RETINAL PIGMENT EPITHELIAL CELLS IN VITRO. BEHAVIOUR AND THE CYTOSKELETON WITH PARTICULAR EMPHASIS ON CYTOKERATINS.

Helen Louise Robey B.Sc.
Department of Clinical Science,
Institute of Ophthalmology,
University of London,
Bath St.,
London EC1V 9AT.

Being a Thesis presented for the degree of Doctor of Philosophy in the University of London. April 1994.

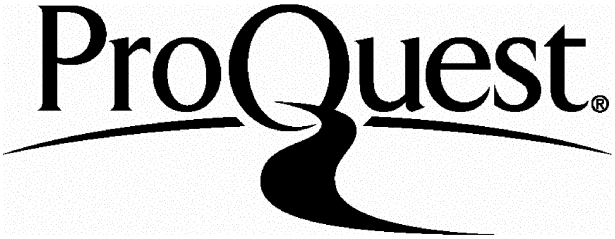

ABSTRACT

Under certain pathological conditions the retinal pigment epithelium (RPE) undergoes changes in shape and behavioural activities, such as phagocytosis, proliferation and mobility. Changes in any of these processes influences the cytoskeleton, which is a cytoplasmic matrix of filaments, consisting of actin microfilaments (AMFs), microtubules (MTs) and intermediate filaments (IFs). The role of AMFs and MTs in these activites is better known than the role of IFs. In the present study immunohistochemical staining techniques were used to identify the cytoskeletal elements, visualise their arrangement in normal and diseased RPE in vitro and examine the possible role of the IFs in RPE phagocytosis, proliferation and migration. Bovine RPE were used as control cells, RCS rat RPE provided a source of diseased RPE and human RPE provided test cells to study proliferation and migration.

Immunohistochemical labelling established that mammalian RPE in vivo and in vitro contained well developed systems of AMFs, MTs and co-expressed vimentin and cytokeratin IFs. The reactivity of cytokeratin monoclonal antibodies used in this study varied both in vivo and in vitro and between neighboring cells. Moreover a sub-population of RPE cells expressed cytokeratin 18 (K18) and cytokeratin 19 (K19) and this sub-population did not appear to be linked to phagocytosis in control rat RPE, but could have an association with phagocytosis in dystrophic cells. K18 fialments showed tortuous arrangements that were unique to dystrophic RPE and this may be the first documentation of a structural difference between control and dystrophic rat RPE.

Using proliferation markers (BrdU & PCNA) it appeared that K18 and K19 were not related to cell proliferation, but were involved in cell migration. Investigations using microchemotaxis chambers showed that human RPE, caught in the process of active migration through the pores of permable membranes, always expressed K18 and K19. The findings demonstrated for the first time a possible functional role for subtypes of cytokeratin IFs in the change of RPE from stationary to motile cells. Antibodies to K18 and K19 may have value as markers for migrating RPE so providing information about the RPE population from sections of ocular pathological material

CONTENTS

TABLE OF FIGURES

CHAPTER 4.

ACKNOWLEDGEMENTS

I would like to acknowledge the British Retinitis Pigmentosa Society for funding 2 years of my study and Professor Ian Grierson for finding funds for the third year. I am grateful to Professor A. Garner, Professor S. Lightman and Pharmax Ltd for letting me use facilities in the departments of Pathology, Clinical Science and Medical.

I am very grateful to Professor Ian Grierson and Dr. N.M. McKechnie, my supervisors, for their guidance, teaching, support, and infinite patience throughout this project. I would also like to thank Professor Grierson for giving me the opportunity to attend four international eye meetings.

Thank you to all my friends and colleagues in the Institute of Ophthalmology for their help, in particular:-

Professor John Marshall, for the use of the RCS rat colony.

Mrs. S. Latta for breeding and maintaining a supply of animals.

Dr. M. Boulton for teaching me the technique to isolate bovine rod outer segments.

Mr. P. West for his help and guidance in computers.

Mrs. J. Willis for teaching me tissue culture techniques.

Mr R. Howes and Mr. S. Davies for all their help in electron microscopy and photography.

Special thanks go to Dr. Paul Hiscott for giving up much of his time to help me, Dr. A. Porter and Dr. M. Goldman for proof reading and moral support..

Thank you to all my family for their support, in particular to my mother and father who have given me endless encouragement, and have so much faith in me that I could not have studied for this degree without them. Finally I am deeply indebted to Mark Nuttall for his infinate understanding, constant moral support and for believing in me.

ABBREVIATIONS

AEC	aminoethylcarbozole
AMF(s)	actin microfilament(s)
BrdU	bromodeoxyuridine
CMB	circumferential microfilament bundle
CMTC	cytoplasmic microtubule complex
COS	cone outer segment (plural COSs)
DAB	3,3'-diaminobenzidine tetrahydrochloride
DIC	differential interference contrast
EDTA	ethylenediaminetetraacetic acid
ERG	electroretinogram
FCS	foetal calf serum
FITC	fluorocein isothyocyanate
GFAP	glial fibrillary acidic protein
IF(s)	intermediate filament(s)
IFAPs	intermediate filament associated proteins
IPM	interphotoreceptor matrix
K18	cytokeratin 18
K19	cytokeratin 19
MAB	monoclonal antibody
MAPs	microtubule associated proteins
MEM	minimal essential media
MT(s)	microtubule(s)
MTOCs	microtubule organising centres
NCS	newborn calf serum
NGS	normal goat serum
PBS	phosphate buffered saline
PCB	paracrystalline bundle
PCNA	proliferative cell nuclear antigen
PVP	polyvinylpyroldone
PVR	proliferative vitreoretinopathy
RCS	Royal College of Surgeons rat
ROS	rod outer segment (plural ROSs)
RP	retinitis pigmentosa
RPE	retinal pigment epithelium
SEM	scanning electron microscopy
SPB	Sorenson's phosphate buffer
TEM	transmission electron microscopy
TRITC	tetramethylrhodamine isothyiocyanate

CHAPTER 1. INTRODUCTION

In the normal adult eye the retinal pigment epithelium (RPE) is a stationary, non-proliferating, phagocytic cell. However, under pathological conditions, such as retinitis pigmentosa and proliferative vitreoretinopathy, RPE undergo behavioural changes, which include proliferation, migration and reduced phagocytosis. The behavioural changes involve radical alterations in shape, function, structure and mobility and are intimately linked to the internal skeleton of the cell or cytoskeleton. The cytoskeleton is an intra-cytoplasmic network of protein fibrils which consists of actin microfilaments, microtubules and intermediate filaments. The role of actin microfilaments and microtubules in the cell is far better understood than that of intermediate filaments. We have studied RPE cells in vitro and have investigated the involvement of the cytoskeleton, in behavioural changes of the RPE. In particular the research has centred on the intermediate filament system.

1.1. THE RETINAL PIGMENT EPITHELIUM

1.1.1. Anatomy & Function

The retina is organised into ten layers (Fig. 1.1.). The innermost layer of the retina is the inner limiting membrane and this layer is in contact with the collagen of the cortical vitreous. Within the retinal layers are blood vessels, Müller cells, astrocytes, four types of neurons (bipolar, ganglion, horizontal, and amacrine cells) and rod and cone photoreceptor cells. The rod and cone photoreceptors (rods and cones) consist of an inner and outer segment. The inner segments contain abundant organelles and play a metabolic role in the photoreceptor, whereas the outer segments consist of stacked discs that contain the photosensitive chemical, rhodopsin (visual purple) (reviewed by De Robertis & Lasansky, 1961). Rods and cones are the visual receptors of the retina and convert light to nerve impulses (the visual process), which are interpreted as images in the occipital lobe of the cerebral cortex.

The RPE forms the outermost layer of the retina and it rests on a basement membrane or Bruch's membrane where it holds a strategic position between the choroidal capillaries and the neurosensitive layers of the retina. This position combined with the anatomy of RPE cells plays a crucial role in the function of the RPE within the eye. The RPE has many complex functions which include adsorption & transport of metabolites, storage of vitamin A, involvement in the visual process, formation of the blood-retinal barrier, retinal adhesion, melanogenesis, and phagocytosis and intracellular digestion of photoreceptor outer segments debris produced by the process of photoreceptor renewal. In particular the role of the RPE in the nourishment of the retina and in photoreceptor

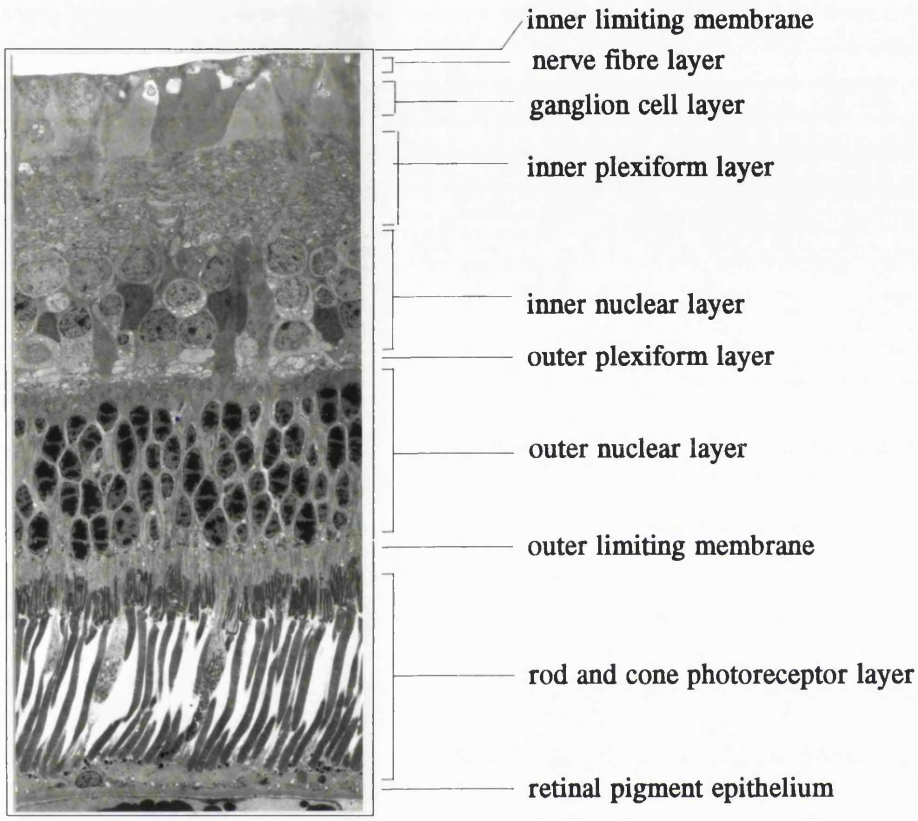

Figure 1.1. Transmission electron micrograph of the normal albino rabbit retina. The ten layer of the retina are demonstrated (x700).

renewal are vital to the integrity and functioning of the retina.

The RPE cell is a stationary, highly differentiated polarised cuboidal cell and it can be divided into two zones, the **basal zone** and the **apical zone**. The **basal zone** contains a large ovoid nucleus, an abundance of mitochondria, a well developed Golgi apparatus and stacks of annulate lamellae (these are the site of active protein synthesis) (Hogan, Alvarado & Weddell, 1971). Microperoxisomes are located both laterally and basally and contain catalase (Leuenberger & Novikoff, 1975). The basal zone is bordered by a basal plasma membrane and lateral plasma membranes. The basal plasma membrane is contorted with numerous infoldings which give rise to coated vesicles (Nguyen-Legros, 1978). The basal infoldings are the adsorption interface of the RPE. The RPE is ideally situated for nutrient adsorption because it rests on Bruch's membrane, which acts as a sieve-like barrier between the choriocapillaries and the RPE.

The RPE adsorbs and transports many essential substances from the choroidal capillaries to the outer retina. The substances include various ions (Steinberg & Miller, 1973; Steinberg & Miller, 1979), amino acids e.g. taurine (Hayes et al, 1975; Schmidt et al, 1977), glucose, glycogen, glycerol (the latter is part of the phospholipid molecule which goes directly into the inner segments (Bibb & Young, 1974a), free fatty acids and fatty acids (Bibb & Young, 1974b), vitamin E (Tappel, 1968, 1970) and vitamin A. Adsorption of some of these substances, e.g. glucose and free fatty acids, requires large amounts of energy. The RPE meets this need through its numerous mitochondria and high levels of oxidative enzymes (the highest in the retina (Pearse, 1961; Hansson, 1970)). On the basal and lateral membranes of the RPE are specific receptors that allow the cell to adsorb vitamin A, or retinol, from the blood stream (Heller, 1975; Heller & Bok, 1976; Bok & Heller, 1976). Once inside the cell cytoplasm retinol, bound to retinol carrier proteins (Saari et al, 1982; Bunt-Milam & Saari, 1983; Bunt-Milam et al, 1984; Bok et al, 1984), can be metabolised (oxidised, isomerized or esterified; Flannery et al, 1990) before being transported, bound to interphotoreceptor retinoid-binding proteins (Liou et al, 1982; Chader & Wiggert, 1984; Pfeffer et al, 1984), to the photoreceptor cells, or stored as retinal (an ester; Zinn & Marmor, 1979; Dowling, 1960; Bridges, 1975) in lipid droplets in the apical cytoplasm of the RPE cell. Retinol and the protein opsin are the essential components of rhodopsin and are necessary elements in the visual process. Through light-induced photoisomerization, opsin is activated and initiates hyperpolarization of the photoreceptor cell membrane and consequently initiating nerve impulses (Darnell, Loddish, & Baltimore, 1986). The RPE plays an essential role in this process through its ability to adsorb, transport and metabolise retinol (Zimmerman, 1974; Chader et al, 1983).

The **apical zone** of the cell is bordered by lateral and apical plasma membranes. The lateral membranes of adjacent RPE run parallel to one another and have a narrow intracellular space. Cell-to-cell junctions, away from the apical membrane, are mostly

gap junctions and macula adherentes. In the apical zone the lateral membranes of adjacent RPE are joined by a continuous belt of zonula adherens followed by a belt of zonula occludens. Zonula adherens, the intermediate junction, is a permeable (gap 20 nm) intercellular junction, which binds neighbouring cells tightly to each other and helps maintain cell shape. Conversly the zonula occludens (or tight junction) is an impermeable junction that fuses adjacent cell membranes and completely obliterates the intercellular space. The belt of zonula adherentes and zonula occludens completely encircle the apical portion of the lateral walls of RPE cells and form the junctional complex. It is through the junctional complex that the RPE forms the blood-retinal barrier. The junctional complex not only controls diffusion of substances between the choriocapillaries and the subretinal space, but also maintains the macromolecular differentiation of the apical and basal membranes.

The apical membrane of RPE cells consists of innumerable microvilli which project into the sub-retinal space. The microvilli form intimate contacts with the rod and cone outer segments (ROS & COS respectively), which also project into the subretinal space (Fig. 1.2.). Long slender microvilli interdigitate with the photoreceptor outer segments and short broad microvilli ensheath the outer segment tips (Spitznas & Hogan, 1970). The short distance between the plasma membrane of apical microvilli and the outer segment plasma membrane is important in the adsorption and transport of substances, such as vitamin A (Dowling, 1960) and amino acids (Young, 1969; Miller & Steinberg, 1976),

The apical cytoplasm contains rough and smooth endoplasmic reticulum, together with free ribosomes, large spindle melanin granules and spherical lipofuscin granules. The melanin granules are formed during RPE cell development and are retained in the RPE as either spherical or ovoid pigment granules (the former being found in the apical microvilli and the latter in the apical cytoplasm). Melanin in the RPE performs several crucial functions (Pathak & Fitzpatrick, 1974). It acts as a neutral density filter, enhancing the resolution of the image by reducing scatter of incoming random light e.g. from the sclera. Melanin also protects the retina from light damage by absorbing radiant energy from visible light and dissipating it in the form of heat. Furthermore it uses this absorbed energy to generate semiquinoid radicles as antioxidants. The lipofuscin granules are residual bodies (Novikoff et al, 1964) containing incompletely degraded photoreceptor discs and are sometimes found around the nucleus as well as in the apical cytoplasm (Streeten, 1961).

Also present within RPE apical cytoplasm are inclusions (Dowling & Gibbon, 1962; Porter & Yamada, 1960), which have a lamella structure (Porter, 1956) and are fragments of ROSs and COSs that are engulfed during the process of photoreceptor renewal (Young, 1967; Young & Bok, 1969). Photoreceptor renewal is a process through which rods (Young, 1967) and cones (Anderson et al, 1978) continually renew their cellular components. Photoreceptor renewal has been described in detail in rods

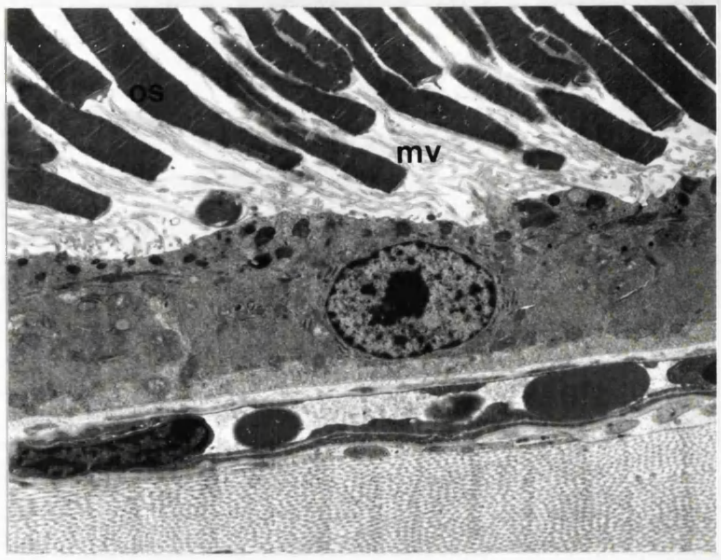

Figure 1.2. TEM of a bovine RPE cell, tapetal region. The outer segments (**os**) of the photoreceptors are intimate with the apical microvilli (**mv**) of the RPE cell (x3,000).

(Young & Droz, 1968). Essentially de novo proteins synthesised in the inner segments of rods, pass into the outer segment and become incorporated into the membrane of a ROS disc situated at the base (at the inner segment end) of the outer segment. These discs undergo continual morphogenesis, the mechanism of which involves evagination of the photoreceptor plasma membrane (Moody & Robertson, 1960; Cohen, 1961a). At each evagination new discs are formed which subsequently displace the preceeding discs (Steinberg et al, 1980). Through continual morphogenesis the discs gradually move through the ROS towards its tip.

The RPE plays a crucial role in photoreceptor renewal through the adsorption and transport of fatty acids and vitamin E. Fatty acids are major constituents of phospholipids, which when associated to proteins, form cell membranes. By maintaining supplies of fatty acids to the outer segments, the RPE ensures disc morphogenesis and photoreceptor integrity. Transport of vitamin E (an antioxidant) by the RPE is also essential to the photoreceptor integrity. A deficiency in this vitamin results in oxidation of the polyunsaturated fats in the outer segment membranes and hence disruption of the ROSs and COSs (Tappel, 1968, 1970; Hayes, 1974).

Young & Bok (1969) noted that despite continual synthesis of discs at the base of a ROS, the length of the outer segment remains constant. This is because there is continuous shedding of effete discs at the outermost tip of the ROS. Using radio-labelled ROS discs, Young & Bok showed that these shed discs were phagocytosed by the underlying RPE cells and formed the lamella inclusions identified in the apical cytoplasm (Dowling & Gibbon, 1962; Porter, 1956; Porter and Yamada, 1960). Since the discovery of phagosomes containing ROS discs the mechanism by which RPE internalise effete ROSs has stimulated intense investigation, particulary with regard to diseased RPE that are unable to phagocytose effectively. Consequently phagocytosis in RPE cells has been investigated in detail both in vivo and in vitro (Hollyfield & Ward, 1974; Hu et al, 1982; Edwards & Szamier, 1977; Feeney & Mixon, 1976; Custer & Bok, 1975; Reich-D'Almeida & Hockley, 1975; Funahashi et al, 1976; Koga et al, 1977; Hollyfield, 1976) and there seems to be two distinct phagocytic mechanisms. RPE from several species including human show non-specific and specific phagocytic mechanisms, which are mediated by non-specific and specific receptors respectively (Philp & Bernstein, 1980 & 1981; Mayerson & Hall, 1986). In vitro, non-specific mechanisms are employed for phagocytosis of polystyrene latex beads and other inert particles, while specific mechanisms are used for selective phagocytosis of ROSs in preference to latex beads (Philp & Bernstein, 1980 & 1981; Mayerson & Hall, 1986). Indeed, kinetic studies have confirmed that ROSs bind to specific receptors on the surface of the cells (Hall & Abrams, 1987). Therefore ROS internalisation by RPE fulfils the main criteria of "true" phagocytosis i.e. that the process is specific.

Phagocytosis occurs in 3 steps: **Recognition and attachment**, **ingestion** or **endocytosis**, and **digestion**. **Recognition and attachment** consists of the interaction of

the ROS membrane with the surface plasma membrane of the RPE cell via specific ligand(s) and receptor(s). So far, the ligand (on the ROS) and receptor (on the RPE) have not been characterised. Glycoproteins on the surface of the RPE might be involved in mediating ROS phagocytosis (Colley et al, 1987) and it has been suggested that either mannose (Hall & Quon, 1980; Seyfried-William et al, 1984; Mayerson & Hall, 1986) or sialic acid (a sugar residue) (Tarnowski & McLaughlin, 1987; McLaughlin & Boykins, 1987) are part of the phagocytic receptor(s).

Ingestion of ROS by the RPE is preceded by ROS detachment or disc shedding. The mechanism of disc shedding is still unclear. However, there are two theories and both are based on electron microscopic analysis of the ROS/RPE juncture. The important difference between the two theories is whether the RPE play an active or passive role in disc shedding. Spitznas & Hogan (1970) describe a continuous cytoplasmic sheath from the RPE, which protrudes inwards from all sides and sequestrates a portion of ROS discs from the tip of the outer segment. This suggests that the RPE is actively involved in "nibbling" off the old discs from the end of the outer segment, implying that disc shedding and ROS ingestion are one process. Alternatively, Young (1971a) portrays a sequence of events initiated by morphological changes in old ROS discs, followed by invagination of the ROS membrane and eventual detachment from the photoreceptor tip. In this mechanism the RPE has a passive role scavenging ROSs released from the photoreceptor and it indicates that disc shedding and ROS ingestion are separate entities. There is evidence to support both theories of disc shedding (Burnside & Laties, 1976; Burnside, 1976; Besharse & Dunis, 1983a,b; Edwards & Bakshian, 1980; Currie et al, 1978; Bok & Young, 1979). However, it is likely that detachment and ingestion involves mechanisms from both photoreceptors and RPE cells. Evidence for mutual involvement has been shown in the frog (Besharse et al, 1984; Besharse, 1984). Using cytochalsin-D (an actin inhibitor) an actin dependent process has been shown to occur in the RPE on activation of disc shedding. Pigment-free pseudopods form in the RPE and disc detachment takes place as the pseudopods envelope the apex of the ROS. Concurrently disc vesiculation, similar to that observed by Currie et al (1978), occurs at the point of separation in the ROS.

Digestion of ROSs by the RPE is a highly efficient system. In several species (rats: LaVail, 1976a,b; frogs: Basinger et al, 1976; Hollyfield et al, 1976; chickens: Young, 1977) discs are shed twice a day, in the morning when the light goes on and at night when it is dark. The ROS load has to be cleared by the RPE and an efficient battery of lysosomes localised in the apical cytoplasm of the cells enables the RPE to cope with the phenomenally large phagocytic load. It has been estimated that frog RPE consume about 600 discs per day, while in the monkey between 2,000-4,000 disc are consumed daily (Young, 1971b) and as many as 250,000-300,000 discs in the rat (Bok & Young, 1979).

The RPE cell has an extensive lysosomal system consisting of at least eight

hydrolytic enzymes (Zinn & Henkind, 1979; Zinn & Marmor, 1979). In situ these enzymes (synthesised in the rough endoplasmic reticulum) are incorporated into vesicles (or primary lysosomes) in the Golgi complex (DeDuve et al, 1955; Novikoff et al, 1956). Primary lysosomes come into contact with ingested ROSs through a network of dynamic filaments (microtubules). The microtubule network extends from the apical membrane to the centre of the cell and may transport ingested phagosomes to lysosomal sites (Burnside, 1976). On contact the phagosome and lysosome membranes fuse (DeDuve, 1964;Young, 1971a). Hydrolytic enzymes are then released into the phagosome (producing a secondary lysosome) and the activated enzymes digest the ROS fragment. The distinct lamellar structure of the phagosome is destroyed as digestion progresses, resulting in small vesicles with a granular matrix and a dense core. These small vesicles appear in the apical and basal part of the cell and occasionally incomplete digestion gives rise to lipofuscin-rich bodies (Novikoff et al, 1964; Feeney et al, 1965).

Clearly the anatomy of the vertebrate RPE underlies the role the RPE plays in the retina. The junctional complex in the apical membrane act as an effective barrier between the choroidal blood supply and the retina, the basal infoldings and coated vesicles indicate adsorption and active transport, while the apical zone of the RPE is clearly orientated towards protein synthesis, phagocytosis of photoreceptor debris, and provides excellent access for transport of substances to the photoreceptors and the neural retina.

1.1.2. Pathology and the RCS rat

The previous section has revealed the RPE monolayer to be a highly complex tissue. The pathological responses of RPE are also complex. The simplest classification has been outlined by Nguyen-Legros (1978) and identifies two cytopathological responses of the RPE:

i) Dysfunction of polarization and pigmentation of the cell, this is often linked to hypertrophy, hyperplasia or metaplasia of the RPE - usually secondary to disorders effecting other parts of the retina or choroid.

Hypertrophy of the RPE may be congenital, such as in Gardener's syndrome (Blair & Trempe, 1980), or acquired where hypertrophic RPE occur as in association with a variety of choroidal lesions. Hyperplasia of the RPE can occur in colobomata (where there is overgrowth of the RPE layer (Duke-Elder, 1963a; Gartner, 1947). However, hyperplasia most often occurs in eyes with retinal detachments (Frayer, 1966). In retinal detachment the RPE proliferate (Machemer & Norton, 1968; Machemer, 1968; Machemer & Laqua, 1975) and undergo metaplastic changes to form a mobile fibroblastic-like cell. The fibroblast-like form of the RPE may migrate

through the retinal layers and become involved in scar formation which ultimately contracts causing retinal detachment and blindness (Machemer & Laqua, 1975; Machemer et al, 1978).

Under certain conditions the RPE will diminish in size (atrophy) and curtail its physiologic activities (Klien, 1958) with depigmentation often being an early indicator of cell atrophy and degeneration. RPE degeneration and loss occurs in choroideremia (Duke-Elder, 1963b; McCulloch, 1950), in central areoler choroidal sclerosis (Ashton, 1953), through bacterial, parasitic and viral infection (eg. in syphilis, toxoplasmosis, onchocerciasis, and rubella), and with ageing (i.e. in senile macular degeneration) (Sarks, 1976). RPE atrophy is one important change associated with the disease retinitis pigmentosa.

ii) Dysfunction of phagocytosis in the RPE cells. In certain pathological conditions, retinal dystrophies (primary failure) and retinal detachment (secondary failure) the RPE fail to phagocytose ROSs. In these disorders, the cells frequently lose their polarity, mobilise, migrate and proliferate.

One group of inherited retinal dystrophies found in both man and animals manifests itself as photoreceptor degeneration and sometimes RPE hyperplasia. In the humans the condition is known as retinitis pigmentosa (RP) and includes autosomal-recessive, autosomal-dominant, dominant and X-linked forms. RP involves a slow degeneration of the photoreceptors and is characterised clinically by an initial RPE cell atrophy followed by cell migration into the retina. The aetiology of the disease or loci of the primary pathology in humans is unknown. However, the primary pathology appears to be in or near the photoreceptors.

Inherited retinal dystrophies have been identified in mice (Keeler, 1924), several breeds of dog (Parry, 1953; Lucas, 1954; Barnett, 1962; Aguirre, 1976), cats (Barnett, 1965; Carlile, 1981; Narfström, 1985), and rats (Bourne et al, 1938). In mice (LaVail & Sidman, 1974) and collie dogs (Santos-Anderson et al, 1980) the disorder occurs early and before the photoreceptors have fully differentiated. In other breeds of dog and in cats, degenerations occur only when the photoreceptors are mature. On the other hand in humans, the degeneration may be linked to photoreceptor development and so occurs slightly later. Therefore it is clear that the dystrophies can be complex and the aetiology of the diseases varies between species. However, the aetiology of retinal dystrophy in the Royal College of Surgeons (RCS) rat is well documented (Herron et al, 1969; Bok & Hall, 1971; LaVail et al, 1972). In addition the end point of the disease in this particular breed of rat shows evidence of RPE migration and hyperplasia (Cogan, 1950), similar to that seen in humans.

In man, the pathogenesis of RP is obscure, primarily because tissue for research is scarce and only available at the natural end of the patients life when the degeneration is in its late stages. Although only limited information can be gained from the human, animal models have enabled detailed study of RP-like behaviour, particularly during the

progression of the disease process.

The RCS rat has a hereditary RP-like lesion (Bourne et al, 1938) of which the primary defect has been localised in the RPE (Herron et al, 1969; Mullen & LaVail, 1976). The degeneration in the rat is relatively simpler than that in dogs and cats, and furthermore it shares three areas of similarity with the human disease (Herron et al, 1974). The three similarities are genetic transmission, progressive loss of electroretinogram (ERG) and the end stage histology.

The aetiology of the degeneration in the dystrophic RCS rat was first documented by Dowling & Sidman in 1962. The first signs of the disease occur 12 days after birth with an accumulation of ROS debris between the surface of the RPE and the ends of the developing rods. Disorganisation and progressive degeneration of the ROSs follows, accompanied by changes in the ERG and an increase in rhodopsin levels. By day 22 the photoreceptor cell nuclei and inner segments begin to degenerate, the latter being entirely lost by day 40. At day 22 the ERG has lost sensitivity, the rhodopsin levels have decreased and the outer segment layer is replaced entirely by a zone of debris. The debris consists of whorls of outer segment and RPE apical microvilli. The RPE, which appears normal up to day 32, is aberrant by day 40. At day 40 some RPE cells appear dedifferentiated and have migrated through the remnant of the outer segments. Adjacent RPE either spread or divide to fill the space on Bruch's membrane vacated by the mobilised cells. These spreading RPE also are dedifferentiated.

The advanced stage of the disease in the rat is reached after 60-72 days. The RPE cells no longer maintain the blood retinal barrier and the debris zone is invaded by macrophages. At the late stages of the disease, invasion of the RPE by retinal capillaries has been described (Bourne et al, 1938; Dowling & Sidman, 1962; Bok & Hall, 1971). The vascularization appears to cause disruption of the remaining inner retina (LaVail, 1979). By this time the outer plexiform zone is gone, the b-wave of the ERG is lost and the animal is blind. In the advanced stages of RP in man loss of photoreceptors, RPE migration (Herron et al, 1974; Kolb & Gouras, 1974) and macrophage invasion of the debris zone (Szamier et al, 1979) also have been noted.

The pathogenesis of the degenerative lesion in the RCS rat has been studied extensively. It was considered that the lesion may lie either in the RPE or in the photoreceptor. Herron et al (1969) showed that up to day 18 the dystrophic rat had normal outer segment renewal rates, but the RPE were non-phagocytic. They proposed that the defect lay with the RPE and its inability to phagocytose ROSs, which resulted in a build-up of ROS debris. The debris forms a barrier cutting off the nutrient supply to the photoreceptor cells and subsequently causes photoreceptor death. Alternatively, Bok & Hall (1971) and LaVail et al, (1972) believed the lesion to lie in the photoreceptors rather than the RPE. They hypothesised that the defect may be an over-production of ROSs, which resulted in debris accumulating in the subretinal space. Both groups found that the renewal rate was either the same or slower than that in the normal

rat and that the RPE failed to phagocytose shed ROS discs. However in 1976, Mullen and LaVail provided even more convincing evidence that the lesion resides in the RPE. The authors produced chimeric rats with an RPE monolayer which was partly normal and partly dystrophic. Where the RPE was normal the overlying neural retina was normal, but where the RPE was dystrophic the retina had degenerated. Later Goldman & O'Brien (1978) showed that dystrophic RPE could phagocytose ROS, but at a greatly diminished rate compared to normal rats.

Extensive research has clearly provided a detailed understanding of the aetiology and pathogenesis of the disease in the RCS rat. The RCS rat has been vital to furthering our understanding of the control of ROS renewal, has emphasised the importance of the RPE to the welfare of the neurosensitive retina and has enabled investigation of the genetic control of cell differentiation. In this study the RCS rat has been used as a source of diseased RPE.

Disease may affect a range of cell functions, change or disrupt features or structures in the cell, or affect interrelations between cells. These processes are difficult to study in vivo and organ culture often provides information which is hard to interpret. The development of tissue and cell culture techniques have provided a simple system to study cell reactions and these provide useful information about cellular behaviour. In this study phagocytois was studied in bovine RPE and rat RPE. Rat RPE was a test model for reduced phagocytosis and was compared with bovine RPE, which were control cells.

1.2. THE CYTOSKELETON

The cytoskeleton is a system of structural protein fibres which are present throughout the cytoplasm of all eukaryotic cells. Cytoskeletal elements form a dynamic cytoplasmic matrix which surrounds, embeds and contacts the cellular organelles. This matrix may determine the position and movement of all other cell structures as well as the overall shape of the cell. There are three classes of cytoskeletal filaments, actin microfilaments (AMFs; 5-7nm diameter), microtubules (MTs; 24nm diameter), and intermediate filaments (IFs; 10nm diameter).

AMFs and MTs are universal components of all eukaryotic cells. Most eukaryotic cells contain one or more type of IF, each of which is assembled from specific proteins.

1.2.1. Actin microfilaments (AMFs)

AMFs consist of 42 kilodalton (KD) globular monomeric protein sub-units (G-actin) which are arranged three-dimensionally to form a helix (F-actin) 70 Å in diameter. An F-actin fibre has the electron micrographic appearance of two strings of

beads wound around each other. Actin is an abundant, highly conserved filamentous protein found in muscle and foremost in the cortical cytoplasm of non-muscle cells. Actin is essential for many forms of cellular motility and its function within the cell relies on its unique structure and its mechanical properties. The mechanical properties are based on the ability of actin to polymerise and depolymerise. Polymerisation and depolymerisation of actin occurs under defined conditions. G-actin formation (depolymerisation) is favoured by low ionic strength, high pH and the presence of Ca^{2+}, whereas F-actin formation (polymerization) is favoured at lower pH and in the presence of Mg^{2+}. Actin polymerisation is controlled by capping proteins and sequestering proteins, such as gelosolin and profilin, respectively. The control of filament formation is crucial and of fundamental importance to the function of AMFs within the cell. Polymerisation provides AMFs with a dynamic versatility. However, the spectrum of AMF function in biological systems is achieved through its associated proteins. These proteins bind to AMFs to form unique structures with specific properties to carry out specific cellular functions. The key proteins include myosin, tropomyosin, calmodulin, fimbrin, fodrin, villin, spectrin, filamin, vinculin, talin, and alpha-actinin. The presence of certain associated proteins defines the organisation and determines the properties of the AMFs.

AMFs have contractile properties when they are associated with myosin and tropomyosin. Myosin molecules interact along the length of F-actin fibres (a process driven by ATP hydrolysis and regulated by Ca^{2+} levels) and this interaction generates the motive force resulting in contraction. AMFs, in the form of well-ordered bundles, provides structural support in the microvilli of intestinal epithelial cells (Mooseker & Tilney, 1975; Geiger et al, 1980, 1981; Hirokawa et al, 1983). The strength of the AMFs is provided through the association of five actin associated proteins, fimbrin, villin, spectrin, fodrin and calmodulin. Fimbrin and villin cross-link adjacent AMFs, whereas spectrin, fodrin and calmodulin form crucial links between AMFs and the plasma membrane. The microvilli in RPE cells are extremely long and thin and contain parallel AMFs along their length. The AMFs provide stability, strength and flexibility so enabling them to offer support and protection to the ROSs (Burnside, 1976; Burnside and Laties, 1976). Vinculin, talin and alpha-actinin interact with the ends of AMFs and mediate attachment of actin structures to the outer cell membrane. Vinculin and alpha-actinin are components of the zonulae adherentes of all epithelial cells, including the RPE, and of focal adhesion plaques (focal contacts) in cultured cells. Vinculin, alpha-actinin and fodrin have also been found in the apical microvilli of RPE cells (Philip & Nachmias, 1985).

A complete AMF system exists in RPE cells (Burnside & Laties, 1976). In situ the RPE cell contains two types of AMF bundles in the apical part of the cell. One is the circumferential microfilament bundle (CMB) and the other is the paracrystalline bundle (PCB). The CMD has random polarity, loose packing, contains myosin (which

is contractile)(Owaribe et al, 1981; 1986) and is associated to the zonulae occludentes and zonulae adherentes of each cell. The PCB is polarised and localised at the apical projections of the RPE cell (Owaribe & Eguchi, 1985). Drug induced disruption of these actin bundles in chick RPE results in loss of cell shape (Crawford, 1979) which indicates that actin organisation in the RPE cells is crucial for the maintenance of cell shape (Owaribe et al, 1979).

In cells, actin exists in a state of equilibrium as nonpolymerised and polymerised forms. Much of the polymerised actin occurs as long bundles consisting of parallel AMFs with myosin, tropomyosin, alpha-actinin (Weber & Groeschel-Stewart, 1974; Lazarides, 1975a,b; Lazarides & Burridge, 1975) and filamin, which is an actin crosslinker (Osborn & Weber, 1979; Pavalko et al, 1989). AMF bundles of this type are called stress fibres and are visible by phase microscopy in well spread cells. Detailed visualisation of stress fibres and other cytoskeletal elements is achieved using electron microscopy of whole or detergent extracted cells (Buckley & Porter, 1967,1975; Wolosewick & Porter, 1976; Brown et al, 1976; Schliwa & Van Blerkom, 1981). Using this procedure the structure of stress fibres have been described (Buckley & Porter, 1967; Small & Celis, 1978). Stress fibres often extend across the whole length of the cell and correspond to the microfilament bundles identified in electron micrographs by Buckley & Porter (1967). Stress fibres terminate at the cytoplasmic face of the plasma membrane at specialised sites known as focal adhesion plaques (Abercrombie et al, 1971; Izzard & Lochner, 1976; Heath & Dunn, 1978). Adhesion plaques contain the attachment proteins talin and vinculin. Talin interacts with both vinculin (Burridge & Mangeat, 1984) and the transmembrane fibronectin receptor which is an integrin (Horwitz et al, 1986). Vinculin links to alpha-actinin (Geiger, 1979), which in turn is directly bound to actin (Maruyama & Ebashi, 1965; Burridge & Feramisco, 1981). Cultured cells are able to attach to an external substrate through the adhesion plaques. Attachment proteins are a vital link between the AMF, the plasma membrane of the cell and the extracellular matrix.

Stress fibres incorporate the same actin associated proteins as those associated with the actin myofibrils in muscle cells. In addition the organisation of stress fibres somewhat resembles that of striated muscle myofibrils. Consequently, it has often been thought that the function of stress fibres in cultured cells is to generate motive force for cell locomotion. However, motile fibroblasts lack stress fibres (Couchman & Rees, 1979; Herman et al., 1981) and, although they have been shown to be potentially contractile in living cells (Kreis & Birchmeir, 1980), this property is not utilised for motive force. It is apparent that stress fibres are associated with strong adhesiveness of cultured cells to the substratum (Willingham et al, 1977) and the adhesive nature of stress fibres has clearly been demonstrated in cultured chick RPE cells (Turksen et al, 1983). Stress fibres, however, are not exclusive to cultured cells and have been demonstrated in situ. The fibres are present in scleroblasts (fibroblasts) in the scales of goldfish (Byers &

Fujiwara, 1982) where they appear to specifically enhance adhesion of the cell to its substrate. Therefore, stress fibres exert isometric rather than isotonic force.

Microinjection techniques and fluorescent probes reveal that in living cells AMFs appear to be able to reorganise and, in particular, stress fibres appear to assemble and disassemble (Wang, 1984; 1987). This dynamic aspect of the AMF system imparts a vasoelastic property to the cell allowing it to change and maintain its shape and internally reorganise one of its major cytoskeletal components.

1.2.2. Microtubules (MTs)

MTs are long hollow tubes and are formed by polymerization of a highly evolutionary conserved globular protein subunit called tubulin. Tubulin is heterodimeric and made of two nonidentical polypeptide chains which have a molecular weight of 55 KD. The wall of the MT is made up of a helical array of repeating tubulin subunits, which are arranged head to tail so giving MTs a defined polarity. MTs are stiff tubes able to resist bending, but transmit tensile and compressive forces along their length (see review Tucker, 1979). A combination of the physical properties of MTs and their organisation provide MTs with a number of functions within the cell and these include:-

1. Development and maintenance of shape
2. Cellular motility
3. Sensory transduction
4. Intracellular transport of material
5. Chromosome movements in cell division.

MT assembly is a well regulated process which gives rise to different arrays of MTs with specific orientation at different phases in the cell cycle. Polymerisation is governed by a number of factors including low pH, the presence of Ca^{2+} ions, Mg^{2+} ions, GTP & GTP hydrolysis and the presence of microtubule associated proteins (MAPs). In the cell a MT exists in a state of dynamic equilibrium dependent on its state of polymerisation and the available pool of tubulin subunits. The phenomenon has been called dynamic instability (Mitchison & Kirschner, 1984) and is crucial to the function of MTs in the cell. In any one period of time, as one set of MTs is being dismantled another set is being erected, possibly by means of recycled subunits from the tubulin pool.

MTs in all cells appear to be organised from specialised anchoring points called microtubule organising centres (MTOCs). In cilia and flagella the MTOCs are the basal bodies and, in interphase, the centrosomes are the MTOCs of the mitotic spindle. MTs assembly is efficient and directional from centrosomes or basal bodies and the filaments formed are known to be more stable than MTs from other anchoring points.

Like AMFs, MTs bundle to form large and diverse structures. There are two

forms of MT bundling; parallel arrays and radial arrays. Parallel arrays are found in sperm flagella, flagella and cilia of protozoa, in cell projections of cultured cells, in neural cell axons (see review Olmsted & Borisy, 1973), and in erythrocytes of certain vertebrates (Behnke, 1971). With the exception of erythrocytes, the arrays are orientated parallel with the long axis of the cellular structure and provide structural support (Byers & Porter, 1964; Burnside, 1971; Warren, 1974). Like AMFs, the MTs perform different functions within the cell according to the different MAPs they contain. In flagella and cilia MTs contain the MAP dynein through which motive force is generated (Gibbons, 1968).

Radial arrays occur in the mitotic spindle and in the cytoplasm of cultured cells. In cultured mammalian cells, during interphase, the MTs are organised into a delicate network of filaments which concentrate around the nucleus and radiate towards the plasma membrane. This is referred to as the cytoplasmic microtubule complex (CMTC) (Brinkley et al, 1980). The CMTC is dynamic and is thought to establish and maintain cell shape as well as be involved in intracellular transport.

Visualisation of the arrangement of the CMTC in cultured cells, as for the rest of the cytoskeleton, can best be achieved using immunohistochemical labelling. Immunohistochemistry involves the labelling of individual proteins with a specific polyclonal or monoclonal antibody. The binding sites are visualised (e.g. with a fluorescent or an enzyme: chromogen reaction - see section 2.3.4) and documented microscopically. Immunohistochemical techniques, especially indirect immunofluorescence, were first used by Lazarides & Weber in 1974, and are now the standard methods of investigating the organisation of the cytoskeleton within the cell. Indirect immunofluorescence and indirect immunoperoxidase were used in the present study to investigate arrangements of cytoskeletal elements in RPE cells undergoing behavioural changes in vitro. Ultrastructural detail of cytoskeletal elements in RPE cells was investigated using TEM of whole and detergent extracted cells.

In RPE in vivo, AMFs are thought to be much more important than MTs in maintaining cell shape (Crawford, 1979; Owaribe et al, 1979). However, there is evidence that MTs play a role in shape changes (dedifferentiation) perhaps by mobilising actin during dedifferentiation (Owaribe et al, 1979). In neural cells, MTs have been shown to transport proteins and organelles between the cell body and the axon (see review by Hyams & Stebbings, 1979). In addition, disrupting MTs stops the movement of chromosomes, nuclei, mitochondria, synaptic vesicles, liposomes, phagosomes, cytoplasmic granules, pigment granules, and ribosomes (reviewed by Burnside, 1975). Time lapse photomicrography of cultured fibroblasts and epithelial cells has been an effective and direct means of showing that MTs function as intracellular transport routes (Freed & Lebowitz, 1970). Therefore it appears that MTs have both structural and transport functions in cells.

1.2.3. Intermediate filaments (IFs)

IFs are the third class of cytoskeletal filaments and are so named because their diameter, 7-11 nm, is intermediate in size between AMFs and MTs. They are enigmatic and intriguing structures that at present do not have a clear cut biological function. Unlike AMFs and MTs, IFs do not appear to be part of the protozoan cytoskeleton, are present in most invertebrate cells, but are not universal components of all eukaryotic cells. There are five major types of IFs which have been distinguished biochemically, immunologically and on the basis of their cell type distribution (see review by Lazarides, 1980). Each type of IF is characterised by a different protein subunit. The IFs are:-

a) vimentin filaments (mol. wgt. 53 KD) - present in all mesenchymal tissues, including connective tissue cells, blood cells, bone and cartilage.

b) desmin filaments (mol. wgt. 52 KD) - present in all types of smooth and striated muscle cells, except certain types of vascular smooth muscle cells that contain vimentin exclusively.

c) glial filaments (mol. wgt. 50 KD) - consists of glial fibrillary acidic protein (GFAP) and are present in astroglial cells.

d) neurofilaments (mol. wgt. 15, 20 & 68 KD) - consist of three proteins and are present in axons of both central and peripheral neurons in vertebrates.

e) cytokeratin filaments (tonofilaments) (mol. wgt. 40-70 KD) - present in most epithelial tissue and the structural proteins of hair, skin and nails. It is the largest group of IFs at least 30 distinct cytokeratin polypeptides.

Each IF type is coded for by a specific gene and there is 23-25% homology between the different genes, which indicates a common ancestry (Steinert & Parry, 1985; Kreig, 1985). Since specific monoclonal antibodies are available for most protein subunits, immunohistochemistry is an ideal tool to evaluate IFs in cells in either culture or in tissue sections. In addition, the cell type specificity of IFs is largely conserved (Franke et al, 1978a,b, 1979a; Hynes & Destree, 1978; Sun & Green, 1978a; Schlegel et al, 1980; Gabbiani et al, 1981) during cell transformation and even in tumour development.

In spite of the diversity of proteins that can polymerise to from IFs, the five IF types share a common molecular structure (see review Steinert & Parry, 1985). Steinert

et al(1980) proposed a common structure for IFs consisting of 2 homologous alpha-helical domains, which are separated and extended by five varying globular domains. The helical domains are twisted like a rope and the rope-like structure is thought to provide the IF with rigid properties. The combination of uniform helical domains and variable globular domains would account for both the structural similarities as well as the chemical and immunological diversity of the different IFs. It has been suggested that IFs share a conserved domain that is responsible for their assembly into 10 nm filaments and, in addition, have class-specific domains that are responsible for their fundamental specificity within different cells (Lazarides, 1980).

Assembly of IF proteins occurs through polymerization of the protein subunits and requires less stringent conditions than those of AMFs and MTs. The three neurofilament proteins (designated light, medium and heavy) readily copolymerise, whereas vimentin and desmin (which are soluble in low salt solutions) polymerize only when the ionic strength reaches physiological levels. In contrast, cytokeratins can polymerise in very dilute salt solutions. The cytokeratins also differ from the other types of IFs in that they are divided into two families, Type I and Type II. The Type I family of filaments are acidic and have lower molecular weights and lower isoelectric points than the neutral-basic Type II family of cytokeratin filaments. In vivo and in vitro assembly of cytokeratin filaments requires both Type I and Type II cytokeratins (Steinert et al, 1976).

In human epithelia there are 19 types of cytokeratin polypeptides. Each cytokeratin can be translated from a unique mRNA species and are therefore distinct protein entities (Fuchs & Green, 1979; Kim et al, 1983; Roop et al, 1983). Using two-dimensional gel electrophoresis, Moll et al (1982) classified the cytokeratin polypeptides 1-19 according to isoelectric pH and molecular weight. The different cytokeratin polypeptides are expressed in different epithelia in different combinations of polypeptides, therefore any given epithelial cell can be characterised by the specific pattern of its cytokeratin IFs (Winter et al, 1980; Fuchs & Green, 1980; Franke et al, 1981a,b; Wu & Rheinwald, 1981). Indeed, cytokeratin expression in epithelial cells appears to follow a set of "rules" (Moll, 1982; Woodcock-Mitchell et al, 1982, Wu et al, 1982, Eichner et al, 1984). The rules include that at least one member of each cytokeratin family (Type I or II) is coexpressed in all epithelia, any given epithelia expresses only a few cytokeratin polypeptides (which in most cases are specific pairs). In coexpressed cytokeratin pairs Type II is always larger than its Type I partner, and the type of cytokeratins expressed correlates with the complexity (differentiation) of the epithelia.

On the basis of chick studies (Crawford et al, 1972. Crawford, 1980; Docherty et al, 1984; Philp & Nachmias, 1985; Owaribe et al, 1986) it was initially thought that RPE contained only vimentin IFs. However, cytokeratin IFs have been identified in amphibian, bovine, rat, rabbit and human RPE (Hiscott et al, 1984; McKechnie et al,

1988; Owaribe et al, 1988; Kasper et al, 1988; Fuchs, et al, 1991). Coexpression of the cytokeratin pair 8 & 18 is generally recognised in mammalian RPE (Owaribe et al, 1988, Kasper et al, 1988; Fuchs, et al, 1991).

Coexpression of two types of IFs, vimentin and cytokeratins, has been reported in other epithelial cell types in vitro (Franke et al, 1978a; Osborn et al, 1980; Virtenen et al, 1981; Henderson & Weber, 1981; Lane et al, 1983; Ramaekers et al, 1983; LaRocca & Rheinwald, 1984). In RPE McKechnie et al (1988) identified vimentin and cytokeratins in normal human RPE in situ and other authors have reported coexpression of these two distinct IFs in guinea-pig RPE and in a sub-population of bovine RPE (Owaribe et al, 1988), in RPE after retinal detachment (Hiscott, 1984; Guèrin et al, 1990), in normal RPE in eyes with uveal melanoma (Fuchs et al, 1991) and in RPE in culture (Owaribe et al, 1988).

IFs, like AMFs and MTs, have associated proteins, which mediate the function of IFs within the cell (Steinert & Parry, 1985). The intermediate filament associated proteins (IFAPs) include filaggrin (mol. wgt. 30 KD), cystein-rich proteins, synemin (mol. wgt. 230 KD), paranemin (mol. wgt. 280 KD), plectin (mol. wgt. 300 KD) and IFAP-300K (mol. wgt. 300 KD). IFAPs are essentially linker molecules increasing IF stability and rigidity. Filaggrin universally aggregates all types of IFs to produce bundles, is prominent in stratum cornea of mammalian epidermis and may be present in other epithelial cells (Steinert et al, 1981). Cystein-rich proteins form disulphide bonds between cytokeratin filaments in hair, producing rigid and insoluble cytokeratin structures (see review by Gillespie, 1983). Synemin and paranemin associate with desmin in ,muscle cells and with vimentin filaments in non-muscle cells (Granger & Lazarides, 1980; Lazarides, 1982). Plectin links IFs to MTs (Wiche et al, 1983) and IFAP-300K and IF linker protein in BHK-21 cells (Lieska et al, 1985). IFs appear chemically stable since they remain even after harsh extraction procedures in which most other cell components are removed, including AMFs and MTs.

Most of the IF proteins exist in their polymerised state in the cell. In cultured cells these filaments form a loose 3-dimensional network throughout the cytoplasm. The central part is concentrated around the nucleus and the peripheral parts radiate towards the plasma membrane. Parallel bundles are found in segments of the network in most cells and are particularly common in the elongated processes of neurons. Cells may respond to extracellular stimuli that require alteration in their morphology by changing the balance between the concentration of polymerised and nonpolymerised cytoskeletal protein. Cytoskeletal alteration is possible with AMFs and MTs, but not with IFs, because they exist in the polymerised state. However the IF network is dynamic and newly synthesised IF proteins can be rapidly incorporated into existing filaments (Vikstrom et al, 1989). Through the dynamic nature of IFs the cell can respond to morphological change by reorganisation and rearrangement of the IF network. It has been shown that under certain conditions, such as mitosis, the IF networks undergoes

reversible reorganisation, for example the rigid IF networks disappear at the onset of cell division (Bershadsky & Vailiev, 1988; see 1.3.2.).

In contrast to the wealth of knowledge about the role and function of AMFs and MTs in cells, very little is known about the IFs (see review by Bloemendal & Pieper, 1989). The insolubility of vimentin filaments in non-ionic detergents would suggest that they play a structural role in the cell. The filaments frequently terminate at the nuclear membrane and in adhesion plaques in cultured fibroblasts (Lehto et al, 1978; Small & Celis, 1978) or in nucleated chick erythrocytes (Virtanen et al, 1979), which suggests that vimentin filaments are the mechanical support for the nucleus constraining its position within the cell (Small & Celis, 1978; Trotter et al, 1978; Lehto et al, 1978; Henderson & Weber, 1980;Lazarides, 1982). Further evidence for vimentin as a structural support comes from its joint role with desmin in the lateral organisation and registration of myofibrils in muscle (Lazarides, 1980). Furthermore, Lazarides (1980) suggested that the cellular arrangement of IFs implies that they hold cellular organelles as well as the nucleus in a defined place in the cell and act as mechanical integrators of cellular space. Evidence to support Lazarides proposal was obtained using stereo paired electron micrographs, which visualised connections between the IFs and the nucleus, centriole, MTs, cytoplasmic vesicles and rough endoplasmic reticulum (French et al, 1982). Goldman et al (1986) suggest that the "IF network represents a cytoskeletal system interconnecting the cell surface with the nucleus" and that it "is involved in transmitting and distributing information amongst the major cellular domains". Such a communication system within cells would be advantageous in maintaining structure and homeostasis. Glial filaments are found randomly dispersed in the cytoplasm of astrocytes and cells of glial origin (Liem, 1978; Schachner et al, 1977; Bignami & Dahl, 1977) and they have also been found to be coexpressed with vimentin in human glioma (Paetau et al, 1979), cultured glial cells (Bennett et al, 1981; Yen & Fields, 1981) and in bovine astrocytes (Yen & Fields, 1981). However, their function is presently undetermined. Neurofilaments are closely associated with MTs in the neuronal axons and may provide tensile strength to the axons (Gilbert et al, 1975).

Cytokeratins in tissues of epidermal origin are called "hard" or alpha-keratins and are resistance to shearing forces. Cytokeratins provide strength to skin, hair and nail (Gillespie, 1983). Cytokeratin filaments (tonofilaments) traverse the epithelial cytoplasm and connect the plasma membrane where desmosomes, or hemidesmosomes (basal membrane) are located. Desmosomes are discoid structures symmetrically distributed on the membrane of two cells in contact with each other and contain a densely stained plaque (Staehelin, 1974; Farquar & Palade, 1963). Arrays of tonofilaments are associated with these types of junctions (Franke et al, 1978b; Sun & Green, 1978a). The filaments bind to the membrane through the desmosomal plaque (Kelly, 1966). The tonofilament/desmosome interaction is thought to provide structural strength and function to dissipate shearing stresses particulary in sheets of epithelial cells that cover

free surfaces (Sun et al, 1979).

1.3. THE ROLE OF THE CYTOSKELETON IN CELL BEHAVIOUR

The cytoskeleton is a dynamic cytoplasmic matrix which is directly involved in many behavioral activities, but of particular importance to the present thesis are phagocytosis, proliferation and migration of RPE.

1.3.1. The cytoskeleton and phagocytosis

Phagocytosis is the incorporation of large particles into a cell and is a property of many types of cell. Unicellular organisms e.g. amoebae and slime moulds, use phagocytosis to internalise and digest nutrients. Several types of phagocytic cells are present in higher organisms e.g. macrophages, which function to rid the organism of invading pathogens, ageing cells and cellular debris. The RPE cell is also a phagocytic cell and is involved largely in the removal of effete ROSs that have been shed during photoreceptor renewal (see 1.1.1.).

The mechanism of phagocytosis in neutrophils and macrophages is well known (see review by Stossel, 1974a,b,c; 1976; Stossel & Hartwig, 1976). From the research on these cells there is an increasing understanding of the phagocytic processes in the RPE (see 1.1.1.). The process of phagocytosis consists of three stages: recognition, ingestion and digestion. The ingestion stage is particulary significant to this study. Ingestion of the particle occurs in three steps:

i) Induction of pseudopod assembly
ii) Movement of pseudopods around the particle.
iii) Fusion of pseudopod tips at the distal end of the particle.

The three steps of ingestion are crucial to the internalisation of the particle. However, in both macrophages and RPE the mechanism of ingestion remains obscure in that the mechanism by which motive force is generated for internalisation of the particle is undetermined. Stossel applied one hypothesis of cell locomotion to present a model for the induction of pseudopod assembly in macrophages (Stossel, 1976; 1982; Stossel & Hartwig, 1976). The model proposes that step one involves an AMF mediated cytoplasmic extension mechanism, which occurs in the cortical cytoplasm. The cortical cytoplasm, which is located immediately below the plasma membrane of cells, is a dynamic gel and controls structure, shape and movement of cellular margins (early microscopists referred to this area as the hyaline ectoplasm). When the level of free Ca^{2+} ions in the cortical cytoplasm is high, short branching AMFs assemble from the G-actin pool. The AMFs contain gelsolin, an auxiliary protein, which increases the

viscosity in the cortical cytoplasm so forming a "gel", which is capable of flow. Under low free Ca^{2+} ion concentration the short filaments are extended to develop an AMF network and this generates a propulsive force. Thus it is thought that the growing AMF network may push on the plasma membrane forming cytoplasmic protrusions. The tip of the cytoplasm protrusion, or pseudopodium, will have a low Ca^{2+} concentration and so the direction of the filament network assembly will be in the direction of the cytoplasmic protrusion, pushing it further and further outwards. As there are attachments between the plasma membrane and the surface of the particle the pseudopodia are guided around the particle until the tips fuse, enclosing it.

RPE, unlike the motile phagocytes, do not have the advantage of being able to flow around the ingested particle. As described earlier (see 1.1.1.) the RPE is stationary embracing the outer photoreceptor segment with long apical microvilli. Consequently the tip of the ROS (from which effete photoreceptor discs are shed) is at the end of a RPE cytoplasmic corridor and only a short distance away from the body of the RPE cell. The microvilli contain AMFs parallel with the axis of the photoreceptor (Burnside & Laties, 1976; Burnside, 1976) and because AMFs are potentially contractile, it is thought that the microvilli may be involved in the directed movement of the shed ROS disc into the body of the RPE cell. In vitro studies, which have identified actin feltworks associated with attached and internalised ROSs in rat RPE, support the role of AMFs in the ingestion of ROS discs (Chaitin & Hall, 1983b). Furthermore it has been proposed that these contractile AMFs could supply the motive force responsible for internalising the discarded tip of the ROS in situ. The studies of Chaitin & Hall (1983b) support Stossel's model and highlight the importance of AMFs in phagocytic processes.

MTs have also been implicated in phagocytosis. Subplasmalemmal MTs have been localised at ingestion sites in macrophages (Reaven & Axline, 1973). In leucocytes disruption of the MTs with cholchicine and vinablastine impaired ingestion and inhibited degranulation (Stossel et al, 1972; Malawista, 1975). It has been suggested that on the basis that MTs are involved in intracellular transport, in phagocytosis they may bring about the fusion of lysosome and phagosome (Malawista, 1975). In both normal and dystrophic RCS rat RPE, Burnside (1976) identified MTs in the apical cytoplasm often in close association with the phagosome and proposed that these filaments were appropriately disposed to transport phagosomes to sites where they can fuse with lysosomes. However, there has been no direct evidence to support Burnside's proposal and the role of MTs in RPE phagocytosis remains unclear.

In vitro studies on phagocytosis in RPE suggested that AMFs alone may not be responsible for ROS ingestion (Chaitin and Hall, 1983b). The dystrophic RCS rat has a reduced ability to ingest ROSs, which is caused by a defect in the phagocytic mechanism (Edwards & Szamier, 1977), yet there is no difference in the organisation of AMFs between normal and dystrophic RPE (Chaitin and Hall, 1983b). These observations would suggest that in the RCS rat there is either a defect in the receptor recogni-

tion system or that some other factor besides AMFs is involved in the ingestion stage of phagocytosis and that this factor is defective. The role of IFs in cell is unclear (see 1.2.3.) and in the present study the role of IFs in phagocytosis of ROS is investigated.

1.3.2. The cytoskeleton and proliferation

During cell division there is total reorganization of morphology and the cytoskeleton plays a vital role in this reorganisation (Bershadsky & Vailiev, 1988). This role is achieved through the dynamic nature of the cytoskeletal elements.

The MTs undergoes the most complex reorganisation during mitosis. Two polar MTOCs are formed from centrioles and the CMTC and the organised actin structures present within the interphase cell are disassembled. These events are accompanied by cell rounding and is associated with a diffuse actin staining throughout the cytoplasm (Sanger, 1975). Subsequently de novo arrays of MTs assemble from each centriole to form the kinetochores (a specialised MTOC developed around the centromeric region of the chromosome) and mitotic spindle, through which the cellular DNA is divided. Cytoplasmic division or cytokinesis occurs at the end of mitosis.

Cytokinesis is dominated by the AMF system. The actin structures are reorganised to form a ring of microfilaments (cleavage ring) containing myosin, alpha-actinin and filamin, at the cell periphery. The cleavage ring contracts invaginating the plasma membrane and forming a cleavage furrow. The furrow proceeds until the cell is divided into two daughter cells.

The involvement of IFs in mitosis is not understood. Blose (1979) reported that the IFs remain assembled throughout mitosis. However, other research workers consider that IFs reorganise during cell division. It has been suggested that at the onset of cell division the vimentin and cytokeratin IF networks, in many types of cultured cell disassemble (Geiger & Sanger, 1980) or partially disappear and form globular aggregates in the cytoplasm (Franke et al, 1982b; 1984). At the end of mitosis the IF networks reassemble. Further research on two types of epithelial cells has revealed that the vimentin filaments undergo dramatic reorganisation at prometaphase, forming a transient cage-like structure around the developing mitotic spindle (Aubin et al, 1980; Blose & Bushnell, 1982). Aubin et al (1980) also described the disappearance of this cage in metaphase and its replacement by elliptical bands surrounding the chromosomes, suggesting that vimentin filaments may be responsible for spindle and chromosome orientation during mitosis.

Cytokeratin filaments have been identified throughout mitosis and resemble their interphase distribution; since AMFs are disassembled, the cytokeratin filaments are thought to play a structural role (Aubin et al, 1980). In PtK2 cells, cytokeratin filaments

identified with MAB KG 8.13 appear to be masked in interphase cell, but unmasked in these cell during mitosis (Franke et al, 1983). Masking describes a specific immunologic determinant that is hidden from immunologic detection, because of the three dimensional arrangement of IF structure. Selective masking and unmasking of cytokeratin filaments during the cell cycle indicates a cell-cycle dependent re-arrangement of cytokeratin filaments (Franke et al, 1983). Using MAB RGE 53, McKechnie et al (1988) identified a sub-population of cultured human RPE cells that stained positively for cytokeratin 18 and that these positively stained cells were proliferating. The researchers proposed that the association seen between cytokeratin 18 expression and proliferation in RPE cells may be similar to the masking phenomenon described by Franke et al (1983). It is uncertain whether masking has any functional application (Franke et al, 1983).

1.3.3. The cytoskeleton and locomotion

Cell locomotion involves reversible reorganisation of the cytoskeletal elements and is initiated by production of pseudopodia. Pseudopodal formation and cell locomotion have been extensively studied in the fibroblast and so serves as a model for cell locomotion (Abercrombie & Ambrose, 1958; Ambrose, 1961; Ingram, 1969; Abercrombie et al, 1970). In vitro motile cells are polarised and undergo directional movement. Examination of the fibroblast in detail has shown that a moving cell develops an anteriorly ruffled lamellapodium and movement of the cell is in the direction of the lamellapodium. This is a broad flattened sheet of thin cytoplasm attached to the substrate via adhesion plaques and contains a meshwork of AMFs in the cortical cytoplasm. The leading edge of the lamellapodium forms close contacts with the substratum (Izzard & Lochner, 1976) and movement forward is achieved through actin meshworks that expand rapidly and directionally. The expansion is stabilised by the lamellapodium and its contacts with the substrate. The AMF meshworks contract above the close contacts, causing tension and so propelling the cell forward (Ingram, 1969; Couchman & Rees, 1979). Studies using an actin disrupting drug, cytochalasin, have indicated that the actin meshworks are crucial to cell locomotion (Spooner et al, 1971). Other models of cell locomotion suggest that a continuous cytoplasmic flow from front to rear provides the motive force for forward movement (Bretcher, 1984) rather that this actin-adhesion model.

Epithelial and fibroblast cells have different locomotory behaviour. In vitro epithelial cells tend to accumulate into sheets containing relatively immobile cells. The

cells in the sheet are contact inhibited, a phenomenon that can occur in fibroblasts, but is seen readily in epithelial cultures (see rev. Abercrombie, 1980 and Heaysman & Pegrum, 1982). Contact inhibition occurs when the pseudopodal attachments between cells are stabilised as a result of cell-cell contact and it is characterised by contraction of the leading lamella (Abercrombie, 1970). The stability of pseudopodal attachments is the key to mobilisation. Unstable pseudopodal attachments easily detached and result in a cell becoming polarized and motile. Epithelial cells at the edge of a sheet appear to loose contact inhibition and become polarised and motile (Takeuchi, 1987). Using the same contact/actin mechanism seen in motile fibroblasts, epithelial cells at the outer edge of the sheet move forward inducing the cell behind to become motile in its turn. The difference between the motile cells at the edge of the sheet and immobile cells within the sheet may be due to the characteristics of pseudopodal activity (i.e. number, shape and attachment of pseudopodia) or the cytoskeleton (i.e. amounts of AMFs and MTs, and the properties of other cytoskeletal components e.g. cytokeratins).

The role of MTs in cell locomotion is not clear. They appear to stabilise cell shape away from the pseudopodal region. Spooner et al (1971) found that colchicine had no effect on undulating membranes or on net cell movement. Yet, Bershadsky & Vasiliev (1988) demonstrated that disruption of MTs in a polarised fibroblast leads to depolarization, pseudopodal formation from all edges of the cell and loss of directional movement. MTs have also been shown to extend into the leading edge of lamellapodia and be associated with vinculin-containing close contacts (Geiger et al, 1984a). It has been suggested that the MTs play an important role in stabilising the lamellapodia, preventing it from contracting once it has advanced, but more importantly may play a role in the spatial coordination necessary for directional movement.

It is not known whether IFs play any direct role in locomotion although it has been proposed that IFs may have a functional role in cell shape and spreading (Goldman, 1971; Goldman & Knipe, 1972). In contrast microinjection of MABs to induce the collapse of the IF network has indicated that the lack of the IF network had no effect on cell morphology, polarity, or spreading (Lin & Feramisco, 1981). However this work does not seem to have been repeated in other cell systems so the case remains in doubt. It is clear that little research has been done and the obvious question arises if IFs have a limited role in the maintenance of shape, what is that role?.

Cell attachment and cell movement are two interlinked processes and how they interact and respond to the environment is crucial to understanding locomotion. The cell surface is thought to be the major site of transfer of information from the extracellular environment to the cell interior. Glycoprotein recongnising receptors, embedded in the plasma membrane, most likely mediate the process of information transfer. The glycoproteins provide a means through which cells can recognise particular signals in the environment that may modulate cellular metabolism. At points of contact, external ligand molecules are thought to bind to the membrane bound receptors and induce

membrane generated signals near the site of pseudopodal extension or lamellapodal ruffling (Geiger, 1982). The external ligands could be various proteins of extracellular matrix, such as collagen, laminin, fibronectin and vitronectin. The ligands, in particular growth factors, can also interact with cell membrane receptors and in doing so can convert a stationary cell to a motile cell (Gherardi, 1991).

Growth factors can induce two types of movement in cells: either random movement (chemokinesis) or, if present in a gradient, movement in the direction of the gradient (chemotaxis) (Carter, 1965; 1967). A factor that not only directs the locomotion of cell but also induces locomotion is a powerful tool for studying mechanisms that underlie and regulate cell locomotion. The glycoprotein, fibronectin has been shown to be a powerful inducer of chemotactic movement in cells (Poselthwaite et al, 1981; Campochiaro et al, 1984; Calthorpe & Grierson, 1990). Chemotactic movement of cells can be assayed in a simple, rapid and reliable system called the Boyden chamber (microchemotaxis chamber; Falk et al, 1980). Within this system cells migrate down a concentration gradient from the upper surface of a polycarbonate membrane to the lower surface of the membrane. It has been demonstrated that chemoattractant membranes provide an excellent substrate to examine the morphology of migrating and motile cells (Calthorpe & Grierson, 1990). Fibronectin was used in a microchemotaxis chamber to investigate the cytoskeleton in migrating human RPE cells.

1.4. JUSTIFICATION AND AIMS

The cytoskeleton is a major intracellular structure which, either directly or indirectly, is implicated in cell shape and function. The dynamic properties of the cytoskeleton provide the basis for the continuous remodelling of the cytoskeletal organisation in the cell, and reorganisation is crucial for processes such as phagocytosis, cell division and cell locomotion. These processes are either affected or induced in the diseased or pathological state in the RPE. Consequently the RPE of normal and dystrophic RCS rat, bovine and human RPE are ideal models in which to study the involvement of the cytoskeleton in behavioural activities.

The role of AMFs and MTs in phagocytosis, proliferation and locomotion in the main are understood, but the role of IFs in cellular activities remain unclear. The cytokeratin IFs, because of their numerous types and variability of expression in different cell types are the most interesting of the IFs, yet their function is obscure.

The aim of this current study is to:

i) Determine any differences in the cytoskeleton between normal and dystrophic RPE.

ii) To investigate the geometry of the cytoskeleton and the possible roles these filaments play in the phagocytosis of ROS.

iii) To examine the cytoskeletal architecture in normal and dystrophic RPE and the possible role it may play in the inability of the RPE to phagocytose ROS.

iv) To assess the role of IFs in RPE proliferation

v) To study the role of the cytoskeleton in the migratory behaviour of the RPE cells.

CHAPTER 2. MATERIAL & METHODS

2.1. CELL CULTURE

2.1.1. Isolation and culture of primary bovine RPE cells

Bovine RPE cells were isolated using a modification of a technique outlined by Basu et al (1983). Bovine eyes were obtained from the local abattoir between 2-3 hours post-mortem and were used within 1-2 hours of arrival at the laboratory. Extraocular muscles, optic nerve and orbital tissue were removed from the globes before they were immersed in 70% methylated spirit (20 seconds). Globes were then soaked for 10 minutes in sterile Ca^{2+}/Mg^{2+}-free phosphate buffered saline (PBS; Oxoid, Unipath Ltd., Basingstoke, England) containing 100 units of penicillin and streptomycin (Gibco Europe Ltd., Paisley, Scotland).

Under sterile conditions, globes were bisected at the ora serrata and the anterior segment, lens, vitreous and retina were removed and discarded. The interior of the eye cup was rinsed with PBS to remove residual vitreal and retinal debris. Three eye cups were positioned on a petri dish and their optic nerve heads were isolated under plastic cylinders weighted with a Brunswick bottle (Fig. 2.1.). Each eye cup was filled with 4 ml of a mixture of 0.25% trypsin (Difco Laboratories, Detroit, Michigan, USA) and 0.02% tetra-sodium ethylenediaminetetraacetic acid (EDTA; BDH, Upminster, England) in Ca^{2+}/Mg^{2+}-free PBS and incubated for 45 minutes at 37°C. The bovine RPE cells detached from Bruch's membrane with gentle pipetting and formed a cell suspension which was aspirated from the eye cup. Cells were seeded, at a concentration of 8.0 $x10^4$ cells/ml, into 25 cm^2 tissue culture flasks (Sterilin, Stone, U.K.) containing 1 ml of Newborn Calf Serum (NCS, Gibco). Five millilitres of culture medium was added to each flask, which consisted of Eagle's Minimal Essential Medium (MEM), containing 20% Foetal Calf Serum (FCS), 2.5 mg/ml amphotericin B, 100 units/ml penicillin & 100 mg/ml streptomycin and supplemented with 2 mM L-glutamine (all Gibco). The medium was buffered with 2.2 g/L sodium bicarbonate (BDH, Upminster, England).

The cells were kept at 37°C in an atmosphere of 5% CO_2 and 95% air and left for a minimum of one week during which time they adhered to the substrate. Primary cultures were fed twice a week by discarding old medium and adding 5 ml of fresh MEM plus 20% FCS. Feeding continued until cells reached confluence. Confluent primary cultures were passaged, providing sub-cultures of bovine RPE (see 2.1.4.).

Figure 2.1. The system used to isolate bovine RPE. The optic nerve heads in each of three eyecups were covered by plastic tubes (arrow) weighted with a Brunswick bottle.

2.1.2. Isolation and culture of control and dystrophic RCS rat RPE cells

The black-eyed congenic control strain of the RCS rat (RCS-rdy$^+$ p/+) was used as a source of control RPE i.e. RPE cells without retinal dystrophy. Dystrophic RPE cells were obtained from the black-eyed dystrophic strain of the RCS rat (RCS-p$^+$) (LaVail et al, 1975). Rat RPE cells were isolated according to Edwards (1977 & 1981a). Animals were taken between 7-9 days post-parturition, a point where retina/RPE microvilli associations are weak and prior to the first signs of retinal degeneration (Weidman & Kuwabara, 1968; LaVail et al, 1975). Eyes were enucleated from animals within a few minutes of death and stored at 4°C overnight in PBS pH 7.8 containing kanamycin (100 g/ml; Sigma Chemical Co. Ltd., Poole, U.K.) and gentamycin (50 g/ml; Sigma).

Two types of rat RPE cultures were established in this study. One type was monodispersed cultures of RPE cells and the other type of culture consisted of aggregates of RPE cells, named "islands". Monodispersed cultures were formed from a suspension of isolated single cells, whereas islands were formed from RPE isolated as sheets of cells. Both single cells and sheets of cells were isolated from globes using the same enzyme digestion technique, however sheets of RPE were obtained by reducing the incubation time from 45 minutes (for single cells) to 25-30 minutes.

Whole globes, after overnight storage, were incubated from 25-30 or 45 minutes at 37°C in Ca^{2+}/Mg^{2+}-free PBS pH 7.8 containing 1 mg/ml trypsin (Difco) and 70 units/ml collagenase (Sigma). Following enzyme treatment, eyes were kept at 37°C in Ham's F-10 culture medium (Gibco) containing 20% FCS, 2.5 g/ml amphotericin B, 100 units/ml penicillin & 100 g/ml streptomycin, kanamycin (100 g/ml), gentamycin (50 g/ml) and supplemented with 2 mM L-glutamine. The media was buffered with 20 mM N-2-hydroxyethylpiparazine N-1-2-ethanesulfonic acid (HEPES, BDH) and 1.2 g/l sodium bicarbonate (BDH).

Ten eyes were dissected at any one time using a Zeiss dissecting microscope and sterile procedures. An incision was made at the ora serrata with an 20ga corneal/scleral ophthalmic V-lance (1.4 mm, Alcon Laboratories, U.S.A.). The incision was extended circumferentially with fine scissors to remove the anterior segment and lens. The back of the globe was submerged in culture medium for 10 minutes, during which time the neurosensitive retina swelled facilitating its removal. Then the eye cup was transferred to another petri dish containing fresh medium (37°C) for removal of the RPE cells. RPE cells were dislodged from Bruch's membrane by first of all stretching the choroid between two forceps, then grasping the optic nerve head and shaking the eye cup vigorously. Most of the RPE was removed in this way, any RPE that remained were teased from the choroid with fine forceps. Single RPE cells or sheets of cells settled to the bottom of the petri dish. These were collected using a pipette and seeded onto 13 mm glass coverslips (pre-coated with FCS) placed in the wells of a 24 well plate (Sterilin). Cells were allowed to settle for 20 minutes before 2-3 ml of Ham's F-10

culture medium (described above) was added. Cultures were maintained at 37°C in 5% CO_2 and 95% air. Cells settled and attached after 48 hours. Rat RPE adhered to the substrate by about 4-5-days. Subsequently fresh medium was added to growing cells every 3rd day until cells had reached confluence, at which point they were used in experiments.

2.1.3. Isolation and primary culture of human RPE cells

Donor eyes from Moorfields Eye Hospital eye bank were obtained up to but not beyond 48 hours post mortem. Age of donors ranged from 6 months to 82 years old. RPE cells were isolated from these eyes following the procedures outlined by Edwards (1981b) and using the modifications described by Boulton et al (1982). Endogenous microorganisms were reduced by soaking the globe for 10 minutes in PBS containing 100 units of penicillin and streptomycin. Subsequently the anterior segment, iris and lens were removed and the vitreous was dislodged by gently shaking the inverted eye cup. The neural retina was teased away from the RPE and the exposed RPE was washed with Ca^{2+}/Mg^{2+}-free PBS (37°C) containing 0.02% EDTA to remove adherent photoreceptor debris.

The posterior eye cup was dissected into three segments and areas of the RPE were isolated by brass cloning rings (Boulton et al, 1982). The RPE were incubated at 37°C for 45-60 minutes, but no more than 90 minutes, in a mixture of 0.25% trypsin and 0.02% EDTA in Ca^{2+}/Mg^{2+}-free PBS. Dissociated RPE cells were aspirated from Bruch's membrane and seeded into 25 cm^2 tissue culture flasks containing 1 ml of FCS. Cell were allowed to settle for 10 minutes before adding 5 ml of Ham's F-10 culture medium containing 20% FCS, 2.5 mg/ml amphotericin B, 100 g/ml streptomycin, supplemented with 0.003 g/ml glucose (BDH) and 2 mM L-glutamine and buffered with 1.17 g/ml of sodium bicarbonate. Cultures were maintained at 37°C in an atmosphere of 95% air and 5% CO_2.

Primary cultures were fed twice a week until confluent, at which point they were passaged and sub-cultures provided the cells for future investigation (see 2.1.4.).

2.1.4. Passaging and sub-culture of RPE cells

Rat RPE failed to survive passaging and were therefore used only at primary culture. Both bovine and human RPE cells could be passaged successfully numerous times, therefore sub-cultures of these two species of RPE were used in this study.

When RPE cells reached confluence they were passaged as follows. The culture medium was discarded and cells were washed with warmed Ca^{2+}/Mg^{2+}-free PBS (37°C)

to remove any residual medium. Cells were then trypsinised. To each flask 2 ml of 0.25% trypsin and 0.02% EDTA (disodium salt) in Ca+/Mg+-free PBS was added for no more than 2 minutes and immediately neutralised using serum to minimise damage to cell membranes. Trypsinisation disrupted cell-substrate attachments releasing the cells into suspension. The cells were then seeded into fresh tissue culture flasks containing 1 ml of NCS and maintained with 5 ml of culture medium (i.e. bovine: MEM containing 15% NCS; human: F-10 containing 20% FCS) in an atmosphere of 5% CO_2 at 37°C. Both bovine and human RPE cells were passaged at a split level of one to three.

In this study bovine and human RPE cells were also grown onto 13 mm glass coverslips, coverslips with gold grids (for TEM of whole cells), and in 4-chambered and 8-chambered tissue culture slides (LabTeks, NUNC Inc, USA). Coverslips were contained in a tissue culture petri dish (Sterilin). Confluent cells were trypsinised, then mixed with 8 ml of warm culture medium (i.e. containing serum), before being pelleted in a centrifuge (Centaur 1, MSE, England) at 800 r.p.m. for 10 minutes. The pellet was resuspended in 1 ml of warm culture medium and cells were counted using a haemocytometer. Serum (bovine: NCS; human:FCS) was added to the flasks (25 cm^2:1 ml), coverslips (0.5 ml), or each chamber of a LabTek slide (4-chambered, 0.2 ml; 8-chambered, 0.1 ml) before they received cells. The RPE cells were seeded at a concentration 7.5 $x10^3$ cells/cm^2.

2.2. MORPHOLOGY

2.2.1. Light microscopy

The morphology and growth of living bovine, rat and human RPE cells in culture were routinely observed using an inverted phase-contrast light microscope (Diaphot, Nikon, Japan). This type of microscope utilises the presence of different refractive indices in various regions of the cell. It enhances the contrast of these regions through the interference effect of two out-of-phase waves allowing visualisation of unstained cells.

The morphology and features of fixed and stained cells were examined using bright field and differential interference contrast (DIC) microscopy (Polyvar, Reichert-Jung, Austria). Cultured cells, that had been stained for cytoskeletal elements using the immunoperoxidase staining technique (see 2.3.4 & 2.3.7), were examined using bright field microscopy.

DIC or Nomarski optics, like phase-contrast, is a type of interference microscopy. However, DIC uses polarized light to reflect changes in regional densities within the cell and presents a 3-dimensional image of the cell. DIC microscopy was used to

observe both stained and unstained cells.

2.2.2. Scanning electron microscopy

Scanning electron microscopy (SEM) allows the surface of unsectioned cells or other specimens to be viewed at a wide range of magnifications. A beam of electrons is scanned (raster) over the specimen and electrons that are scattered (secondary electrons) are detected to give a 3-dimensional image of the specimen. Surface morphology of cultured RPE cells, isolated ROSs, and cells on migration membranes were investigated using SEM. For cultured cells the culture medium was discarded and cells were washed in warmed (37°C) PBS before processed for SEM.

Specimens were fixed in 2.5% glutaraldehyde (EM grade vacuum distilled Fisons Polaron, Loughborough, U.K.) in Sorenson's phosphate buffer (SPB) pH 7.4, 304 mOsmols for 1 hour (primary fixation). The tissues or cells were then washed in 3 changes of SPB (15 minutes per change) before being post-fixed for 1 hour in 1% osmium tetroxide buffered with SPB (secondary fixation). Post-fixed specimens were washed once in SPB for 15 minutes, then 3 times in distilled H_2O (10 minutes each change), before dehydrated through a graded series of ethanol (AnaLar grade, BDH) solutions of 30%, 50%, 70%, 85%, 95%, and 3 times 100%. Subsequently the specimens were critical point dried (Polaron, Hemel Hempstead, U.K.) and mounted on metal stubs with either double-sided adhesive tape or silverdag (Bio-Rad, Hemel Hempstead, U.K.). Finally mounted specimens were gold coated (approx. 12-16 nm thickness) using a Polaron sputter coater before being viewed in an Hitachi S-520 scanning electron microscope (Hitachi, Tokyo, Japan) using secondary electron detection.

2.2.3. Transmission electron microscopy

Transmission electron microscopy (TEM) was required for viewing whole cells and thin sections of tissue and cultured cells. TEM is used for viewing thin sections of tissue and cells at high magnifications. The specimen is exposed to a beam of electrons and the image obtained is dependent on the absorption of incident electrons by various molecules in the preparation.

Primary and secondary fixation of specimens for TEM was the same as that described for SEM (see 2.2.3.). Following the post-osmication buffer wash the specimens were washed in 3 changes of distilled H_2O (10 minutes each change) before being dehydrated through the same series of graded ethanol solutions used for SEM. After the third change of 100% ethanol the specimens were subsequently embedded in Araldite resin (Agar Scientific). Specimens were exposed to 2 changes of 100% propylene oxide

(15 minute each change), then for 2 hours each in 75%:25%, 50%:50% and 25%:75% propylene oxide:Araldite resin, respectively. Finally the specimens were left for 24 hours in 100% Araldite for maximum infiltration, then placed in fresh resin and polymerised at 60°C for 24 hours. The blocks were allowed to cure for 1-2 days before cutting.

Ultrathin sections (50-70 nm) were cut with an Ultracut E (Reichert-Jung, Milton Keynes, U.K.). The sections were flattened with chloroform, collected on 200 mesh copper grids (3.05 mm, Bio-Rad) and stained for 15 minutes with 1% uranyl acetate. Grids were then rinsed in distilled H_2O and stained in 0.4% Reynolds lead citrate for 6-7 minutes, followed by another rinse in distilled H_2O and then dried overnight. Sections of tissue were viewed in an Hitachi H-600 transmission electron microscope.

For TEM of whole cultured cells, the cells were grown until they formed a monolayer in the flask. Then the culture medium was discarded, the cells were washed in warmed PBS (37°C), before being fixed and processed for TEM as described above with one modification. After the third change of 100% ethanol propylene oxide was added to the flask for one minute. The propylene oxide dissolved the plastic, releasing the cultured cells as a complete sheet. The sheet was taken from the flask and any residual plastic was removed by washing in several changes of fresh 100% propylene oxide. Then the cells were embedded in Araldite as described above.

RPE were grown on gold grids for TEM of whole cells. The gold grids (3.05 mm square mesh, Bio-Rad) were coated with a 70 nm thin film of formvar plastic (from a 0.5% w/v solution of formvar in ethylene dichloride) and mounted on 13 mm glass coverslips (3 grids per coverslip). The gold grids with their formvar support film were given a fine coating of carbon (10-20 nm thick) to provide a desirable surface for cell growth and to add strength to the formvar. Gold grids were sterilised using ultra-violet light (245 nm) for 24 hours, before being placed on the base of tissue culture petri dish (see 2.1.4.). The RPE cells were grown to pre-confluence, before being processed for TEM as described above. However, whole cells were stained with 1% uranyl acetate in 25% ethanol for 15-20 minutes during the alcohol dehydration step. After dehydration in graded ethanol the cells were critical point dried, coated with carbon, and viewed in an Hitachi H-600 transmission electron microscope.

The carbon coat stabilises the formvar under the electron beam by dissipating electron charge build-up, this prevents the formvar heating up and splitting. The carbon coat also provides some contrast to the specimen. Cells were viewed using conventional transmission imaging in a Hitachi H-600 electron microscope.

2.2.4. Rhodamine 123 staining of mitochondria in bovine and human RPE cells.

The morphology of the mitochondria of living RPE cells were visualised using the fluorescent dye rhodamine 123 (Addai & Ockleford, 1986). Bovine and human RPE cells were grown to pre-confluence on 8-chambered LabTeks (see 2.1.4.). The culture medium was discarded and the cells were incubated for 20 minutes, at 37°C, in culture medium containing rhodamine 123 (10 g/ml; Sigma). Cells were then washed with warm PBS, before immediately mounted with water and viewed using epi-fluorescent optics (Polyvar).

2.3. CYTOSKELETON.

2.3.1. Preparation of fresh tissue for frozen sections

Bovine and human eyes were dissected as described earlier (see 2.1.1. & 2.1.3.) and a 3 cm^2 section of sclera with intact choroid, RPE and neural retina was cut from the eye cup. The choroid/RPE/retina complex was released from the sclera using fine forceps and embedded in OCT Compound (Raymond A Lamb, London, U.K.), before being quick frozen in liquid nitrogen. Control and dystrophic RCS rat eyes were enucleated, punctured at the ora serrata with an ophthalmic lance, embedded in OCT and frozen in liquid nitrogen.

Cryostat sections of frozen tissue were collected on glass microscope slides and stored at -20°C.

2.3.2. Preparation of fresh rat RPE cells for immunohistochemistry

Fresh RPE cells, isolated from the eye cup as described earlier (see 2.1.2), were suspended in PBS (pH 7.2, 37°C) containing 15% NCS and were centrifuged for 10 minutes at 800 rpm. The serum was removed by washing the cells twice with warm PBS and then the final cell pellet was resuspended in 1 ml of PBS. The cells were air dried onto microscope slides which had been coated with 1% normal goat serum (NGS; Sigma). The slides were stored at -20°C and when the cells were required they were rehydrated in PBS, before being processed for indirect immunofluorescence (see 2.3.4.).

2.3.3. Fixation of cultured cells.

The culture medium was discarded and the cells were washed with warm PBS. The cells were fixed for 5 minutes in pre-cooled methanol (-20°C) followed by pre-cooled acetone for 2 minutes (-20°C). The cells, grown on plastic substrate (i.e. flasks) were fixed in pre-cooled methanol for 7 minutes. After fixation the RPE were air dried and then either used immediately for immunocytochemistry or stored at -20°C until required. The cells that were frozen were rehydrated in PBS for 5 minutes before being processed for immunocytochemistry.

2.3.4. Immunocytochemical staining techniques

Three types of immunocytochemical staining procedures were used in the present thesis and these were **indirect immunofluorescence, indirect immunogold/silver** and **indirect immunoperoxidase**.

Essentially immunocytochemical staining involved two steps. First of all the antigen was labelled with a primary antibody, which was either a monoclonal antibody (MAB) or an antiserum. Then the primary antibody was labelled with a secondary antibody, which in turn was conjugated to either a fluorochrome (immunofluorescence), colloidal gold (immunogold/silver) or horseradish peroxidase (HRP, immunoperoxidase). The secondary antibody was raised to the immunoglobulin of the species in which the primary antibody had been developed. Two types of fluorochromes where used in this study fluorocein isothyiocyanate (FITC) and tetramethylrhodamine isothyiocyanate (TRITC).

For immunofluorescence and immunogold/silver staining, cells or tissue was incubated for 10 minutes in 1% NGS in PBS (pH 7.5) before being incubated in the primary antibody. This reduced background fluorescence and prevented false positive staining. For immunoperoxidase specimens were incubated for 20 minutes in 1% hydrogen peroxide solution followed by a wash in tap water, before being incubated in 1% NGS for 20 minutes. The primary and secondary antibodies were diluted to their appropriate titre (as recommended by the manufacturer or as determined in the laboratory) using 1% NGS in PBS. The primary antibody was applied to the specimen for 45 minutes, then the specimen was washed for 5 minutes with 3 changes of PBS before the secondary antibody was applied for a further 45 minutes. The specimen was washed and, for immunofluorescence, immediately mounted under a glass coverslip using fluorostab (Euro-Diagnostics BV, Holland). For immunogold/silver, the tissue was then processed for silver enhancement of the gold labelled tissue according to the manufacturers instructions (Janssen Pharmaceuticals, Middlesex, U.K.). The peroxidase labelled specimens were incubated in 3% hydrogen peroxidase and either aminoethyl-carbazole

(AEC see Appendix I.) or 3,3'-diaminobenzidine tetrahydrochloride (DAB see Appendix I.). The incubation resulted in either a red (AEC) or brown/black (DAB), insoluble polymeric oxidation product in association with the antigenic sites.

Immunofluorescent stained specimens were viewed in a Polyvar 111 microscope equipped for epi-fluorescence (Polyvar, Reichert-Jung). Immunogold/silver stained specimens were detected using epi-polarization illumination (Polyvar) and immonoperoxidase stained specimens were viewed by bright field microscopy.

Negative controls were obtained by incubating tissue with 1% NGS instead of a primary antibody. Absorption controls were not undertaken, because purified antigen of either bovine ROSs or cytoskeletal elements were not readily available. However, using immunoblotting the commercial anti-cytoskeleton MABs that were used in this study did appear to identify the proteins specified in the data sheet. The specificity of the cytokeratin antibodies used in this study was investigated and reported by McKechnie et al, 1988.

2.3.5. Detergent extraction of whole cells

Cells grown to pre-confluence on formvar coated gold grids were extracted with Triton-X 100 detergent (Schilwa & van Blerkom, 1981). The cells were washed in warmed PHEM buffer pH 6.9, consisting of 60 mM piperazine 1,4 diethylsulfonic acid, 25 mM HEPES, 10 mM ethylene glycol-bis(-aminoethyl ether), 2 mM $MgCl_2$ and 120 mM KCl, before being prefixed in fresh 1% paraformaldehyde in PHEM for 5 minutes at 4°C. Extraction was in chilled PHEM (Bell, 1981) buffer containing 0.15% triton-X 100 for 1-1.5 minutes. The extracted RPE were then fixed in 1% glutaraldehyde in PHEM for 1 hour (Schilwa & van Blerkom, 1981). Following fixation, the extracted cells were washed in PHEM buffer pH 6.9, at room temperature before being post-fixed in 0.5% osmium tetroxide in PHEM for 1-2 minutes. The extracted cells were then processed for TEM exactly the same as whole cells and viewed in an Hitachi H-600 transmission electron microscope.

2.4. ROD OUTER SEGMENTS.

2.4.1. Isolation of bovine ROSs

Bovine retinae were the source of photoreceptor outer segment material used to challenge the RPE cells. Rod outer segments (ROSs) were isolated according to Papermaster (1982). As little mechanical or chemical damage as possible was ensured

by strictly adhering to the recommended values for the ionic strength, composition and osmolarity of all the solutions required in the isolation. In addition light damage was prevented by isolating the ROSs under reduced light and wrapping the tubes containing ROS preparations in aluminium foil. The ROSs were prepared under sterile conditions, all solutions were passed through a 0.2 μm mesh filter (Sartorius Instruments, Ltd., Surrey, U.K.) and chilled on ice.

Twenty bovine eyes at a time were dissected as described earlier (see 2.1.1.). The retinae were removed and placed in 10 ml of chilled sucrose homogenising medium (see Appendix II.) and homogenised using a Uni-Form PTFE pestle running in a glass body with a volume capacity of 15 ml and a gap of 0.126 mm (Jencons (Scientific) Ltd., Leighton Buzzard, U.K.). The pestle was passed 3 times in the body of the homogeniser. The homogenate was centrifuged at 40000 r.p.m for 4 minutes then the supernatant, containing the ROSs, was decanted into a pre-chilled 100 ml glass bottle and stored on ice for 5 minutes.

One molar tris-acetate buffer (see Appendix II.) was carefully added to the supernatant until the volume of the supernatant had tripled. The buffer and supernatant were gently mixed then centrifuged at 4000 r.p.m. for 4 minutes. The resulting pellet contained the ROSs, both the pellet and the supernatant were stored in ice for 10 minutes before the supernatant was decanted and discarded. All the ROS pellets were resuspended and pooled with 0.5 ml of 0.77 M sucrose solution (Density: 1.10 g/ml, see Appendix II.) prior to being layered on top of a sucrose gradient.

Sucrose gradients were prepared in 50 ml high speed centrifuge tubes using a cannula. Firstly, 7 ml of 0.84 M sucrose solution (density: 1.11 g/ml, see Appendix II.) was slowly injected through the cannula followed by 9 ml of 1.0 M sucrose solution (density: 1.13 g/ml, see Appendix II.) and then 9 ml of 1.14 M sucrose solution (density: 1.15 g/ml, see Appendix II.) to create sucrose solutions with a greater density at the bottom of the tube. The ROS suspension was layered on top of the 0.84 M sucrose solution and the sucrose gradients were centrifuged for 30 minutes, at 40,000 g, in an angle rotor (350°) using a Suprafuge 22 (Heraus, Brentwood, U.K.).

The ROSs formed two bands after centrifugation, one at the interface of 1.11/1.13 g/ml sucrose solutions and the other at interface of the 1.13/1.15 g/ml sucrose solutions. Retinal debris formed a pellet at the bottom of the tube. The ROSs were carefully aspirated from each band and either used immediately for phagocytic challenge or stored over night in 1.11 g/ml sucrose solution (0.84 M) at 4°C in the dark and used the next day. The ROSs were pelleted from the sucrose by diluting with an equal volume of 10 mM tris-acetate buffer then centrifuged at 10,000 g for 5 minutes. The final ROS pellet was resuspended into 1 ml of MEM or PBS supplemented with 2.5% sucrose, which reduces ROS swelling without interfering with ROS attachment (Mayerson & Hall, 1986).

2.4.2. Air dried ROSs

The ROSs were isolated as described earlier (see 2.4.1.). The final ROS pellet was resuspended in 1 ml of PBS containing 2.5% sucrose and ROSs were air dries on microscope slides pre-coated with 5% NGS. The slides were stored at -40°C until required.

2.5. PHAGOCYTOSIS

2.5.1. Phagocytic challenge of cultured RPE cells with bovine ROSs

Cultures of bovine and rat RPE cells were grown on either 4-chambered LabTek (bovine) or 13 mm glass coverslips (rat) as described in sections 2.1.4. and 2.1.2, respectively. For SEM, bovine RPE were grown on 13 mm coverslips. When the RPE cells reached confluence they were challenged with bovine ROSs. ROSs were isolated from bovine retinae as described earlier (see 2.4.1.) and the final pellet of ROSs was resuspended in 1 ml of serum-free culture medium (bovine: MEM; rat: Ham's F-10) containing 2.5% sucrose. The number of ROSs in the suspension was counted using a haemocytometer and then diluted to give a concentration of 1.88 $x10^7$ ROSs/ml. This concentration gave an optimum ROSs settlement rate of 5 x 10^5 ROSs/cm^2/hour. LabTeks and coverslips on which RPE were growing were overlaid with 0.8 ml and 1 ml, respectively of growth medium containing ROSs at the optimum concentration (7.5 million ROS/cm^2). Initially the cells were challenged for various time intervals. Following challenge, the cells were washed several times in warmed PBS (37°C) before attached and internalised ROSs were visualised using an indirect double immunofluorescent labelling technique (see 2.5.2.). The specimens were either viewed using a Polyvar 111 microscope or processed for SEM in the conventional manner and viewed in a Hitachi S520 (see 2.2.3.).

For each chamber of a LabTek (bovine) and for each coverslip (rat) the number of ROSs and cells were counted in 10 microscopic fields under the x40 oil immersion lens of the Polyvar light microscope.

2.5.2. Indirect double immunofluorescent staining of cultured RPE cells challenged with ROSs

A modification of an indirect double immunofluorescent technique developed by Chaitin & Hall (1983a) was used to visualise ROSs attached to the cell surface and

ROSs that had been internalised by the cell. Essentially the technique consisted of two parts. The first part was conducted on unfixed cells and only labelled ROSs on the outside of the cells (as these cells were live all the solutions were warmed to 37°C). The second part of this staining technique was conducted on fixed cells. Fixation perforated the membrane of the cell and through these openings antigenic sites inside the cell were accessible. Thus internalised ROSs were labelled. The procedure was as follows:-
1) The culture medium was discarded, cells were washed in PBS and then exposed to 1-2% paraformaldehyde in PBS for 10 minutes. The cells were washed once more before being exposed to 1% NGS in PBS for 10 minutes. Following this the cells were incubated for 30 minutes with a monoclonal antibody (MAB) to ROS, named 1F4 (for details of this MAB see 3.3.1.), which was diluted 1:2 with 1% NGS in PBS. Thereafter the cells were washed and then incubated for a further 30 minutes in a goat anti-mouse IgG conjugated to TRITC and finally washed once more.
2) The cells were methanol/acetone fixed (see 2.3.3.) and then washed before being incubated for 10 minutes 1% NGS in PBS. Then the cells were incubated for 45 minutes in MAB 1F4, before being washed and incubated for another 45 minutes in goat anti-mouse IgG conjugated to FITC. Then the cells were mounted with fluorostab and viewed using a Polyvar 111 microscope with epi-illumination optics.

In the first part of the staining procedure, ROSs that had been attached to the surface of the cells were labelled with the fluorescent probe TRITC. ROSs stained in this way, fluoresced red when the cells were illuminated with green light (550 nm). While in the second part of the staining procedure, both attached and internalised ROSs were labelled with the FITC probe and fluoresced green when illuminated with blue light (495 nm).

2.5.3. Indirect double immunofluorescent staining of cultured rat RPE cells: cytokeratin 18 (K18) and ROS challenge

Rat RPE cells were methanol/acetone fixed as described previously (see 2.3.3.) following challenge with ROSs. Fixed cells were incubated in 1% NGS in PBS for 10 minutes and then for 45 minutes in a cocktail of MABs including 1F4 and RGE 53 (Bio-nuclear Services, Cornwall, U.K.) The latter is a MAB against an intermediate filament called cytokeratin 18. After the incubation the cells were washed in PBS and then incubated for a further 45 minutes in a cocktail of secondary antibodies consisting of anti-mouse IgG FITC conjugate, and anti-rabbit IgG TRITC conjugate. Then the cells were washed once more before being mounted with fluorostab and viewed with epi-illumination optics (Polyvar 111 microscope).

In the staining procedure the ROSs (labelled with FITC) fluoresced green when illuminated with blue light, and the cytoskeletal elements (labelled with TRITC) fluo-

(BrdU+/K18+, BrdU+/K19+), positive for BrdU and negative for K18 or K19 (BrdU+/K18-, BrdU+/K19-), negative for BrdU and positive for K18 or K19 (BrdU-/K18+, BrdU-/K19+), and negative for BrdU and K18 or K19 (BrdU-/K18-, BrdU-/K19-). The number of cells in each group were counted in 15 microscopic fields from 8 chambers of a LabTek, under x40 objective (Polyvar).

2.6.2. Proliferating cell nuclear antigen (PCNA) and K18 staining of cultured cells

PCNA is a nuclear antigen that begins to accumulate in the G1 phase of the cell cycle, is most abundant during S-phase and declines during the G2/M phase (Tan et al, 1987; Kurki et al, 1988). It is also a marker of cell proliferation, however stains more than the S-phase of the cell cycle.

Human RPE cells were prepared and fixed in the same way as for BrdU (2.6.1.). However, for PCNA there was no need to incubate the cells in a proliferation marker prior to fixation. PCNA was detected in proliferating cells using the MAB, anti-PCNA (25 g/ml; Boehringer Mannheim Biochemica, Germany). Labelled nuclei were visualised using the avidin/biotin indirect immunoperoxidase staining (see 2.3.4.). After the PCNA staining the specimens were then stained for cytokeratin 18 in the same way as with BrdU (see 2.6.1.).

Cells were divided in four groups, PCNA+/K18+, PCNA+/K18-, PCNA-/K18+, PCNA+/K18- and the number of cells in each group were counted in 15 microscopic fields from 8 chamber of a LabTek, under x40 objective (Polyvar).

2.6.3. Growth curve and K18 staining of cultured cells

Confluent cultures of human RPE were trypsinised and seeded onto either LabTek slides or tissue culture flasks as described previously (see 2.1.4.). Cells were cultured up to 72 hours and growth curves were established by counting the number of cells at 12 hour time intervals. At each time interval cells were methanol/acetone fixed (see 2.3.3.) before being labelled for K18 using MAB RGE 53 (Bio-nuclear Services) and stained using immunoperoxidase staining procedure (see 2.3.4.). Using a combination of bright field microscopy (for K18 labelled cells, which were stained red when developed in AEC) and DIC microscopy (for unstained cells), the number of cells and the number of cells positive for K18 were counted in a total of 120 fields per LabTek or flask (15 fields/8-chambered LabTek and 120 fields/8 cm^2 area in each flask (representative of the total area of a LabTek)) using x40 objective (Polyvar).

(BrdU+/K18+, BrdU+/K19+), positive for BrdU and negative for K18 or K19 (BrdU+/K18-, BrdU+/K19-), negative for BrdU and positive for K18 or K19 (BrdU-/K18+, BrdU-/K19+), and negative for BrdU and K18 or K19 (BrdU-/K18-, BrdU-/K19-). The number of cells in each group were counted in 15 microscopic fields from 8 chambers of a LabTek, under x40 objective (Polyvar).

2.6.2. Proliferating cell nuclear antigen (PCNA) and K18 staining of cultured cells

PCNA is a nuclear antigen that begins to accumulate in the G1 phase of the cell cycle, is most abundant during S-phase and declines during the G2/M phase (Tan et al, 1987; Kurki et al, 1988). It is also a marker of cell proliferation, however stains more than the S-phase of the cell cycle.

Human RPE cells were prepared and fixed in the same way as for BrdU (2.6.1.). However, for PCNA there was no need to incubate the cells in a proliferation marker prior to fixation. PCNA was detected in proliferating cells using the MAB, anti-PCNA (25 g/ml; Boehringer Mannheim Biochemica, Germany). Labelled nuclei were visualised using the avidin/biotin indirect immunoperoxidase staining (see 2.3.4.). After the PCNA staining the specimens were then stained for cytokeratin 18 in the same way as with BrdU (see 2.6.1.).

Cells were divided in four groups, PCNA+/K18+, PCNA+/K18-, PCNA-/K18+, PCNA+/K18- and the number of cells in each group were counted in 15 microscopic fields from 8 chamber of a LabTek, under x40 objective (Polyvar).

2.6.3. Growth curve and K18 staining of cultured cells

Confluent cultures of human RPE were trypsinised and seeded onto either LabTek or tissue culture flasks as described previously (see 2.1.4.). Cells were cultured up to 72 hours and growth curves were established by counting the number of cells at 12 hour time intervals. At each time interval cells were methanol/acetone fixed (see 2.3.3.) before being labelled for K18 using MAB RGE 53 (Bio-nuclear Services) and stained using immunoperoxidase staining procedure (see 2.3.4.). Using a combination of bright field microscopy (for K18 labelled cells, which were stained red when developed in AEC) and DIC microscopy (for unstained cells), the number of cells and the number of cells positive for K18 were counted in a total of 120 fields per LabTek or flask (15 fields/8-chambered LabTek and 120 fields/8 cm^2 area in each flask (representative of the total area of a LabTek)) using x40 objective (Polyvar).

2.7. MIGRATION

2.7.1. Migration of human RPE cells

A 48-well micro chemotaxis chamber (Neuro Probe, Cabin John, USA) was used to study the migration of human RPE cells (Fig. 2.2.). Principally a chamber consisted of a series of upper and lower wells in register. A chemoattractant was placed in the lower wells, and cells were placed in the upper wells. Sandwiched between these wells was a polycarbonate membrane perforated with 10 μm diameter pores (as determined from preliminary experiments the 10 μm pores were an optimum size for epithelial cell to pass through). The chamber was incubated for 5 hours under normal culture conditions during which time the cells settled onto the upper surface of the membrane and migrated through the pores to the lower surface of the membrane. Cells on the lower surface were counted in 20 high-power fields (x 1000) per well using conventional bright field microscopy (Zeiss, Germany) which gave an index of migratory ability.

Polyvinylpyroldone (PVP) gelatin coated polycarbonate membranes were used for all migration assays (Calthorpe & Grierson, 1990). PVP membranes were coated in gelatin as follows. Membranes were placed into a 0.5% solution of acetic acid at 60°C for 20 minutes, then washed twice in distilled water before immersed for 1 hour in 500 mls of boiling distilled water containing 0.5 mls of a 5 mg/ml solution of type 1 porcine gelatin of 300 bloom (Sigma). Then the membranes were air dried before being dried for 1 hour at 100°C.

To conduct migration assays, the chamber was dismantled into its component parts and 27 μl of chemoattractant, diluted in serum-free culture medium was placed into the lower wells. Bovine fibronectin (Sigma) was used as the chemoattractant, because previous studies had shown that it was a potent inducer of human RPE migration (Campochiaro et al, 1984). The optimum dose was calculated from a dose response curve (see 2.7.2. & 3.5.1). The gelatin coated membrane was placed on top of the lower wells, followed by a gasket and then the upper chamber was secured in place with six screws. The upper wells were covered with a glass slide to prevent evaporation while the chamber was allowed to equilibrate at 37°C.

Human RPE cells between 5th and 7th passage were used for the migration assays. Confluent cultures of RPE cells were trypsinised, as described earlier (see 2.1.4.) and diluted with Ham's F-10 culture medium containing 50% FCS. The cell suspension was centrifuged for 10 minutes at 800 r.p.m. then the pellet was resuspended in serum-free Ham's F-10 medium and centrifuged as before. The washing procedure was repeated once more until finally, the RPE were resuspended in 1 ml of medium and counted in a Coulter counter (Coulter Electronics, Luton, U.K.). A volume of 50 μl of serum-free medium containing 80,000 RPE cells was placed into the upper wells of the

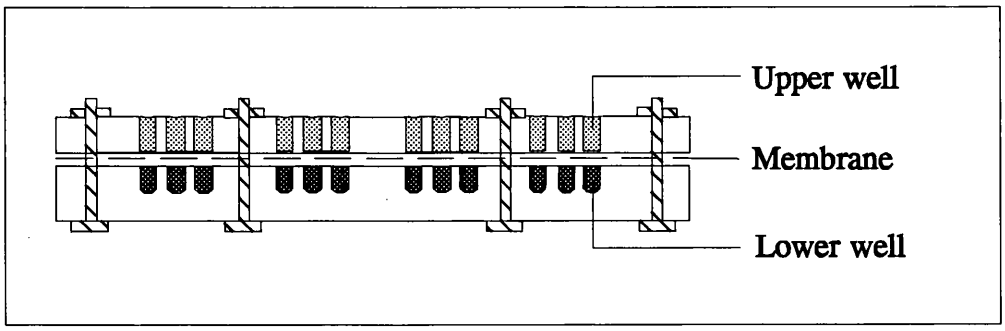

Figure 2.2. A cross-section of a 48-well micro chemotaxis chamber as used for the migration assays.

micro chemotaxis chamber. The apparatus was incubated for 5 hours at 37°C in 95% air and 5% CO_2 and then it was dismantled. The membrane was removed and fixed according to the treatment outlined in section 2.7.4.

2.7.2. Fibronectin dose response curve for migrating human RPE cells

The optimum dose of fibronectin that induced maximum migration of human RPE cells was determined using the micro chemotaxis chamber described previously (see 2.7.1.). Fibronectin was diluted with Ham's F-10 medium and a range of concentrations from 0 to 50 μg/ml was added to the lower wells. At the end of the assay the membrane was fixed in ethanol for 30 seconds then air dried before being immersed in haematoxylin for 30 minutes. Following destaining in cold tap water, the membrane was mounted in aqueous mount (IMMUNO-MOUNT, Shandon Scientific Ltd., UK), viewed and counted as described in 2.7.1.

2.7.3. SEM of migration membranes

Membranes with migrated human RPE cells (see 2.7.1.) were washed twice in PBS to remove any culture medium. Then the cells were fixed in 2.5% glutaraldehyde in SPB for 4 hours. The specimens were processed for SEM as described previously (see 2.2.3.). The membranes were orientated on stubs so that both the upper and lower surfaces could be examined on the same specimen in a Hitachi S520 scanning electron microscope.

2.7.4. Indirect immunofluorescent staining of the cytoskeleton in human RPE cells on a migration membranes

Human RPE migration assays were conducted using the micro chemotaxis chambers described above (see 2.7.1.). The membranes were fixed in methanol (-20°C) for 7 minutes and air dried. The membranes were immersed for 5 minutes in PBS then incubated for 10 minutes in 5% NGS in PBS, before being incubated in primary antibody. The primary antibodies used were anti-actin (clone C4, 1:100, ICN Biomedicals Ltd., High Wycombe, U.K.), anti-beta-tubulin (clone TUB 2.1, 1:100, ICN Biomedicals Ltd.), anti-vimentin (clone VIM 13.2, 1:100, Sigma), anti-cytokeratin 18 (clone RGE 53, 1:20, Bio-nuclear Services Ltd.) and anti-cytokeratin 19 (clone K4.62, 1:20, ICN Biomedicals Ltd.). As cells on both sides of the membrane were of interest, the upper side of the membrane was incubated for 30 minutes in primary antibody then

the membrane was turned over and the lower side of the membrane was exposed to primary antibody (30 minutes). The double exposure was followed by 3 washes in PBS. Then the membranes were incubated for 30 minutes each side in secondary antibody (anti-mouse IgG conjugate to FITC (1:40, Sigma)). Finally the membrane was washed, mounted under a coverslip with Fluorostab and observed using epi-fluorescence (Polyvar).

Immunofluorescent labelled cells on both the upper and lower sides of the membrane were counted in 20 high-power fields/well under the x40 oil immersion lens (Polyvar). Then the membranes were counter stained with haematoxylin as described previously (see 2.7.2.) and cell nuclei were counted in the same manner as the immunofluorescent cells.

2.7.5. Indirect immunoperoxidase staining of K18 and K19 in human RPE cells on a migration membrane

Migration assays were conducted with human RPE cells using the micro chemotaxis chamber (see 2.7.1.). Cells were fixed and labelled for K18 and K19 as described in the previous section (see 2.7.4.) however the secondary antibody was an anti-mouse IgG peroxidase conjugate (1:50 DAKO). Labelled cytokeratin filaments were stained red using AEC (see 2.3.4.). The cells were counter stained with haematoxylin (see 2.7.2.), before being mounted and viewed by light microscopy (Polyvar). The cells on the both sides of the membrane were counted in 20 high-power fields/well under the x40 oil immersion lens (Polyvar).

2.8. STATISTICAL EVALUATIONS

For statistical evaluation of the data, student's t-test, paired t-test, Chi-squared analysis, and Mann-Whitney-U test were done using appropriate software (CSTAT, Oxtech, Oxford, UK). The Mantel-Haenszel test for stratified data was done using EGRET, 1988, statistics & epidemiology research cooperation, Seattle, Washington, USA. The correlation matrix was done using MICROSTAT II (Ecosoft Inc.)

CHAPTER 3. RESULTS

3.1. CULTURE AND MORPHOLOGY OF RPE CELLS

3.1.1. Culture of bovine, rat and human RPE

Bovine and human RPE were morphologically similar in both primary culture and sub-cultures. After 7 days in culture the RPE were established in colonies which consisted of small, pigmented, polygonal cells. Mitotic figures were identified in these colonies indicating that the cells were undergoing division while enlarged heavily pigmented cells were thought to be non-dividing (Flood et al, 1980; Flood & Gouras, 1981; Boulton et al, 1982). Within 2-3 weeks these colonies grew and eventually merged to form a monolayer of tightly packed, homogenous cuboidal cells. Monolayers of primary bovine and human RPE exhibited a mosaic pattern (Fig. 3.1a) (although this pattern was more common in bovine cells), which was subsequently lost in sub-culture.

Sub-cultures of bovine and human RPE consisted of unpigmented flattened, discoid-shaped cells (Fig. 3.1b) which reached confluence between 3-4 days post-passage. Bovine RPE cells could be sub-cultured up to 13th passage after which large, spread, multinucleate cells were apparent, dividing cells were rare and cell death was common. Before this stage was reached the cultures were discarded. The number of sub-cultures achieved in human RPE varied according to the age of the donor and as young eyes were rare the maximum passage reached, before degenerative changes were observed, was 11th passage. Consequently bovine and human RPE cells between 5th and 7th passage were thought to be appropriate for the study.

Control and dystrophic RCS rat cultures were similar in all features. Rat RPE cells isolated as single cells established monodispersed cultures within 5 days (Fig. 3.1c). These cultures were pre-confluent at day 5 and consisted of pigmented, flattened, often bi-nucleate, discoid-shaped cells with close cell-to-cell associations. Within 7-9 days the monodispersed cultures of rat RPE cells reached confluence. Rat RPE cells isolated as aggregates adhered to the substrate and established islands of cells within 4-5 days (Fig. 3.1d). These islands consisted of heavily pigmented cells in the centre and flattened, well spread, unpigmented cells at the periphery. Peripheral cells were discoid-shaped whereas the shape of central cells could not be clearly distinguished under phase-contrast microscopy because of their heavy pigmentation. Cells between the centre and the periphery were small, polygonal cells with variable pigmentation. Islands increased in size circumferentially until, after 9 days, the periphery of adjacent islands came into contact. At the 9 day stage, the cultures were determined as confluent.

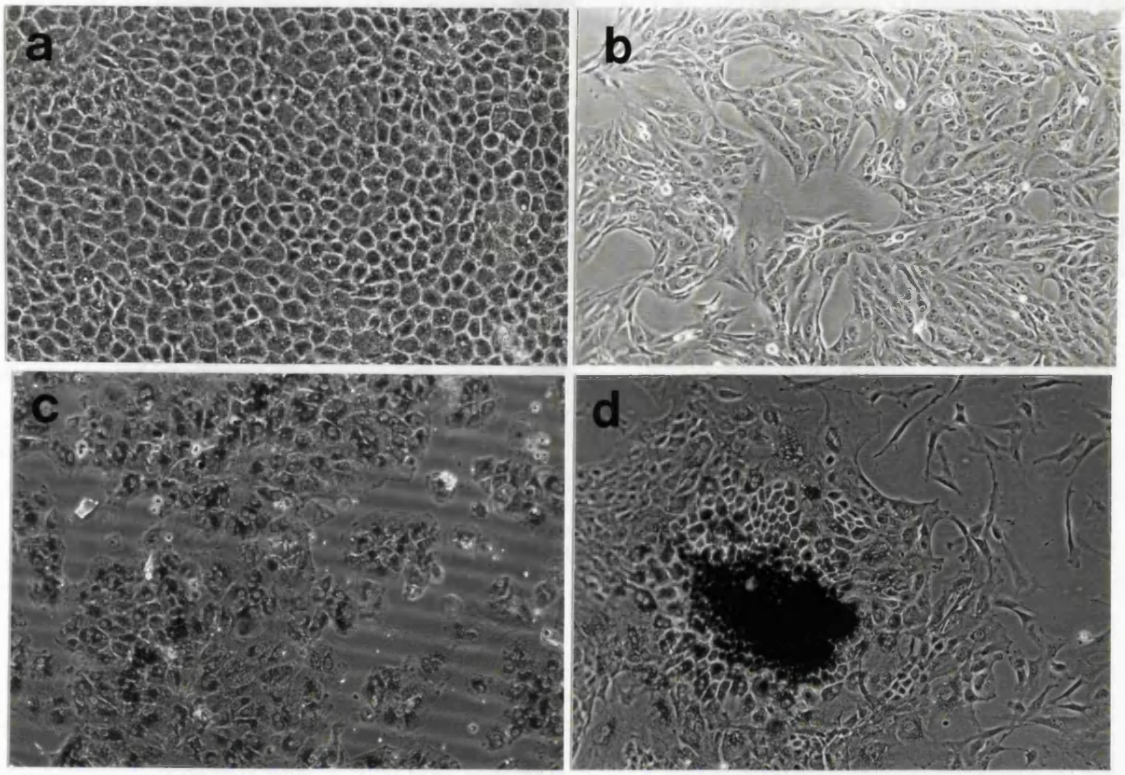

Figure 3.1. Phase micrographs of cultured bovine (**a**), human (**b**) and rat (**c-d**) RPE cells. **a**) After 2-3 weeks in vitro bovine and human primary cultures formed a monolayer of tightly packed polygonal cells which displayed a mosaic pattern. The mosiac pattern was best demonstrated in bovine cultures. **b**) Sub-cultures of bovine and human RPE lost the mosiac pattern and consisted of non-pigmented flattened, well spread, discoid-shaped cells. The cultures were confluent within 4-5 days and this Figure shows preconfluent human cells. **c**) Rat RPE cells isolated as single cells established monodispersed cultures within 4-5 days and consisted of pigmented, flattened, often bi-nucleate, discoid-shaped cells. **d**) Rat RPE cells isolated as aggregates established islands of cells within 4-5 days. Islands consisted of heavily pigmented cells in the centre and unpigmented, flattened, discoid-shaped cells at the periphery. Cells between the centre and the periphery were small, polygonal cells with variable pigmentation. (Magnifications: **a-d** x100).

3.1.2. Morphology of bovine, rat and human RPE

In culture, bovine and human RPE cells shared similar morphologies. SEM revealed that both cell types were flattened, well spread and discoid-shaped with a large ovoid nucleus below the plasmalemma (Fig. 3.2a). The cells were mostly denude of surface microvilli. The cellular organelles were seen by TEM to have been concentrated around the nucleus and dispersed in the peripheral cytoplasm (Fig. 3.2b). In both bovine and human RPE, ribbon-like structures were seen extending from the perikaryon into the periphery of the cell (Fig. 3.2b). The ribbon-like structures were large branching organelles that formed a complex overlapping network (Fig. 3.3.). At higher magnification the presence of distinct cristae (Fig. 3.3. inset) identified these structures as mitochondria. The long ribbon-like nature of mitochondria was not an artifact of electron microscopy processing because these elongated networks were seen in live cells using the fluorescent dye, rhodamine 123 (Fig. 3.2c). The length of a randomised selection of mitochondria was measured from electron micrographs using a MOP video plan image analysis system. Some were found to be over 10 μm long, they were termed "giant" mitochondria and appeared to be aligned within the cytoplasm to cytoskeletal elements (Fig. 3.4.), particularily stress fibres.

When ultrathin sections of cultured RPE cells were studied by TEM the cytoplasm was shown to be replete with organelles (Fig. 3.5a) including micropinocytotic vesicles, Golgi cisternae and Golgi vesicles, lysosomal bodies, rough endoplasmic reticulum, AMFs, MTs and IFs. Mitochondria with their distinctive cristae were identified in abundance surrounding the nucleus and throughout the perikaryon (Fig 3.5a). It was clear that conventional thin sections which showed mitochondria as round or sausage-shaped structures (Fig. 3.5b) provided little insight of their complex elongated structure as seen by whole cell viewing.

In the periphery of the cell away from the perikaryon the cytoplasm was thin and this allowed the cytoplasmic substructure to be seen clearly (Fig. 3.6a). A characteristic feature of well spread cells were dense bands radiating from the cell centre (Fig. 3.6a). At high magnification the dense bands were seen to be a coalescence of filaments, particularly AMFs (Fig. 3.6b). The bands have been recognised in other cell types where they were called stress fibres and in the present cells measured between 200 and 500 nm in width. Following detergent treatment the cytoskeleton was freed from associated organelles and the overlapping network of various sized filaments could be seen (Fig. 3.6c). The filaments measured between 5 and 25 nm in diameter and were presumed from their sizes to have been a mixture of AMFs, MTs and IFs (Fig 3.6c and insert).

The morphology of control and dystrophic rat RPE in culture was similar. The individual cells in monodispersed cultures of rat RPE were well spread, flattened, discoid and were therefore like bovine and human RPE (Fig. 3.7a). Rat RPE appeared

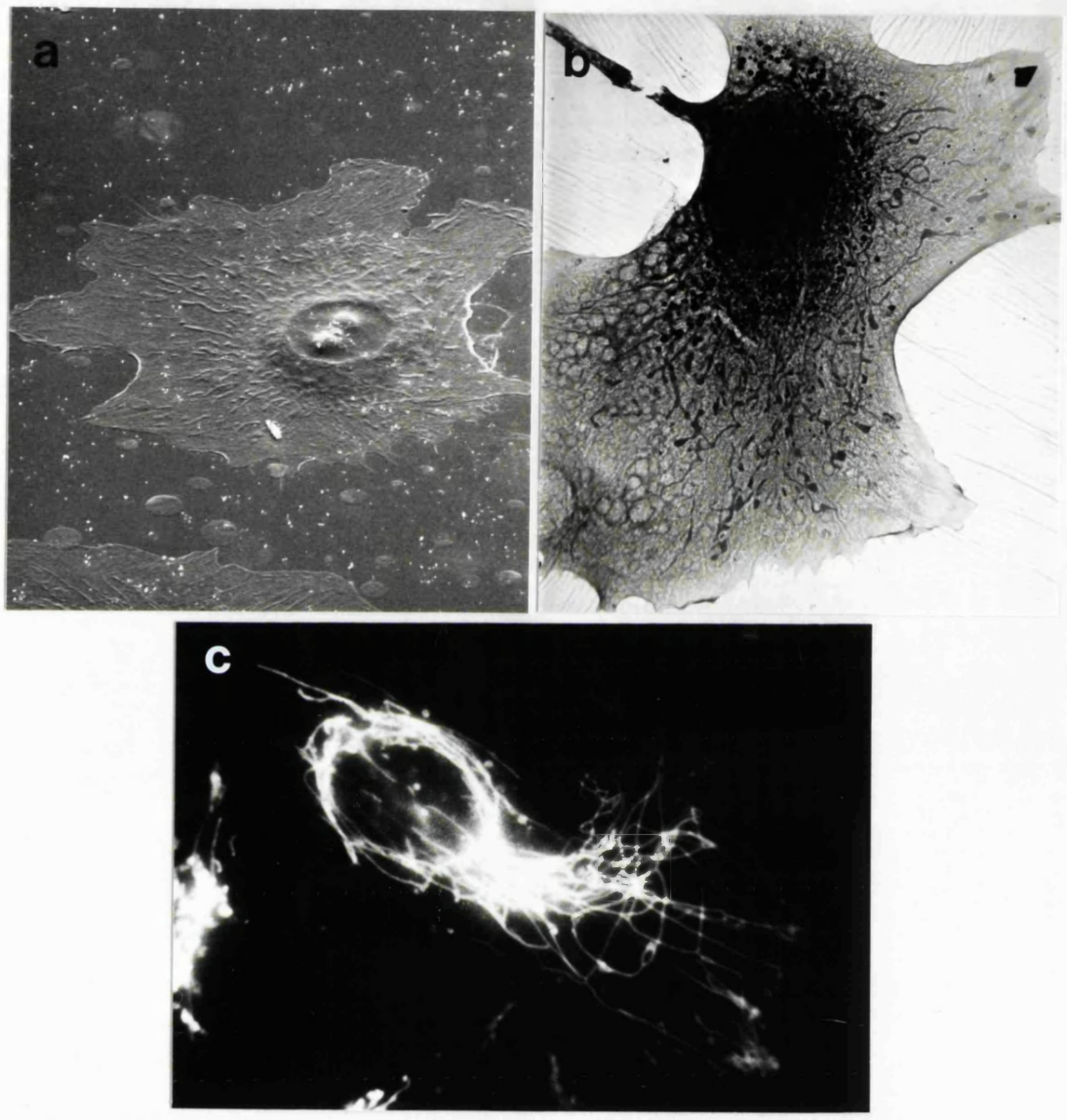

Figure 3.2. SEM (**a**; human), TEM of a whole cell (**b**; bovine) and fluorescent micrograph (**c**; human) of cultured RPE. **a**) In vitro RPE cells were flattened, well spread discoid-shaped cells with a large ovoid nucleus (arrow). Cells had no surface microvilli. **b**) TEM revealed that cell organelles were concentrated around the nucleus and that ribbon-like structures extended throughout the perikaryon and into the peripheral cytoplasm. **c**) Rhodamine 123, a specific dye for mitochondria, visualised the mitochondrial network in live cells. (Magnifications: **a** & **b** x1,500, **c** x1,200).

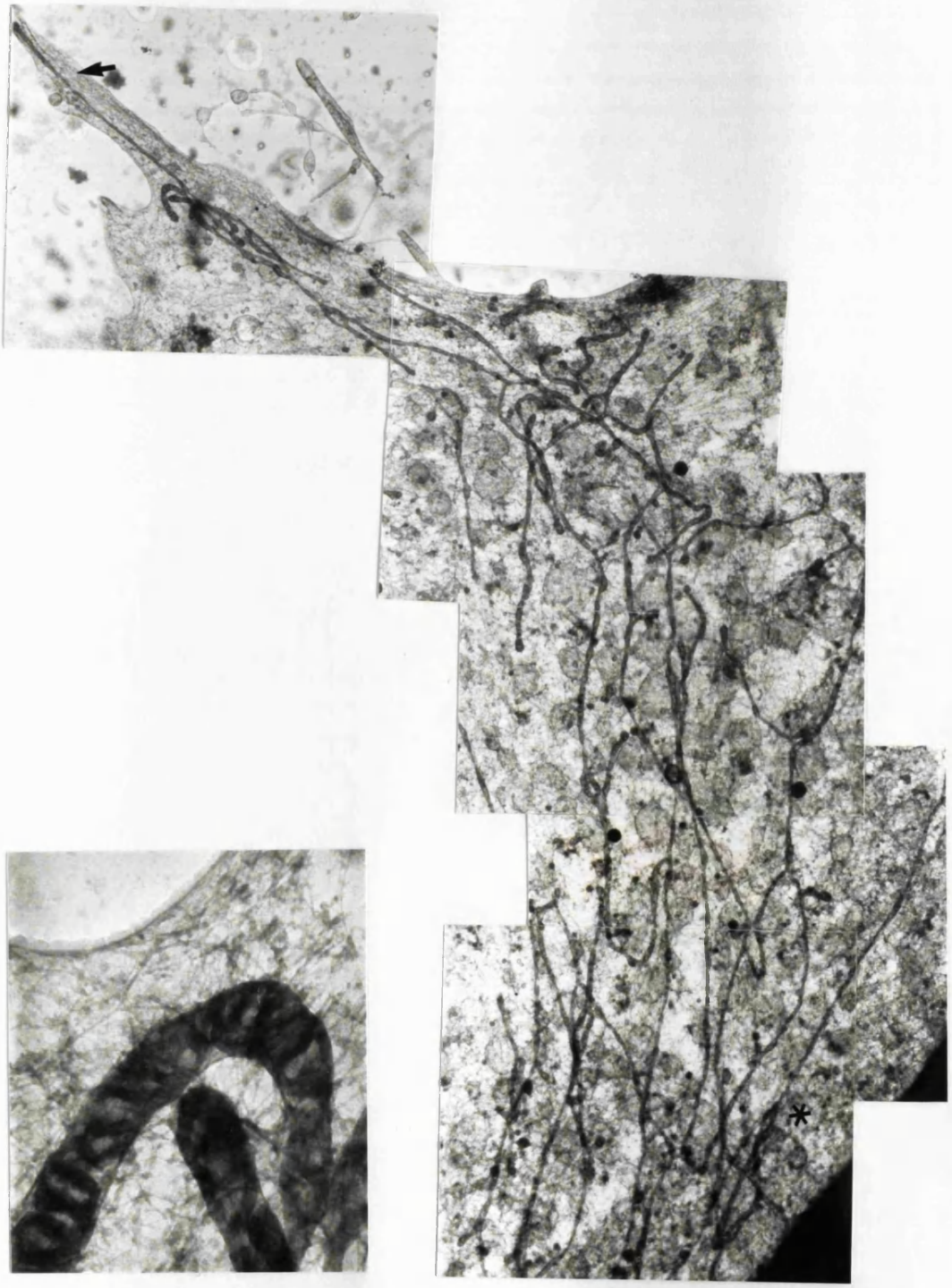

Figure 3.3. Whole cell viewing by TEM shows the network of ribbon-like organelles in the cytoplasm of cultured bovine RPE cells (x7,500). These organelles were identified as mitochondria by their distinctive cristae (insert, x65,000). The mitochondrial network extended from the perikaryon (the edge of which is denoted by an (✱) to the cell periphery and even into cell processes (arrow)

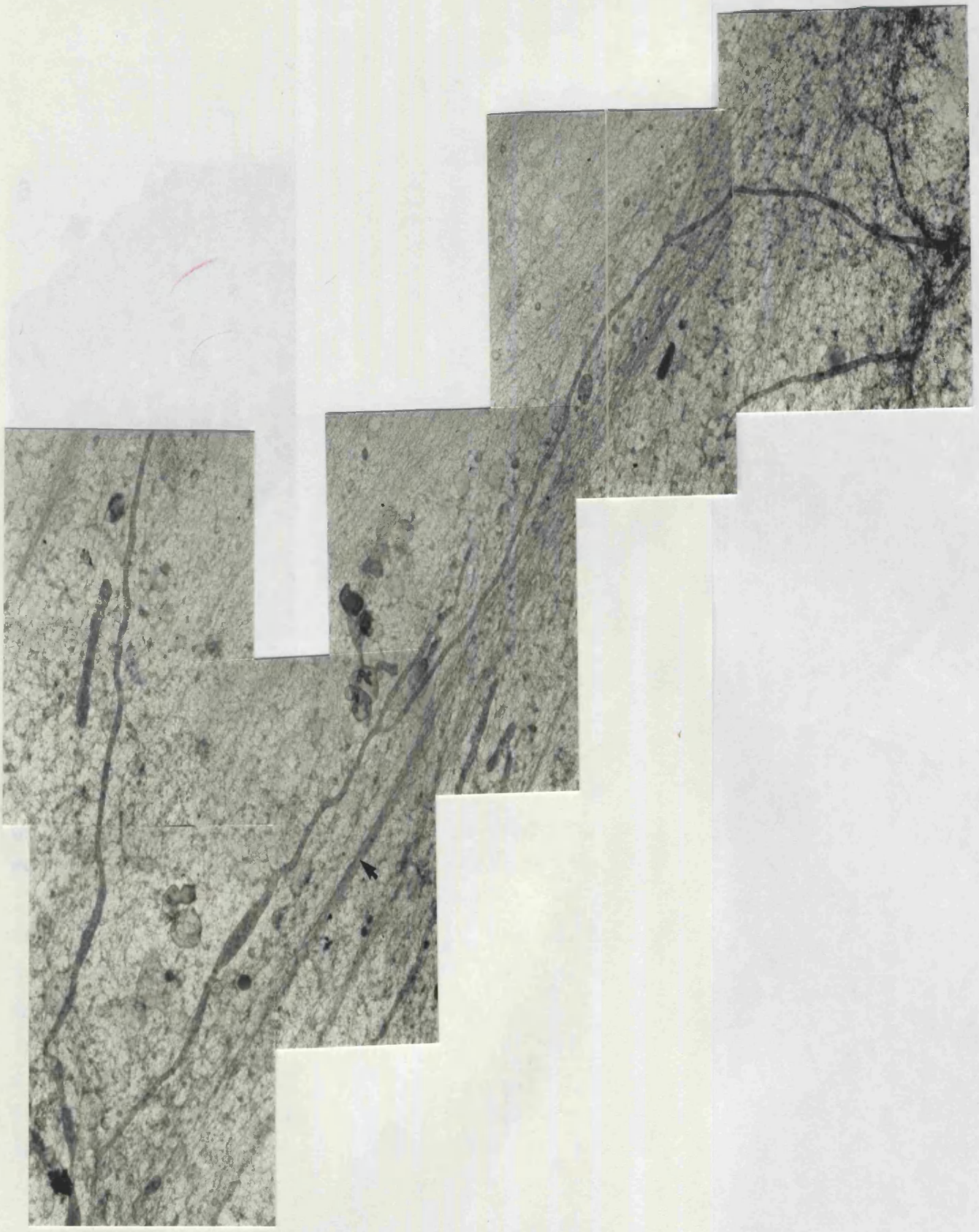

Figure 3.4. TEM of a "giant" mitochondrion located in a cultured human RPE cell. This long branching mitochondrion measured 9.9 μm long and was aligned with cytoskeletal elements, particularily stress fibres (arrow) (x12,000).

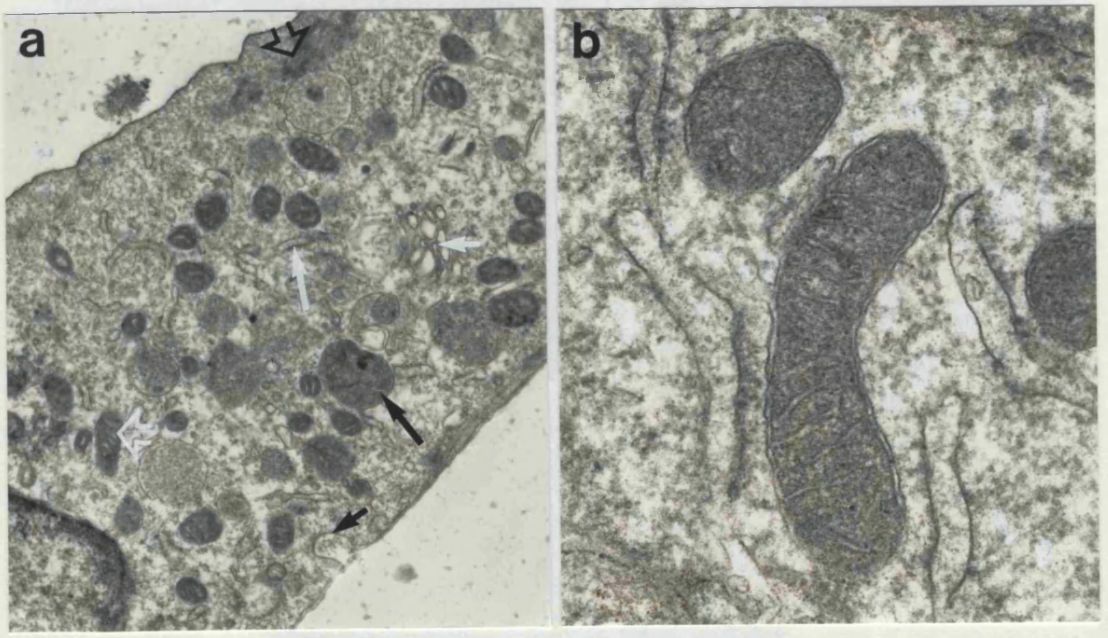

Figure 3.5. TEM of ultrathin sections of bovine RPE. **a**) TEM revealed the cytoplasm to be replete with micropinocytotic vesicles (short black arrow), Golgi cristae (short white arrow), lysosomal bodies (long black arrow), rough endoplasmic reticulum (long white arrow), cytoskeletal filaments, particulary AMFs (black open arrow), and ovoid mitochondria (white open arrow). **b**) The mitochondria appeared as round or sausage-shaped structures in thin section with dense matrices and obvious christae. (Magnifications: **a** x16,500, **b** x53,500).

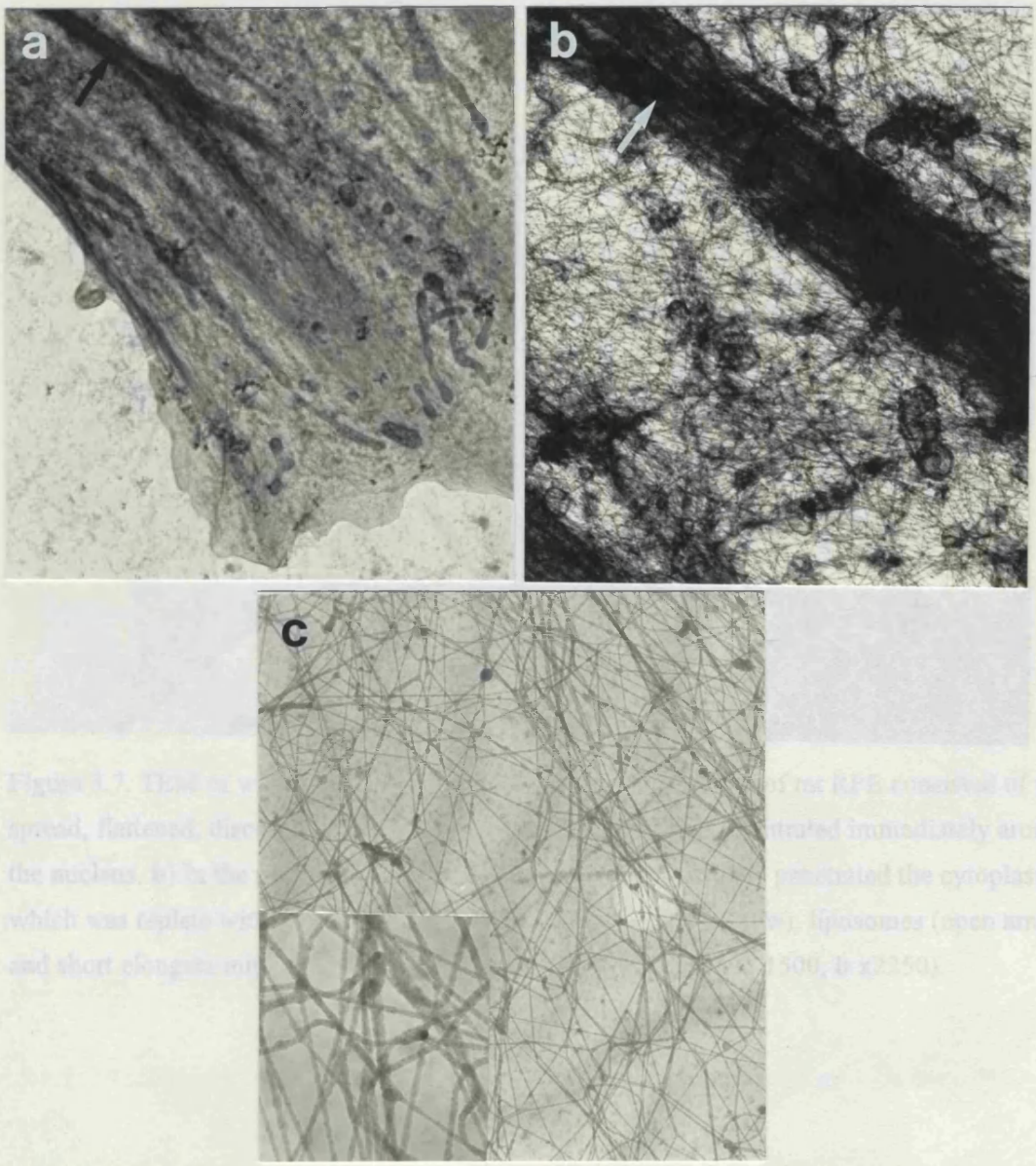

Figure 3.6. TEM of whole bovine RPE cells. **a**) The thin cytoplasm at the cell periphery allowed visualisation of cytoplasm substructure which, in well spread cells, contained dense parallel bands (black arrow). **b**) The dense bands consisted of bundles of AMFs (white arrow). These stress fibres were surrounded by a 3-dimensional network of smaller fibres. **c**) Detergent extracted cells showed the cytoskeleton to be a network of heterogenously sized filaments, which measured between 5-25 nm diameter and were presumed by their size to be a mixture of AMFs, MTs and IFs (insert). (Magnifications: **a** x7000, **b** x 40,000, **c** x30,000,insert x80,000).

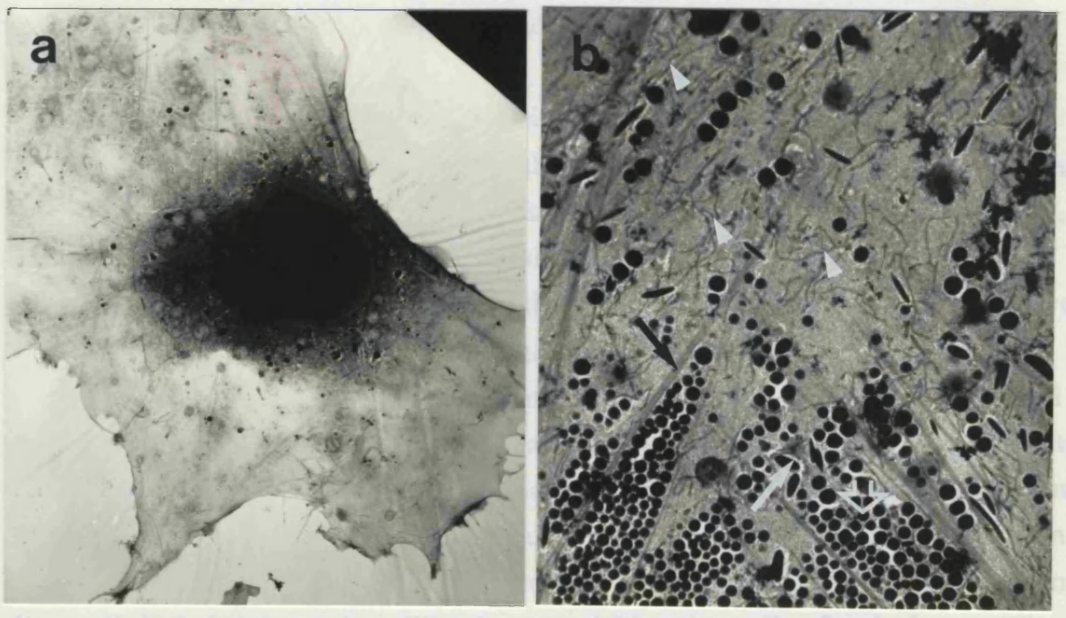

Figure 3.7. TEM of whole rat RPE cells. **a**) Monodipersed cultures of rat RPE consisted of well spread, flattened, discoid-shaped cells whose organelles were concentrated immediately around the nucleus. **b**) In the perikaryon, parallel stress fibres (black arrow) penetrated the cytoplasm, which was replete with organelles such as melanosomes (white arrow), liposomes (open arrow) and short elongate mitochondria (arrow heads) (Magnifications: **a** x1500, **b** x2250).

to have few organelles in the spread cytoplasm, most of the organelles were concentrated immediately around the large ovoid nucleus (Fig. 3.7b). Stress fibres were identified in the perinuclear cytoplasm and these were dispersed among large numbers of electron dense bodies presumed to be melanosomes and liposomes. The mitochondria in rat RPE, when compared to those in bovine cells, were shorter and did not form a network (Fig. 3.7b). SEM revealed that cells in monodispersed cultures were devoid of microvilli (Fig. 3.8a) and the margins of adjacent cells overlapped where there were numerous microspikes (Fig. 3.8b).

Islands of rat RPE contained cells with a variety of morphologies. Cells in the centre of the islands formed mosaics of cuboidal cells. The surfaces of these cells were covered with a forest of microvilli that obscured the plasmalemmae underneath (Fig. 3.8c). Peripheral cells were large, flattened, well spread cells (Fig. 3.8d). At higher magnification SEM showed that some of these cells had small stumpy microvilli, overlapping cell margins and microspikes (Fig. 3.8e). The cells were similar to those in monodispersed cultures. The cells between the periphery and the centre of the island were termed intermediate cells. Intermediate cells were larger, flatter and thinner than the cells in the centre, but not as well spread as the peripheral cells (Fig. 3.8f). Intermediate cells had shorter microvilli than the cells in the centre and more microvilli than peripheral cells. However the number of microvilli was variable. Some of the intermediate cells had abundant microvilli, whereas neighbouring cells often had none (Fig. 3.8f). Distinct cell-to-cell boundaries were also a feature of intermediate cells (Fig. 3.8f insert).

3.2. THE CYTOSKELETON

3.2.1. Identification of the cytoskeletal elements in bovine, rat and human RPE cells.

The cytoskeletal elements were visualised in bovine, rat and human RPE cells using immunocytochemical staining techniques and a panel of monoclonal antibodies (MABs; see Appendix III). The cultured cells of all 3 species stained positively for actin and tubulin. The organisation of these two types of filament in all three species of RPE was similar (Fig. 3.9.). In small epithelioid cells actin staining was diffuse with short filaments of actin in the peripheral cytoplasm (Fig. 3.9a). However, in large well spread cells the cytoplasm contained parallel actin bundles, called stress fibres, which traversed the cell (Fig. 3.9b). Tubulin staining revealed fine filaments which radiated from the perinuclear zone into the periphery of the cells (Fig. 3.9c). The filaments radiated from MTOCs adjacent to the nucleus (Fig. 3.9d).

In vivo bovine RPE showed positive staining with an anti-vimentin MAB, VIM-

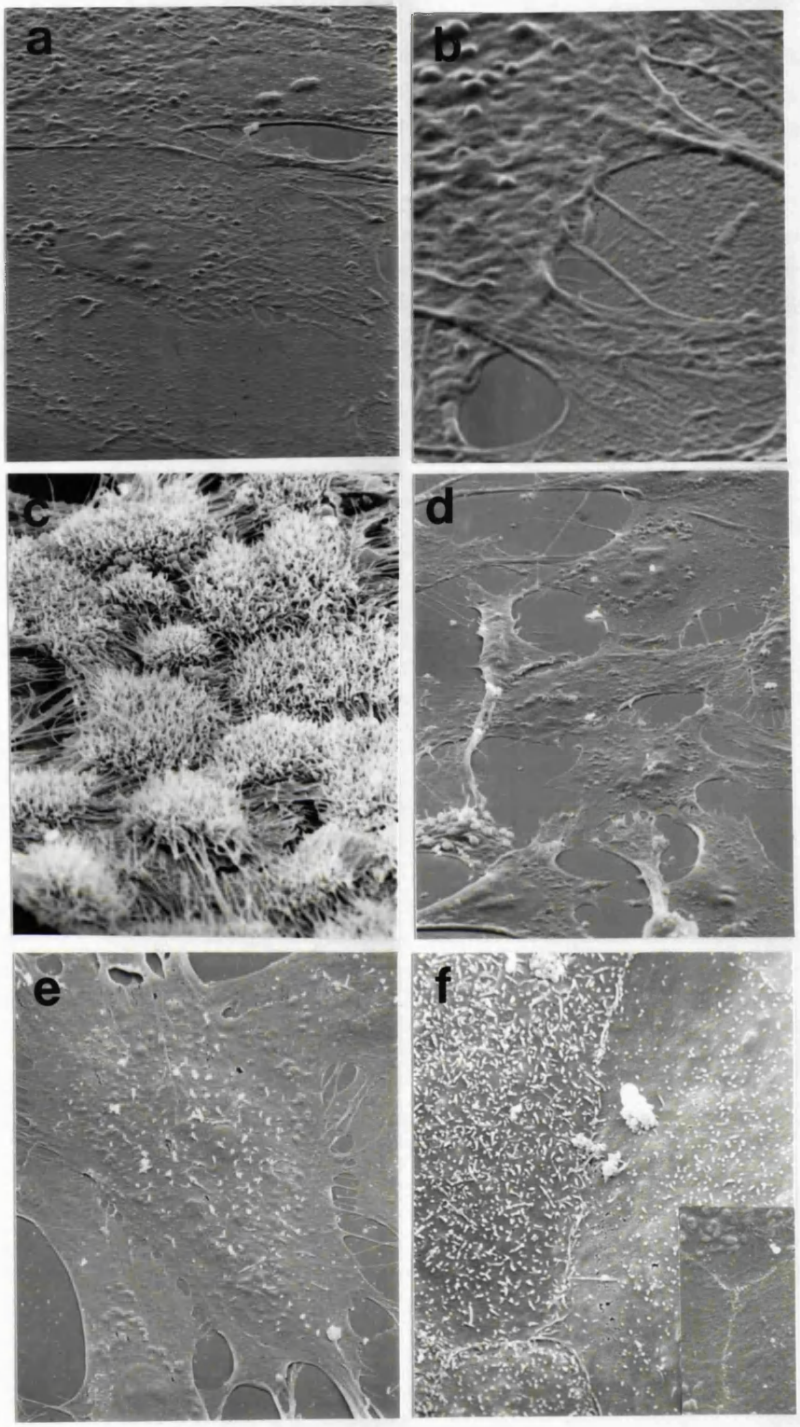

Figure 3.8. SEM of rat RPE. Monodipersed cultures (**a** & **b**), and islands (**c-f**). **a**) The cells in monodispersed cultures were devoid of microvilli. **b**) The margins of adjacent cells overlapped and numerous microspikes extended between adjacent cells. **c**) Islands of rat RPE consisted of three distinct cell morphologies. Cells in the centre of an island were cuboidal with long apical microvilli. **d**) Peripheral cells were flattened, well spread, discoid-shaped cells and as such were similar to the cells in monodipersed cultures. **e**) Stumpy microvilli were present on the surface of the peripheral cells. **f**) Cells between the centre and the periphery, the intermediate cells, had short variable surface microvilli and distinct cell-to-cell boundaries (insert). (Magnifications: **a** x1300, **b** x3500, **c** x1200, **d** x600, **e** x900, **f** x 1900, insert x1700).

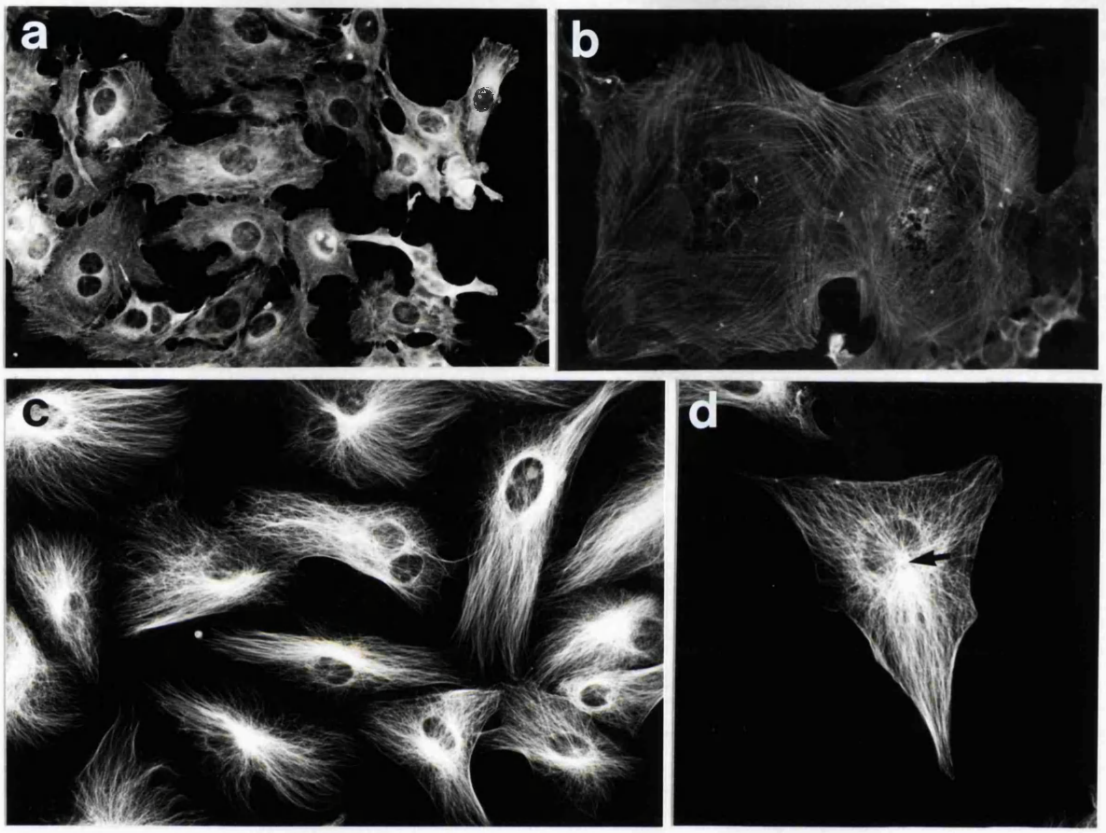

Figure 3.9. Immunofluorescent micrographs of AMFs (**a**; bovine & **b**; rat) and MTs (**c** & **d**; human) in cultured RPE cells. **a**) In small epithelioid cells actin staining was diffuse with short filament in the peripheral cytoplasm. **b**) Large well spread cells had traversing parallel actin stress fibres. **c**) Tubulin staining revealed fine filaments radiating throughout the cell. **d**) These filaments emerged from microtubule organising centres adjacent to the nucleus (arrow). (Magnifications: **a** x65, **b** x160, **c** x340, **d** x360).

13.2 and with all but three of the anti-cytokeratin MABs. The epithelium did not stain with MAB NCL-5D3, RGE 53 and K4.62. Positive cytokeratin staining of bovine RPE in situ is illustrated in cells labelled with MABs K8.13 (Fig. 3.10a & b) and RCK 102 (Fig. 3.10c). Both control and dystrophic rat RPE showed positive staining with MABs VIM-13.2, K8.13, AE3, RCK 102, K8.60 and K8.12, in vivo. Cytokeratin staining of rat RPE, illustrated in figure 3.10c, shows cells labelled with the K8.13, which identifies a wide range of cytokeratins. Rat RPE did not stain with MABs RCK 105, AE1, RGE 53, K4.62 and NCL-5D3. Frozen sections of human RPE were stained using immunogold/silver technique (see 2.3.4.), because pigmentation and autofluorescence hampered visualisation of the immunofluorescent staining. Human RPE stained positively for vimentin with MAB VIM-13.2 and for cytokeratins with MABs K8.13 and RCK 102 (Fig. 3.10d-f). Some cells stained faintly positive with MABs NCL-5D3 and RGE 53 and were negative with MABs K8.12 and K4.62. We have found that in situ bovine, rat and human RPE co-express both vimentin and cytokeratin IFs.

RPE cells from all three species stained positively for vimentin in vitro. Cells stained for vimentin contained a filamentous network that surrounded the nucleus, extending throughout the cytoplasm and terminated at the margins of the cell. Vimentin IFs showed focal concentration adjacent to the nucleous (Fig. 3.11a). Vimentin IFs did not always form a network of radiating filaments, some cells showed diffuse staining for vimentin in the perikaryon with filamentous networks only at cell margins (Fig. 3.11a).

Cultured RPE from all three species expressed cytokeratins, but staining for cytokeratins varied between the three species. There were four types of cytokeratin staining patterns identified:-

A All cells showed uniform positive staining.
B All cells stained, but some cells stained intensely and others stained faintly.
C Some cells stained, others did not.
D No cells stained.

Some anti-cytokeratin MABs showed the same type of staining pattern in more than one species. Bovine and rat RPE shared the same type of staining pattern with MABs AE3 and NCL 5D3 (Fig 3.12.). Whereas bovine and human shared the same type of staining when labelled with MAB AE1. Human and rat RPE demonstrated the same type of staining with several MABs, such as RCK 102, RCK 105, K8.12 and K4.62 (Fig 3.12.). MAB RGE 53 was the only one that revealed the same staining pattern in all three species.

MAB AE3 showed staining type A in bovine and rat RPE and revealed a network of intensely stained, fine filaments within the cytoplasm (Fig. 3.11b). However the same MAB showed staining type B in human RPE and revealed both faintly stained

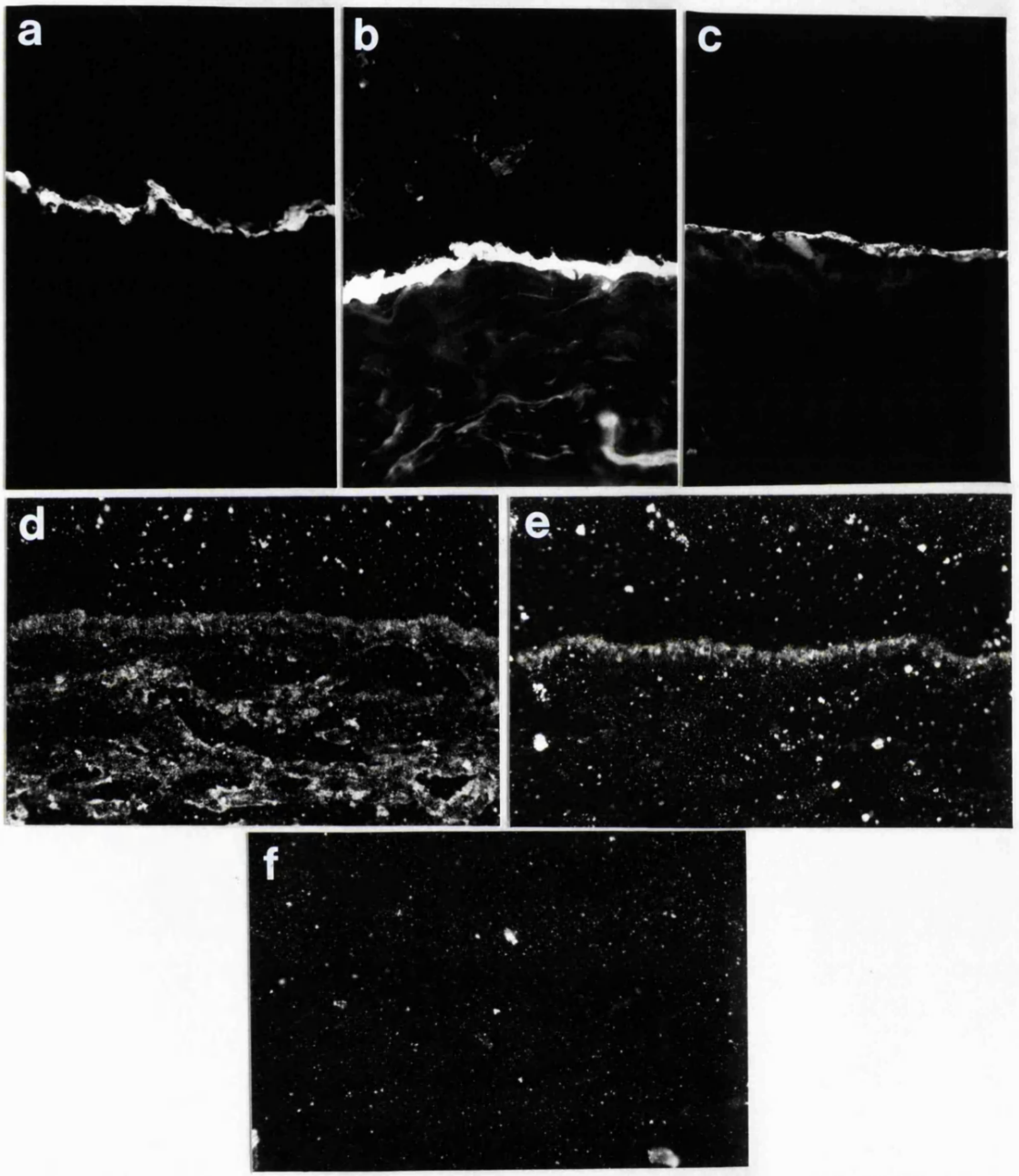

Figure 3.10. Immunofluorescent micrographs demonstrating cytokeratin staining of RPE in situ from bovine (**a** & **b**) and rat (**c**). The sections were labelled using MAB K8.13 (**a** & **c**) and RCK102 (**b**) and show intense fluorescence at the RPE monolayer. Immuno-gold/silver staining of cryostat sections of RPE in situ from human tissue (**d-f**). Using epi-polarization, immunostaining was detected for vimentin in RPE (arrow), choroid and sclera (**d**) and cytokeratins using MAB K8.13 showed the RPE only (**e**). Negative control showed only background staining (**f**). (Magnifications: **a** x220, **b-f** x 250).

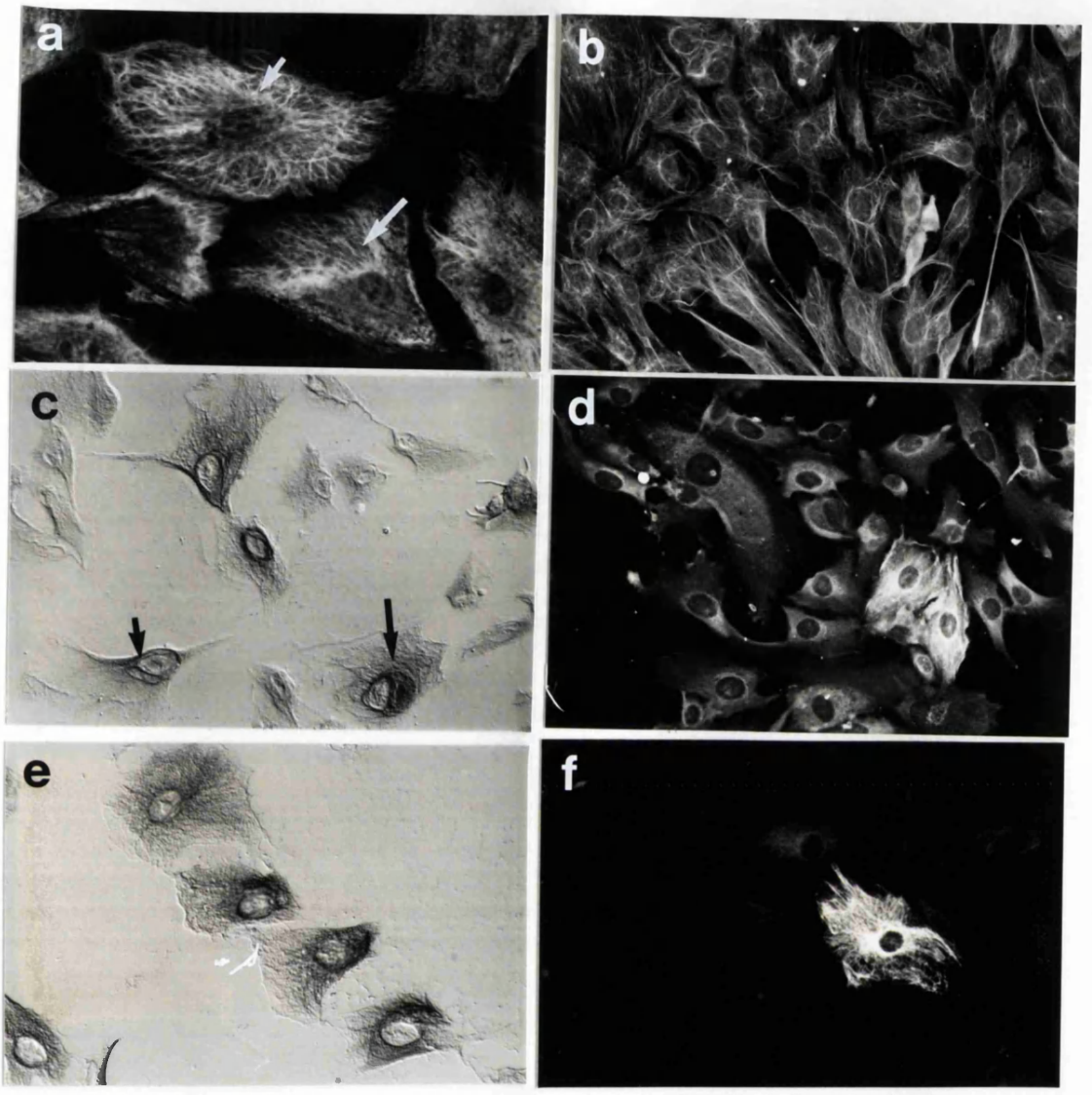

Figure 3.11. Micrographs of cultured human (**a**, **c**, & **e**), bovine (**d** & **f**), and rat (**b**) demonstrating vimentin IFs (**a**) and cytokeratin IFs (**b-f**). Cells were stained using immunofluorescenc (**a**,**b**,**d** & **f**) and immunoperoxidase (**c** & **e**). **a**) All cells stained positive for vimentin and consisted of a filamentous network surrounding the nucleus and radiating throughout the cytoplasm. Staining was concentrated at the juxtanuclear region of the cell (short arrow). In some cells vimentin staining was diffuse in the perikaryon, but filamentous at cell margins (long arrows). **b**) Staining type **A** was shown by MAB AE3 in bovine and rat RPE and consisted of prominent cytokeratin IFs within the cytoplasm. **c**) Whereas in human RPE MAB AE3 showed staining type **B** where some cells contained faintly stained filaments (short arrow) and others contained intensly stained fialments (long arrow). **d**) This combination of faint and intensley stained cells was also shown in bovine RPE labelled with MAB K8.13. However the faintly stained cells demonstrated a diffuse staining pattern and the intensley stained cells revealed a filamentous pattern. **e**) In contrast MAB K8.13 consistently showed staining type **A** in human RPE, where all cells contained intensely stained filaments within the cytoplasm. **f**) Type **C** staining was seen in bovine cells with MAB AE1. Most cells were negative, but some cells contained intensely stained cytokeratin networks.(Magnifications: **a** x450, **b-e** x250, **f** x200).

Type of staining	Anti−cytokeratin MABs		
	Bovine RPE	Rat RPE	Human RPE
A	AE3, K4.62, RCK 102 & K8.12	AE3	K8.13
B	K8.13	–	–
C	RGE 53 & AE1	K8.13, RCK 102, RCK 105, RGE 53, K4.62 & K8.12	RCK 102, RCK 105, AE1, NCL 5D3, K8.12, RGE 53 & K4.62
D	RCK 105 & NCL 5D3	AE1 & NCL 5D3	–

Figure 3.12. The type of staining revealed in bovine, rat and human RPE when labelled with anti−cytokeratin monoclonal antibodies (MABs).

filaments in some cells and intensely stained filaments in other cells (Fig. 3.11c). This combination of faintly stained cells and intensely stained cells was also seen in bovine RPE labelled with MAB K8.13. However, the faintly stained cells showed a diffuse staining pattern, while the intensely stained cells contained a filamentous pattern (Fig 3.11d). In human RPE K8.13 consistently stained all cells (type A) revealing intensely stained filaments throughout the cytoplasm (Fig 3.11e). In contrast rat RPE demonstrated type C staining with K8.13.

Type C staining was the most common type of staining seen. For both rat and human RPE six (rat) and seven (human) of the anti-cytokeratin MABs showed type C staining, whereas only two MABs showed type C staining in bovine RPE, MAB AE1 and RGE 53. With these MABs the majority of bovine RPE cells showed negative staining but some cells contained intensely positively cytokeratin filaments (Fig. 3.11f). The proportional staining was most pronounced with MAB RGE 53, which consistently showed the type C staining in all three species. As only a proportion of cells stained this was best demonstrated using either immunoperoxidase staining, where both positive and negative stained cells could be visualised (Fig. 3.13a) or a combination of immunofluorescence and DIC micrographs (Fig 3.13b & c). Using these staining technique it was clear that some cells contained intensely stained filaments, whilst adjacent cells were negative for cytokeratin (Fig. 3.13a). Other MABs such as RCK102, RCK105, K8.12 and K4.62 showed an identical staining pattern to RGE 53 in both rat and human RPE in vitro (Fig. 3.13c & d). MABs RGE 53 and K4.62 recognise cytokeratin 18 (K18) and cytokeratin 19 (K19), respectively. Therefore in cultured human, and rat, RPE, K18 and K19 were expressed only in a sub-population of cells.

Despite the various types of staining there was no difference in the expression of cytokeratins between control and dystrophic rat RPE in vitro. However, there was a difference in the pattern of K18 filaments identified with MAB RGE 53. In some dystrophic cells the cytokeratin IFs were organised in highly convoluted and tortuous arrays (Fig. 3.14a) which were never seen in control cells (Fig. 3.14b). The variation in cytokeratin staining patterns was also seen in islands of cultured rat RPE cells. In particular islands of both control and dystrophic RPE labelled with MABs RCK 102 and RGE 53 (identified cytokeratins 5 & 8, and K18, respectively), which together identify the cytokeratin pair K8 & K18, showed a distinct staining pattern. Cells in the centre, which by phase microscopy were highly pigmented and by SEM were cuboidal, stained positive although a filamentous network was not visualised (Fig. 3.14c). Well spread cells at the periphery, and those cells described by SEM as intermediate, contained intricate networks of cytokeratin IFs similar to those described above in monodispersed cultures. Peripheral and intermediate cells consisted of both K18 positive (K18+) and K18 negative (K18-) populations of cells and showed variation in the staining pattern between K18+ cells, although the greatest variation in staining pattern was seen in intermediate cells (Fig. 3.14d).

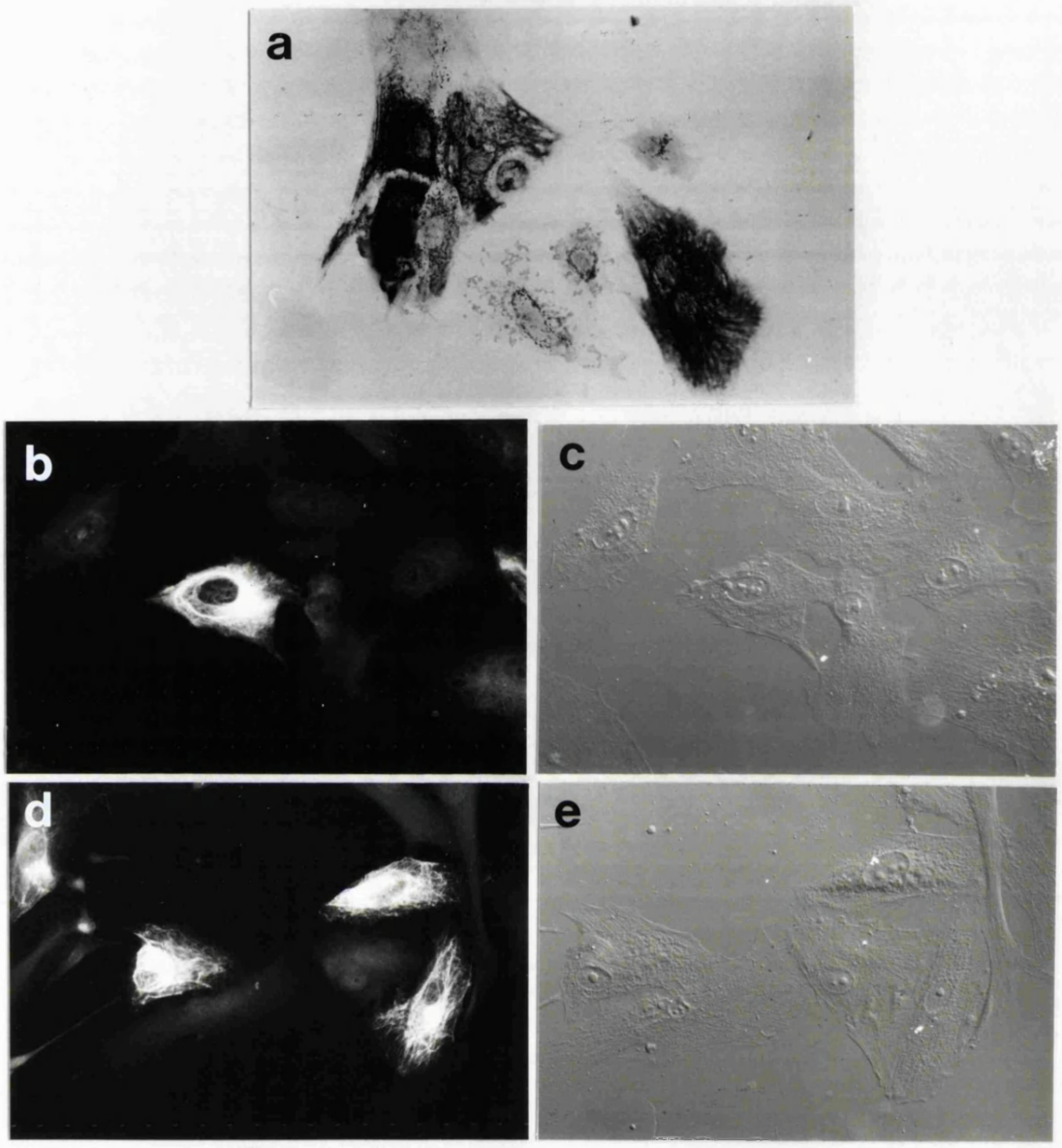

Figure 3.13. Micrographs of cultured rat (**a**) and human (**b-e**) RPE labelled with anti-cytokeratin MABs. Cells were stained using immunoperoxidase (**a**) and immunofluorescent with corresponding DIC micrographs (**b-e**). **a**) MAB RGE 53, which identifies K18, showed type **C** staining in rat RPE (control). Only a proportion of cells stained positive. **b**) Similarily in human RPE MAB RGE 53 identified an intensley stained filamentous network throughout the cytoplasm. **c**) These networks appeared only to be present in a sub-population of human RPE cells. **d-e**) MAB K4.62, which identifies K19, also labelled a filamentous network (**d**) in a sub-population of RPE cells (**e**). (Magnifications: **a-e** x250).

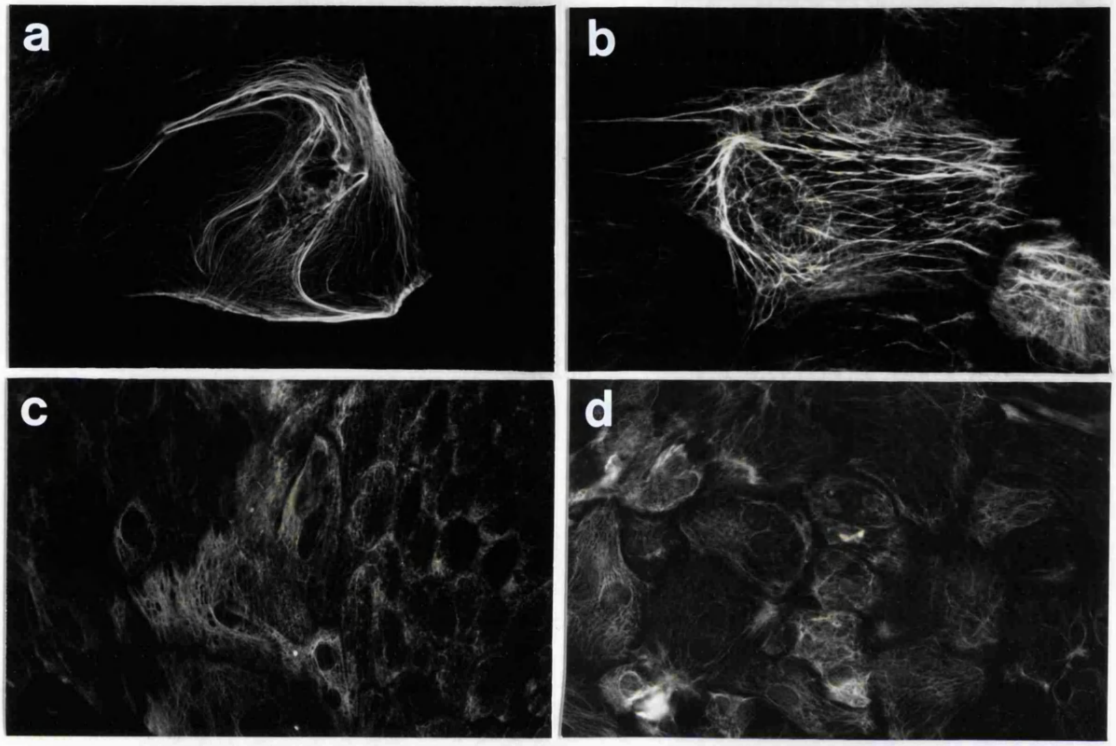

Figure 3.14. Immunofluorescent micrographs demonstrating cytokeratin IFs in cultured rat RPE. Dystrophic RPE (**a**) and control RPE (**b**) in monodispersed cultured labelled with MAB RGE 53. Islands of RPE labelled with MABs RCK 102 (**c**) and RGE 53 (**d**). **a**) MAB RGE 53 identified convoluted K18 filaments in dystrophic RPE. **b**) Such chaotic patterns were not seen in control rat RPE where an ordered intricate network surrounded the nucleous and spread throughout the cytoplasm. **c**) Islands of rat RPE deomonstrated a variation in cytokeratin staining. Cells in the centre of an island stained positively, although a clearly filamentous pattern could not be distinguished. **d**) Intermediate cells, like peripheral cells and cells in monodispersed cultures, contained a network of cytokeratin IFs. Although variation in staining pattern was seen in the peripheral cells, the greatest variation was seen in the intermediate cells. (Magnifications: **a** x700, **b** x600, **c** x200, **d** x250).

3.2.2. Quantification and characterisation of the K18 and K19 sub-population of human RPE cells

Confluent cultures of human RPE were stained for K18 alone, K19 alone and for both K18 & K19 using RGE 53, K4.62, and a cocktail of these two MABs, respectively. Using immunoperoxidase labelling and DIC microscopy both cytokeratin positive and negative cells were visualised and were counted in the photographic field under x40 objective (Polyvar). Fifteen fields were counted per LabTek chamber so that a total of 1354 cells were examined and evaluated.

The sub-population of human RPE cells that expressed K18 and K19 was 46.8% and 14.9%, respectively (Fig. 3.15.). The proportion of cells that stained with both monoclonals was 44.9%. This did not exceed the proportion of cells that were K18+. Therefore, cells which are positive for K19, as identified with K4.62, were considered to be a sub-set of the K18 population (identified with RGE 53).

3.3. PHAGOCYTOSIS

3.3.1. Selection and characterisation of a MAB to isolated ROSs.

MABs raised to bovine photoreceptors were characterised in our laboratory (Shallal et al, 1988). Three MABs, 1F4, 4A2 and 4C4 were used and from western blot analysis and TEM/immunogold labelling these identified either rhodopsin (1F4 & 4C4) or peripherin (4A2). Two key criteria had to be met by the MABs used in this study: 1. They had to identify isolated ROSs; 2. They had to tolerate the fixation regime used in the indirect double immunofluorescent staining procedure of cultured cells challenged with ROSs (see 2.5.2.).

The localisation, titre and effect of fixation of all three MABs against ROSs were determined on frozen sections of bovine retina. Tissue culture supernatants of MABs 1F4 and 4A2 positively stained the ROSs of bovine retina specifically and intensely at a dilution of 1:2 (Fig. 3.16a & b). Staining was far greater than the negative control where the MAB was omitted (Fig. 3.16c). MAB 4C4, at the same dilution stained ROSs intensely, however background fluorescence was unacceptably high and 4C4 was abandoned. MAB 4A2 appeared to stain features in the inner retina, possibly axons of neurons. The reactivity of 1F4 and 4A2 were compared on isolated bovine ROSs air dried onto a microscope slide (see 2.4.2.). MAB 1F4 stained the isolated ROSs intensely and with a lower background fluorescence than 4A2 (Fig. 3.16d). From these results MAB 1F4 was used to identify ROSs challenged to cultured RPE cells.

Cytokeratin character	Total numbers of cells	Mean +/− SD	% K+ cells
K18+	234	7.80 +/− 2.44	46.8
K18−	266	68.87 +/− 2.99	
K19+	56	2.07 +/− 1.07	14.9
K19−	320	10.63 +/− 2.94	
K18+ & K19+	179	5.97 +/− 2.44	44.9
K18− & K19−	219	7.30 +/− 2.32	

KEY
K18+ cytokeratin 18 positive
K18− cytokeratin negative
K19+ cytokeratin 19 positive
K19− cytokeratin 19 negative

Figure 3.15. The number of K18, K19 and both K18 & K19 positive cells in cultures of human RPE. K18 and K19 IFs are expressed in a sub−population of human RPE cells and K19+ cells are a sub−set of the K18+ cells.

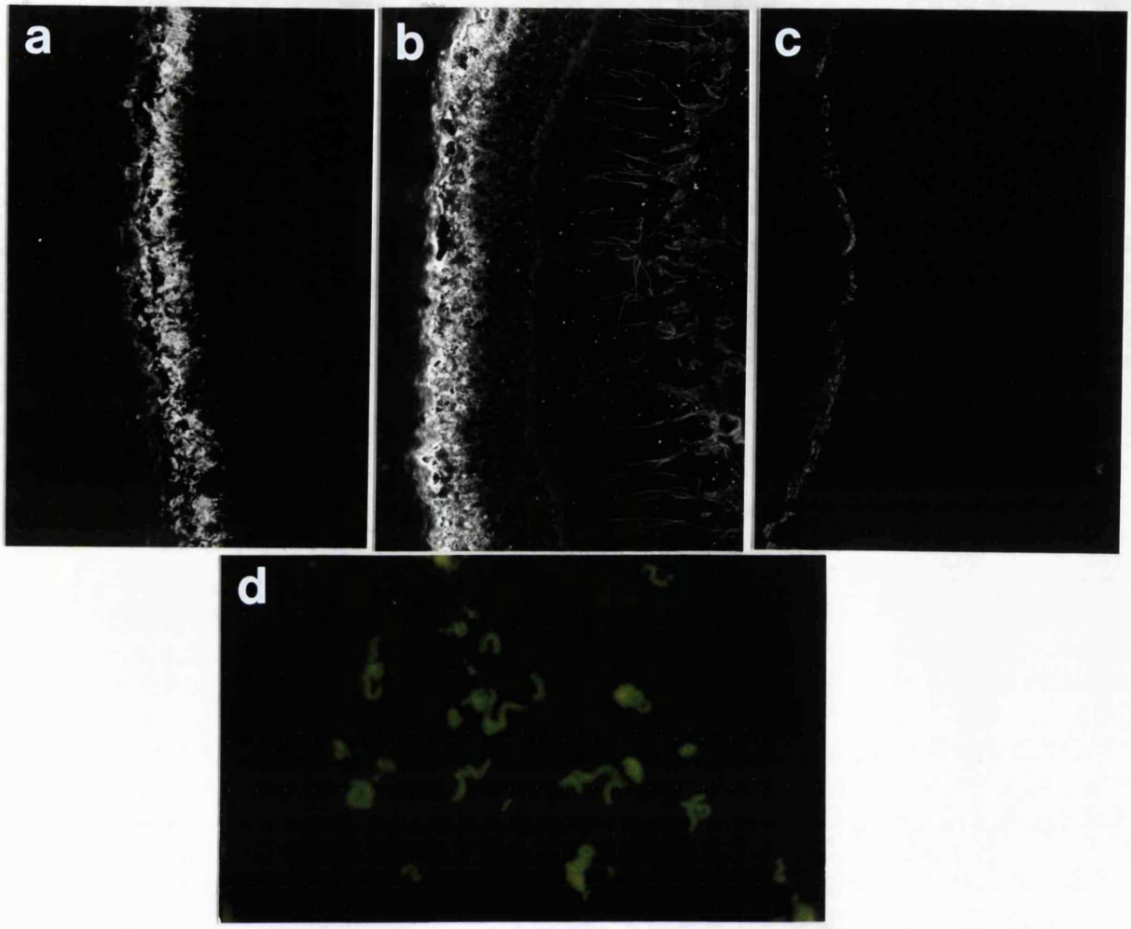

Figure 3.16. Immunofluorescent micrographs demonstrating the localisation of anti-ROS MABs 1F4 (**a** & **d**) and 4A2 (**b**). Immunolabelling of cryostat sections of bovine retina (**a-c**) demonstrated that MABs 1F4 (**a**) and 4A2 (**b**) identified photoreceptors outer segments specifically. However, 4A2 also stained features of the inner retina. The negative control (**c**) showed no background staining. **d**) Isolated ROSs stained positive with MAB 1F4, staining was more intense with 1F4 than 4A2. (Magnifications: **a-c** x200; **d** x500).

3.3.2. Phagocytosis of ROSs by cultured bovine RPE cells.

Bovine RPE cells were challenged with ROSs for 1, 2, 3 and 4 hours. Attached and internalised ROSs were visualised using the double immunofluorescent labelling procedure (see 2.5.2.) and challenged cells were viewed using DIC microscopy (Fig. 3.17.). ROSs attached to the cell surface were labelled with TRITC and so fluoresced red (Fig. 3.17a). Both attached and internalised ROSs were labelled with FITC and fluoresced green when the illuminating light was changed from green to blue (Fig. 3.17b). The difference in the numbers of red and the numbers of green fluorescing ROSs is the amount of ROS internalised and therefore the index of phagocytic ability. When immunofluorescent micrographs were compared with DIC micrographs (Fig. 3.17c) it was clear that the labelled ROSs had a cellular localisation. The phagocytosis of bovine ROSs by cultured RPE cells was quantified using this technique.

Cultured bovine RPE cells were found to attach and internalise ROSs, however from the fluorescent micrographs it appeared that the number of TRITC and FITC labelled ROSs was the same (Fig. 3.17). Therefore bovine RPE had attached more ROSs than they had internalised. Counts were taken, as described previously (see 2.5.1.) and expressed as the percentage ROSs and the mean number of ROSs attached and internalised in a sample of 10 random microscopic fields (x40 objective, Polyvar) plotted against time (Fig. 3.18.). The data on bovine RPE phagocytosis was generated from 4 experiments. The mean number of cells per 10 random microscopic fields was also recorded.

Bovine RPE cells attached and internalised ROSs at 1, 2, 3 & 4 hours (Fig. 3.18) and appeared to attach between 32.6%-69.8% more ROSs than they internalised (Fig. 3.18a). Indeed bovine RPE attached significantly more ROSs than they internalised at 2, 3 and 4 hours (paired t-test, $p<0.01$), but there was no difference between ROS attachment and internalisation at 1 hour.

There was a linear relationship between the mean number of ROSs attached and time (Fig. 3.18b), with a minimum of 30 ROSs attached at 1 hour which increased to a maximum of 67 ROSs at 2 hours. The mean number of ROSs internalised decreased from just under 14 to nearly 8, between 1 and 2 hours, thereafter reaching a maximum of 34 ROSs at 4 hours. However, the numbers of ROSs was low when the counts were taken from a sample of 10 random microscopic fields which contained an average of 711 cells. The largest number of ROSs counted were those that had attached to bovine RPE cells at 4 hours (67 ROSs). Therefore there would be approximately 0.09 ROSs attached per cell. The data indicates that bovine RPE attach few ROSs during ROS challenge and consequently internalise even less ROSs.

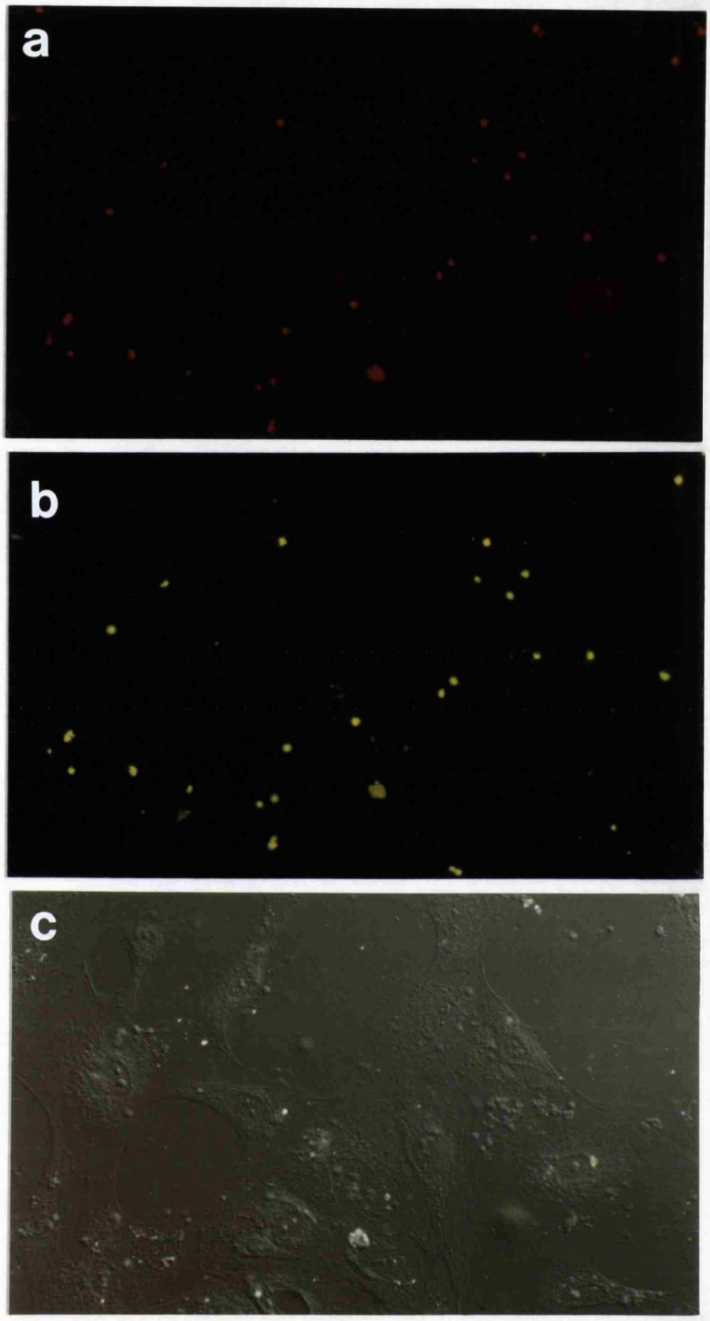

Figure 3.17. Immunofluorescent micrographs (**a** & **b**) and corresponding DIC micrograph (**c**) of cultured bovine RPE cells challenged with ROSs for 3 hours. The register between the red dots (**a**; attached ROSs) and the green dots (b; attached and internalised ROSs) means that six ROSs have been phagocytosed (Magnifications **a-c** x250).

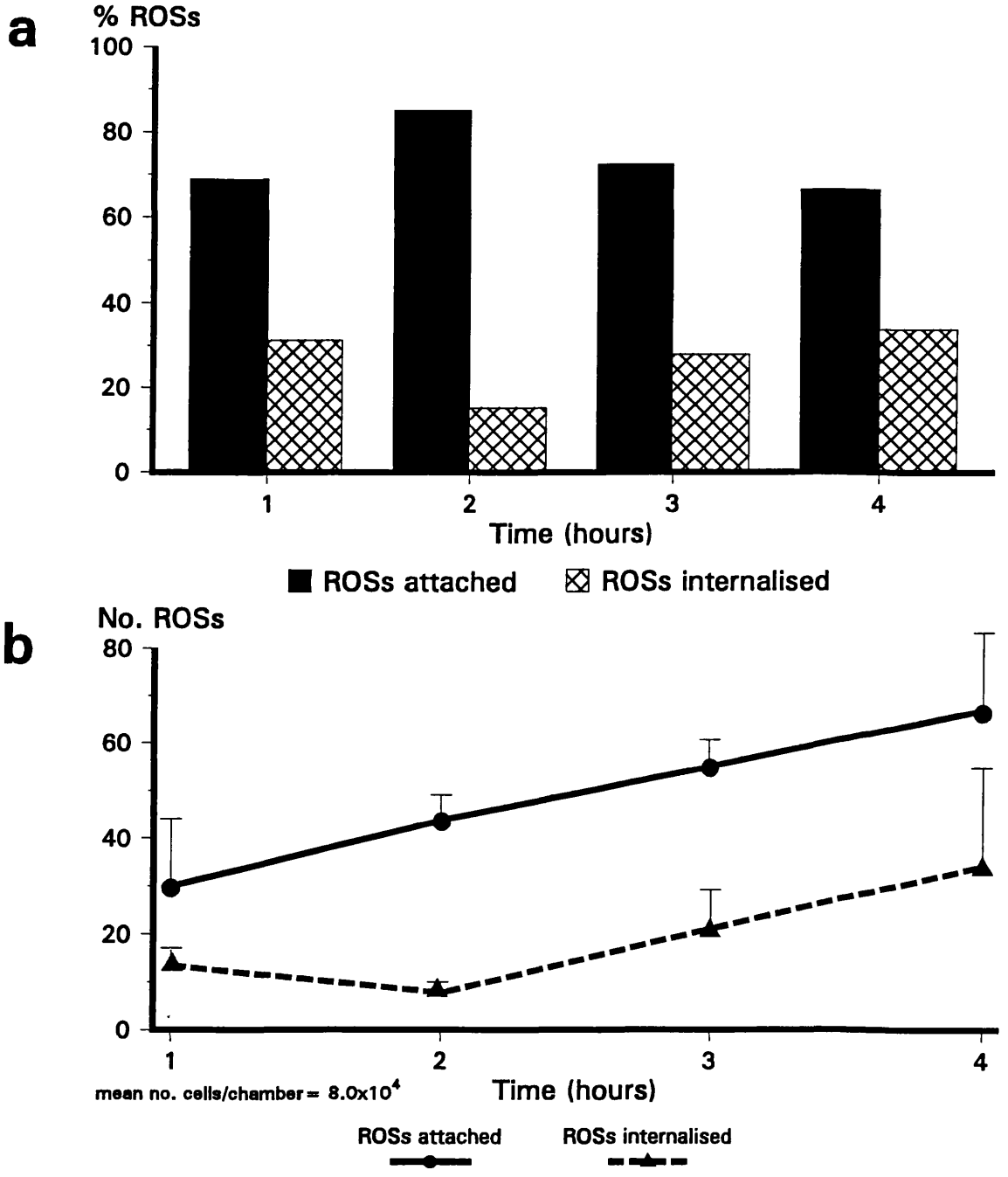

Figure 3.18. Phagocytosis of ROSs by cultured bovine RPE. Bovine cells were challenged with ROSs for 1,2,3 & 4 hours. a) Percentages of ROSs. Bovine RPE attached significantly more ROSs than they internalised between 2-4 hours (paired t-test, $p<0.01$). b) Mean number of ROSs. Each point is generated from 4 challenge experiments and the bars show the standard error of the mean (SE). The mean number of ROSs attached increased with time. Internalisation of ROSs decreased after 1 hour, thereafter increasing. However, the number of ROSs is low when compared to the number of cells per culture. The maximum number of ROSs were attached at 4 hours and compared to the mean number of cells this is approximately 0.09 ROS/cell.

3.3.3. Phagocytosis of ROSs over a 3 hour time course by control & dystrophic RCS rat RPE in vitro.

Rat RPE cells were challenged with ROSs for 1, 2 and 3 hours. Attached and internalised ROSs were detected and visualised in control and dystrophic cells following the protocol adopted for the bovine studies (see 3.3.2.). Immunofluorescent micrographs revealed that in control rat RPE there were considerably more FITC labelled ROSs (Fig. 3.19a) than TRITC labelled ROSs (Fig. 3.19b). In comparison dystrophic cells appeared to have almost equal numbers of TRITC and FITC labelled ROSs (Fig. 3.19c & d). Therefore immunofluorescent staining indicated that both control and dystrophic cultured rat RPE cells attached and internalised ROSs, but the dystrophic rat RPE cells appeared to internalise far fewer ROSs than control cells.

ROSs were counted as described previously (see 2.5.1.) and counts were expressed as the mean number of ROSs attached and internalised in a sample of 10 random microscopic fields (x40 objective, Polyvar) against time. The congenic breed of control RCS rat appeared to be prone to disturbance which often led to mothers killing their young. This was more prominent in control animals, consequently in this study there were more dystrophic than control RPE cell cultures available for investigation. In addition when compared to bovine, rat RPE proved difficult to grow in vitro and less able to withstand the lengthy phagocytic challenge. Inevitably cultures were lost during culturing and during the ROS challenge. Consequently the data was generated from 2 control cultures and from 5 dystrophic cultures per time period. The mean number of cells per 10 random microscopic fields was also recorded (Fig. 3.20.).

In control RPE the profiles of ROS attachment and ROS internalisation differed (Fig. 3.20a). Within 1 hour comparable quantities of ROSs were both attached and internalised. Between 1-2 hours there was very little increase in the amount of ROSs attached however, after 2 hours ROS attachment rapidly increased reaching a maximum at 3 hours. In contrast the number of ROSs internalised gradually increased between 1-2 hours reaching a maximum at 2 hour, before decreasing to a minimum at 3 hours. Indeed significantly more ROSs were internalised at 2 hours than at 1 and 3 hours (Student's t-test, $p< 0.01$).

In dystrophic RPE, ROSs were attached and internalised (Fig. 3.20b). From the onset of challenge ROSs were attached by dystrophic cells. The numbers of ROSs attached increased reaching a maximum at 2 hours, thereafter decreasing to a minimum at 3 hours. Although there was no difference in the numbers of ROSs attached between 1 and 2 hours, significantly more ROSs were attached by dystrophic cells at 2 hours than at 3 hours (Student's t-test, $p<0.01$).

Some ROSs were internalised by dystrophic cells however, dystrophic cells internalised between 8-14 fold fewer ROSs than control cells even though they attached on average just under 1½ times more ROSs than control cells. There were on average

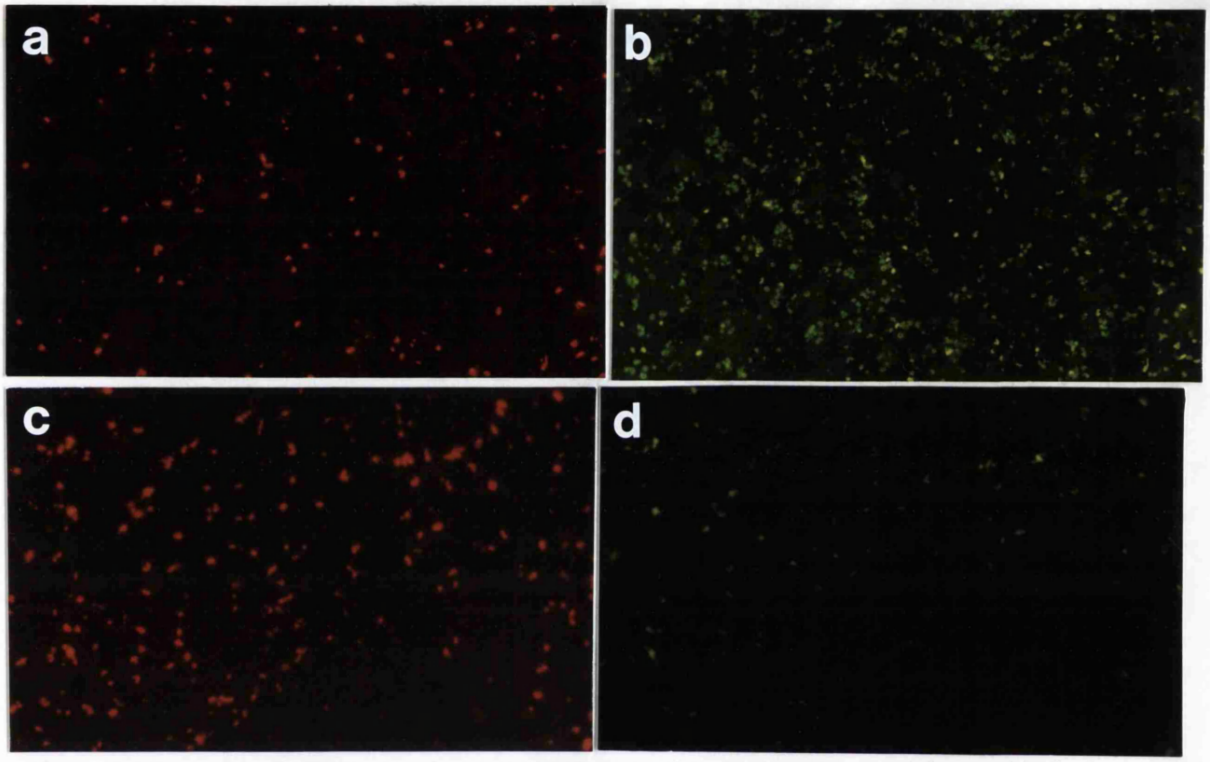

Figure 3.19. Immunofluorescent micrographs of cultured control (**a** & **b**) and dystrophic (**c** & **d**) rat RPE challenged with ROSs for 2 hours. Attached ROSs were identified with TRITC (**a** & **c**) and both attached and internalised ROSs were identified with FITC (**b** & **d**). The difference between the number of red dots (**a**) and the number of green dots (**b**) indicates that control RPE have internalised a large number of ROSs. Whereas in dystrophic RPE there appears to be almost equal numbers of red (**c**) and green (**d**) dots thus far fewer ROS have been ingested. (Magnification **a-b** x160, **c-d** x250).

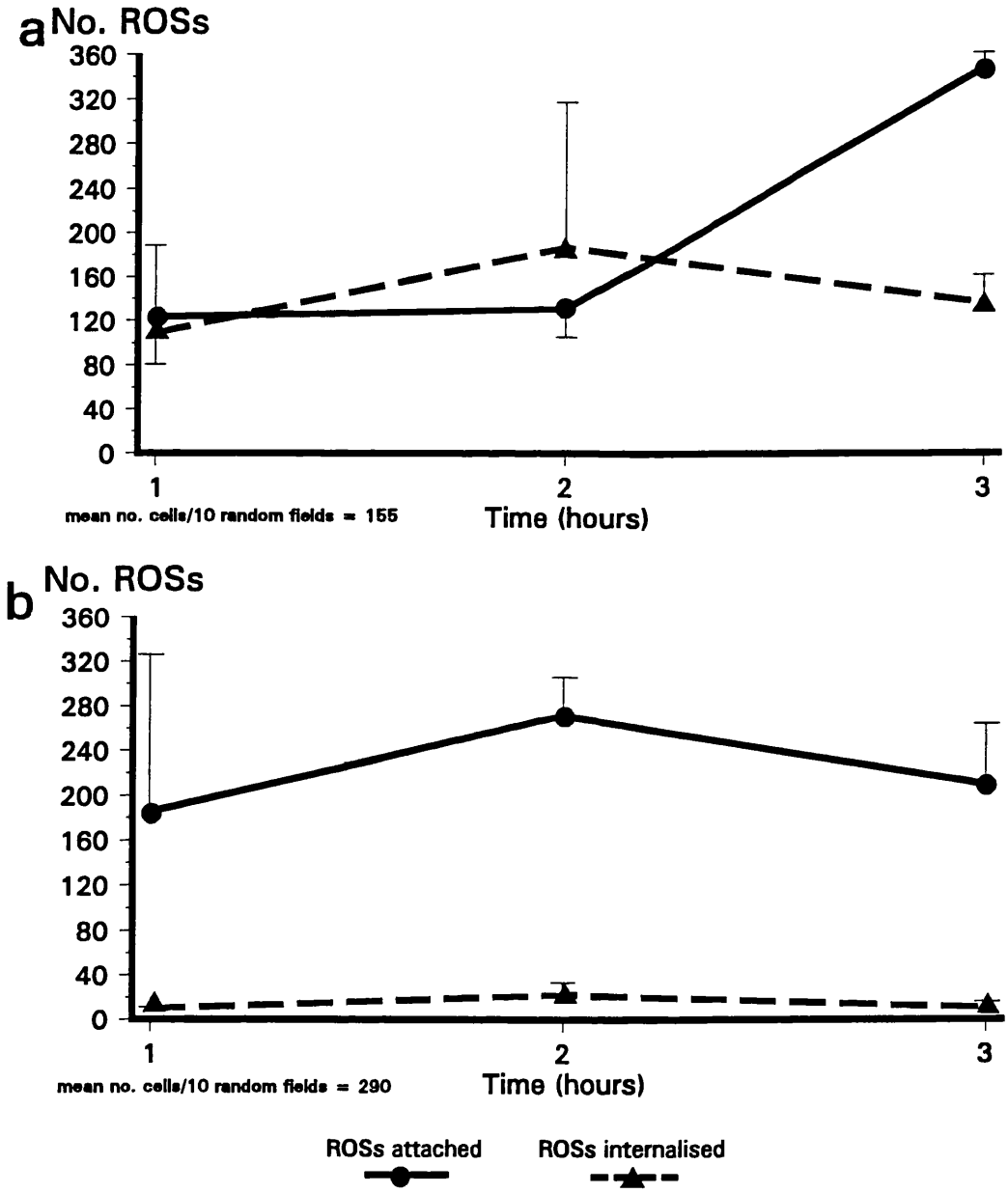

Figure 3.20. Phagocytosis of ROSs by cultured RCS rat RPE. RPE cells were challenged with ROSs for 1, 2 and 3 hours. Bars show SE. a) Mean number of ROSs attached and internalised by control cells. Each point was generated from counts taken from 2 cultures. Maximum internalisation of ROSs was seen at 2 hours (Student's t-test, $p<0.01$). b) Mean number of ROSs attached and internalised by dystrophic cells. Each point was generated from counts taken from 5 cultures. Significantly more ROSs were attached at 2 hours than at 3 hours (Student's t-test, $p<0.01$). Thus 2 hours is an optimum time for ROS challenge where there is maximum phagocytosis (control) and attachment (dystrophic). Comparing the number of ROSs attached at 2 hours and the mean number of cells there are approximately 0.85 ROSs/cell (control) and 0.94 ROSs/cell (dystrophic).

2½ times more dystrophic cells than control cells and this may account for the superior ROS attachment seen in dystrophic cells, however this further emphasises the ability of control cells to internalise ROSs.

Control rat RPE cells showed optimal ROS phagocytosis and dystrophic RPE cells show optimal ROS attachment at 2 hours of ROS challenge. As a result further investigations of ROS phagocytosis were conducted at this time period.

3.3.4. Phagocytosis of ROS by control and dystrophic cultured RCS rat RPE cells.

Monodispersed cultures of control and dystrophic RPE cells were challenged with ROSs for 2 hours. Using a combination of immunofluorescence and DIC both the ROSs and RPE cells were visualised (Fig. 3.21.). Attached and internalised ROSs were identified (Fig. 3.21a). When compared to the corresponding DIC micrograph (Fig. 3.21b) it was clear that some cells were devoid of ROSs and this was true for both control and dystrophic cells. The proportion of cells that accumulated ROSs was quantified. Both the number of cells, and the number of ROSs, were counted as described previously (see 2.5.1.) from 10 control and 6 dystrophic cultures (see Appendix IV.). The data is expressed as the percentage of cells with and without ROSs by the two cell types and as the percentage of ROSs attached and internalised (Fig 3.22.).

In control RPE 71.8% of cells accumulated ROSs (with ROSs) and 29.3% of cells were devoid of ROSs (without ROSs), whereas 57.8% of dystrophic cells had accumulated ROSs and 42.2% were without ROSs (Fig. 3.22a). The number of cells with ROSs was significantly greater in control cultures than dystrophic (Chi-squared, $p<0.01$, Fig 3.22a).

Both control and dystrophic RPE attached and internalised ROSs (Fig. 3.22b). Control RPE attached and internalised similar amounts of ROSs (attached 59.5%, internalised 40.5%). Whereas, dystrophic RPE attached more ROSs (95%) than they internalised (5%) and this difference was significant (Student's t-test $p<0.01$, Fig. 3.22b). Control RPE attached a total of 2852 and internalised 1941 ROSs whereas dystrophic cells attached and internalised a total of 1430 and 76 ROSs, respectively. Chi-squared analysis showed this difference to be significant ($p<0.01$). It is apparent that cultured dystrophic RPE, when compared to control, had a reduced ability to phagocytose ROSs.

The results indicate that in both control and dystrophic rat RPE in vitro there is a variability in the ability of cells to attached and consequently internalise isolated bovine ROSs.

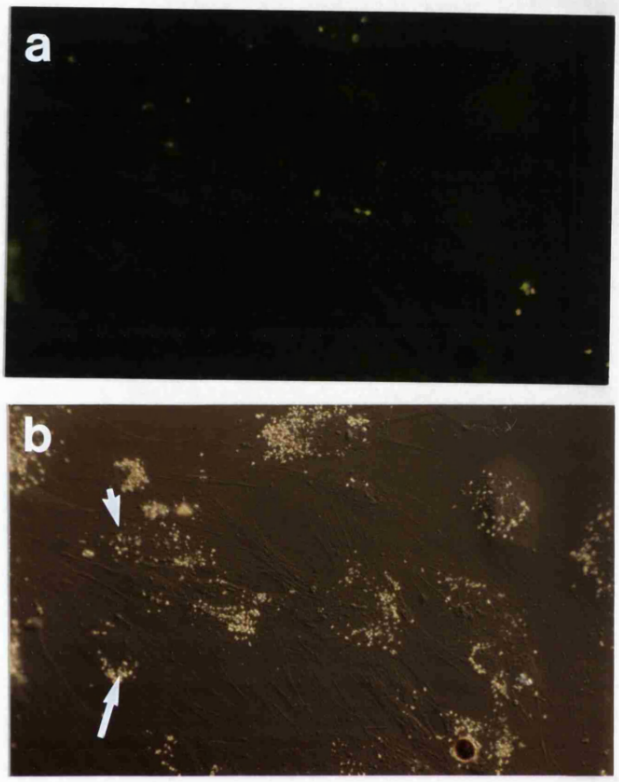

Figure 3.21. Immunofluorescent micrographs (**a**) and DIC (**b**) of cultured rat RPE challenged with ROSs for 2 hours. **a**) Attached and internalised ROSs were identified with FITC. **b**) Corresponding DIC showing confluent RPE cells. Comparing the immunofluorescent and DIC micrographs rat RPE showed variation in ROS attachment and internalisation. ROSs were present in some cells (small arrow), whilst other cells were devoid of ROSs (large arrow). (Magnifications **a** & **b** x225).

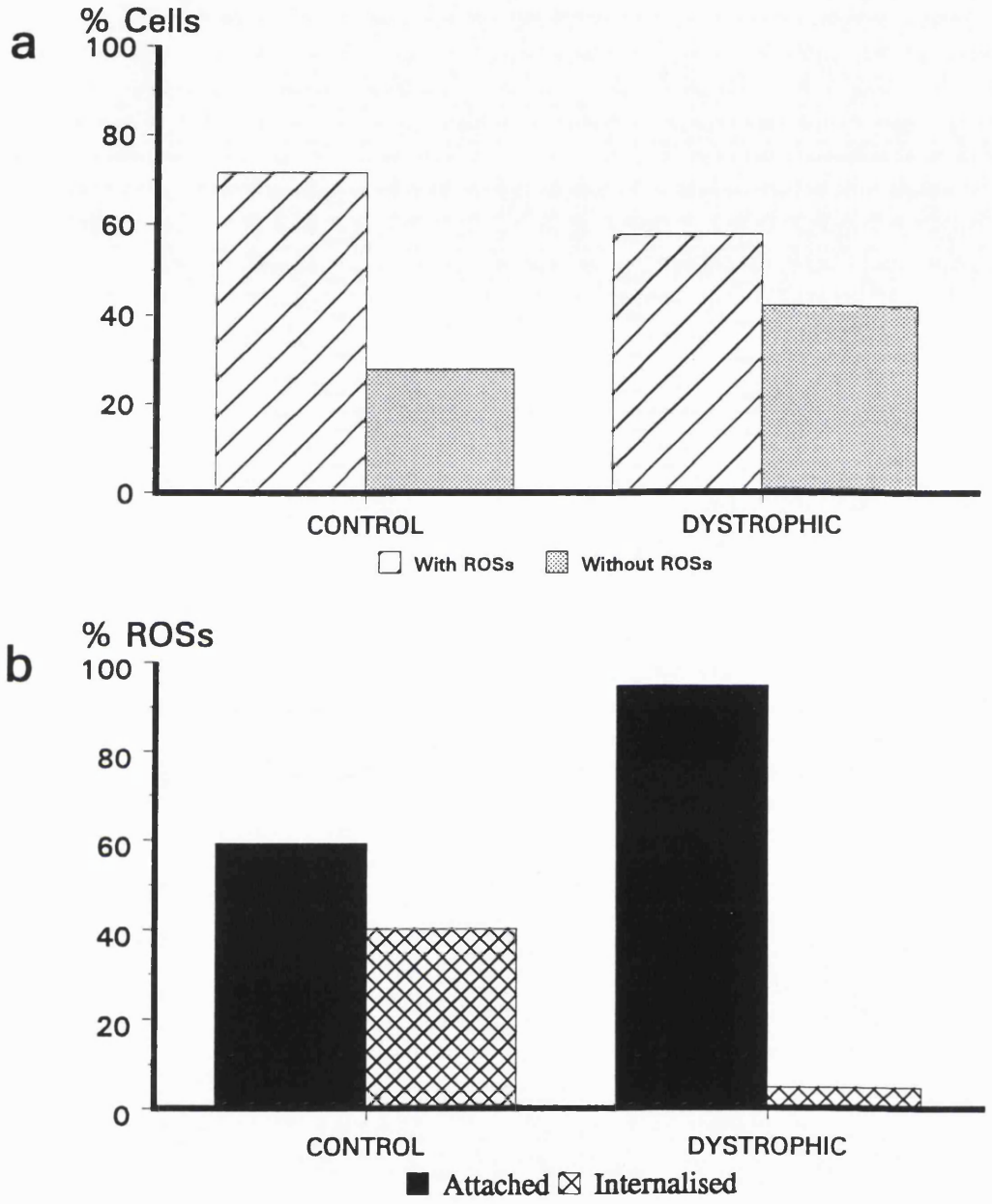

Figure 3.22. Phagocytosis of ROSs by monodispered cultures of control and dystrophic rat RPE. Cells were challenged for 2 hours. The data was generated from 10 control and 6 dystrophic cultures. a) Percentage of RPE cells that accumulated ROSs (with ROSs) and that were devoid of ROSs (without ROSs). There were more cells with ROSs than without ROSs in control cells. In dystrophic cultures there were similar proportions of cells with and without ROSs. The number of cells with ROSs was significantly greater in control than dystrophic (Chi-squared, $p<0.01$). b) Percentages of ROSs. Control RPE attached and internalised a similar amounts of ROSs, but dystrophic attached more ROSs than they internalised. Dystrophic RPE, compared to control, had a reduced ability to phagocytose ROSs (Chi-squared, $p<0.01$).

3.3.5. The variation in phagocytosis of ROSs by control and dystrophic RCS rat RPE.

The variation in the ability of rat RPE to attach and internalise ROSs was investigated using islands of RPE challenged with ROSs for 2 hours. Using immunofluorescent microscopy a remarkable pattern of ROS attachment was seen in islands of control and dystrophic cells (Fig. 3.23a & b). Fluorescently labelled ROSs whether attached (Fig. 3.23a) or internalised (Fig. 3.23b) formed a doughnut-like pattern in the islands. At higher magnifications a comparison of an immunofluorescent micrographs (Fig. 3.23c) with the corresponding DIC micrographs (Fig. 3.23d) of RPE islands revealed that the cells at the centre and the edge of the island were devoid of ROSs (attached and internalised) and half way between the centre and the edge of the RPE island there was a zone of cells which avidly attached and internalised ROSs. From the figure the intermediate cells accumulated about 30 times more ROSs in the centre and 8 times more ROSs than cells at the edge of an island.

The ROSs were counted from whole islands of rat RPE (data see Appendix V.). The counts showed that the just under 35% and 40% of control and dystrophic cells, respectively, accumulated ROSs and 65.3% (control) and 60.16% (dystrophic) cells were devoid of ROSs (Fig. 3.24a). Chi-squared analysis showed that in islands of both control and dystrophic cells there was no significant difference in the proportion of cells with or without ROSs. The proportion of cells in the islands with and without ROS were similar to those proportions in monodispersed cultures.

The phagocytic profile in islands of RPE was similar to that seen in monodispersed cultures (Fig. 3.24b). Control RPE attached 58.8% of ROSs and internalised 41.2% of ROSs. Whereas, dystrophic RPE attached 88.8% of ROSs and internalised only 11.2% ROSs. Chi-squared analysis of the data showed that control RPE internalised more ROSs than dystrophic RPE and the latter had a reduced ability to phagocytose ROSs ($p<0.01$).

The results indicate that islands of RPE exhibited the same phagocytic profile and the variation of ROS attachment and internalisation that was seen in monodispersed cultures. However, unlike monodispersed cultures, attached and internalised ROSs showed a distinct distribution pattern on islands of RPE. This pattern was zonal and appeared to be linked to the position of the cell within the island. SEM of islands of RPE revealed 3 types of regionally distinct cell morphologies zonally arranged (see 3.1.2.) therefore, the pattern of ROS attachment and internalisation and cell morphology was investigated.

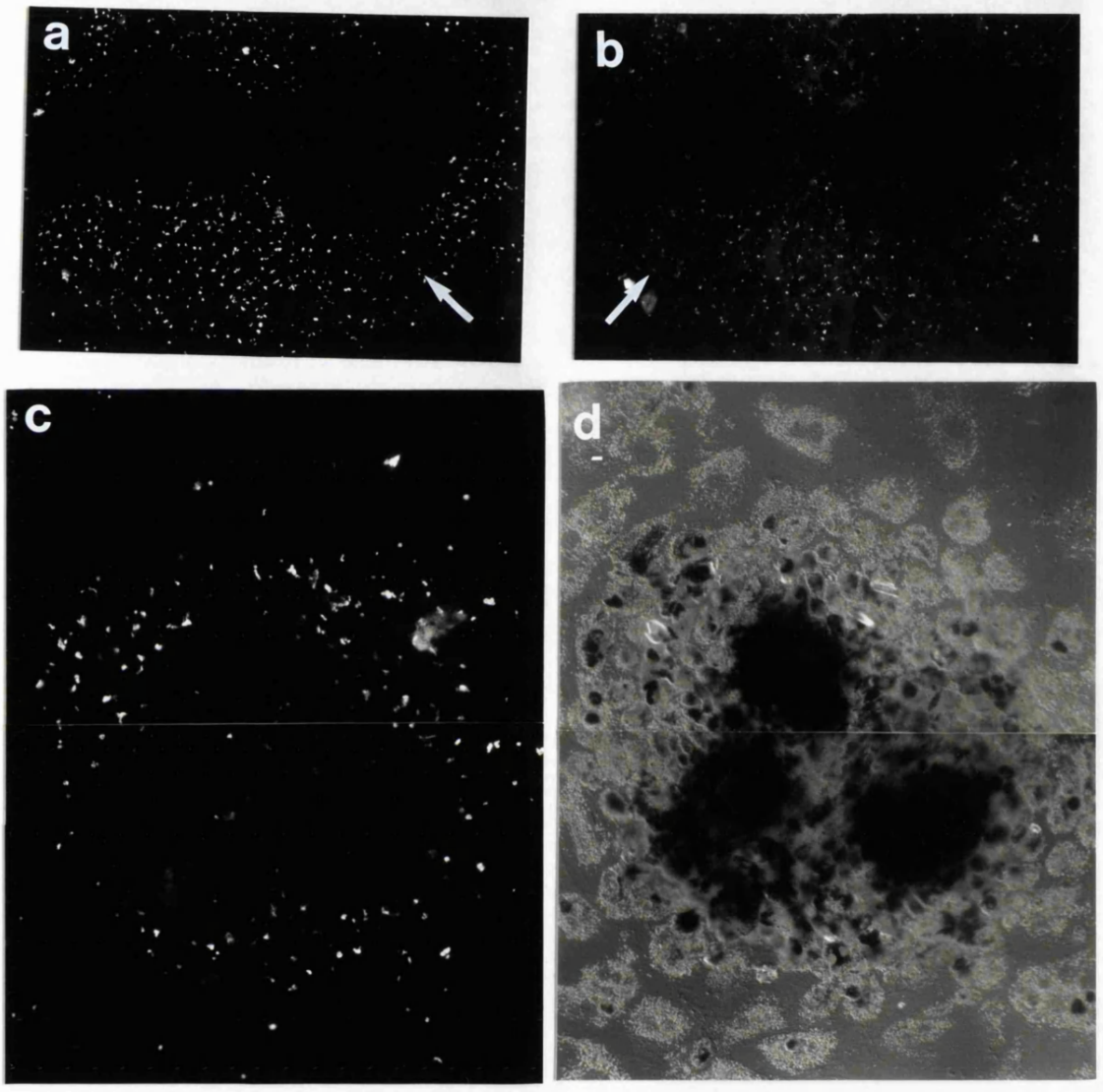

Figure 3.23. Immunofluorescent micrographs (**a-c**) and DIC micrograph (**d**) of islands of cultured dystrophic rat RPE. In islands of RPE, TRITC labelled ROS (**a**; attached) and FITC labelled ROSs (**b**; internalised) formed a doughnut-like pattern. ROSs appeared to accumulated in a distinct zone of cells (arrow). **c**) The doughnut-like pattern of attached and internalised ROSs was compared to the DIC micrograph of the RPE island (**d**). The zone in which most of the ROSs were found consisted of intermediate cells. Three ROSs were identified at the centre, 90 ROSs accumulated at the intermediate cell zone and 11 ROSs were associated with cells at the edge of the island. (Magnifications **a-b** x100; **c-d** x200).

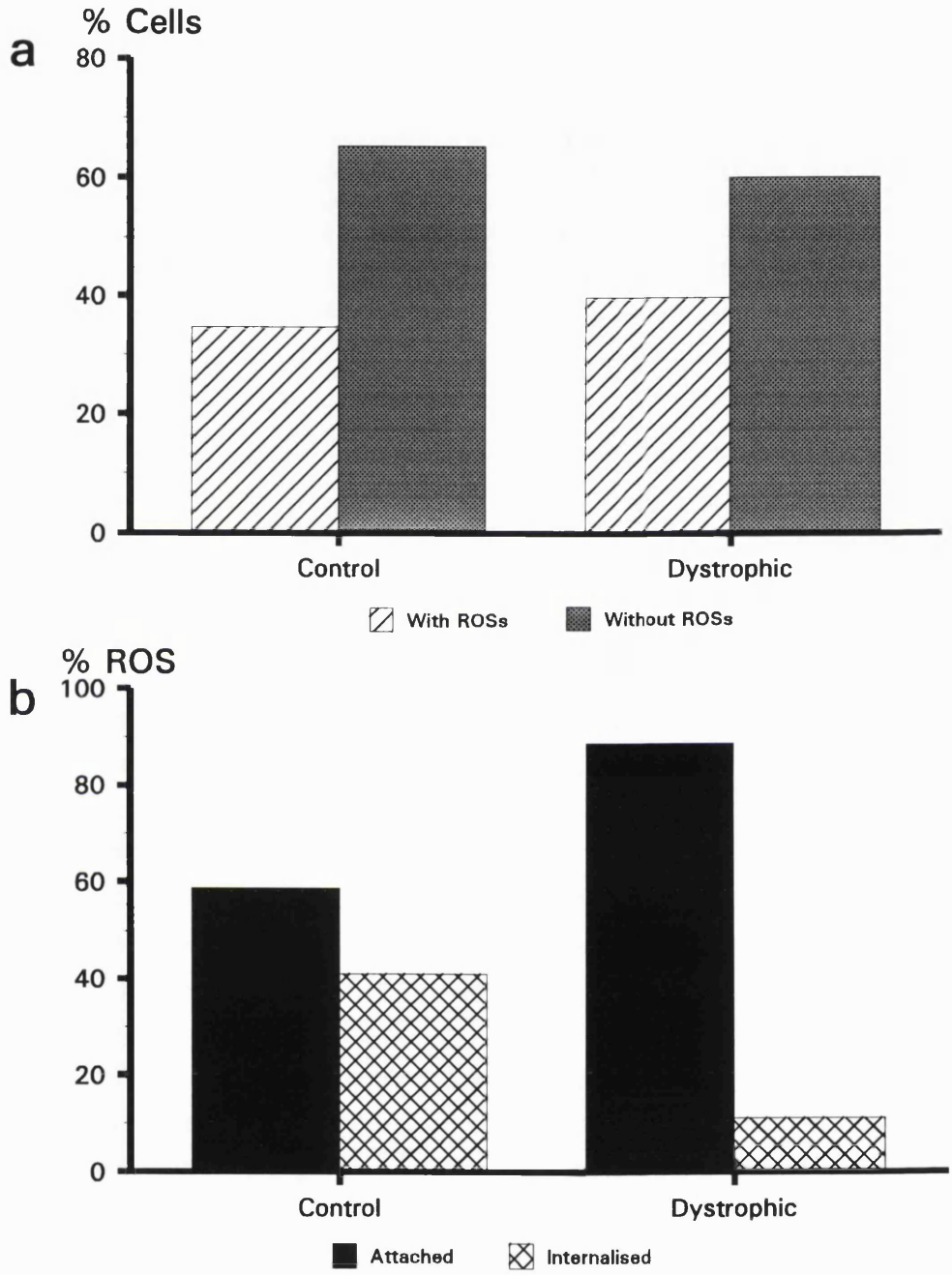

Figure 3.24. Phagocytosis of ROSs in islands of cultured control and dystrophic RPE. Cells were challenged for 2 hours. The data was generated from 4 control and 10 dystrophic RPE islands. a) Islands of RPE from both control and dystrophic tissue had the similar proportion of cells with and without ROSs (chi-squared $p > 0.01$). b) Percentages of ROSs. Control cells attached and internalised similar amounts of ROSs, but dystrophic show a reduced ability to phagocytose ROSs (Chi-squared, $p < 0.01$).

3.3.6. SEM of islands of rat RPE challenged with ROSs.

SEM was used to illustrate the pattern of ROS association in islands of RPE. SEM showed that cells at the centre of an island of RPE, which had previously been described as cuboidal cells, had a multitude of long surface microvilli (see 3.1.2.). The cuboidal RPE were always found to have very few or no ROSs attached to their cytoplasm (Fig. 3.25a). However, some of the flattened, well spread discoid-shaped cells at the periphery attached some ROSs (Fig. 3.25b). Although many of the peripheral cells were also devoid of ROSs. Cells which were located in the intermediate zone had an abundance of ROSs on their surface (Fig. 3.25c). At high power these ROSs were intimately associated with stumpy surface microvilli (Fig. 3.25d). SEM showed that the distinct doughnut-like pattern of ROS accumulation revealed by immunofluorescence in islands of RPE (see 3.3.5.) appeared to be related to cell morphology.

3.3.7. Investigation of ROS association and cytokeratin expression.

Previously it had been noted that anti-cytokeratin MABs revealed a distinctive staining pattern for cytokeratin IFs in rat RPE and the pattern appeared to be related to the location of the cell within the island (see 3.2.1.). Consequently as ROS accumulation also appeared to be related to the position and morphology of the cell in an island, island cultures of RPE were challenged with ROSs and both ROS phagocytosis and cytokeratin staining was investigated. MAB RGE 53 was used to identify cytokeratin IFs, because only this MAB had indicated a difference in the staining pattern between control and dystrophic rat RPE (see 3.2.1.)

Cultures of islands of control and dystrophic rat RPE cells were challenged with ROSs for 1, 2 and 3 hours. A time course was chosen in this case, so that information correlating K18 expression with peaks in ROS attachment (2 hours, control & dystrophic) and internalisation (3 hours, control) could be made (Fig. 3.20). Using double immunofluorescent labelling procedure ROSs were labelled with FITC (attached and internalised could not be differentiated) and K18 filaments were labelled with TRITC (see 2.5.3.).

MAB RGE 53 identified staining type C, where only a proportion of cells stained, in islands of RPE challenged with ROSs (see 3.2.1.). A combination of immunofluorescent and DIC micrographs visualised both ROSs and K18+ and K18- cells (Fig. 3.26). This technique revealed a combination of patterns between K18 expression and ROS accumulation, which was true for both control and dystrophic cells. In some cells the majority of ROSs appeared only to be accumulated by K18- cells and K18+ cells accumulated very few ROSs (Fig. 3.26a-c). However, the opposite was also seen where K18+ cells accumulated most of the ROSs. This exclusive accumulation by

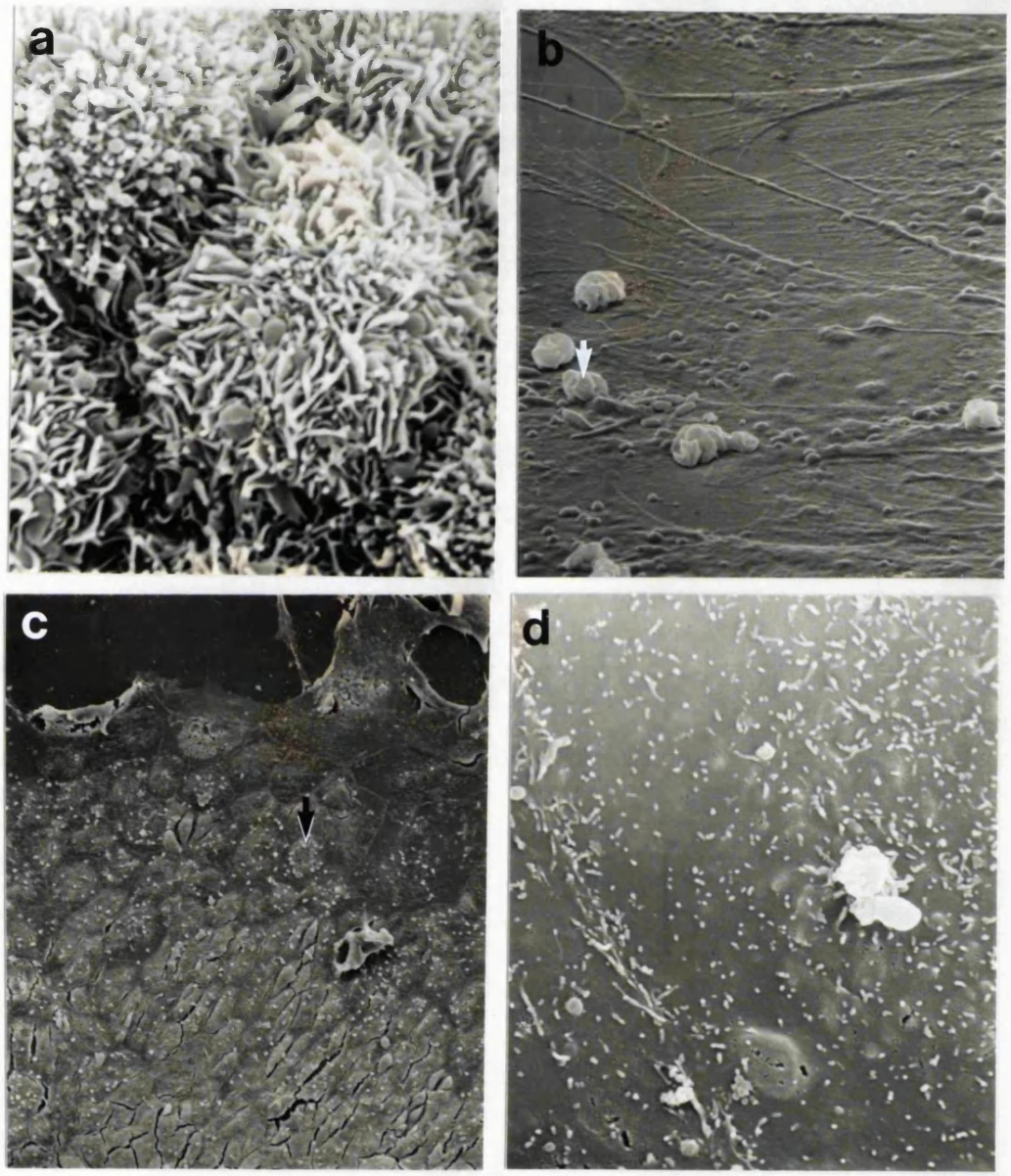

Figure 3.25. SEM micrographs of islands of dystrophic rat RPE revealed the morphology of the cells that did and did not accumulate ROSs. Cell were challenged with ROSs for 2 hours. **a**) Cuboidal cells in the centre of the island had numerous long microvilli, but were often devoid of ROSs. **b**) Well spread, flattened, peripheral cells in the main were devoid of ROSs, although some cells did attach ROSs (white arrow) **c**) Cells in the intermediate zone of the RPE island had an abundance of ROSs on the surface of cells (black arrow). d) ROSs present on the surface of intermediate cells were associated with small stumpy surface microvilli. (Magnifications **a** x 4,000, **b** x2,500, **c** x125, **d** x5,000).

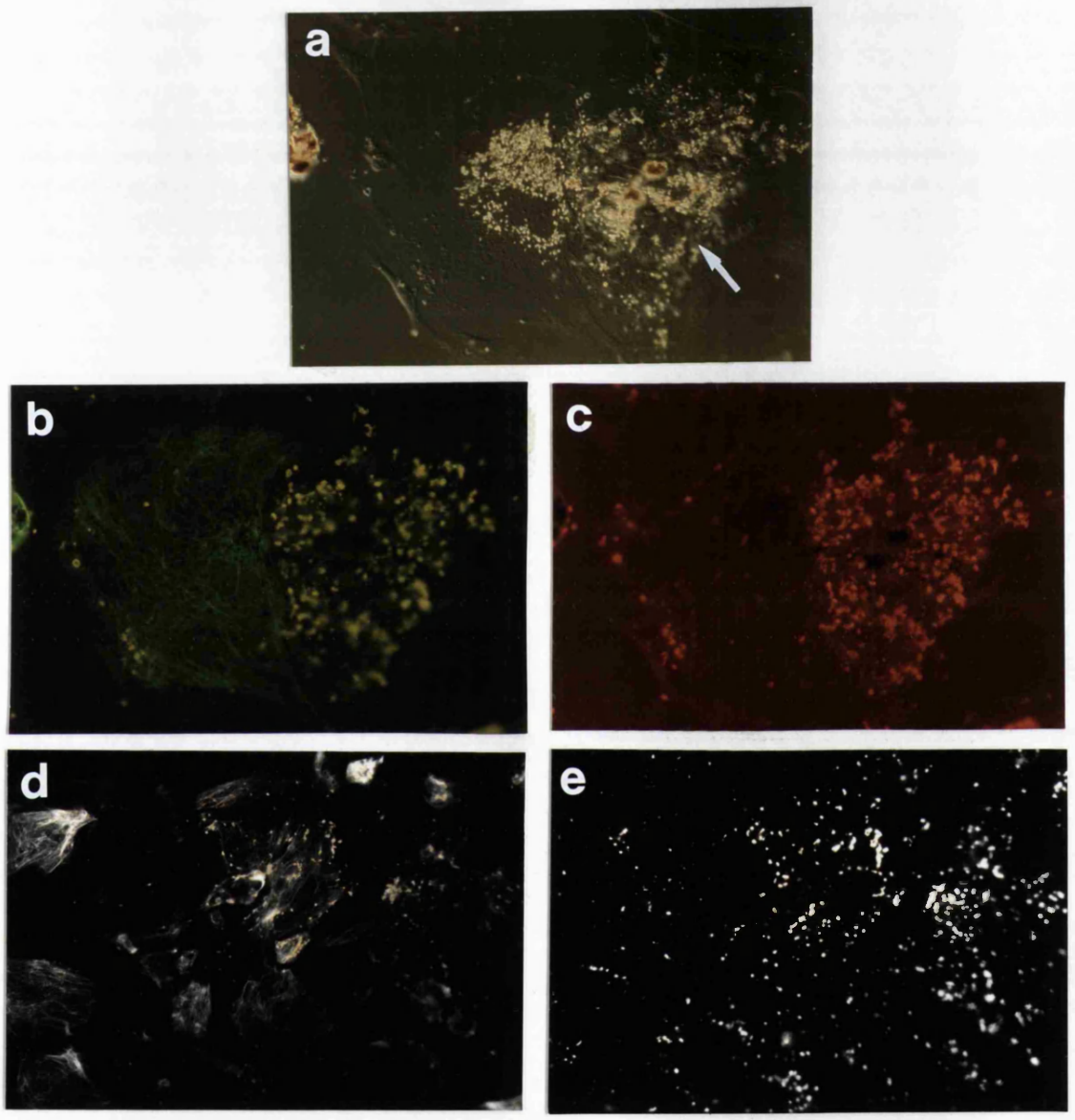

Figure 3.26. DIC micrograph (**a**) and immunofluorescent micrographs (**b-e**) of an island rat RPE (dystrophic) challenged with ROSs for 2 hours. K18 IFs identified with MAB RGE 53 were labelled with FITC (**b** & **d**). ROSs identified with MAB 1F4 were labelled with TRITC (**c** & **e**). **a**) Two adjacent peripheral cells. Cells were large well spread and contained brown pigmentation (arrow) **b**) The cell on the left contained K18+ filaments and the cell on the right was K18-. **c**) An abundance of ROS were present on the K18- cell however, the K18+ cell only accumulated a few ROSs. This exclusive accumulation of ROSs by K18- cells was not seen in all cultures of control and dystrophic RPE. **d**) Intermediate cells, which showed a large variation in K18 staining patterns, often accumulated similar amounts of ROSs by both K18+ and K18- cells with divergent staining patterns (**e**). (Magnifications **a-c** x250, **d-e** x100).

either K18+ or K18- cells was common in cells at the periphery. However, in some cultures of control and dystrophic RPE, K18 expression appeared unrelated to ROS attachment and phagocytosis. This was particularly evident in intermediate cells, where K18+ cells as well as K18- cells accumulated similar amounts of ROSs (Fig. 3.26d-e).

The amount of ROS accumulated by K18+ and K18- cells was counted as described previously (see 2.5.3.). The data (see Appendix VI.) was generated from a total of 8 control cultures (3 cultures challenged for 1 & 2 hours and 2 cultures challenged for 3 hours) and 9 dystrophic cultures (3 for all three time intervals). From this data, combining counts from all time intervals, the population of K18+ and K18- rat RPE cells were similar for control and dystrophic tissue (Appendix VI.). Here just under 51% were K18+ and just over 49% K18- in control cells and 58% were K18+ and 42% K18- in dystrophic cells. The data for ROSs accumulation and K18 expression was expressed as the mean number of ROSs accumulated at each time interval by K18+ and K18- cells (Fig 3.27a & b) and as the number of ROSs accumulated by the K18+ and K18- cell populations in each culture (Fig. 3.27c & d).

The profile of ROSs accumulation and expression of K18 appeared to be consistent at all 3 time intervals in both control and dystrophic cells (Fig. 3.27a & b). In control RPE there was a trend suggesting that more ROSs were accumulated with K18- cells than K18+ (Fig. 3.27a), whereas in dystrophic cells this trend was reversed where more ROSs appeared to be accumulated with K18+ cells (Fig. 3.27b). Indeed in control cells the K18- cells significantly accumulated more ROSs (Student's t-test, $p<0.01$), whereas in dystrophic cells there was no difference in the amount of ROSs accumulated with K18+ and K18- cells (Student's t-test $p>0.1$).

The relationship between the amount of ROSs accumulated by the two K18 cell populations was expressed in figure 3.27 c & d. The number of ROSs accumulated to the K18+ and K18- populations appeared to be similar in control cultures. However, there were 2 data points which recorded between 2½-4½ times more ROSs than the rest of the data and both of these were for K18- cells. The significant difference in the amount of ROSs accumulated between K18+ and K18- control cells (see above) may have been influenced by these two large values. In dystrophic cells the two K18 cell populations appeared to accumulate similar amounts of ROSs.

Comparing K18+ cell populations between control and dystrophic tissue, there were far more ROSs accumulated by dystrophic cells than with control cells (Student's t-test, $p<0.01$). Whereas there was no difference in the number of ROSs accumulated by the K18- cell populations between the two cell types.

There was considerable variation in the number of ROSs accumulated by apparently the same number of cells (Fig. 3.27c & d). In control cells, for example, 40 cells accumulated 809 ROSs and yet in another culture 116 ROSs were accumulated by the same number of cells. In dystrophic cells from one culture 60 cells accumulated 143 ROSs, whereas 392 ROSs were accumulated by 60 cells in another culture (see also

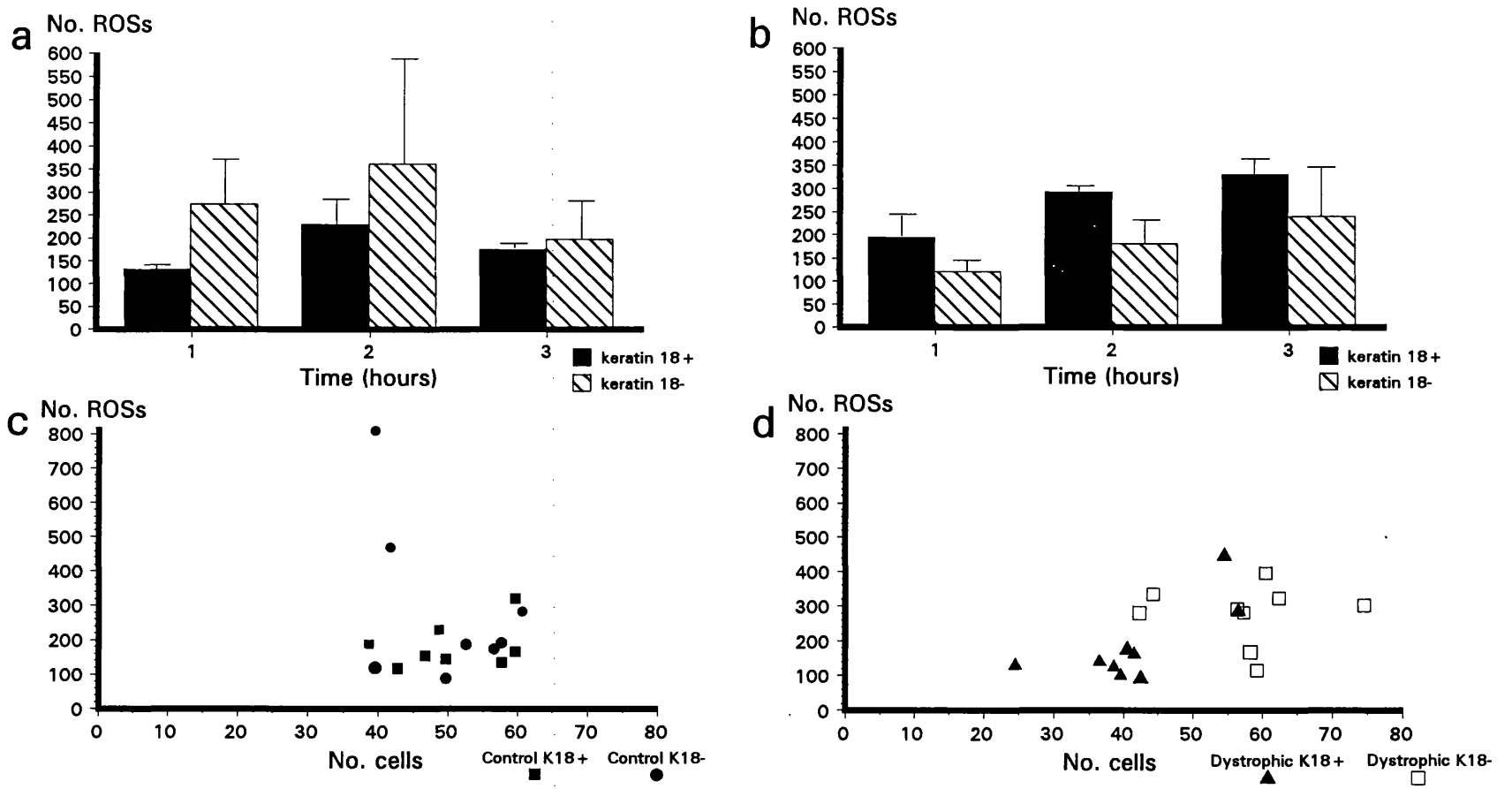

Figure 3.27. The effect of ROS accumulation on the expression of K18 in control (**a** & **c**) and dystrophic (**b** & **d**) rat RPE cells. **a** &**b**).Mean number of ROSs (Bar +/- SE) accumulated by K18+ and K18- cell populations at 1, 2, and 3 hours.**a)** In control cells significantly more ROSs were accumulated by K18- cell population (Student's t-test, $p < 0.01$), whereas in **b)** dystrophic cells both types of K18 populations accumulated similar numbers of ROSs (Student's t-test, $p < 0.01$). **c** &**d**) The relationship between the number of ROSs acuumulated by K18+ and K18- cell population. **c)** In control cells similar numbers of cells accumulated similar numbers of ROSs. Whereas in dystrophic cells **(d)** the K18+ and K18- populations appear more diverse. The K18+ population is a smaller group with fewer number of ROSs when compared to the K18- population (Student's t-test, $p < 0.01$).

data Appendix VII.).

The variation in phagocytosis which was seen previously (3.3.4. & 3.3.5.) was also evident and the data showing the number of cells with and without ROSs are presented in the table in figure 3.28. Using a Mantel-Haenszel procedure for stratified data in control cultures a significantly higher proportion of K18+ cells were without ROSs ($p=0.018$, prevalence ratio=35.64/27.85=1.28, confidence limits 1.04-1.57). However, in dystrophic RPE the situation was reversed with a higher proportion of K18- cells without ROSs ($p=0.018$, prevalence ratio=22.75/29.74 =0.70, confidence limits 0.61-0.96). The significant difference between the prevalence ratio of the control and dystrophic cells establishes that this reverse phenomenon is real and not a sampling phenomenon. In the K18+ cells, comparing control and dystrophic RPE there was a significantly higher proportion of control cells devoid of ROSs ($p=0.00002$, prevalence ratio = 35.64/22.75 = 1.57, confidence limits 1.27-1.93). Whereas, there was no difference in the proportion of K18- cells without ROSs between control and dystrophic RPE ($p=0.56$, prevalence ratio = 27.85/29.74 = 0.94, confidence limits 0.75-1.17).

3.4. PROLIFERATION

Pre-confluent cultures of human RPE cells were grown and LabTeks and proliferating cells were identified by two proliferation markers, BrdU and PCNA (see 2.6.1. and 2.6.2, respectively). Expression of both K18 and K19 (the latter a subset of K18, see 3.2.2.) were investigated in conjunction with incorporation of BrdU, whereas only expression of K18 was investigated in conjunction with PCNA. This was because BrdU is a well known marker of cell proliferation and it specifically labels the S-phase of the cell cycle. PCNA, on the other hand is a relatively new marker of proliferating cells, it identifies of a wider spectrum of the cell cycle and was therefore used only to confirm the results from the BrdU investigations.

A combination of immunoperoxidase and immunofluorescent staining was used to identify BrdU and K18 (see 2.6.1.). Under DIC microscopy BrdU positive (BrdU+) cells had black nuclei (Fig. 3.29a) and cells positive for K18 were visualised by immunofluorescence (Fig. 3.29b). A double immunoperoxidase procedure was used to identify BrdU and K19 (see 2.6.1.) and both BrdU labelled nuclei and K19 filaments were visualised in bright field micrographs (Fig. 3.29c). Some cells co-labelled for both the proliferation marker and the cytokeratins (Fig. 3.29.) however, the majority of cells labelled with BrdU did not stain for either K18 or K19.

BrdU labelling and cytokeratin expression in human RPE cells was quantified. Cells were counted as described previously (see 2.6.1.) and the data is given in Appen-

	Type of K18 population	Total no. of cells	No. of cells with ROSs	No. of cells without ROSs	% cells without ROSs
Control	K18+	404	144	260	35.6
	K18−	395	110	285	27.9
Dystrophic	K18+	510	116	394	22.8
	K18−	380	113	267	29.7

Figure 3.28. The number of cells with and without ROSs in the K18+ and K18− cell populations of cultured control and dystrophic rat RPE.

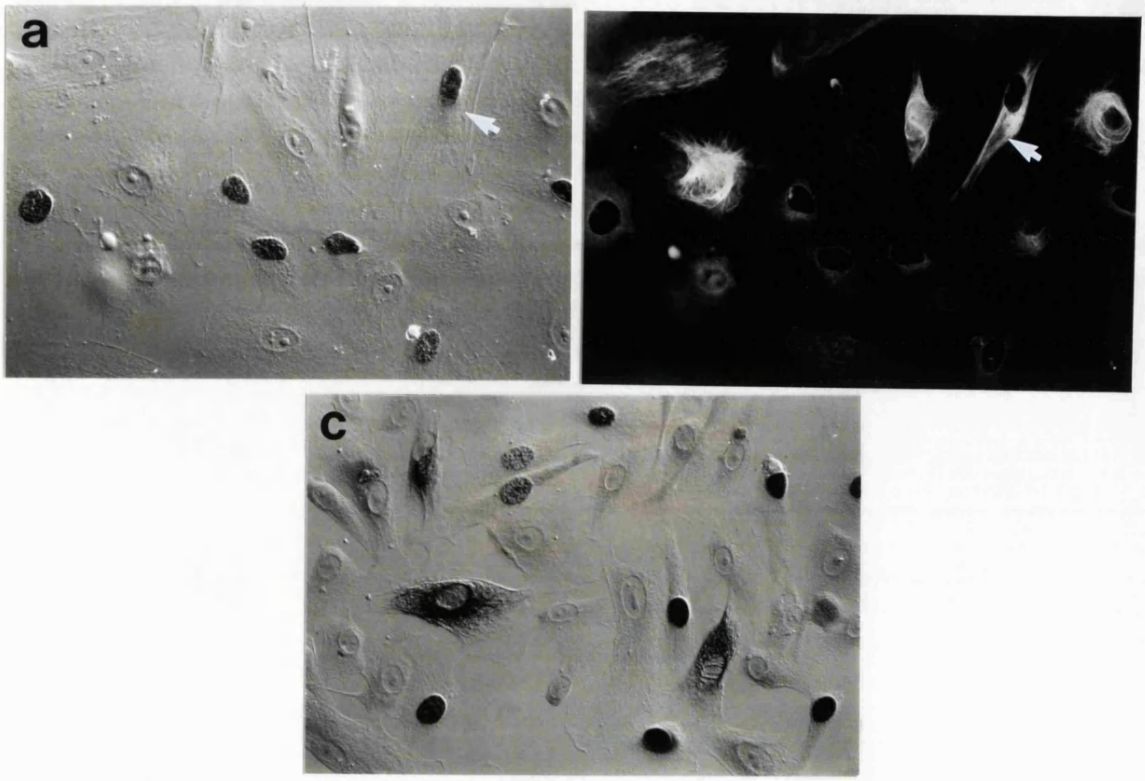

Figure 3.29. DIC (**a** & **c**) and immunofluorescent (**b**) micrographs of pre-confluent human RPE cells. Proliferating cells were labelled with BrdU and identified using MAB anti-BrdU. K18 or K19 were identified in the same cells using MAB RGE 53 or MAB K4.62, respectively. **a** & **b**) Cells stained for BrdU (immunoperoxidase) and K18 (immunofluoresecent). **a**) Cultures of human RPE contained a sub-population of proliferating cells, which were identified by their black nuclei. **b**) The same cells also contained a sub-population of K18+ cells. Comparing DIC and immunofluorescent micrographs some cells co-labelled for BrdU and K18 (arrow). **c**) Cells stained for BrdU and K19 (double immunoperoxidase). Sub-populations of BrdU+ and K19+ cells were revealed, however most cells that were K19+ were not positive for BrdU. (Magnifications **a-c** x200).

dix VIII. The results revealed that in these cells between 31.9% and 35.9% labelled positively for BrdU. In the BrdU+ population only 3.3% expressed K18 and 5.8% expressed K19, whereas in the BrdU negative (BrdU-) population 87.5% of cells were K18- and 84% were K19-. Using PCNA (for data see Appendix IX.) the same trend seen with BrdU and K18 was also prevalent with PCNA and K18. There was a far smaller proportion of cells in the PCNA+/K18+ subset (10.7%) than in the PCNA-/K18+ (16.4%) and the largest sub-set of cells were PCNA+/K18- (89.3%).

The apparent poor colabelling of K18 and K19 with proliferation markers indicate that K18 and K19 are not associated with proliferation and this supported by growth curve experiments. Growth curves of human RPE were established on two types of substrate, glass (LabTek) and plastic (Tissue culture flask) and at 12, 24, 48 and 72 hours cells were stained for K18 (see 2.6.1.). As K19+ cells is a sub-set of K18+ cells staining was conducted only for K18 in growth curve experiments. Both glass and plastic substrates were used to ensure cytokeratin expression was not affected by the nature of the substrate. Stained and unstained cells were counted as described previously (see 2.6.1.) from six LabTeks and six 25cm^2 flasks (see Appendix X.) and the data was expressed as the number of cells and the percentage of K18+ cells against time (Fig. 3.30.).

In both LabTeks and flasks there was as increase in the overall cell population between 12-72 hours, during which time there was either only a slight increase, in the case of LabTeks (Fig. 3.30a) or no increase, in the case of flasks (Fig. 3.30b), in the number of cells expressing K18. Between 24-72 hours there was a marked increase in cell numbers (Fig 3.30a & b). However, despite this period of marked cellular proliferation the percentage of human RPE staining for K18 dramatically decreased from 12 hours onwards on both substrates (Fig. 3.30c & d).

The largest percentage of cells expressing K18 was at 12 hours, the shortest time interval. To establish the complete profile of K18 expression growth curves of human RPE were set up including pre-12 hour time intervals. Cells were grown in tissue culture flasks (only flasks were used seen as the choice of substrate appeared to have no effect on the cytokeratin expression) and cells were stained for 2, 4, 12, 24 & 72 hours. The data generated from 6 flasks (see Appendix X.) was expressed as described above and are shown in figure 3.31.

Between 2-72 hours there was almost no change in the number of K18+ cells (Fig. 3.31a) and in particular there was no change in the number of K18+ cells between 24-72 hours, a period of acute cell proliferation. The proportion of K18+ cells varied with time (Fig. 3.31b). At 4 hours K18+ cells represented over 50% of the total cell population. Thereafter there was a steady decrease in the percentage of K18+ cells up to confluence at 72 hours.

The results from both the proliferation markers and growth curves indicate that

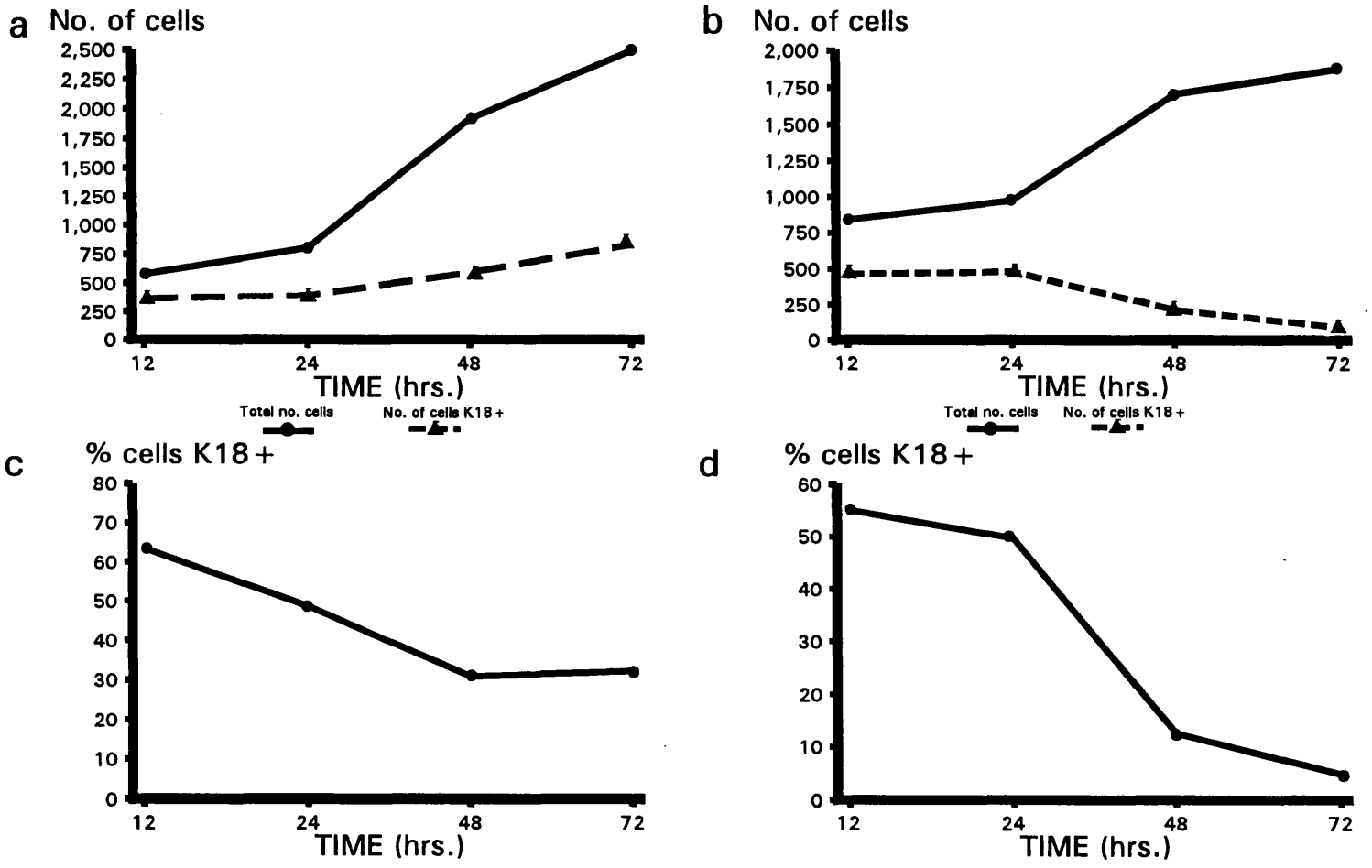

Figure 3.30. Growth curve of cultured human RPE and the expression of K18. Cells were grown in 6 LabTeks (**a** &**c**) and 6 flasks (**b** &**d**) at 12, 24, 48 & 72 hours.**a** & **b**) As the cell population increased over 72 hours in culture the number of K18+ cells either increased slightly (LabTeks) or showed no increase (flasks). **c** & **d**) During this time the percentage of K18+ cells decreased with time in both the Labteks and flasks. The largest percentage of K18+ cells was seen at 12 hours.

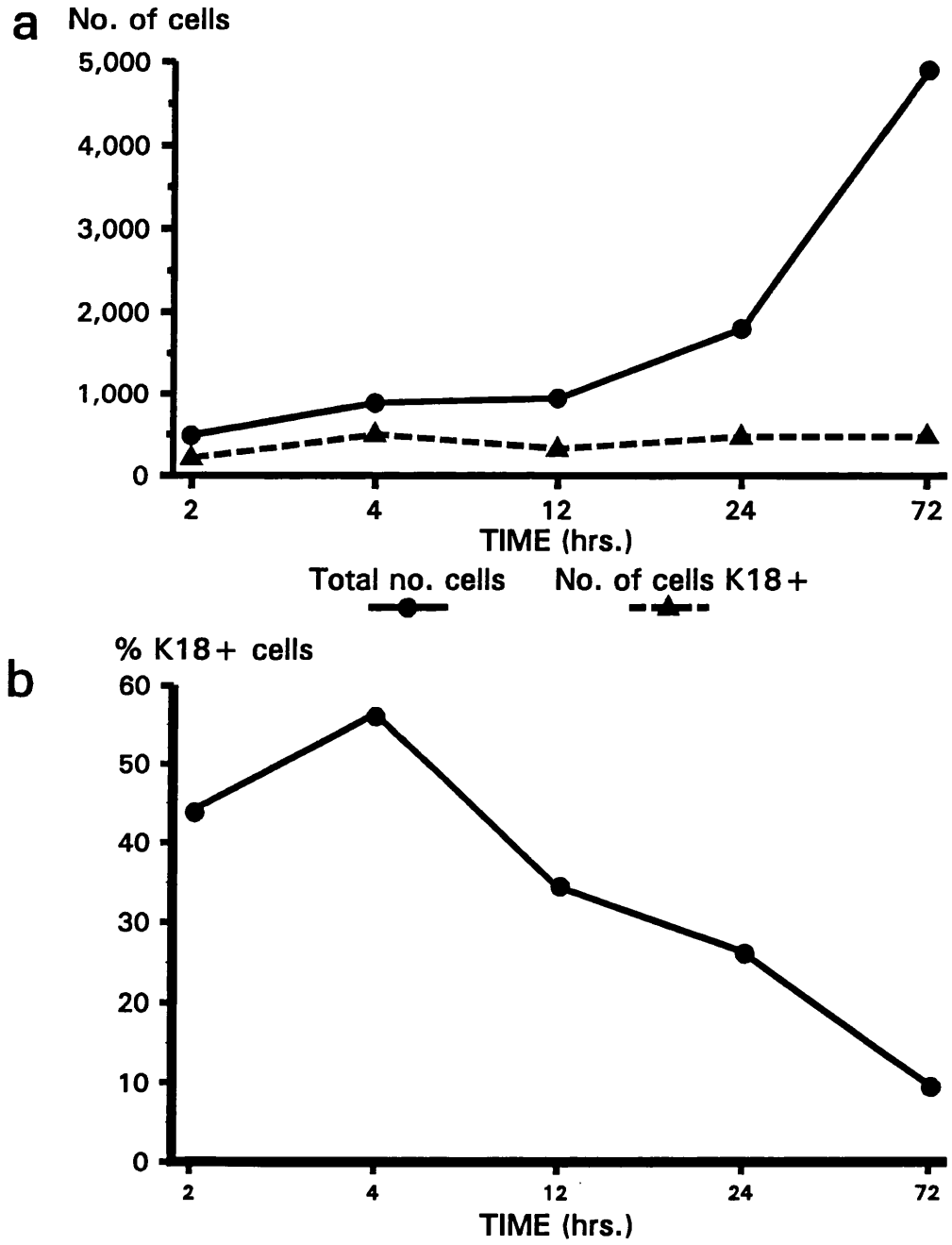

Figure 3.31. Growth curve of cultured human RPE cells and the expression of K18. Cells were grown in 6 flasks for 2, 4, 12, 24 & 72 hours. a) The cell population increased until confluence was reached at 72 hours. However, during this time there was little or no change in the number of K18+ cells. b) The percentage of K18+ cells increased after 2 hours reaching a peak at 4 hours thereafter decreasing as the overall cell population increased. The maximum expression of K18 in cultured human RPE was seen at 4 hours.

K18 and K19 are not involved in proliferation of human RPE in vitro.

3.5. MIGRATION

3.5.1. Migration of human RPE cells

Human RPE cells at pre-confluence were used in migration studies. Migration assays were conducted using the 48-well micro chemotaxis chamber (Boyden chamber) as described previously (see 2.7.1).

Fibronectin, which has been shown to be a chemoattractant for other cell types (Calthorpe & Grierson, 1990), was chosen as a possible chemoattractant for human RPE. The optimum migratory response for human RPE was established through a dose response curve (Fig. 3.32a). Human RPE cells migrated to fibronectin at concentrations between 5-50 μg/ml and the maximum migration (between 4.3% and 5%) of human RPE cells occurred with 10 μg/ml. The migration of human RPE cells to 10 μg/ml of fibronectin was compared to another chemoattractant, foetal calf serum (FCS) used at an optimal 1% concentration (Fig. 3.32b). In two migration assays (Run 1 & 2) 10 μg/ml of fibronectin stimulated between 3 to 4 fold more migration of human RPE cells than the 1% FCS. Consequently all following migration experiments were conducted using 10 μg/ml of fibronectin as the chemoattractant for human RPE cells.

3.5.2. Morphology of migrating human RPE cells

Human RPE cells were migrated using the Boyden chamber. At the end of the assay membranes were removed and fixed in 2.5% glutaraldehyde in SPB and processed for SEM. Pieces of the membrane were mounted such that cells on the upper (settled) and lower (migrated) sides of the membrane of the same well could be viewed. The topography of the migrating RPE cells at different stages of migration could be appreciated using SEM.

On the upper or settled side of the membrane the cell phenotype varied from rounded to flattened cells (Fig. 3.33a). The rounded cells were recently settled cells which had attached to the membrane. This could be established, because immediately prior to fixation, membranes were thoroughly washed to remove any cells which were not attached. After attachment the cells spread and became flattened. These flattened cells had numerous small microvilli and well developed cell processes (Fig. 3.33b). In the initial stages of migration the cell processes could be seen probing into nearby pores (Fig. 3.33c). The cell process extended deeper into the pore so that in a cell committed to migration, the bulk of the cytoplasm was constricted (Fig. 3.33d). In more advanced stages of migration most of the cell was within the pore and only a rounded knot of cell

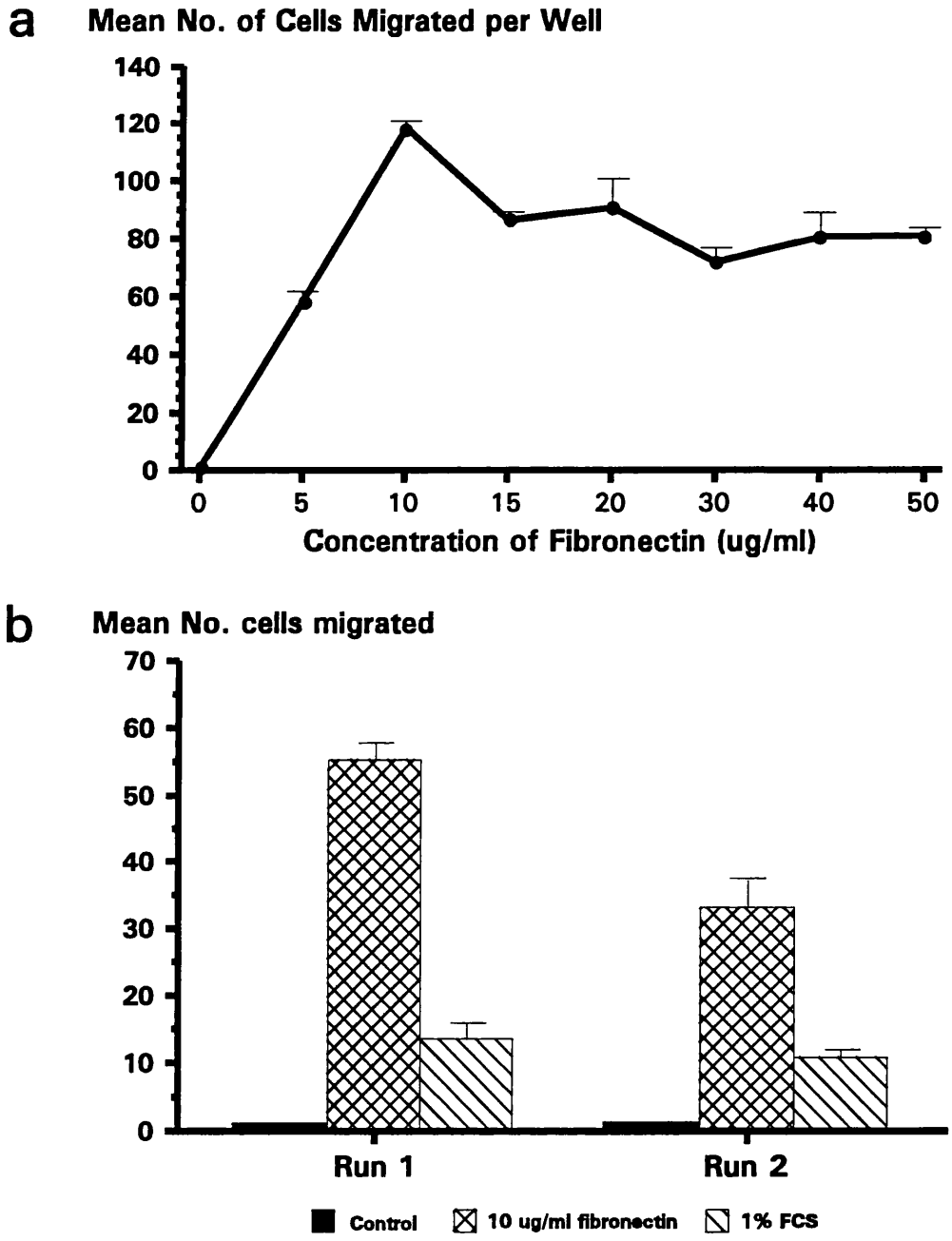

Figure 3.32.a) Dose response curve of human RPE. Cells were exposed to fibronectin for 4 hours at concentrations of 5, 10, 15, 20, 30, 40, & 50 μg/ml. O is the response of the control cells. the optimum migratory response occured at a concentration of 10 ug/ml.Bars show SEM. b) Ten μg/ml of fibronectin stimulates between 3-4 fold more migration of human RPE cells than 1% foetal calf serum (FCS), an alternative chemoattractant.

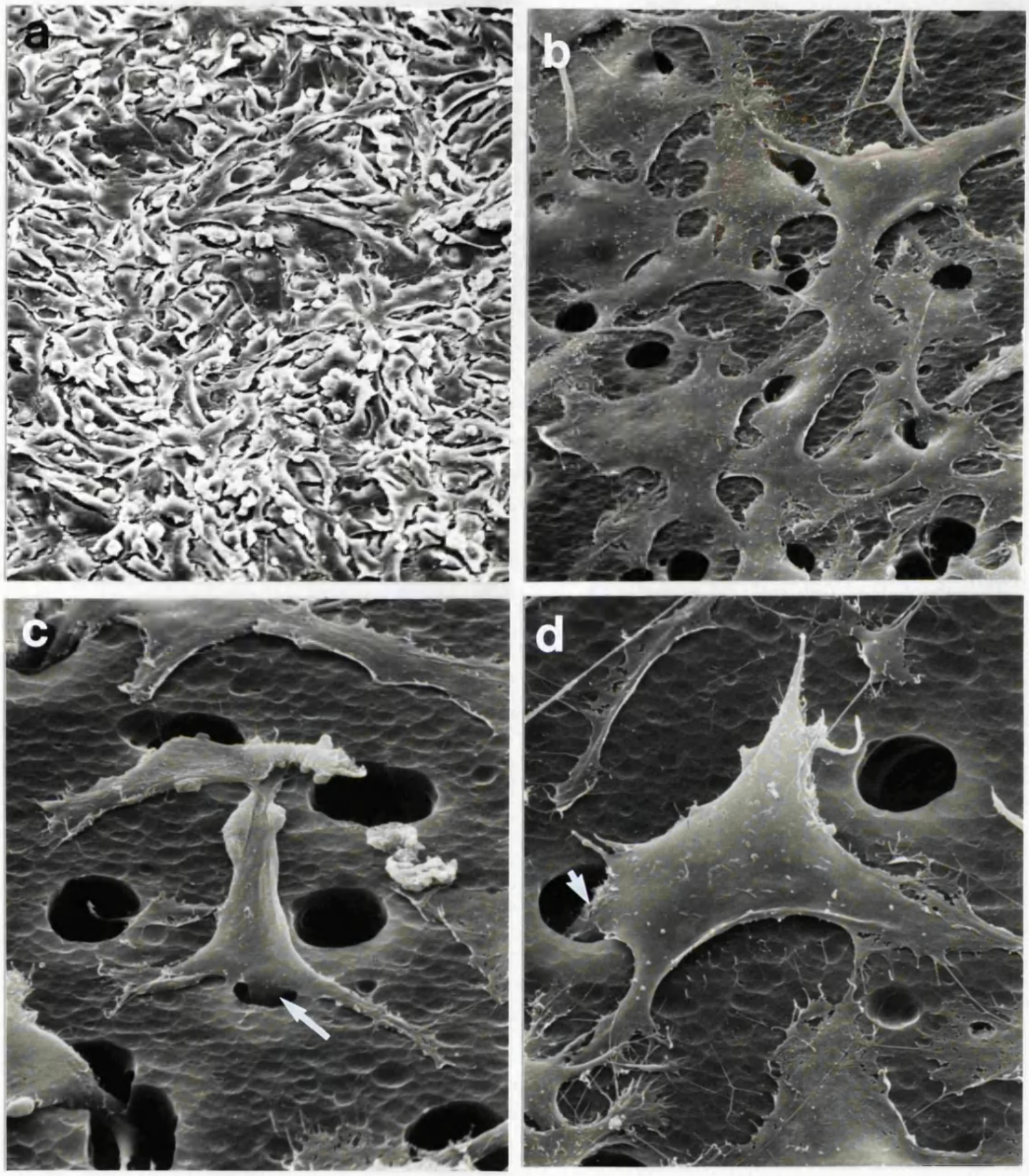

Figure 3.33. SEM of migrating human RPE cells on the upper surface of a migration membrane. **a**) Cells on the upper surface had phenotypes varying from rounded (black arrow) to flattened (white arrow). **b**) The flattened cells had well developed cytoplasmic processes and surface microvilli. **c**) Some cells appeared to be in the initial stages of migration with tips of cell processes probing into a pores (arrow) or **d**) even extending the whole cell process into a pore (short arrow). (Magnifications **a** x600, **b** x2500, **c** x6000, **d** x5500).

cytoplasm remained on the upper side of the membrane (Fig. 3.34a).

Examination of the pores on the lower or migrated side of the membrane showed that some contained the cytoplasm of RPE in transit through the membrane. The earliest stage was a small bulbous projection of cytoplasm with numerous microspikes making contact with the lower surface (Fig. 3.34b). Other cells exhibited more advanced extension out of the pore (Fig. 3.34c); until in the final stages of migration the perikaryon had passed through the pore and was evident on the lower surface (Fig. 3.34d). Cells which had emerged from the pores had an elongated kite-like shape and were smooth-surfaced with microspike at the periphery and no surface microvilli. The RPE which had completed the migration through the pores were well spread, extremely flattened cells so that their nuclei were prominent (Fig. 3.34b, foreground & 3.35.a). These cells were larger, uniform in shape and more epithelioid than those seen on the upper surface. The migrated cells had numerous long microvilli (Fig. 3.35b).

3.5.3. Identification of the cytoskeletal elements in migrating human RPE cells

The organisation of AMFs, MTs and vimentin IFs were investigated in cells on both the upper (settlement) and lower (migrated) sides of the migration membrane.

Cells on the settlement side of the membrane showed a variable staining pattern for actin. Rounded and poorly spread cells had diffuse cytoplasmic staining as did those in passage through pores (Fig. 3.36a). A filamentous staining pattern was seen in spread cells, however well developed stress fibres were rare (Fig. 3.36a). Focusing through the pore revealed that cytoplasm within the pore stained intensely, but diffusely for actin, whereas AMFs were seen in cytoplasm that had emerged from a pore and was spread onto the lower surface of the membrane (Fig. 3.36b). This cell resembled the kite-like shaped cell described from SEM (Fig. 3.34d) and was in the final stages of migration. Migrated cells on the lower side of the membrane had distinct AMFs throughout the cytoplasm (Fig. 3.36c). These cells, which by SEM, were described as a well spread flattened cells (Fig. 3.34b, foreground & Fig. 3.35a) had abundant actin stress cables traversing the cytoplasm (Fig. 3.36d).

Cells on both the settlement and migrated side of the membrane contained faintly stained fine MT filaments (Fig. 3.37.). Rounded, recently settled cells stained intensely, but individual MTs could not be distinguished (Fig. 3.37a). However, settled and spread cells contained a network of MTs that surrounded the nucleus and radiated towards the periphery of the cell (Fig. 3.37b). Cells in the final stages of migration (described by SEM Fig. 3.34d) contained a network of MTs within the cytoplasm (Fig. 3.37c). Well spread, flattened post-migrational cells, which contained abundant actin stress fibres, also contained a radiating network of fine MTs throughout the cytoplasm (Fig. 3.37d).

All cells on the settlement side of the membrane stained positively for vimentin

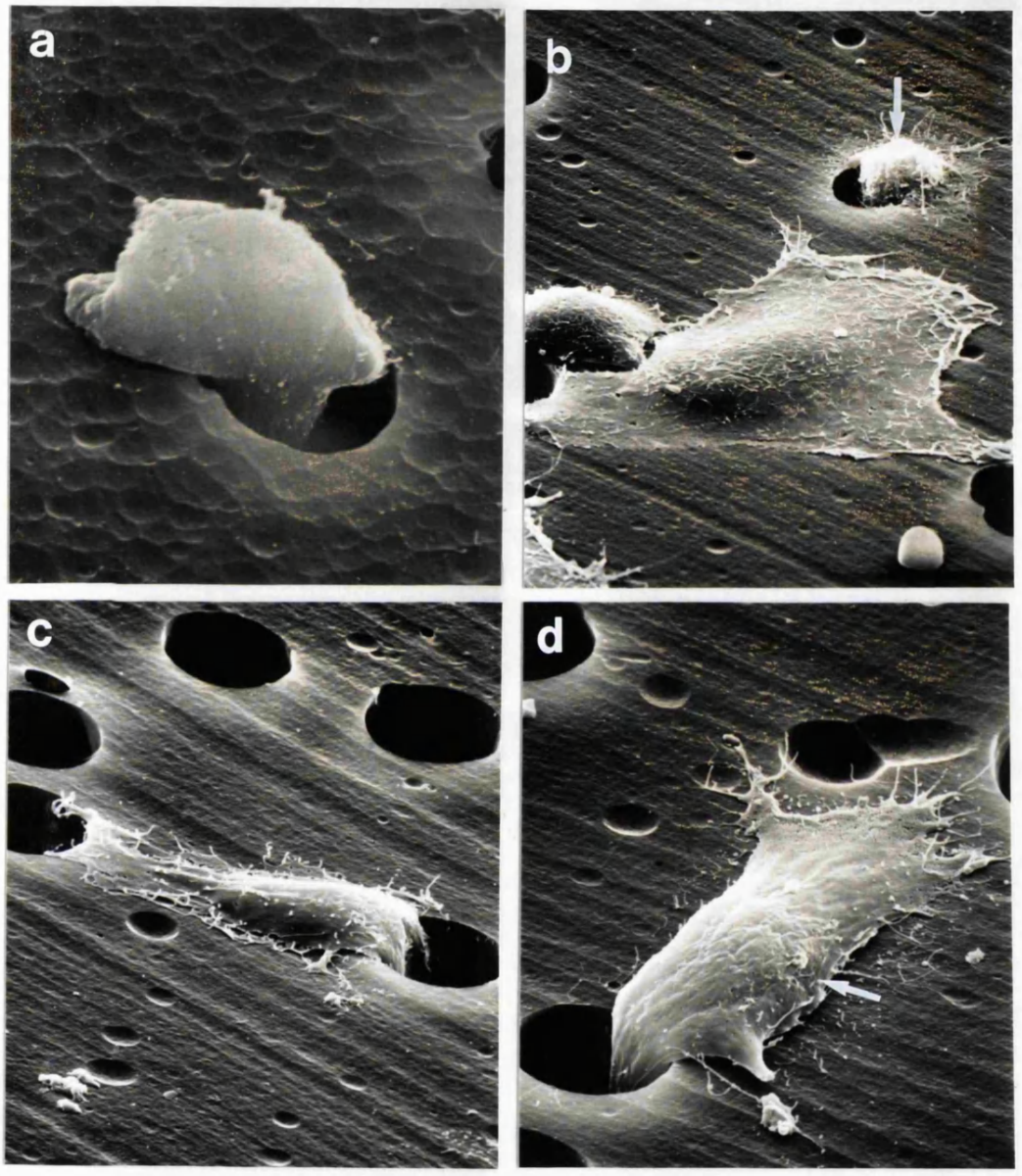

Figure 3.34. SEM of migrating human RPE cells. **a**) A cell on the upper side of the membrane in an advanced stage of migration. Only a remnant of cell cytoplasm remains on the upper surface. **b**) On the lower side of the membrane a small bulbous projection of cytoplasm protrudes from a pore indicating a cell emerging onto the lower side of the membrane (arrow). **c**) Other cells showed more advanced stages of emergence with spread cytoplasm extending onto the lower surface. **d**) In the final stages of migration the perikaryon was evident on the lower surface (arrow). (Magnificationa **a** x11 000, **b** x4500, **c** x7500, **d** x6500).

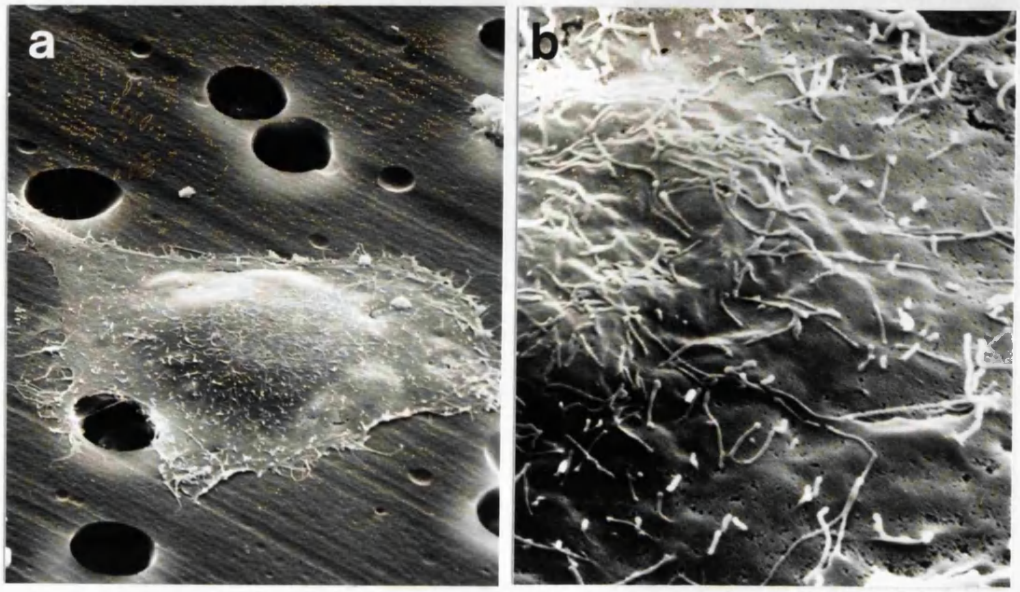

Figure 3.35. SEM of migrated human RPE cells. **a**) Cells which had completed migration were well spread flattened discoid shaped cells. **b**) The surface of migrated cells had abundant long microvilli. (Magnifications **a** x5000, **b** x20 000).

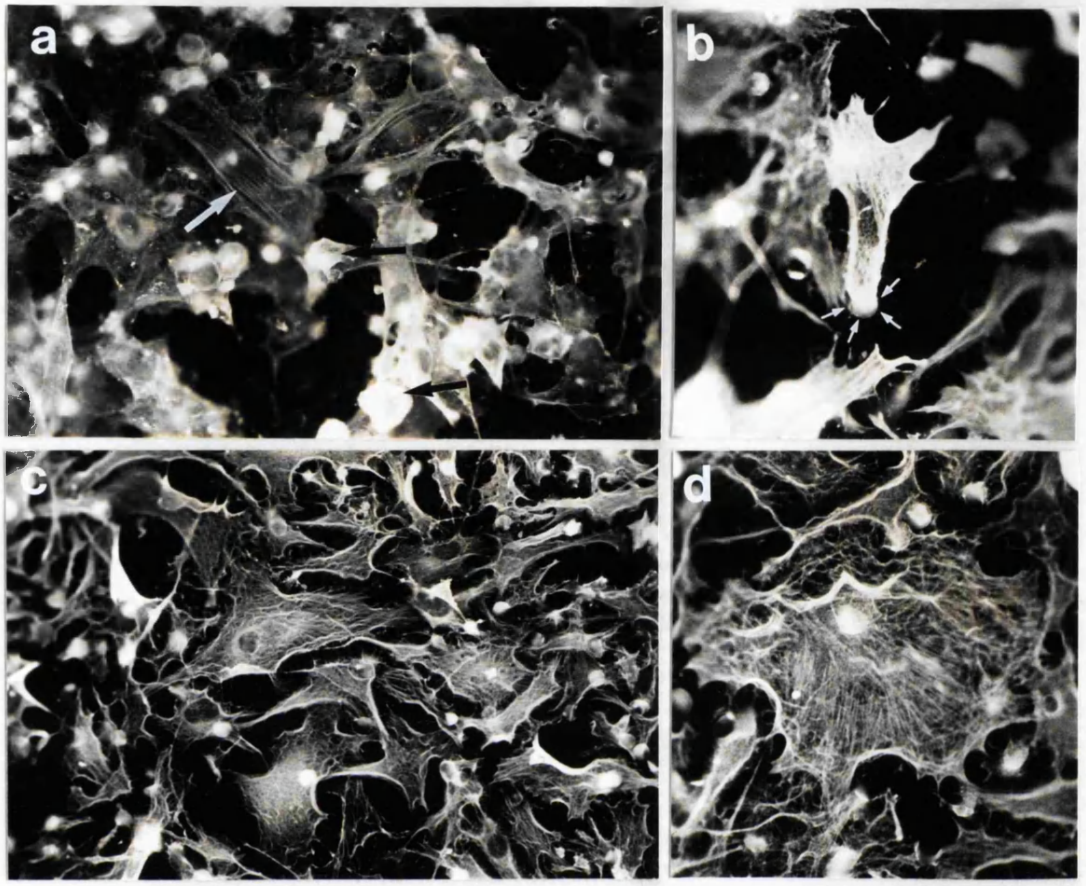

Figure 3.36. Human RPE on the upper (**a**) and lower (**b-d**) side of a membrane were stained for AMFs and visualised by immunofluorescence. **a**) On the upper side of the membrane rounded poorly spread cells (black arrow) had a diffuse actin staining pattern. Whereas spread cells (white arrow) had a filamentous staining pattern. **b**) This filamentous staining was seen in cytoplasm of cells in advanced stages of emergence from a pore (arrow heads) and **c**) in many cells on the lower side of the membrane. **d**) Large flattened discoid shaped migrated cells had abundant actin stress fibres throughout the cytoplasm. (Magnifications **a** x250, **b** x400, **c** x259, **d** x400).

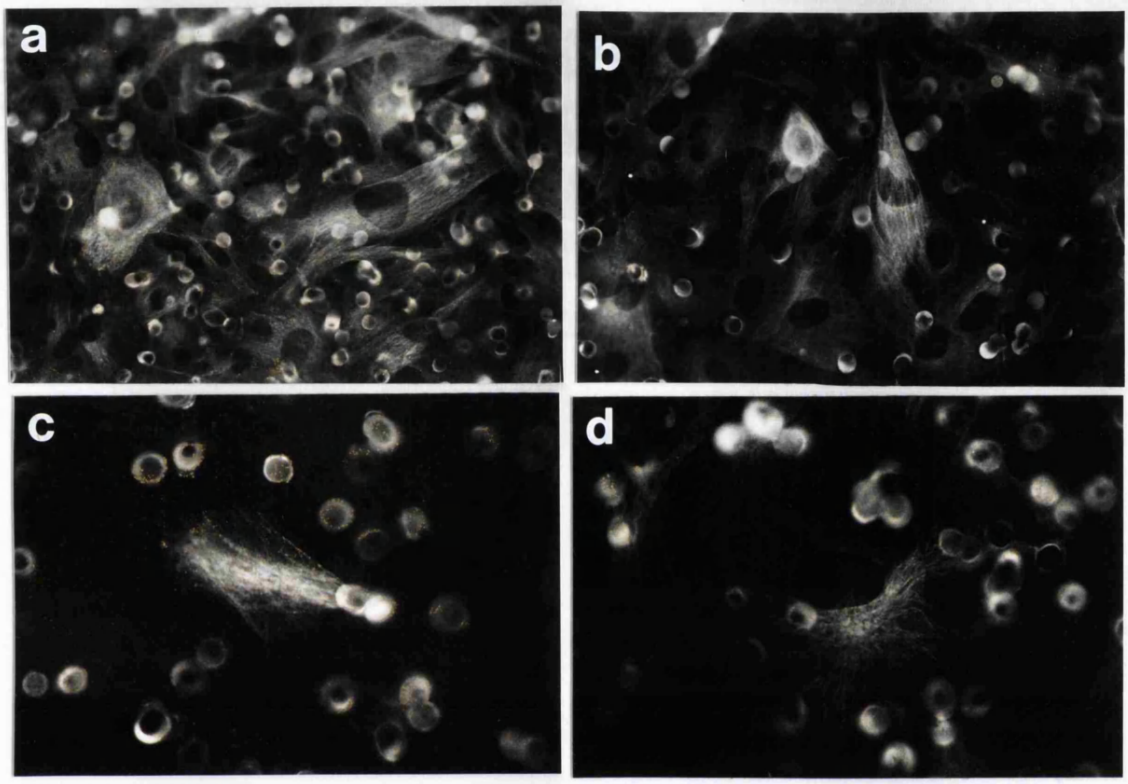

Figure 3.37. Migrating human RPE cell on the upper (**a** & **b**) and lower (**c** & **d**) side of a membrane were stained for MTs and visualised by immunofluorescence. **a**) Rounded cells stained intensely, but diffusely for MTs and **b**) spread cells showed faint staining of tubules within the cytoplasm. **c**) Cytoplasm emerging and spreading onto the lower also contained fine MT filaments. **d**) MTs formed a radiating network in the migrated flattened discoid shaped cells. (Magnifications: **a** x250, **b** x200, **c** & **d** x400).

IFs. Both rounded, recently settled cells and cells in transit through a pore cells stained intensely for vimentin but a filamentous pattern was difficult to determine (Fig. 3.38a). Spread cells exhibited a clear network of vimentin IFs (Fig. 3.38a). Cells on the migrated side of the membrane showed variable staining patterns for vimentin. Cytoplasm emerging from a pore and spreading onto the lower surface (Fig. 3.34c) was distinguished by having a faint and diffuse vimentin staining pattern (Fig. 3.38b). In other cells distinct vimentin IFs could be seen within the spread cytoplasm (Fig. 3.38b). Post-migrational cells usually had a patchy staining pattern for vimentin (Fig. 3.38c).

3.5.4. K18 and K19 in migrating human RPE cells.

The organisation of K18 and K19 were investigated in migrating cells using MABs RGE 53 and K4.62, respectively. The staining of cells on the settlement side of the membrane by immunofluorescence revealed that rounded cells stained intensely, but diffusely for both K18 and K19 and there was some variation in the staining pattern in the spread cells (Fig. 3.39a & b). This finding was in agreement with the staining of cells on LabTeks (see 3.2.1.). Of interest was cells that contained intensely stained K18 and K19 networks and had cell processes probing around and into pores (arrow, Fig. 3.39a).

On the lower side of the membranes, positively stained K18 and K19 filaments were seen associated with pores (Fig. 3.39c; illustrated with K18). When the K18 and K19 stained membranes were compared with those membranes stained for actin (Fig. 3.36c), it was apparent that there were far fewer cells stained positive for K18 and K19 than the amount of cells present on the lower surfaces. It was clear that on both upper an lower surfaces of the membrane only a sub-set of human RPE cells stained positively for K18 and K19 and from a cursory examination there was more cytokeratin staining on the migrated side of the membrane.

The population of K18+ and K19+ cells and the total number of cells were counted adopting my standard counting procedure (see 2.6.4.). The data (K18, see Appendix XI & K19 see Appendix XII.) was expressed as the percentage of cells K18+ and K19+ on the settled and migrated side of the membrane (Fig. 3.40.). Sub-populations of K18+ and K19+ RPE were present on both sides of the migration membrane (Fig. 3.40a). Moreover it was apparent that there were more positive cells on the migrated than the settlement side of the membrane. Indeed just over 8% were K18+ on the settlement side whereas 45% were positive on the migrated side. Only 2.5% were K19+ on the settled side while over 21% were positive on the migrated side. The differences were significant in both cases using Chi-squared analysis and the Mann-Whitney U test ($P<0.001$).

It should be noted here that the figure of 8.2% K18+ and 2.5% K19+ cells on the

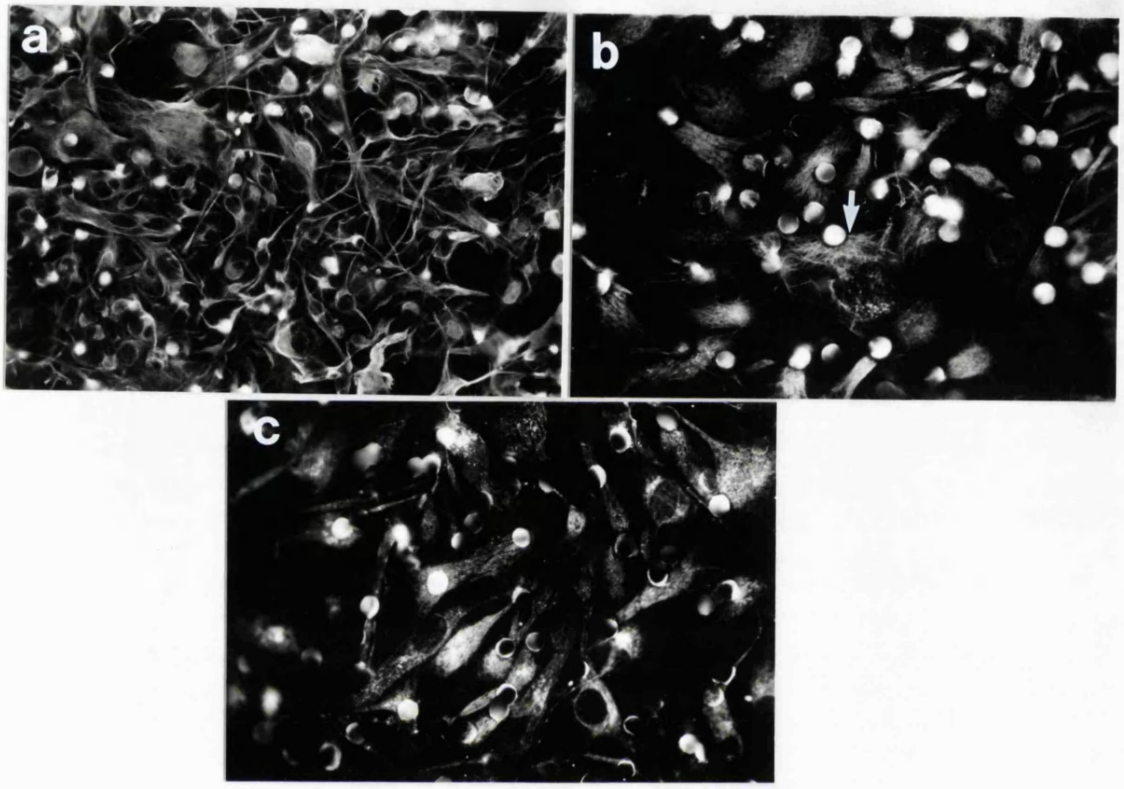

Figure 3.38. Human RPE cells on the upper (**a**) and lower (**b** & **c**) of a migration membrane were stained for vimentin IFs and visualised with immunofluorescence. **a**) Rounded cell on the upper surface stained intensely for vimentin IFs. Distinct filamentous vimentin was seen in spread cells. **b**) Cells emerging onto the lower side of a membrane showed variation in vimentin staining. Filaments were identified in cytoplasm of cells which was emerging from a pore (arrow). **c**) However in the main the vimentin staining was patchy in cells on the lower side of a membrane. (Magnifications: **a** x200, **b** x300, **c** x250).

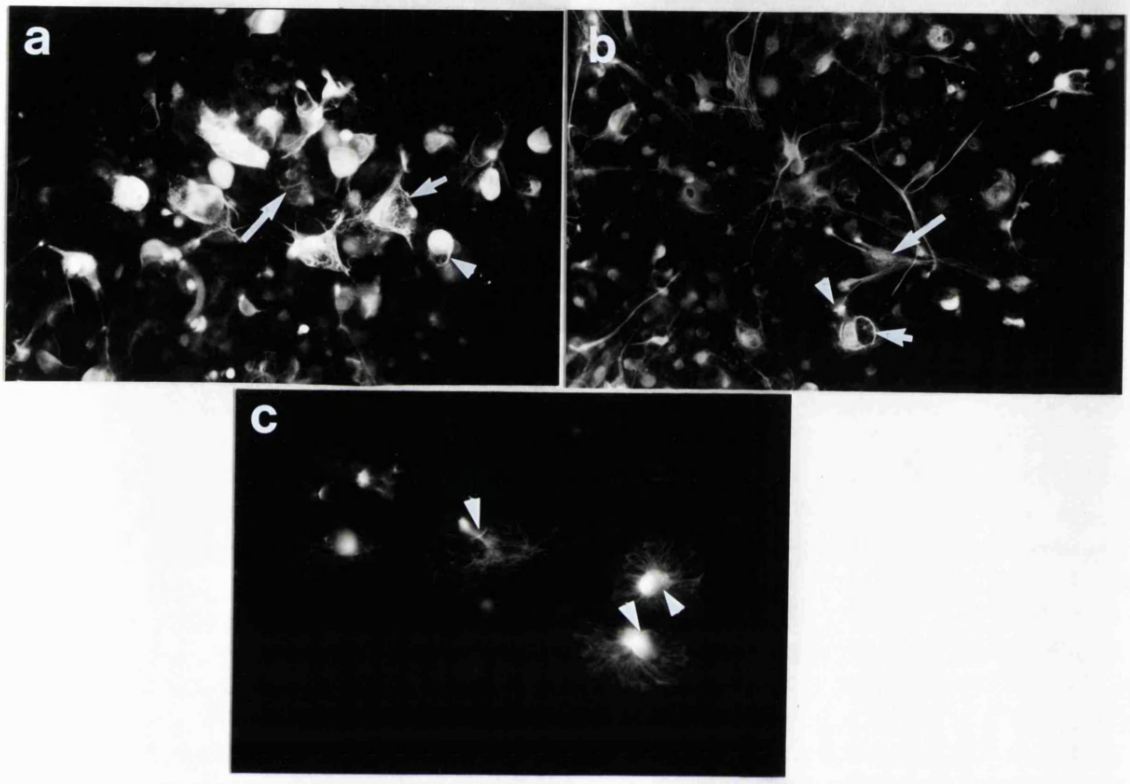

Figure 3.39. Migrating human RPE were stained for K18 (**a** & **c**) and K19 (**b**) using MABs RGE 53 and KG4.62, respectively. A subset of cells stained positively for K18 (**a**) and K19 (**b**) on the upper side of the migration membrane. Rounded cells stained intensely, but diffusely and staining in spread cells varied from filamentous (short arrow) in some cells to faintly positive in others (long arrow). Filamentous cytokeratin networks were seen in cells associated with pores (arrow heads) on both the upper (**a**) and lower (**c**) side of the membrane (Magnifications: **a** & **b** x200, **c** x400).

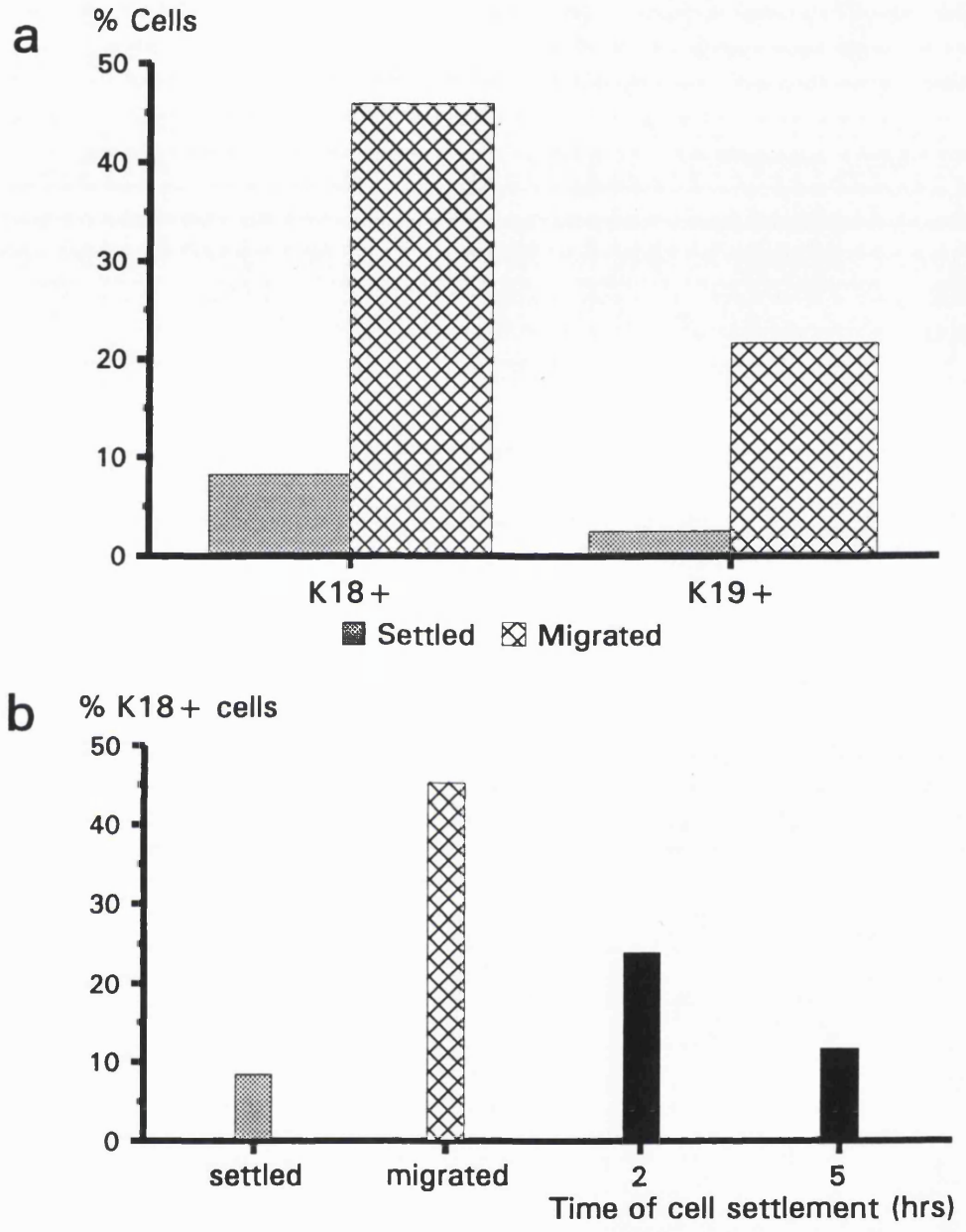

Figure 3.40. a) The expression of K18 and K19 in migrating human RPE cells. Cells were migrated in a micro chemotaxis chamber and then stained for K18 and K19. Cells that stained were counted and represented as a percentage of the total cells on each side of the membrane. The K18 and K19 subset was larger on the migrated (lower) side of the membrane than on the settled side of the membrane (Chi-squared, $p<0.01$). b) A comparison of the K18+ subset of human RPE cells on the migration membrane with cells in a flask seeded at the same call density used in a migration assay. Cells were allowed to settle for 2 and 5 hours then they were stained for K18. At high cell densities the K18+ subset was reduced.

settlement side of the membrane may appear to be considerably lower than that of 47% (K18+) and 14.9% (K19+) present in a confluent culture (see above 3.2.2). This discrepancy in the differences in cytokeratin expression seen in flasks and on the membrane may have been due either to substrate or cell density. This required further investigation and because, K19+ cells are a sub-set of K18+ cells (see 3.2.2.) staining was conducted only for K18.

Cells seeded into a 25 cm^2 culture flasks at the same cell density used in migration assays were allowed to settle for 2 and 5 hours, before being stained for K18 and counter stained with haematoxylin exactly as described for migration membranes (see 2.7.5.). Cells were counted using the standard counting procedure adopted for growth curve experiments (see 2.6.1.). From a total of 14, 543 cells, 24.06 % were K18+ at 2 hours and this decreased to 11.67% (from a total of 18, 253 cells) at 5 hours. This is comparable to the percentage K18+ population (8.2%) on the membranes (Fig. 3.40b). Clearly cell density and the short time in culture account for the discrepancy between the K18+ population on upper surface of the migration membranes and that seen in a confluent culture.

Quantification of immunofluorescent stained cells showed that on the migrated side of the membrane there is a larger subset of K18+ and K19+ cells than on the settled side. As the finding was intriguing, the membranes were examined in more detail. On the upper surface of the membrane intensely stained rounded cytoplasm was identified adjacent to the pores (Fig. 3.41b K18 and Fig. 3.41d, K19). In the same microscopic field the lens was focused through the pores and onto the lower side of the membrane. Positively stained cytokeratin IFs were seen emerging from the pores, spreading in a kite-like shape onto the lower surface (Fig. 3.41a, K18 and Fig. 3.41c, K19). The intensely stained, cytokeratin positive rounded cytoplasm on the upper surface of the membrane corresponded to the remnant of cellular cytoplasm identified by SEM in a cell migrating through a pore (see Fig. 3.34a). The filamentous array seen spreading in a kite-shaped pattern from the pore resembled the phenotype described by SEM of a cell in the advanced stages of migration (Fig. 3.34d). The cells in figure 3.41. were migrating human RPE cells captured in transit through a pore. These cells expressed K18 and K19 and therefore provide the first indication of a possible link between migratory activity of human RPE cells and K18 and K19 filaments identified by MABs RGE 53 and K4.62.

That K18+ and K19+ staining was associated with cells in transit through pores, was supported by using a technique which visualised both cytokeratin positive and cytokeratin negative cells simultaneously. Cells were stained using a combination of immunoperoxidase staining and counter staining with haematoxylin (see 2.7.5.). This technique (illustrated with K18) was used to establish that cytokeratin negative cells do not inhabit pores.

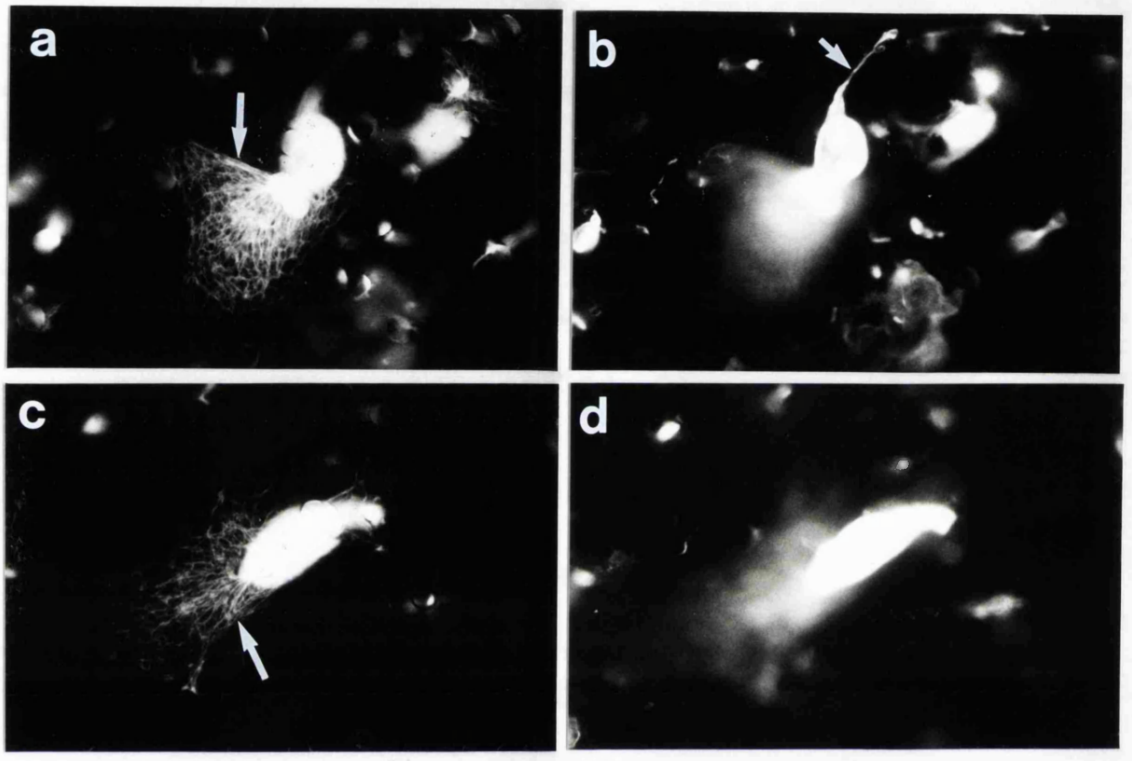

Figure 3.41. Migrating human RPE cells stained for K18 (**a** & **b**) and K19 (**c** & **d**) at two levels of focus. The cells are intransit through a pore. On the lower (migrated) side of the membrane a filamentous array of K18 (**a**) and K19 (**c**) filaments has emerged from the pore (arrows) and spread onto the lower surface. While on the upper (settled side) surface the cytoplasm within the pore, that remaining on the upper surface and a cell process (**b**, arrow) stain diffusely for K18 (**b**) and K19 (**d**). (Magnifications: **a-d** x400).

On the upper surface of the membrane (Fig. 3.42a) the majority of these cells were K18-, as has been shown previously (Fig. 3.40a). Rounded cells were stained dark blue and were always negative for (K18-). Foci of K18+ staining was seen adjacent to the nucleus in some of the partially spread cells. RPE with a more flattened polarised morphology were positive for K18 and showed a fibrillar staining pattern. These cells usually had cytoplasmic processes extending into adjacent pores (Fig. 3.42a). On the migrated side of the membrane (Fig. 3.42b) the large flattened non-polarised epithelioid (discoid) shaped cells (which invariably had abundant actin stress fibres, see 3.5.3.) were negative in the main. The vast majority of the positive cells were smaller bipolar cells often with cytoplasm still within a pore (Fig. 3.42b). **Cells in transit through pores were always K18+ and no exceptions were found in over 300 wells examined.** In other words K18 and K19 were expressed by human RPE involved in active migration through the pores.

Seven stages of migration were identified and are summarised in figure 3.43. **Stage 1** consisted of rounded, recently settled cells on the upper surface of the membrane. These cells were negative for K18 and K19 and exhibit diffuse staining for actin. **Stage 2** was a spread cell which was mostly cytokeratin negative and by SEM had numerous surface microvilli. Whereas, **stage 3** was a spread cell with a foci of K18+ staining adjacent to the nucleus. **Stage 4** consisted of well spread cells with cytoplasm invading the pores. These cells had prominent processes, seen by both light microscopy and SEM, and were always positive for K18 and K19. The cells had a filamentous cytokeratin and actin network within the cytoplasm. Cells in transit through pores were represented by **stage 5** and were always positive for K18 and K19. The cytokeratin formed an intricate filament network within the cytoplasm that spread onto the lower surface of the membrane, but the cytoplasm in the pore and the remnant on the upper surface exhibited a diffuse staining pattern. In this stage of migration actin showed the same staining morphology as the cytokeratins. Cells in **stage 6** were identical to cells in stage 4, only on the opposite side of the membrane and were K18+ and K19+. Finally, **stage 7** consisted of large well spread and flattened migrated cells with well developed actin stress cables in their cytoplasm. They were negative for K18 and K19.

The 7 stages of migration were quantified. As K19+ cells were a subset of K18+ cells the proportion of K19+ cells at each stage would be much smaller than the proportion of K18+ cells and therefore difficult to quantify accurately. Thus only membranes stained for K18 were quantified for this study. From 24 wells the number of cells corresponding to each of the 7 stages were counted and the data (see Appendix XIII.) showed that in agreement with previous results (see 3.5.1.) 3.8% of human RPE cells had migrated and 0.9% of cells were in transit through the pores. The K18+ stages (3, 4, 5, & 6) of migration were analysed separately (Fig. 3.44a). Stage 4 consisted of the largest proportion of cells with just under 50%, while stages 5 and 6 were just over and under 10%, respectively. The proportion of K18+ cells in stage 3 was just over 30%,

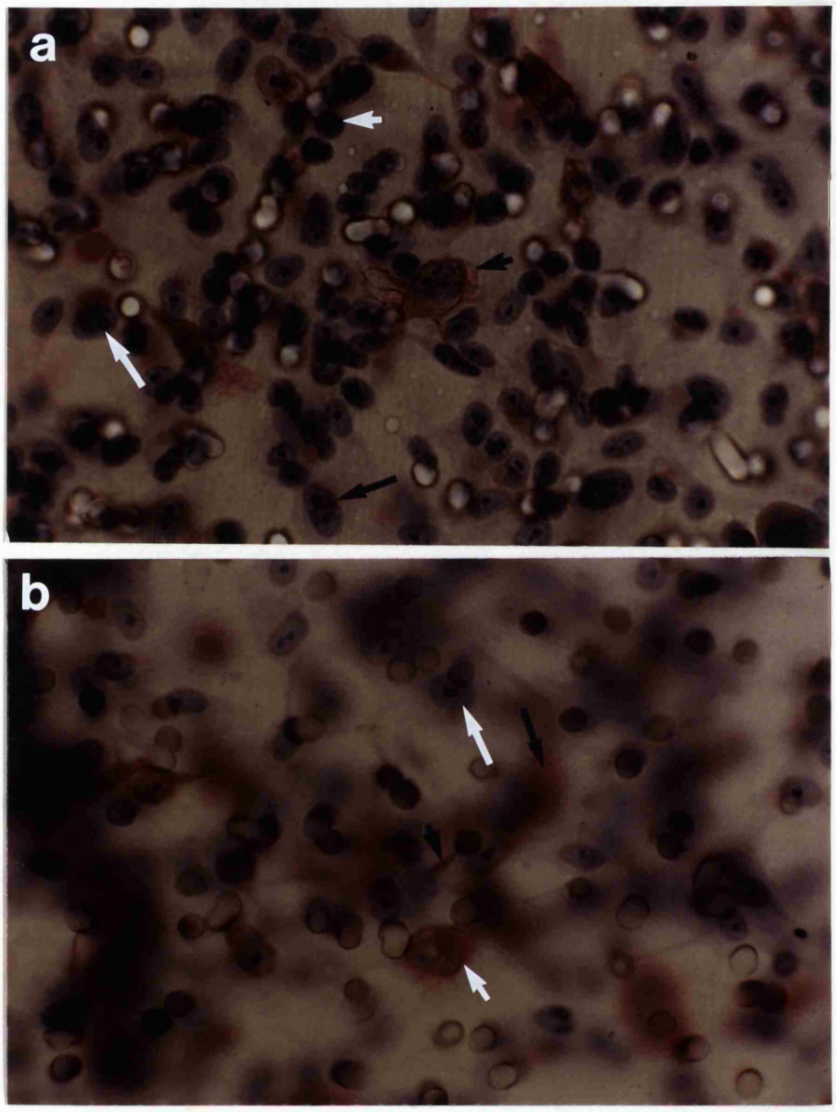

Figure 3.42. Immunoperoxidase staining of K18 in human RPE on the upper (**a**) and lower (**b**) sides of a migration membrane. Cells were counter-stained with haematoxylin. **a**) Upper surface: rounded cells were K18- (short white arrow) and spreading cells had localised K18 staining adjacent to the nucleus (long white arrow). Cells in the initial stages of migration were K18+ and had a fibrillar staining pattern. These cells often had a cell process extending into a pore (short black arrow). Spread stationary cells were K18- (long black arrow). (**b**) Lower surface: K18+ cells were small polarised cells often with some of their cytoplasm still within a pore (short white arrow). Cytokeratin negative cells were large flat non-polarised epithelioid cells (long white arrow). K18+ cytoplasm could be seen extending out of the pores and spreading onto the lower surface (short black arrow) (comparable to Fig. 3.34**c**). This spreading cytoplasm comes from K18+ cells on the upper surface which, because the micrograph is focused on cells on the lower side of the membrane, appears as a diffuse red shadow (long black arrow). N.B. the density of cells on the lower side of the membrane is the same as that in Fig. 3.36**c**. (Magnifications: **a** & **b** x 280).

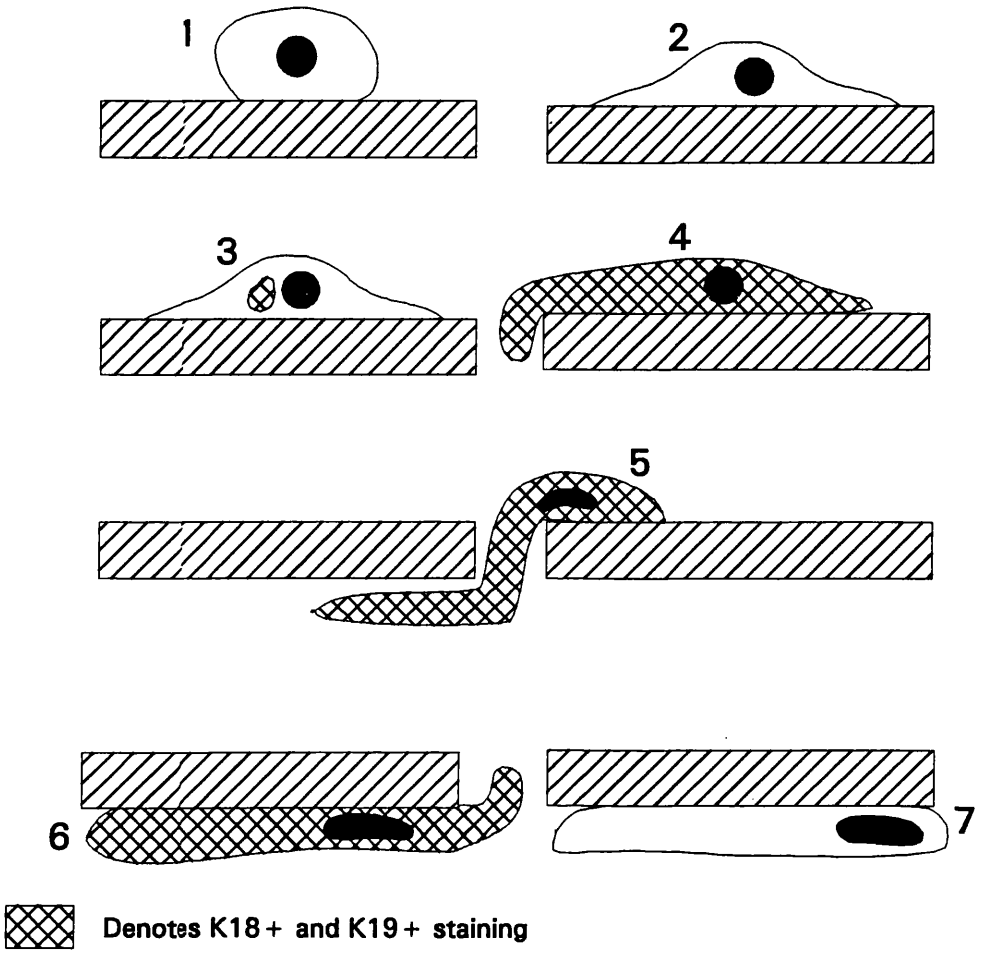

Figure 3.43. Migration of human RPE in vitro and the role of K18 & K19. The migration process consists of severn stages. Stage 1. A rounded cell with diffuse actin staining is negative for K18 and K19. Stage 2. A spread cell with diffuse or filamentous actin, but is still K18- and K19-. Stage 3. A spread cell that has diffuse filamentous actin and which had an intense staining non-filamentous aggregate adjacent to the nucleus. Stage 4. A well-spread flattened cell with a cell process placed in a pore, has filamentous actin and is always K18+ and K19+. Stage 5. A cell actively migrating through a pore has filamentous actin and is K18+ and K19+. Stage 6. This is identical to stage 3 although the cell is on the lower surface rather than the upper surface and has a foot process within the pore. Stage 7. A large flattened migrated cell with actin stress cables and negative for K18 and K19.

a

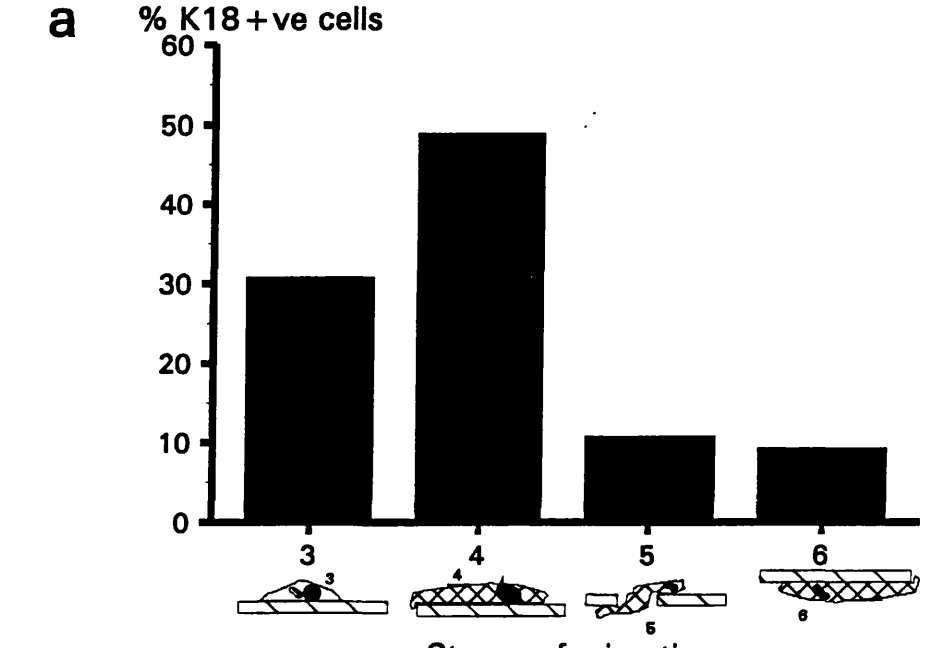

Denotes K18+ and K19+ staining

b Correlation

	stage 1	stage 2	stage 3	stage 4	stage 5
stage 1	1.000000				
stage 2	.233565	1.000000			
stage 3	.442533	.327831	1.000000		
stage 4	.024222	-.543974	-.035583	1.000000	
stage 5	.037856	.484750	.099725	-.470469	1.000000
stage 6	.211266	.582670	.148631	-.758551	.677802
stage 7	.112227	.445699	.137631	-.559638	.286097

Figure 3.44. a) The percentage of K18+ cells in the four stages of human RPE migration that stain positively for cytokeratins. Stage 4 had the largest proportion of K18+ cells and stage 6 had the smallest. Very few cells were were in transit through the membrane (stage 5) and stage 3 was a larger group than it had appeared to be from microscopy. b) A correlation matrix of the stages of human RPE cell migration, where type=stage. The correlation indicates that on a migration membrane with an increase in the number of cells in stage 5 there is a corresponding decrease in the number of cells in stage 4, but an increase in stage 6. this analysis fits the proposed model for K18 in migrating human RPE cells.

which is larger than what it had appeared form the light micrographs. Clearly in the 4 hour migration assay the majority of K18+ cells are in the initial stages of migration (stage 4). The data on all 7 stages of migration was entered into a data base and a correlation matrix was performed (Microstat-II, Ecosoft Inc.). From the matrix (Fig. 3.44b) stages 4 and 6 showed the highest negative correlation at -0.76 and stages 5 and 6 showed the highest positive correlation at +0.68. Thus on a migration membrane as the number of cells in stage 5 increases there is a corresponding decrease in the number of cells in stage 4. As the number of cells in stage 5 increases there is a corresponding increase in the number of cells in stage 6. This analysis and correlation continue to fit the proposed model for the involvement of K18 in migrating human RPE cells.

CHAPTER 4. DISCUSSION

4.1. GROWTH AND MORPHOLOGY OF CULTURED RPE CELLS

4.1.1. Growth of RPE in vitro

The growth and culture of bovine, human and rat RPE cells has been well documented (Basu et al, 1983; Albert et al, 1972; Mannagh et al, 1973; Flood et al, 1980; Boulton et al , 1982; Edwards, 1977). In culture bovine and human RPE shared similar growth characteristics and cell morphology, whereas rat RPE had markedly different growth characteristics and minor morphological differences. In the present study bovine and human RPE could be sub-cultured up to as many as 13th and 11th passage, respectively, and therefore had the advantage over rat RPE, which could not be sub-cultured and therefore could only be used as primary cultures. As a result, work with rat RPE required a constant supply of tissue for experimentation.

Control and dystrophic rats were used in the study to obtain normal and diseased RPE. It was found that there were no differences in either growth or morphology of cultured rat RPE whether or not the cells were obtained from control or dystrophic tissue. This indicates that the lesion in dystrophic RCS rat does not affect the growth or appearance of RPE cells in vitro.

The study concentrated on two types of rat RPE culture which could be grown in vitro, monodispersed and island cultures. Monodispersed cultures of rat RPE showed similar growth and morphology characteristics to that already described by Edwards (1977). However, for the first time this study describes islands of rat RPE that resembled the morphology of embryonic chick RPE (Crawford, 1975). The islands demonstrated an outstanding feature that was seen in all the three species of RPE, this feature was phenotypic change. When removed from the eye, RPE cells appeared as uniform hexagonal, pigmented cells, but in vitro the RPE formed mosaic growth patterns (bovine and human), lost their pigment and eventually became spread, flattened discoid or epithelioid shaped cells (bovine, human and monodispersed rat). Phenotypic changes in cultured RPE have been described before (Albert et al 1972; Flood et al, 1980). However, in islands of rat RPE the stages of phenotypic change could be identified in cells within distinct zones. Cells in the centre of the island resembled RPE in vivo, whereas cells at the edge of an island, which showed the greatest phenotypic change, resembled rat RPE in monodispersed cultures. Island cultures of rat RPE present a model system in which to study the functional responses of RPE cells in relation to their in vivo and their in vitro morphological states. In this study islands were used to study one of the functional responses of RPE, that of phagocytosis (see 4.3.).

4.1.2. Morphology of RPE in vitro

The fine structure of whole cells using TEM has been reported previously (Buckley & Porter, 1967; Wolosewick & Porter, 1976; Byers & Porter, 1977). TEM of whole cells provides excellent images of cellular organelles and the interrelationships of the organelles with the cytoskeleton. Ultrastructural organisation of cytoskeletal elements in intact whole cells could only be observed in the thinner parts of the cell. In whole RPE cells from all three species used in this study, the cytoskeleton consisted of a complex network of filaments. One of the filaments through its size and that it formed dense bands that traversed the cytoplasm (see 4.2.), was identified as AMFs. The AMFs associated with cellular organelles and were often aggregated to form stress fibres (see 4.2.). The limitation of TEM of whole cells is that fine detail and identification of filaments is difficult. Consequently cells were detergent extracted with non-ionic detergents in PHEM buffer, which preserved all the major cytoskeletal elements (Schliwa & Blerkom, 1981). In extracted cells the cytoskeleton appeared to consist of an interactive network of filaments, similar to that described in other cells (Schliwa & Blerkom, 1981; Grierson et al, 1986).

TEM whole cell viewing did not reveal any differences in the ultrastructure between control and dystrophic rat RPE. However, the rat RPE showed some differences in ultrastructure from that of bovine and human RPE. The shape and frequency of organelles were similar in bovine and human RPE, but rat cells contained an abundance of pigment granules which were sparse in bovine and human RPE cells. Bovine and human RPE have been shown to loose pigmentation in culture (Albert, 1972) and this loss occurs in cells undergoing cell division (Flood et al, 1980). Therefore, the abundance of pigment in rat RPE would suggest that these cultures contain cells that are either non-dividing or slow to divide. The lack of proliferation may account for the failure to sub-culture rat RPE in this study.

The examination of whole cells of bovine and human RPE by TEM combined with rhodamine 123 staining in live cells has given us new information about the mitochondria in cultured RPE cells. The mitochondria were large branching organelles that formed an extensive network throughout the cytoplasm. Mitochondria have been described before as "elongate and branching", "meandering forms", "filamentous" and "anastomising networks" in a variety of eukaryotic cells (Kilarski & Koprowski, 1976; LeFurgey et al, 1983; Johnson et al, 1980 & 1981; Addai & Ockleford, 1986), in yeast (Keddie & Barajas, 1969; Davison & Garland, 1975) and recently in cultured human RPE (Oliver & Newsome, 1992). Clearly mitochondria deviate from their original description as ovoid bodies 1-4 μm in length and 0.3-0.7 μm wide (Palade, 1952 & 1953; Sjostrand, 1953). TEM of ultrathin sections of RPE cells in this study and in other studies (Hogan et al, 1971; Zinn & Marmor, 1979; Flood et al, 1980) revealed a

cytoplasm replete with ovoid-shaped mitochondria. In the RPE this appears to be a cross section of the mitochondrial network identified in whole cells.

Whether mitochondrial networks exist in the RPE in vivo was not demonstrated in this study. However the formation of the mitochondrial network in the RPE in vitro is intriguing. The mechanism by which elongate mitochondria form and eventually associate into a network within the cytoplasm is not fully understood. However, it has been shown in cultured cells that mitochondria can elongate by fusion of smaller rod-shaped mitochondria (Lewis & Lewis, 1915). These elongate mitochondria appear to form from fusion of smaller mitochondria and these in turn appear to enlarge to form networks, which may also enlarge further (Lewis & Lewis, 1915; Stevens, 1974; Osafune, 1973). There is evidence to suggest that such networks may be supported by MTs (Johnson et al, 1980; Cambrey-Deakin et al, 1988), which are thought to act as guidelines for the mitochondria (Ball & Singer, 1982), and the position of these networks may be maintained by IFs (Eckert, 1986; see review by Carmo-Fonseca & David-Ferreira, 1990).

The function of mitochondrial networks is not understood. However it has been shown that giant mitochondria form in the presence of glucose in yeast during active growth (Stevens, 1974). Giant mitochondrial also appear to be common in highly active tissue in rats, i.e. in liver (Brandt et al, 1974), nephron (Bergeron et al, 1980), diaphragm muscle (Bakeeva et al, 1978), as well as in cultured cells derived from active tissue, i.e. in chick heart muscle (LeFurgey et al, 1983) and rat embryo (Buckley & Porter, 1975). This evidence suggests a link between mitochondrial network formation and the physiological state of the cell. In vivo the RPE cell has a high level of oxidative enzymes (Pearse, 1961; Hansson, 1971) and we know from functional studies that RPE have high metabolic and transport demands. The mitochondrial networks identified in bovine and human RPE by this study may be either a consequence of its function in vivo, or may be an adaption to the energy requirements needed for growth in culture. If energy requirements were the factor that influenced mitochondria morphology, then the absence of mitochondrial networks in rat RPE could be explained. Rat RPE, being primary cultures grew much slower than sub-cultured bovine and human RPE. Consequently these slow growing cells would have a low metebolic rate, therefore lower energy requirements and have no demand for mitochondrial networks.

4.2. THE CYTOSKELETON OF RPE CELLS

4.2.1. Actin Microfilaments (AMFs)

AMFs were visualised in cultured bovine, human and rat RPE cells by

immunofluorescent labelling with MABs to actin. These filaments were seen to be arranged in patterns similar to AMFs that have been previously identified in RPE cells (Owaribe et al, 1979; Chiatin & Hall, 1983b) and other types of cultured cells (Lazarides & Weber, 1974; Lazarides, 1975a). Actin staining consisted of two types of patterns, diffuse staining with short peripheral filaments and bundles of parallel AMFs (stress fibres) spanning the cell cytoplasm. The diffuse staining indicates an unpolymerised, non-filamentous form of actin (Lazarides, 1975a), which is associated with cell motility (Herman et al, 1981). However, stress fibres, which were also identified in RPE cells using TEM of whole cells (see 4.1.2.) and have been found in many tissue culture systems, are large AMF bundles and are thought to be a feature of stationary cells (Bradley et al, 1980 ; Herman et al, 1981). Stress fibres are abound in cells which strongly adhere to the underlying substrata (Willingham et al, 1977). The fibres are contractile (Kreis & Birchmeier, 1980), terminate in focal contacts (Abercrombie et al, 1971) and may maintain tension between the cells and their rigid substrate (isometric forces) (Heath & Dunn, 1978; Grierson et al, 1988) thus providing the tractional force for the cell to adhere to the substrate (Burridge, 1981).

4.2.2. Microtubules (MTs)

MTs were also identified by immunofluorescence and anti-tubulin MAB. In bovine, human and rat RPE MTs formed fine radiating filaments that appeared to delineate the shape of the cell and resembled the cytoplasmic microtubule complex described by Brinkley et al (1980). The radiating filaments were typical of the MT patterns that have been described in RPE cells (Turksen et al, 1983; Irons & Kalnins, 1984) and in other cells types (Weber et al, 1975a & b; Osborn & Weber, 1976a). MTs are organised from organising centres (Osborn & Weber, 1976b) which are easily identifiable in RPE cells. The radial organisation of MTs reflects the role of MTs in the cells. In colchicine sensitivity studies, MTs have been shown to be important in the maintenance of cell shape (Goldman, 1971; Goldman & Knipe 1972) and are involved in the intracellular movement of organelles (Freed & Lobowitz, 1970; Goldman 1971; Wang & Goldman, 1978). In the RPE MTs appear to be part of a mechanism contributing to pigment migration in teleost (Burnside 1976; Troutt & Burnside, 1989) and have been identified in association with phagosomes (Feeney and Mixon, 1976). The phagosome/MT association was also reported by Burnside (1976) who suggested that MTs might be involved in the movement of the phagosome in the cell leading to phagosome-lysosome fusion. Clearly bovine, human and rat RPE in vitro share a common organisation of their AMFs and MTs with many other cell types. Further more the study has confirmed that there are no differences in either AMFs or MTs arrangements between normal and dystrophic RCS rat RPE cells in vitro.

4.2.3. Intermediate filaments (IFs)

Historically, the IF complement in RPE cells has been controversial. Chick RPE has been reported to expresses vimentin IFs only (Docherty et al, 1984; Owaribe et al, 1986) and RPE from several species (Owaribe et al, 1988) and human (Kasper et al. 1988; Fuchs et al, 1991) have been shown to express only cytokeratin IFs. However, the present study has shown that bovine, rat and human RPE co-express both vimentin and cytokeratin IFs, in vivo and in vitro.

The results of the present study that show co-expression of vimentin IFs and cytokeratin IFs in bovine, rat and human RPE support the suggestions of previous authors. Co-expression of vimentin IFs and cytokeratin IFs in human RPE has been reported from this laboratory (McKechnie et al,1988) and from other laboratories in RPE of guinea-pig and in sub-populations of bovine RPE (Owaribe et al, 1988). Co-expression is also common in other cultured epithelia (Franke et al, 1979c & d; Henderson & Weber, 1981; LaRocca & Rheinwald, 1984) and in parietal endodermal cells (Lane et al, 1983). Conversely chick RPE has been found to express only vimentin IFs (Owaribe et al, 1988), but McKechnie et al (1988) suggested that chick RPE was markedly different from human RPE in terms of IF expression and Owaribe et al (1988) proposed that the IF expression in chick RPE could not be generalised for all RPE. The results of other authors, (Kasper et al. 1988; Fuchs et al, 1991), who have identified only cytokeratin IFs in RPE cells may be due to differences between the multitude of commercially available anti-vimentin MABs that have been used to identify the vimentin in these studies.

Cytokeratins were identified using immunofluorescence and anti-cytokeratin MABs. MABs specifically identify presence or absence of different cytokeratins according to the presence of specific antigenic determinants. Therefore MABs were prefered in this study to eliminate possible problems of cross-reaction which could occur with antisera. It was found that there was similar positive staining in the RPE of all three species in vivo and in vitro with anti-cytokeratin MABs K8.13 and RCK 102. K8.13 identified a wide spectrum of cytokeratins (1,5,6,7,8,10,11 & 18) and RCK 102 identified cytokeratins 5 & 8. Thus the results appear to agree with previous reports that simple epithelia are characterised by cytokeratins 8, 18 & 19 (Moll et al, 1982) and that the major cytokeratin IFs present in RPE are cytokeratins 8 & 18 (a polypeptide keratin pair) (Kasper et al, 1988; Owaribe et al, 1988; Fuchs et al, 1991), which highlights the epithelial character of the cells.

It should be noted that cytokeratin filaments consist of an acidic (low molecular weight and low isoelectric point) and a basic (high molecular weight and high isoelectric point) cytokeratin protein and these are termed "keratin pairs". Cytokeratins 8 & 18 and 7 & 19 are thought to be pairs and the 7 & 19 pair has been reported to be present in simple epithelia (Cooper et al, 1985). Unfortunately MABs that recognised

cytokeratin 8 alone were not available and although MAB RCK 105 is supposed to recognise only cytokeratin 7, immunoblotting analysis has shown that RCK 105 also identified cytokeratins 14 & 15 as well as cytokeratin 7 (McKechnie et al, 1988), which defeats its' reliability as a single cytokeratin marker. Consequently due to lack of suitable MABs this study was not able to show that cytokeratins 7 & 8 were present alongside cytokeratins 18 & 19 in the various RPE either in vivo or in vitro.

In contrast immunoreactivity to some of the anti-cytokeratin MABs varied between the three species used in this study. Human RPE stained faintly positive with the MAB NCL 5D3 (identified cytokeratins 8, 18 & 19) in vivo and in vitro, whereas both bovine and rat consistently showed no immunoreactivity to this MAB either in situ or in culture. Similarly human RPE showed a faint positive reaction to MAB RGE 53 in situ, but both bovine and rat RPE gave a negative response to this MAB. Variation in reactivity to cytokeratin MABs did not only occur between human RPE verses bovine and rat RPE. In vitro human and bovine RPE were both positive with MAB AE1 (identified cytokeratins 10,14,15,16 & 19), but rat RPE were negative. The variation in immunoreactivity reported in the study supports previous findings that there are interspecies differences in the cytokeratin complement of RPE cells. Interspecies differences in the cytokeratin components of RPE has been documented in detail before (Owaribe, 1988). He proposed that as all RPE shared similar functions, therefore the difference in cytokeratin composition could not be related to their function in the eye. Therefore to date the reason why there is variation in cytokeratin expression between different species remains to be determined.

This study revealed that immunoreactivity of RPE cells to MABs RGE 53 and K4.62 changed in response to culture. In situ bovine and rat RPE were negative for MAB RGE 53 (identified cytokeratin 18, K18) and K4.62 (identified cytokeratin 19, K19) and human RPE showed only a faint positive reaction to these MABs. However, when the three species of RPE were cultured, RGE 53 produced intense positive staining in a sub-population of cells. Similarly K4.62 identified a sub-population of K19+ cells in rat and human RPE. Quantitation of the sub-populations of K18+ and K19+ cells in cultured human RPE revealed that 46.8% of cells expressed K18 and 14.9% of cells expressed K19, further more those cells that were K19+ were a subset of the K18 population. Thus culturing appears to have induced a change in expression of K18 & K19 in the RPE studied. Culture induced changes in cytokeratin staining, which indicated an increased composition in cytokeratin expression has not been reported before in RPE. Changes in cytokeratin expression involving a reduction in cytokeratin composition however, has been reported in RPE (Owaribe et al, 1988) and other epithelia (Connel & Rheinwald, 1983) and is thought to be due to loss during adaptation to culture conditions (Connel & Rheinwald, 1983). However, increased expression of cytokeratins that had been linked to cell morphological changes has been identified in corneal epithelial cells (Fuchs & Green, 1980) and in RPE cells (Vinores et al, 1990).

Vinores et al showed that the population of cytokeratin positive cells increased as RPE cells invaded bovine vitreous in vitro, and that cytokeratin expression decreased as the migratory behaviour of RPE diminished.

It would appear that the expression of cytokeratin IFs in epithelial cells is a dynamic process where expression and loss of expression may be influenced by environmental factors which result in morphological change. The in situ environment is considerably different to the in vitro environment and the transition from in situ to in vitro during culturing induces morphological and behavioral changes in RPE cells. These changes undoubtably influence the IF population of the cells, in particular such changes may explain the immunoreactivity of bovine, rat and human RPE to MABs RGE 53 and K4.62.

Immunocytochemical analysis of cultured RPE revealed that immunoreactivity to MABs that recognised acidic cytokeratins was consistent in all three species of RPE. However, interspecies differences were identified in the immunoreactivity to MABs that identified basic cytokeratins. The expression of basic cytokeratins appears to more prone to change than acidic cytokeratins in cultured cells. The change from in vivo to in vitro has induced changes in the expression of only basic cytokeratins in epidermal cells, keratinocytes (Steinert & Yuspa, 1978; Sun & Green, 1978b; Fuchs & Green, 1978 & 1980) and other epithelial derived cells (Doran et al , 1980; Schmid et al, 1983). The susceptibility of basic cytokeratins to change could be linked to cell differentiation. Certain acidic and basic cytokeratins are specific to different types of epithelia (Tseng et al, 1982). Simple epithelia express acidic cytokeratins while more specialized, differentiated epithelia express basic cytokeratins.

The changes in the expression of basic cytokeratins seen in RPE in this study could also be linked to cell differentiation. In culture RPE cell morphology alters (see 4.1.) and concomitant complex molecular changes take place within the cell which results in loss of their highly differentiated state (Albert et al, 1972; Mannagh et al, 1973; Israel et al, 1980). Vitamin A, for example, is a known cellular differentiation agent (Strickland & Mahdovi, 1978; Strickland et al, 1980) and one of the culture-induced molecular changes that occurs within RPE cells is loss of vitamin A (Flood et al, 1983). Thus what was once a cell with high levels of retinoid (Zinn & Marmor, 1979), in culture it becomes a cell relatively lacking in retinoid. Vitamin A has been linked to cytokeratin expression. In keratinocytes, vitamin A reversibly suppresses the expression of the 67 kD basic cytokeratin (cytokeratin 1; Fuchs & Green, 1981) and modulates the expression of cytokeratins 8 & 18 in mesothelial cells (Kim et al, 1987). Consequently, the disruption of the retinoid balance in RPE in vitro may precipitate the changes in IF expression. The results of this study indicate that IF changes in RPE as a result of culturing are more likely to involve the basic than the acidic cytokeratins.

Changes in IFs in RPE in situ have been reported in human RPE cells which were in close proximity to choroidal melanoma (Fuchs et al, 1991) and in eyes with

retinal detachment (Guérin et al, 1990). In retinal detachment and other pathological conditions, such as RP, the RPE have been subjected to environmental changes. Such changes have lead to the RPE changing from a stationary phagocytic, highly differentiated cell to a mobile, de-differentiated cell. The disease-induced behavioral and morphological changes (such as motility and hyperplastic changes) in the RPE cells appeared to compare favourably with those which occur when cells are placed in culture. Therefore the IF changes we have identified in cultured cells in this study may be relevant to those which take place in RPE in situ during disease.

A feature that was identified in cultured bovine RPE was that these cells exhibited inconsistent immunoreactivity to our panel of anti-cytokeratin MABs. Bovine cells were often negative for cytokeratin IFs, only occasionally were subsets of cells in some cultures found to stain positively for cytokeratins. The loss of cytokeratin staining in cultures has been described before as a feature of bovine RPE (Owaribe et al, 1988) and has been seen in other epithelia by Connel & Rheinwald (1983), who suggested that the loss was due to rapid de-differentiation. However, lack of cytokeratin staining in some bovine cultures could be due to selective masking of the immunologic determinant or epitope. Franke et al (1983) found mitotic PtK2 cells were positive with MAB K8.13, yet interphase cells remained negative and described the existence of cell cycle-dependant selective masking of cytokeratin epitopes. The phenomenon of epitope masking highlights one of the pitfalls of using MABs and immunofluorescence to identify the subtypes in the cytokeratin family. The results of this study and those of others (Smedts et al, 1990; Fuchs et al, 1991) indicate that care must be taken when identifying cytokeratins in cells or tissue through immunostaining techniques, because the phenomenon of masking could lead to an ambiguous result. Definitive identification of the cytokeratins must be obtained using gel electrophoresis and immunoblotting. Immunohistochemistry is best when the location of cytoskeletal elements is required and is particularly valuable for studies comparing cell morphology and staining patterns.

In this study immunohistochemical staining techniques were used to identify patterns of cytoskeletal elements, particular cytokeratins in cultured RPE cells. In bovine, human and rat RPE the pattern of fine cytokeratin filaments radiating throughout the cytoplasm forming a delicate network was comparable to the classic networks which have been described in other epithelia (Franke et al, 1978b; Franke et al, 1979a; Osborn et al, 1980). This study did not identify any differences in the organisation of vimentin IFs or of most of the cytokeratin IFs between cultured control and dystrophic rat RPE. The one exception was K18 networks identified with MAB RGE 53.

For the first time a difference in the organisation of a componant of the cytokeratin IF network between control and dystrophic rat RPE in vitro has been identified. MAB RGE 53 identified a filamentous network consisting of K18 filaments

in a sub-population of cultured rat RPE cells. In dystrophic rat RPE the sub-population of K18+ cells contained a network of filaments organised into highly tortuous webs which were not evident in control rat RPE. The function or role that these tortuous networks may play in the dystrophic rat is unknown.

A distinctive feature of the cytokeratin network in all three species of RPE cells was the considerable variation in the staining patterns between cells. Variation in cytokeratin patterns visualised by immunofluorescence has been noted before in cultured epithelia (Lane & Klymkowsky, 1981). As the cytokeratin networks are thought to be complex, dynamic systems in a continuous state of flux (Geiger et al, 1984b; Lane & Klymkowsky, 1981) it is probably not surprising that these cytoskeletal elements varied between neighbouring cells. The importance of a dynamic cytokeratin IF network was considered by Boller et al (1987). The authors suggested that the differential distribution of cytokeratin in cells meant that different cytokeratin filaments present within cells could have different function in these cells. Thus, the variation in cytokeratin staining may reflect the intrinsic state of the cell, possibly in the cell cycle or in behavioral modes.

Variation in the staining pattern of K18 was most obvious in islands of both control and dystrophic rat RPE. Staining varied according to the location of the cell in the island. In particular there was greater variation in cells described as having an intermediate morphology. It is possible that in islands of rat RPE the variation seen in the K18 staining pattern may be due to the differential stages of cell adaptation to culture. Cells in the centre of an RPE island showed the least morphological change as a result of the transition from an in situ to an in vitro environment. The central cells maintained an in situ-like morphology. Whereas cells at the edge of the island, which had in situ been surrounded by cells bound by tight contacts (zonula occludens & zonula adherens), had been subjected to an extreme environmental change and when in culture had contact-free cytoplasmic borders. In response to this extreme change, edge cells showed the most marked morphological change and appeared dedifferentiated (indistinguishable from the in situ phenotype). However, intermediate cells showed a morphology that was half way between the in situ-like cells of the centre and the de-differentiated cells at the edge. The intermediate cells showed the greatest variation in both morphology and in the K18 staining patterns. The variation in morphology suggests that the cells in this zone were not demonstrating synchronous morphological change. The variation in the staining patterns between intermediate cells may reflect the de-differentiated state of the cell and consequently the behavioral response of the cell to environmental change.

In conclusion RPE cells contain both vimentin IFs and cytokeratin IFs. The immunoreactivity of RPE cells to anti-cytokeratin MABs alters with culture induced changes which in turn effect IF expression. The staining patterns of cytokeratin IFs

link with change in cell morphology in the RPE cells as they respond to environmental change. Culture induced changes of IFs may reflect alterations in cytokeratin expression in RPE cells in response to disease in the eye, such as PVR and RP. In particular the IFs, K18 and K19 responded to environmental change and may be markers of cell behavioural changes, such as de-differentiation and adaptation to culture, and these behavioral changes may correlate to changes that occur during disease. In the dystrophic RCS rat the organisation of K18 networks differs strikingly from that of controls and some association between this and the dystrophic lesion cannot be ruled out.

4.3. EVALUATION OF PHAGOCYTOSIS IN CULTURED BOVINE AND RAT RPE

Using a MAB (developed in this laboratory) that was highly specific for isolated bovine ROSs and double immunofluorescent staining, attached and internalised ROSs were visualised and quantified in cultured bovine and rat RPE. This technique was developed by Chaitin & Hall (1983) and, besides imaging ROS phagocytosis in a large number of cells it also gives direct quantitation of ROS phagocytosis. Using this technique it appeared that bovine RPE cells were far less effective at attaching and internalising ROSs than control rat RPE. Bovine RPE, like chick RPE (Masterson et al, 1981) appeared to be poor phagocytes. The present study has shown, as have others (Goldman & O'Brien, 1978; Chaitin & Hall, 1983), that dystrophic RCS rat RPE in vitro have an impaired ability to phagocytose ROSs whereas, cultured control RCS rat RPE effectively phagocytose ROSs.

The results also revealed that in bovine and in both types of rat RPE cultures challenged with ROSs, phagocytosis of ROSs varied between cells. From observation of micrographs and from the quantitation of phagocytosis, the number of ROSs attached and internalised by bovine RPE was markedly low. From the ROS concentration (1.88×10^7 ROS/ml), ROS settlement rate (5×10^5 ROSs/cm^2/hour) and the mean number of bovine RPE cells per cm^2 (4×10^4 cells/cm^2), it could be calculated that the mean number of ROSs available at the suface of each cell at 1 hour was 12.5 and at 4 hours was 50. As the mean number of ROSs attached per cell at 4 hours by bovine RPE was 0.09 then clearly some cells were failing to attach any ROSs. Similarly, with both control and dystrophic rat at 2 hours (maximal ROSs attachment in dystrophic cells; see Fig 3.20) the mean number of ROSs per cell was 0.85 (control) and 0.94 (dystrophic). In any given culture while some cells attached and internalised ROS, other cells failed to accumulate any ROSs. The variability in phagocytic ability of RPE has not been reported in the literature before to my knowledge.

The island cultures of rat RPE showed that the phagocytic variability of ROSs by

RPE cells was directly correlated to cell morphology and a model showing the role of cell morphology and ability to accumulate ROSs is proposed (Fig. 4.1.). In situ the RPE cell (Fig. 4.1.A) is a cuboidal, highly polarised cell with an abundance of long thin apical microvilli which interdigitate with the outer segments of rod photoreceptor cells. Phagocytosis of the outer segment discs at the RPE end of the rod photoreceptor cells involves a receptor recognition system (Hall & Abrams, 1987). The receptors are thought to be localised on the RPE cell membrane closest to the tip of the ROS. In island cultures of RPE, cells in the centre of an island shared similar morphological features to RPE cells in situ (Fig 4.1.B). Central cells were cuboidal with a forest of apical microvilli on their surface. When these cells were challenged with ROSs it was not possible to mimic the situation in situ, consequently challenged ROSs do not interdigitate with the RPE apical microvilli. In fact in vitro , the microvilli may act as a barrier between the ROSs and the receptor recognition system on the cell membrane preventing ROS phagocytosis. Phagocytosis occured in cells described as intermediate cells (Fig 4.1.C). As RPE adapt to culture they undergo morphological changes (see 4.1.) some of these changes had occured in intermediate cell, which were flattened, epitheloid and had short and sparse microvilli. In these cells the receptors on the apical membrane would be exposed, ROSs were accumulated and subsequently phagocytosed. Well spread cells at the edge of the island showed the greatest morphological changes. These edge cells had some stumpy surface microvilli and were devoid of ROSs. The lack of ROSs phagocytosis in edge cells may be due to an insufficient number of receptors or result because cells were actively engaged in cell division or other cellular activities that supressed phagocytosis of ROSs.

In conclusion the variability of phagocytosis in rat RPE in vitro appears to be a function of cell morphology and ultimately may be a function of the behavioural state of the cell as it adapts to the environmental change imposed by tissue culture.

4.4. EVALUATION OF THE INVOLVEMENT OF CYTOKERATIN IN THE PROCESS OF PHAGOCYTOSIS AND ITS POSSIBLE ROLE IN THE DEFECT IN THE RCS RAT.

In the experimental system in vitro the RPE has had to adapt from zero phagocytic load to a large phagocytic load presented during ROS challenge. It is possible that in order to accommodate such change there could be an alteration in the cytoskeleton. AMFs and MTs have been shown not to be involved in the defect of the RCS rat (Chaitin & Hall, 1983; Irons & Kalnins, 1984) and so far the role, if any, of IFs in the phagocytic process has not been explored. The present study has identified a difference in K18 expression and ROS association between control and dystrophic RCS rat RPE.

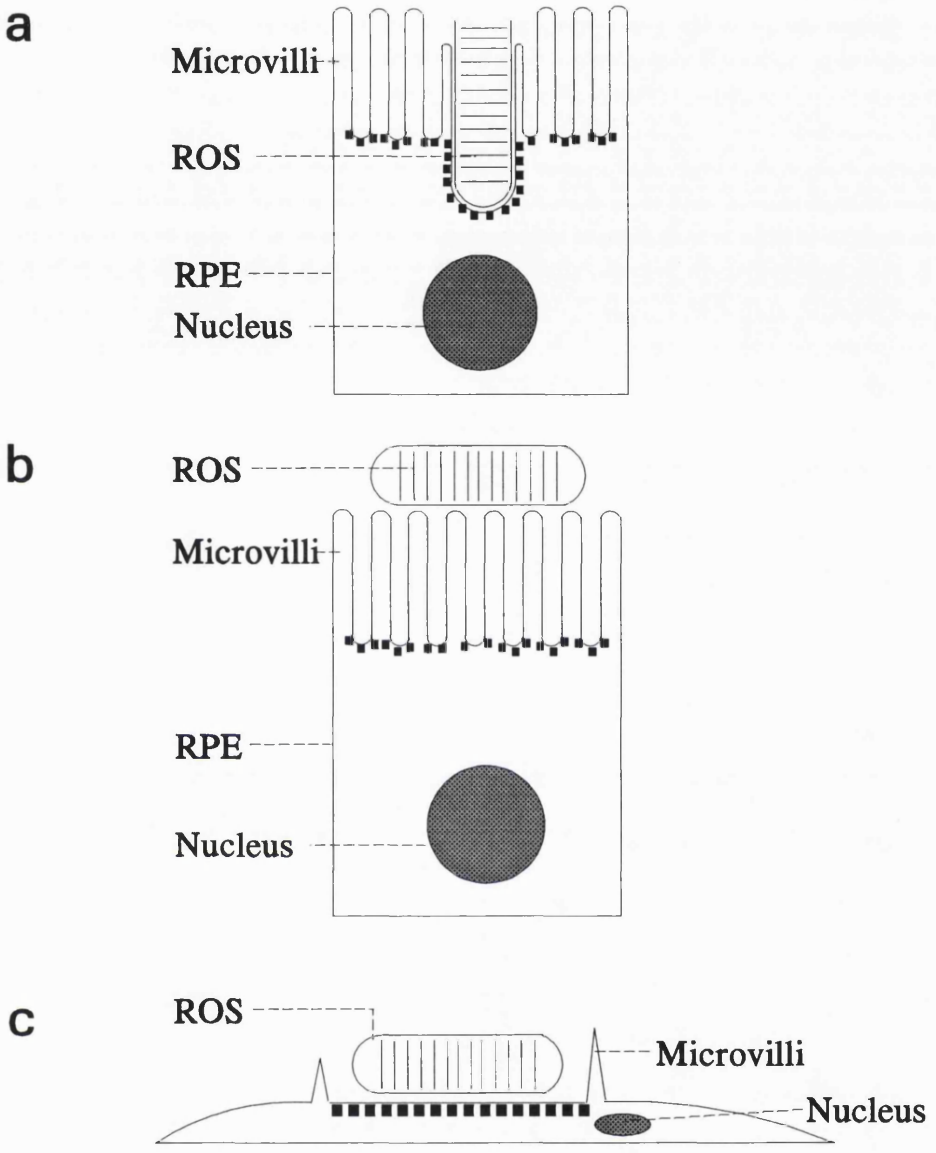

▪ Receptor

Figure 4.1. A model for the involvement of cell morphology in the variability of phagocytosis of ROSs by cultured rat RPE. a) A RPE cell in situ. Photoreceptor outer segment interdigitate with the long microvilli. If there is a receptor for ROSs it must be in contact with the tips of the photoreceptor outer segments and therefore would be located at the base of the microvilli. b) A cell in the centre of an RPE island. In vitro ROSs can not be orientated as they are in vivo and thus the forest of microvilli acts as a barrier between the ROSs and the receptor system of the cell. c) An intermediate cell adapting to culture. The cell has spread and the microvilli are reduced in number and size. In these cells the receptors are accessable to ROSs challenged to the cells and phagocytosis is possible.

Using a double immunofluorescent staining technique, especially developed for this investigation, both ROSs and cytokeratin IFs were visualised in rat RPE cells. The quantitative studies have shown that K18- control RPE cells accumulated more ROSs than the K18+ cells. This indicates that the expression of K18 in control RPE does not appear to be related to ROS attachment and internalisation. Whereas, in dystrophic cells K18+ and K18- cells accumulated equal amounts of ROSs. The results expose an anomaly in the expression of K18, IFs and ROS phagocytosis in cultured RCS rat RPE. Furthermore, when comparing control and dystrophic cells, the trend in control RPE suggests that K18- cells are more effective in accumulating ROSs, whereas the trend was reversed in dystrophic RPE, i.e. K18+ cells accumulated more ROSs.

Previously the dystrophic cells were noted to contain tortuous and convoluted K18 networks (see 4.2.), K18 organisation was influenced by cell morphology (see 4.2) and cells in the process of morphological change (i.e. the intermediate cells in islands of rat RPE) were more effective at associating ROSs. It has been shown that cytokeratin gene expression was affected, either positively or negatively, by complex factors such as cell shape, cell-cell interactions and growth rate (Ben Ze'ev 1984; 1985; Connell & Rheinwald, 1983) as well as by vitamin A and EGF (Eckert & Green, 1984; Kim et al, 1984; 1987). However the mechanism by which the factors influence shape and growth rate is unknown. As the cytokeratin genes can be influenced by external factors, it might be that the genetic lesion in the dystrophic rat, which effects the mechanism of phagocytosis, may also effect the K18 genome, directly or indirectly, such that the organisation of the K18 network is abnormal. This may account for the anomaly in the different trends that has been identified between control and dystrophic rat RPE in K18 expression and ROS accumulation.

Unfortunately the present investigation has not clarified the involvement of IFs in the phagocytosis of ROSs or in the defect in the dystrophic RCS rat RPE. However, clearly there is no simple mechanism operating between K18 expression and ROS association.

4.5. EVALUATION OF THE INVOLVEMENT OF CYTOKERATIN IN PROLIFERATION OF RPE CELLS

The organisation of cytokeratin IFs in epithelial cells has been shown to alter with changes in cell behaviour, particularly during cell division (Aubin et al, 1980; Horwitz et al, 1981; Lane et al, 1982; Franke et al, 1982 and 1983). In human RPE K18 (identified by RGE 53) was expressed in a sub-population of cells and was linked to cell proliferation (McKechnie et al, 1988). In this present study K18, and its' sub-set K19, have been identified in sub-populations of RPE cells and the variation in K18 staining patterns identified in these cells have been suggested to be linked to behavioural change during adaptation to culture conditions (see 4.2). Proliferation is a

process that may occur during environmental change and is a key behavioural response in cell culture. The expression of K18, and its' sub-set K19, were investigated in cultured human RPE using markers of cell proliferation. Far from establishing a link between replication and K18 & K19 expression, the present study has demonstrated that human RPE expressing K18 & K19 are less likely to be actively dividing.

MABs that detected proliferating cells via BrdU incorporation or accumulation of PCNA enabled direct quantitation of dividing cells. This technique, when combined with immunohistochemical staining for K18 & K19, also enabled assessment of cytokeratin expression and cell proliferation in the same cultures. There were between 8-30 times more dividing cells that were negative for K18 & K19 than there were of dividing cells that were positive for these two cytokeratins. Clearly in human RPE cells the expression of K18 is not linked to cell proliferation.

It has been shown in the present study and from the work of others (McKechnie et al, 1988) that the incidence of K18+ and K19+ cells steadily decreased as the number of cells increased. The obvious interpretation of the growth curve findings is that there is a relationship between K18 and K19 expression and proliferation because cell division rate is high in sparse cultures when K18 and K19 expression is high and division and cytokeratin expression plummits at confluence. At first it might seem that the growth curve findings are at odds with the BrdU and PCNA labelling which emphatically demonstrated that proliferation and cytokeratin expression are not related. On the other hand as the cells approach confluence not only does cell division rate decrease, but their mobility is impaired. Mobility is also compromised at high seeding density. At high seeding density K18+ cells were found to make up a significantly lower percentage of the population than in cultures seeded at lower density, when comparable time peroids were evaluated.

RPE play a key role in retinal scar formation but they are difficult to identify on phenotype alone (Kampik 1981). Consequently it is important to identify a marker for proliferating RPE cells. The findings of this study do not support the suggestion by McKechnie et al (1988) that in cultured human RPE expression of K18 may be cell cycle related. Therefore MAB RGE 53 and K4.62 cannot be recommended for use as markers for RPE proliferation in either culture or in pathological tissues, such as retinal scars. Indeed it is more likely that K18 & K19 may be linked to cell mobility and our evidence is discussed in the next section (see 4.6.).

4.6. EVALUATION OF THE CYTOSKELETON IN MIGRATING RPE CELLS

Many cell types are capable of directed migration in response to a particular stimuli and epithelial cells are no exception. Chemoattractants, such as serum and fibronectin (Campochiaro et al, 1984) induce cell locomotion and when presented as a

concentration gradient it induces directed movement (Calthorpe et al, 1991). Fibronectin at 10 μg/ml was found to produce an optimal migrational response in human RPE. Migrating human RPE cells were used to investigate the organisation of AMFs MT and IFs in motile cells.

Immunofluorescent and immunoperoxidase staining was used to visualise the cytoskeletal elements in migrating cells. The techniques have not been used before on a permeable chemotaxis membrane and proved excellent for imaging the arrangement of the cytoskeletal proteins within the cell cytoplasm of cells at various stages of migration.

The AMF and MT organisation in the multi-processed cells on the upper (settled) and lower (migrated) sides of the permeable membrane followed the established decription reported in the literature (Couchman & Blencowe, 1985; Herman et al 1981; Geiger et al, 1984). The diffuse and filamentous actin staining and the MTs orientated parallel to the direction of movement in cells on the upper surface, indicated cell motility. Whereas the actin stress fibres present in the flattened, well spread cells on lower surface indicated that these cell were stationary (Herman et al, 1981).

The organisation of IFs in motile epithelial cells has not been described before. The investigation revealed that vimentin IFs formed a radiating network throughout the cytoplasm of cells on the settled side of the membrane, but staining for vimentin was diffuse in cells on the migrated side. The change from an organised filamentous vimentin network to disordered non-filamentous vimentin suggested that the vimentin IFs had undergone reorganisation. It appears that as human RPE cells migrate through the membrane the vimentin IF system is reorganised. Reorganisation of vimentin IFs has been described in cells during mitosis (Franke et al, 1982; Franke et al, 1984) and is thought to neccessary because of the rigid nature of these filaments. The rigidity if the radiating vimentin IF assembly might hamper the movement of the RPE cells through the small 10 μm pore of the permeable membrane and therefore vimentin IF reorganisation occurs in this situation as it does in cell division .

Vimentin reorganisation in migrating RPE does not necessarily suggest a role for vimentin IFs in RPE cell migration. However the chemoattraction assays provided strong evidence that K18 & K19 IFs do have a role in human RPE cell migration. On the migrated side, the percentage of K18+ human RPE cells was 5 times greater than on the settled side. The same trend was true for K19 with a 10 fold increase in the K19+ population on the migrated side of the membranes. The enhancement of the K18 and K19 populations from upper to lower sides of the membranes occurred because all cells caught in transit through the pores in the membrane were positive for these two cytokeratins. Cells intransit through pores were, at the time of staining, actively migrating cells. Therefore K18 and K19 were expressed by human RPE involved in active migration.

The present study identified seven stages in the process of RPE migration and

these were outlined and summarised in section 3.5.4. and figure 3.43 respectively. The early stages of the migration process consisted of stages 1, 2, 3, and 4, where RPE cells progressed from rounded and partially spread cells that were mostly negative for K18 and K19 and stained diffusely for actin (stage 1 & 2), to well spread cells with cytoplasm invading pores that were positive for K18 and K19. Positive staining was either seen as non-filamentous aggregates adjacent to the nucleous in recently settled cells (stage 3) or as filamentous cytoplasmic networks that extended into cytoplasm that probed into nearby pores (stage 4). Stage 4 cells also contained a filamentous actin network within the cytoplasm. Actively migrating cells in tansit through pores (stage 5) were always K18+ and K19+ and contained intricate webs of filamentous cytokeratin in the cytoplasm that was spread on the under side of the membrane and diffuse staining for cytokeratin in the remnant of cytoplasm on the upper surface. Similarily stage 5 cells had a distinctive actin network in the cytoplasm spread on the under side of the membrane, but the cytoplasm in the pore and the remnant on the upper surface exhibited a diffuse staining pattern. In the advanced stages of migration (stages 6 & 7) cells demonstrated loss of cytokeratin staining. Stage 6 cells (which were identical to stage 4 except they were on the bottom of the membrane rather than the top) contained a filamentous K18 and K19 cytoplasmic network, but stage 7cells were negative for these cytokeratins. Stage 7 cells were extremely large and flat with well developed actin cables or stress fibres in their cytoplasm. Clearly human RPE committing (stage 4) and committed (stage 5) to migration became more spread and mobile and exhibited K18 and K19 staining whereas human RPE on the upper surface which were not yet involved in migration were negative. In the post migrational phase on the lower surface of the membrane, staining was progressively lost (stages 6 and 7). The post migrational cells (stage 7) were well spread and flat but were probably immobile given the presence of stress fibres in their cytoplasm. It has been said that cytokeratins help cultured epithelium to remain flat and spread (Aubin et al, 1980) but this would not be the case with K18 and K19 which are present during spreading which leads to locomotion and during locomotion itself, but cannot be detected in sedentary human RPE.

A current area of research interest has been altered cytokeratin subtype expression with the emergence of premalignant or malignant epithelial lesions (Smedtds et al, 1990; Cintorino et al, 1990; Schaafsma et al, 1990; Nagle et al, 1991). It has been observed that the expression of cytokeratins 8, 18 or 19 may be upregulated in premalignant or malignant lesions of various tissues including the cervix, prostate and tongue. In addition, infiltrating cells of transitional cell carcinomas were shown to be strongly immunoreactive for K18 (Schaafsma et al, 1990). Furthermore, it has been shown in transfected mouse L cells that expression of cytokeratins 8 and 18 is associated with significantly increased invasive ability (Chu et al, 1990). Invasive epithelia would be expected to be highly motile but in addition an association between cell flexibility and K18 expression has been made (Schaafsma et al, 1990).

Undoubtedly human RPE in transit through pores would need to be highly flexible and to some extent this was born out by our SEM studies which demonstrated the complex distortion of cell shape required to successfully negotiate the pore channels through the membrane.

Our observation of an apparent specific association between migratory activity of RPE cells in vitro and immunoreactivity to MABs RGE 53 and K4.62 suggests that cytokeratins 18 and 19 may play a fuctional role in RPE cell motility. Furthermore expression of K18 & K19 can be used as markers of motile human RPE cells. Thus MAB RGE 53 and K4.62 could be used as tools for immunohistochemical identification of motile RPE cells in pathological tissue, such as retinal scars. Indeed, we have already documented the presence of a subset of K18+ RPE cells in situ in some retinal scars (Hiscott et al, 1991) and it is also possible that K18 & K19 may be useful in the detection of migratory activities by other simple epithelia.

4.7. FINAL COMMENT AND FUTURE INVESTIGATIONS

Until now, no functional role has been assigned to IFs in cells. However through investigating RPE cell behaviour the present study has shown that IFs may have a functional role in cell migration or motility and possibly in cell flexibilty. As part of its response to environmental change (i.e from in situ to in vitro or from normal to diseased state), the RPE cell changes its activity and this in turn effects the organisation of the cytoskeletal elements, and in particular the cytokeratin IFs. In RPE K18 & K19, cytokeratin IFs appear to be expressed in association with actively migrating cells, but these cytokeratins are not markers of proliferation. The way in which K18 & K19 are involved in intracellular mechanisms engaged in cell migration was not investigated, but remains an important area for future research. In addition it would be necessary to investigate whether there is de novo expression of K18 & K19 and this could be determined using mRNA probes, in situ hybridisation and immunoblotting techniques.

Evidence in the literature indicated that K18 increased invasive ability of cells. Human RPE cells invading the neurosensitive retina are a major feature in PVR. Therefore it would be important to examine whether K18 & K19 are also expressed in RPE cells undergoing invasion. An invasive in vitro assay system would consist of video time lapse imaging of a human RPE seeded onto a monolayer of glial cells. The glial cell monolayer would be representative of the neural retina in situ. At various stages of invasion, RPE cells would be stained for K18 & K19 and the the role of these two cytokeratins in the invasive behaviour of human RPE could be determined. Indeed preliminary studies using the invasive assay system described above have revealed that human RPE that were active (mobile) on the surface of the glial monolayer probed the glial monolayer with cellular processes and were positive for K18 and K19. Staining for

K18 and K19 became intense in RPE cells as they invaded the monlayer. Invaded RPE cells spread onto the substrate, were quescent and negative for K18 and K19. The preliminary results suggests a link between invasive activity of RPE and expression of cytokeratins 18 and 19. Therefore a study on K18 and K19 expression in simple epithelia melanomas would be of considerable interest.

K18 & K19 are co-expressed with K8 & K7, respectively as keratin pairs. This study did not investigate the co-expression of keratin pairs in proliferating and migrating RPE, because of the lack of MABs that identify K8 or K7. It would be meaningful to look for expression K8 & K7 in human RPE on permeable membranes and in an invasion assay, as well as K8 & K7 synthesis through in situ hybridization.

The study has shown that dystrophic rat RPE differ from control rat RPE in the staining pattern of K18 filaments. Unfortunately the present study failed to determine whether IFs have a role in phagocytosis of ROSs, but the study did indicate an anomaly in K18 expression and phagocytic capability between control and dystrophic RPE. During the study it was found that immunofluorescence analysis was clearly was not adequate to investigate IF association with ROS phagocytosis or to try to determine the anomaly in K18 expression and phagocytosis. However, a combination of TEM of detergent extracted whole cells and immunogold labelling could be used to follow the movement of ROSs from attachment at the cell surface to incorporation into the secondary lysosome during phagocytosis, by specifically labelling both the K18 filaments and ROS material. Other means of investigating the involvement of IFs with ROS phagocytosis could be achieved by disrupting the K18 network, possibly by microinjection of the corresponding anti-K18 MAB. Following treatment cells would be challenged with ROSs and phagocytosis would be compared between control and dystrophic RPE.

Vitamin A has been indicated in the literature to influence the expression of cytokeratins as a result of culture induced changes such as dedifferentiation. Recently Campochairo et al (1991) and Verstraten et al (1992) have published results that have shown that vitamin A inhibits cell growth, proliferation, migration (i.e. wound closure) and contraction in vitro. The authors suggested that vitamin A, or rather depletion of vitamin A, may play a role in the pathogenesis of PVR and could have potential therapeutic applications. The experimental model used in this study for RPE proliferation and migration would be ideal to investigate the possible use of vitamin A or other retinoids as agents for the treatment of PVR.

APPENDICES

APPENDIX I

Peroxidase substrates

Aminoethylcarbozole substrate (AEC)

Dissolve 15 mg aminoethylcarbozole into 3 ml diethylformamide.
Add 50 ml 0.02 M acetate buffer and pH solution to 5.2, filter and prior to use add 0.5 ml of 3% hydrogen peroxide.

3,3'–diaminobenzidine tetrahydrochloride (DAB)

To 30 mg of DAB add 50 ml 0.05 M Tris–HCL buffer and pH solution to 7.6, filter and prior to use add 0.5 ml of 3% hydrogen peroxide.

APPENDIX II

Solutions for isolation of bovine ROSs

42% Sucrose (1.465M)

210 g sucrose
290 g dH_2O

2M Tris (hydroxymethyl)methylamine

24.2 g Tris (hydroxymethyl)methylamine
100 ml dH_2O

2M Acetic acid

48 ml acetic acid
200 ml dH_2O

1M Tris-acetate buffer (pH 7.4)

100 ml 2M Tris (hydroxymethyl)methylamine
82 ml 2M acetic acid

1M Sodium chloride

5.84 g NaCl
100 ml dH_2O

0.1M Magnesium Chloride

2.03 g $MgCl_2$
100 ml dH_2O

2mM di-Sodium EDTA

0.074 g Na_2EDTA
100 ml dH_2O

2mM Calcium Chloride

0.044 g $CaCl_2$
100 ml dH_2O

1mM Calcium EDTA

100 ml 2mM Na_2EDTA
100 ml 2mM $CaCl_2$

10mM Tris-acetate Buffer

0.5 ml 1M tris-acetate
0.5 ml 0.1M $MgCl_2$
7 ml 1M NaCl
5 ml 1mM CaEDTA

Sucrose Homogenising Media

1.91 g 42% sucrose
13 ml 1M NaCl
0.4 ml 0.1M $MgCl_2$
1.0ml 1M Tris-acetate buffer
Add 230 g dH_2O

Sucrose Gradient Solutions (50 ml)

Solution	Density g/ml (Sucrose molarity)			
	1.10 (0.77M)	1.11 (0.94M)	1.13 (1.0M)	1.15 (1.14M)
42% sucrose	31.2 g	34.2 g	40.7 g	46.5 g
1M Tris-acetate	0.5 ml	0.5 ml	0.5 ml	0.5 ml
0.1M $MgCl_2$	0.5 ml	0.5 ml	0.5 ml	0.5 ml
1.0mM CaEDTA	5.0 ml	5.0 ml	5.0 ml	5.0 ml
add dH_2O to get	55.0 g	55.5 g	56.6 g	57.5 g

APPENDIX III

Monoclonal antibodies used to identify the cytoskeletal elements

MONOCLONAL ANTIBODY	CYTOSKELETAL ELEMENT	IG CLASS	SUPPLIER
Anti–actin C4 clone	actin microfilaments	IgG1	*ICN
Anti–beta tubulin TUB 2.1	microtubules	IgG1	ICN
Anti–vimentin VIM–13.2	vimentin intermediate filaments	IgM	#SIGMA
K8.13	cytokeratin 1, 5, 6, 7, 8, 10, 11 & 18	IgG2a	ICN
AE3	cytokeratin 1, 2, 3, 4, 5, 6, 7 & 8	IgG	ICN
RCK 102	cytokeratin 5 & 8	IgG1	"BIONUCLEAR SERVICES
RCK 105	cytokeratin 7 (? 14 & 15)	IgG1	BIONUCLEAR SERVICES
K8.60	cytokeratin 1, 10 & 11	IgG1	ICN
AE1	cytokeratin 10, 14, 15 16 & 19	IgG	ICN
NCL–5D3	cytokeratin 8, 18 & 19	IgG2a	BIONUCLEAR SERVICES
K8.12	cytokeratin 13 & 16	IgG1	ICN
RGE 53	cytokeratin 18	IgG1	BIONUCLEAR SERVICES
K4.62	cytokeratin 19	IgG1	ICN

*ICN Biomedical Ltd., High Wycombe, U.K.

#Sigma chemical Co. Ltd., Poole, U.K.

"Bionuclear Services, Cornwall, U.K.

APPENDIX IV

Phagocytosis of ROSs by monodispersed cultures of control and dystrophic rat RPE

CULTURE	CONTROL				DYSTROPHIC			
	Total number of ROSs		Total number of cells		Total number of ROSs		Total number of cells	
	Attached	Internalised	With ROSs	Without ROSs	Attached	Internalised	With ROSs	Without ROSs
1	193	151	97	79	487	17	191	54
2	325	249	166	47	495	9	225	58
3	410	260	103	34	144	4	44	78
4	284	210	80	34	116	18	34	50
5	206	124	81	41	63	20	24	75
6	382	247	87	23	131	8	52	101
7	463	257	92	6				
8	302	309	127	33				
9	138	58	59	27				
10	149	149	53	47				
TOTAL	2852	1941	945	371	1430	76	570	416
%	59.5	40.5	71.8	28.2	95	5	57.8	42.2

APPENDIX V

Phagocytosis of ROSs by islands of cultured control and dystrophic rat RPE

	Island	Number of ROSs attached	Number of ROSs internalised	Number of cells with ROSs	Number of cells without ROSs
CONTROL	1	135	69	62	103
	2	153	120	52	63
	3	62	46	33	77
	4	16	21	14	60
TOTAL		366	256	161	303
%		58.8	41.2	34.7	65.3
DYSTROPHIC	1	113	11	42	37
	2	106	9	43	28
	3	137	12	62	68
	4	136	16	48	33
	5	102	21	59	92
	6	231	17	88	89
	7	113	7	19	29
	8	53	0	30	53
	9	163	8	78	115
	10	186	8	94	139
	11	259	80	156	308
	12	290	48	91	232
TOTAL		1889	238	810	1223
%		88.8	11.2	39.8	60.2

APPENDIX VI

The expression of K18 and the association of ROSs in cultures of control RCS rat RPE

Time (hours)	Cultures	Cytokeratin 18+		Cytokeratin 18−	
		Number of cells	Number of ROSs	Number of cells	Number of ROSs
1	1	47	150	53	186
	2	42	117	58	173
	3	58	133	42	467
Mean +/− SE		49.0 +/−4.7	133.3 +/−9.5	51.0 +/−4.7	275 +/−95.9
2	4	50	143	50	89
	5	49	238	51	188
	6	60	318	40	809
Mean +/− SE		53.0 +/−3.5	227.7 +/−50.5	47.0 +/−2.9	362 +/−225
3	7	60	165	40	116
	8	39	186	61	281
Mean +/− SE		49.5 +/−10.5	175.5 +/−10.5	50.5 +/−10.5	198 +/−82.5
%		50.6	38.4	49.4	61.6

APPENDIX VII

The expression of K18 and the association of ROSs in cultures of dystrophic RCS rat RPE

Time (hours)	Cultures	Cytokeratin 18+		Cytokeratin 18−	
		Number of cells	Number of ROSs	Number of cells	Number of ROSs
1	1	57	286	43	90
	2	60	143	40	105
	3	58	160	42	172
Mean +/− SE		58.3 +/−0.9	196.3 +/−45.1	41.7 +/−0.9	122.3 +/−2529
2	4	63	315	37	137
	5	74	295	26	126
	6	43	272	57	284
Mean +/− SE		60.0 +/−9.1	294 +/−12.4	40.0 +/−9.1	182 +/−50.9
3	7	58	275	42	159
	8	60	392	40	122
	9	45	330	55	443
Mean +/− SE		54.3 +/−4.7	323.3 +/−33.8	45.7 +/−4.7	241.3 +/−101.4
%		57.5	60.1	42.4	39.9

APPENDIX VIII

The expression of K18 after post–seeding event in human RPE cells

Substrate	Time (hours)	Number of K18+ cells	Total number of cells	% K18+ cells
Flask	12	463	840	55.00
	24	483	973	49.64
	48	215	1704	12.60
	72	90	1874	4.80
LabTek	12	366	577	63.47
	24	391	804	48.63
	48	592	1914	30.93
	72	831	2490	32.29
Flask	2	214	487	43.94
	4	499	885	56.40
	12	325	943	34.46
	24	473	1793	26.31
	72	480	4906	9.78

APPENDIX IX

The expression of K18 and K19 in human RPE cells labelled with the proliferation marker BrdU

LabTek chamber	BrdU+				BrdU−			
	K18+	K18−	K19+	K19−	K18+	K18−	K19+	K19−
1	7	106	6	98	38	208	25	159
2	4	111	8	79	42	204	25	151
3	4	99	3	79	27	193	31	146
4	1	92	3	77	24	190	20	138
5	4	99	3	68	23	195	25	181
6	4	116	4	78	18	200	28	201
7	1	102	8	105	24	213	32	148
8	3	88	6	77	26	173	27	204
TOTAL	28	813	41	661	222	1576	213	1328
%	3.3	96.7	5.8	94.2	12.3	87.7	16.0	84.0
BrdU	841		702		1796		1541	
%	31.9		31.3		68.1		68.7	

APPENDIX X

The expression of K18 and K19 in human RPE cells labelled with MAB anti−PCNA a proliferation marker

LabTek chamber	PCNA+		PCNA−	
	K18+	K18−	K18+	K18−
1	23	259	1	21
2	43	388	11	19
3	48	255	0	15
4	25	277	2	11
5	27	253	0	16
6	24	221	0	20
7	37	230	4	26
8	32	281	10	15
TOTAL	259	2164	28	143
%	10.7	89.3	16.4	83.6
PCNA	2423		171	
%	93.4		6.6	

APPENDIX XI

The expression of K18 in migrating human RPE cells

Well	Settled (upper)		Migrated (lower)	
	Number of K18+ cells	Number of cells	Number of K18+ cells	Number of cells
1	225	2427	20	105
2	158	2446	22	93
3	184	2342	17	101
4	209	2625	50	88
5	169	2364	88	105
6	167	2360	49	94
7	192	2612	49	126
8	226	2892	57	171
9	241	2166	74	113
10	165	2175	54	148
11	228	2668	–	194
12	207	1899	–	109
Mean	197.6	2414.6	48	114.4
SD	27.7	264.9	23.1	26.7
%	8.2		45.9	

APPENDIX XII

The expression of K19 in migrating human RPE cells

Well	Settled (upper)		Migrated (lower)	
	Number of K19+ cells	Number of cells	Number of K19+ cells	Number of cells
1	115	2307	57	504
2	51	2631	47	210
3	39	3031	49	190
4	45	2591	49	184
5	31	2438	32	150
6	29	2423	38	158
7	126	3165	49	205
8	45	2499	83	198
9	84	2461	46	297
10	113	2878	–	–
11	74	2711	–	–
12	28	2595	–	0
Mean	65	2644.2	50	232.9
SD	36.3	260.3	14.9	110.0
%	2.5		21.5	

APPENDIX XIII

The profile of the cytokeratin 18 stages on a migration membrane

Well	Number of cells in each stage of migration							Total cells on upper side	Total cells on upper & lower side
	1	2	3	4	5	6	7		
1	47	628	28	36	10	3	10	748	762
2	108	684	25	42	5	5	20	864	889
3	85	560	30	51	7	1	5	733	739
4	82	707	24	30	6	11	47	849	907
5	67	721	28	38	7	8	34	861	903
6	69	833	28	25	12	7	27	967	1001
7	47	809	24	26	16	15	40	922	977
8	58	772	23	30	9	14	36	892	942
9	55	868	13	32	13	9	25	981	1015
10	45	663	22	27	13	12	32	770	814
11	57	788	29	26	8	8	14	908	930
12	60	834	29	20	9	14	45	952	1011
13	29	648	16	43	5	0	9	741	750
14	34	637	17	44	5	1	11	737	749
15	53	624	20	27	8	8	21	732	761
16	37	597	12	39	4	2	18	689	709
17	48	691	14	37	7	5	17	797	819
28	29	582	23	41	9	5	35	684	724
29	42	623	11	28	6	5	27	710	742
20	46	748	33	33	0	1	28	860	889
21	52	646	11	19	9	10	29	737	776
22	51	680	16	42	4	2	31	793	826
23	44	544	16	37	1	4	20	642	666
24	49	555	18	38	6	4	23	666	693
Total	1294	16,442	510	811	179	154	604	19,236	19,994
%	6.5	82.2	2.5	4.1	0.9	0.8	3.0		

REFERENCES

Abercrombie, M. 1970. Behaviour of cell towards one another. Advances in Biology of the skin. **5**: 95-112.

Abercrombie, M. 1980. The crawling movement of metazoan cells. Proc. R. Soc. Lond. B **207**: 129-147.

Abercrombie, M., & Ambrose, E.J. 1958. Interference microscope studies of cell contacts in tissue culture. Exp. Cell Res. **15**: 332-345.

Abercrombie, M., Heaysman, J.E.M., & Pegrum, S.M. 1970. The locomotion of fibroblasts in culture. I. Movements of the leading edge. Exp. Cell Res. **59**: 393-398.

Abercrombie, M., Heaysman, J.E.M., & Pegrum, S.M. 1971. The locomotion of fibroblasts in culture. IV. Electron microscopy of the leading lamella. Exp. Cell Res. **67**: 359-367.

Addai, F.K. & Ockleford, C.D. 1986. Mitochondria in living cells from human chorionic villi: the effects of colchicine on numbers and distribution. J. Anat. **147**: 219-233.

Aguirre, G.D. 1976. Inherited retinal degeneration in the dog. Trans. Am. Acad. Ophthalmol. Otolaryngol. **81**: 667-676.

Albert, D.M., Tso, M.O.M., & Rabson, A.S. 1972. In vitro growth of pure cultures of retinal pigment epithelium. Arch. Ophthalmol. **88**: 63-69.

Ambrose, E.J. 1961. The movements of fibrocytes. Exp. Cell Res. suppl **8**: 54-73.

Anderson, D.H., Fisher, S.K., & Steinberg, R.H. 1978. Mammalian cones: disc shedding, phagocytosis, and renewal. Invest. Ophthalmol. Visual Sci. **17**: 117-133.

Ashton, N. 1953. Central areolar choroidal sclerosis: histopathological study. Br. J. Ophthalmol. **37**: 140-147.

Aubin, J.E., Osborn, M., Franke, W.W., & Weber, K. 1980. Intermediate filaments of the vimentin-type and the cytokeratin-type are distributed differentially during mitosis. Exp. Cell Res. **129**: 149-165.

Ball, E.H. & Singer, S.J. 1982. Mitochondria are associated with microtubules and not with intermediate filaments in cultured fibroblasts. Proc. Natl. Acad. Sci. USA **79**: 123-126.

Barnett, K.C. 1962. Hereditary retinal atrophy in the poodle. Vet. Rec. **74**: 672-675.

Barnett, K.C. 1965. Retinal atrophy. Vet. Rec. **77**: 1543-1552.

Basinger, S., Hoffman, R., & Mattes, M. 1976. Photoreceptor shedding is initated by light in the frog retina. Science **194**: 1074-1076.

Basu, P.K., Sarkar P., Menon I., Carré F., & Persad S. 1983. Bovine retinal pigment epithelial cell cultured in vitro: Growth characteristics, morphology, chromosomes, phagocytosis ability, tyrosine activity and effect of freezing. Exp.Eye Res. **36**: 671-683.

Behnke, O. 1971. Microtubules in disk-shaped blood cells. Int. Rev. expl. Pathol. **9**: 1-91.

Bakeeva, L.E., Chentsov, Y.S., & Skulachev, V.P. 1978. Mitochondrial framework (reticulum mitochondriale) in rat diaphram muscle. Biochim. Biophys. Acta. **501**: 349-369.

Bell, P.B. Jr. 1981. The application of scanning electron microscopy to the study of the cytoskeleton of cells in culture. Scanning Electron Microscopy II: 139-157.

Ben-Ze'ev, A. 1984. Differential control of cytokeratins and vimentin synthesis by cell-cell contact and cell spreading in cultured epithelial cells. J. Cell Biol. **99**: 1424-1433.

Ben-Ze'ev, A. 1985. Cell density and cell shape related regulation of vimentin and cytokeratin synthesis. Exp. Cell Res. **157**: 520-532.

Bennett, G.S., Tapscott, S.J., Kleinbart, F.A., Antin, P.B. & Holtzer, H. 1981. Different proteins associated with 10 nm filaments in cultured chick neurons and non-neural cells. Science **212**: 567-569.

Bergeron, M., Guerette, D., Forget, J., & Thiery, G. 1980. Three-dimensional characteristics of the mitochondria of the rat nephron. Kidney International **17**: 175-185.

Bershadsky, A.D., & Vasiliev, J.M. 1988. Reorganization of Cytoskeleton. Cell Division. In Cytoskeleton. Cellular Organelles. Series editor: Philip Siekevitz. Plenum Press. N.Y. & London. 251-266.

Besharse, J.C. 1984. Photoreceptor disc shedding and phagocytosis mechanism and regulation. J. Cell Biol. **99**: 115a.

Besharse, J.C., Forestner, D.M., & Green berger, L.M. 1984. Mechanism of rod disc shedding: Induction of pigment epithelial ensheathing and phagocytosis in eye cups. Invest Ophthalmol. Vis. Sci. **25** (suppl.): 243.

Besharse, J.C. & Dunis, D.A. 1983a. Rod photoreceptor disc shedding in eye cups: Relationship to bicarbonate and amino acids. Exp. Eye Res. **36**: 567-580.

Besharse, J.C. & Dunis, D.A. 1983b. Methoxyindoles and photoreceptor metabolism: Activation of rod shedding. Science **219**: 1341-1343.

Bibb, C., & Young, R.W. 1974a. Renewal of glycerol in the visual cells and pigment epithelium of frog retina. J. Cell Biol. **62**: 378-389.

Bibb, C., & Young, R.W. 1974b. Renewal of fatty acids in the membrane of visual cell outer segments. J. Cell Biol. **62**: 327-343.

Bignami, A. & Dahl, D. 1977. Specificity of the glial fibrillary acidic protein for astroglia. J. Histochem. Cytochem. **25**: 466-469.

Blair, N.P. & Trempe, C.L. 1980. Hypertrophy of the retinal pigment epithelium associated with Garner's syndrome. Am. J. Ophthalmol. **90**: 661-667.

Bloemendal, H. & Pieper, F.R. 1989. Intermediate filaments: Known structure, unknown function. Biochemica et Biophysica Acta. **1007**: 245-253.

Blose, S.H. 1979. Ten-nanometer filaments and mitosis: Maintenance of structural continuity in dividing endothelial cells. Proc. Natl. Acad. Sci. U.S.A. **76**: 3372-3376.

Blose, S.H., & Bushnell, A. 1982. Observations on the vimentin-10-nm filaments during mitosis in BHK21 cells. Exp. Cell Res. **142**: 57-62.

Bok, D., & Hall, M.O. 1971. The role of the pigment epithelium in the etiology of inherited retinal dystrophy in the rat. J. Cell Biol. **49**: 664-682.

Bok, D. & Heller, J. 1976. Transport of retinol from the blood to the retina: an autoradiographic study of the pigment epithelial cell surface receptor for plasma retinol binding protein. Exp. Eye Res. **22**: 395-402.

Bok, D., Ong, D.E., & Chytil, F. 1984. Immunocytochemical localization of cellular retinol-binding protein in the rat retina. Invest. Ophthalmol. Vis. Sci. **25**: 877-883.

Bok, D. & Young, R.W. 1979. Phagocytic properties of the retinal pigment epithelium. In The Retinal Pigment Epithelium. Ed. K.M. Zinn & M.F. Marmor. Publ. Harvard University Press. London.pp 148-174

Boller, K., Kemler, R., Baribault, H., Doetschman, T. 1987. Differential distribution of cytokeratins after microinjection of anti-cytokeratin monoclonal antibodies. Europ. J. of Cell Biol. **43**: 459-468.

Boulton, M.E., Marshall, J., & Mellerio, J. 1982. Human retinal pigment epithelial cells in tissue culture: A means of studying inherited retinal diseases. Birth Defects: Original Article Series **18**: 101-118.

Bourne, M.C., Campbell, D.A., & Tansley, K. 1938. Hereditary degeneration of the rat retina. Br. J. Ophthalmol. **22**: 613-623.

Bradley, R.A., Couchman, J.R. & Rees, D.A. 1980. Comparison of the cell cytoskeleton in migratory and stationary chick fibroblasts. J. Muscle Res. & Cell Motility. **1** : 5-14.

Brandt, J.T., Martin, A.P., Lucas, F.V., & Vorbec, M.L. 1974. The structure of rat liver mitochondria: A re-evaluation. Biochem. & Biophys. Res. Comm. **59**: 1097-1103.

Bretcher, M.S. 1984. Endocytosis: relation to capping and cell locomotion. Science (Wash DC). **224**: 681-686.

Bridges, C.D.B. 1975. Storage, distribution and utilization of vitamins A in the eye of adult amphibians and their tadpoles. Vision Res. **15**: 1311-1323.

Brinkley, B.R., Fistel, S.H., Marcum, J.M., & Pardue, R.L. 1980. Microtubules in cultured cells; Indirect immunofluorescent staining with tubulin antibody. Int. Rev. Cytol. **63**: 59-95.

Brown, S., Levinson, W., & Spudich, J.A. 1976. Cytoskeletal elements of chick embryo fibroblasts revealed by detergent extraction. J. Supramolecular Structure. **5**: 119-130.

Buckley, I.K., & Porter, K.R. 1967. Cytoplasmic fibrils in living cultured cells. A light and electron microscope study. Protoplasma **64**: 349-380.

Buckley, I.K. & Porter, K.R. 1975. Electron microscopy of critical point dried whole cultured cells. J. of Microscopy. **104**: 107-120.

Bunt-Milam, A.H. & Saari, J.C. 1983. Immunocytochemical localization of two retinoid-binding proteins in vertebrate retina. J. Cell Biol. **97**: 703-712.

Bunt-Milam, A.H., Eisenfeld, A.J., & Saari, J.C. 1984. Immunocytochemical localization of retinoid-binding protein in adult and developing retinas. Invest Ophthalmol. Vis Sci. Suppl. **25**: 276.

Burnside, B. 1971. Microtubules and microfilaments in newt neurulation. Devel. Biol. **26**: 416-441.

Burnside, B. 1975. The form and arrangement of microtubules: An historical, primarily morphological review. Ann. N.Y. Acad. Sci. **253**: 14-26.

Burnside, B. 1976. Possible roles of microtubules and actin filaments in retinal pigment epithelium. Exp Eye Res. **23**: 257-275.

Burnside, B., & Laties, A.M. 1976. Actin filaments in apical projections of the primate pigmented epithelial cell. Invest Ophthalmol. **15**: 570-578.

Burridge, K. 1981. Are stress fibres contractile? Nature **294**: 691-692.

Burridge, K., & Feramisco, J.R. 1981. Non-muscle -actinins are calcium-sensitive actin-binding proteins. Nature. **294**: 565-567.

Burridge, K. & Mangeat, P. 1984. An interaction between vinculin and talin. Nature **308**: 744-746.

Byers, H.R., & Fujiwara, K. 1982. Stress fibers in cell in situ: Immunofluorescence visualization with anti-actin, anti-myosin, and anti--actinin. J. Cell Biol. **93**:804-811.

Byers, B., & Porter, K.R. 1964.Orientated microtubules in elongating cells of the developing lens rudiment after induction. Proc. Natl. Acad. Sci. USA **52**: 1091-1099.

Byers, H.R. & Porter, K.R. 1977. Transformations in the structure of the cytoplasmic ground substance in erythrophores during pigment aggregation and dispersion. J. Cell Biol. **75**: 541-558.

Calthorpe, C.M. & Grierson, I. 1990. Fibronectin induces migration of bovine trabecular meshwork cells in vitro. Exp. Eye Res. **51**: 39-48.

Calthorpe, C.M., Grierson, I. & Hitchings, R.A. 1991. Chemoattractants produced by ocular cells unduce trabecular meshwork cell migration. Int. Ophthalmol. **15**: 185-191.

Cambrey-Deakin, M.A., Robson, S.J. & Burgoyne, R.D. 1988. Colocalisation of acetylated microtubules, glial filaments, and mitochondria in astrocytes in vitro. Cell Motility and the Cytoskeleton **10**: 438-449.

Campochiaro, P.A., Jerden, J.A., & Glaser, B.M. 1984. Serum contains chemoattractants for human retinal pigment epithelial cells. Arch. Ophthalmol. **102**: 1830-1833.

Carlile, J.L. 1981. Feline retinal atrophy. Vet Rec. **108**: 311.

Carmo -Fonseca, M. & David-Ferreira, J.F. 1990. Interactions of intermediate filaments with cell structures. Electron Micros. Rev. **3**: 115-141.

Carter, S.B. 1965. Principles of cell motility: The direction of cell movement and cancer invasion. Nature **208**: 1183-1187.

Carter, S.B. 1967. Effects of cytochalasins on mammalian cells. Nature **213**: 261-264.

Chader, G.J. & Wiggert, B. 1984. Interphotoreceptor retinoid-binding protein. Characteristics in bovine and monkey retina. Vision Res. **24**: 1605-1614.

Chader, G.J., Wiggert, B., Lai, Y-L., Lee, L. & Fletcher, R.T. 1983. Interphotoreceptor retinol-binding protein: A possible role in retinoid transport to the retina. *In*: Progress in Retinal Research. 2. Eds. N. Osborne & G. Chader. pp.163-189.

Chaitin, M.H., & Hall, M.O. 1983a. Defective ingestion of rod outer segments by cultured dystrophic rat pigment epithelial cells. Invest. Ophthalmol. Vis. Sci. **24**: 812-820.

Chaitin, M.H., & Hall, M.O. 1983b. The distribution of actin in cultured normal and dystrophic rat pigment epithelial cells during the phagocytosis of rod outer segments. Invest. Ophthalmol. Vis. Sci. **24**: 821-831.

Chu, Y-W., Oshima, R.G., & Hendrix, M.J.C. 1990. Expression of keratins 8 and 18 in mouse L cells results in an increase in migratory and invasive ability. J. Cell Biol. **3** (ASCB abstracts, 30th Ann. Meeting.):41a.

Cintorino, M., Petracca, R., Vindigni, C., Tripodi, S.A., & Leoncini, P. 1990. Topography-related expression of individual cytokeratins in normal and pathological (non-neoplastic and neoplastic) human oral mucosa. Virchows Arch. **417**: 419-426.

Cohen, A.I. 1961a. Some preliminary electron microscopic observations of the outer receptor segments of the *Macaca rhesus*. In: The Structure of the Eye. Ed. G.K. Smelser. Acedemic Press, New York. pp.151-158.

Colley, N.J., Clark V.M., & Hall M.O. 1987. Surface modification of retinal pigment epithelium cells: Effects on phagocytosis and glycoprotein composition. Exp. Eye Res. **44**: 377-392.

Connell, N.D. & Rheinwald, J.G. 1983. Regulation of the cytoskeleton in mesothelial cells: Reversible loss of keratin and increase in vimentin during rapid growth in culture. Cell **34**: 245-253.

Cooper, D., Schermer, A. & Sun, T-T. 1985. Classification of human epithelia and their neoplasms using monoclonal antibodies to keratins: Strategies, applications & limitstions. Lab. Invest. **52**: 243-256.

Couchman, J.R. & Blencowe, S. 1985. Adhesion and cell surface relationships during fibroblast and epithelial migration in vitro. Expl. Biol. Med. **10**: 23-38.

Couchman, J.R., & Rees, D.A. 1979. The behaviour of fibroblasts migrating from chick heart explants: Changes in adhesion, locomotion and growth, and in the distribution of actinonysin and fibronectin. J. Cell Sci. **39**: 149-165.

Crawford, B.J. 1975. The structure and development of the pigmented retinal clone. Can. J. Zool. **53**: 560-570.

Crawford, B.J. 1979. Cloned pigmented retinal epithelium. The role of microfilaments in the differentiation of cell shape. J. Cell Biol. **81**: 301-315.

Crawford, B.J. 1980. Developement of the junctional complex during differentiation of chick pigmented epithelial cells in cloned culture. Invest. Ophthalmol. Vis. Sci. **19**: 223-237.

Crawford, B., Cloney R.A., & Cahn R.D. 1972. Cloned pigmented retinal cells; the affect of cytochalasin B on ultrastructure and behaviour. Z. Zellforsch. **130**:135-151.

Custer, N.V. & Bok, D. 1975. Pigment epithelium-photoreceptor interactions in the normal and dystrophic rat retina. Exp. Eye Res. **21**: 153-166.

Currie, J.R., Hollyfield, J.G., & Rayborn, M.E. 1978. Rod outer segment elongate in constant light: Darkness is required for normal shedding. Vision Res **18**: 995-1003.

Darnell, J., Loddish, H., & Baltimore, D. 1986. Molecular Cell Biology. Publ. Scientific American Books. U.S.A.

Davison, M.T. & Garland, P.B. 1975. Mitochondrial structure studied by high voltage electron microscopy of thick sections of Candida utilis. J. General Microbiol. **91**: 127-138.

DeDuve, C. 1964. From catases to lysosomes. Fed. Proc. **23**: 1045-1049.

DeDuve, C., Pressman, B.C., Gianetto, R., Wattiank, R., & Appleman, F. 1955. Tissue fraction studies: intra-cellular distribution patterns of enzymes in rat-liver tissue. Biochem. J. **60**: 604-617.

De Robertis, E. & Lasansky, A. 1961. Ultrastructure and chemical organisation of photoreceptors. *In*: The Structure of the Eye. Eds. G.K. Smelser. Pub. Academic Press, London. pp. 29-49.

Docherty, R.J., Edwards, J.G., Garrod, D.R. & Mattey, D.I. 1984. Chick embryonic pigmented retina is one of the group of epitheliod tissues that lack cytokeratins and desmosomes and have intermediate filaments composed of vimentin. J. Cell Sci. **71**: 61-74.

Doran, T.I., Vidrich, A. & Sun, T-T. 1980. Intrinsic and extrinsic regulation of the differentiation of skin, corneal and esophageal epithelial cells. Cell **22**: 17-25.

Dowling, J.E. 1960. Chemistry of visual adaption in the rat. Nature. **188**: 114-118.

Dowling, J.E., & Gibbon, I.R. 1962. The fine structure of the pigment epithelium in the albino rat. J. Cell Biol. **14**: 459-474.

Dowling, J.E., & Sidman, R.L. 1962. Inherited retinal dystrophy in the rat. J. Cell Biol. **14**: 73-109.

Duke-Elder, S. 1963a. System of Ophthalmology, **vol. 3** part II: 626. London: Kimpton

Duke-Elder, S. 1963b. System of Ophthalmology, **vol. 3** part II: 619-623. London: Kimpton

Eckert, B.S. 1986. Alteration of the distribution of intermediate filaments in PtK1 cells by acrylamide II: Effect on the organisation of cytoplasmic organelles. Cell Motility and the Cytoskeleton **6**: 15-24.

Eckert, R.L. & Green, H. 1984. Cloning of cDNAs specifying vitamin-A-responsive human keratins. Proc. Natl. Acad. Sci. USA **81**: 4321-4325.
Eichner, R., Bonitz, P. & Sun, T-T. 1984. Classification of epidermal keratins according to their immunoreactivity, isoelectric point, and mode of expression. J. Cell Biol. **98**: 1388-1396.

Edwards, R.B. 1977. Culture of rat retinal pigment epithelium. IN VITRO **13**: 301-304.

Edwards, R.B. 1981a. The isolation and culturing of retinal pigment epithelium of the rat. Vision Res. **21**: 147-150.

Edwards, R.B. 1981b. Culture of mammalian retinal pigment epithelium and neural retina. In Visual Pigments and Purple Membranes. Methods of Enzymology **81** Ed. L. Packer. New York: Academic Press: 39-43.

Edwards, R.B. & Bakshian, S. 1980. Phagocytosis of outer segments by cultured rat pigment epithelium reduction by cyclic AMP and phosphodiesterase inhibitors. Invest. Ophthalmol. Vis. Sci. **19**: 1184-1188.

Edwards, R.B. & Szamier, R.B. 1977. Defective phagocytosis of isolated rod outer segments by RCS rat retinal pigment epithelium in culture. Science, **197**: 1001-1003.

Farquhar, M.G. & Palade, G.E. 1963. Junctional complexes in various epithelia. J. Cell Biol. **17**: 375-412.

Feeney, L., Grieshaber J.A., & Hogan, M.J. 1965. Studies on human ocular pigment. In the structure of the eye. Ed. J.W. Rohen. Stuttgart: F.K. Schattauer-Verlag, pp 535-548.

Feeney, L. & Mixon, R.N. 1976. An in vitro model of phagocytosis in bovine and human retinal pigment epithelium. Exp. Eye Res. **22**: 533-548.

Flannery, J.G., O'Day, W., Pfeffer, B.A., Horwitz, J., & Bok, D. 1990. Uptake, processing and release of retinoids by cultured human retinal pigment epithelium. Exp. Eye Res. **51**: 717-728.

Flood, M.T. & Gouras, P. 1981. The organization of human retinal pigment epithelium in vitro. Vis. Res. **21**: 119-126.

Flood, M.T., Gouras, P., & Kjeldbye, H. 1980. Growth characteristics and ultrastructure of human retinal pigment epithelium in vitro. Invest. Ophthalmol. Vis. Sci. **19**: 1309-1320.

Flood, M.T., Bridges, C.D.B., Alvarez, R.A., Blaner, W.S., & Gouras, P. 1983. Vitamin A utilization in human retinal pigment epithelial cell in vitro. Invest. Ophthalmol. Vis. Sci. **24**: 1227-1235.

Franke, W.W., Schmid, E., Osborn, M. & Weber, K. 1978a. Different intermediate-sized filaments distinguished by immunofluorescence microscopy. Proc. Natl. Acad. Sci. USA **75**: 5034-5038.

Franke, W.W., Weber, K., Osborn, M., Schmid, E. & Freudenstein C. 1978b. Antibody to prekeratin. Decoration of tonofilament-like arrays in various cells of epithelial character. Exp. Cell Res. **116**: 429-445.

Franke, W.W., Schmid, E.A., Weber, K., & Osborn, M. 1979a. HeLa cells contain intermediate-sized filaments of the prekeratin type. Exp. Cell Res. **118**: 95-109.

Franke, W.W., Schmid, E.A., Winter, S.,Osborn, M., & Weber, K. 1979b. Widespread occurance of intermediate-sized filaments of the vimentin-type in cultured cells from diverse vertebrates. Exp. Cell Res. **123**: 24-46.

Franke, W.W., Denk, H., Kalt, R., & Schmid, E. 1981a. Biochemical and immunological identification of cytokeratin proteins in hepatocytes of mammalian liver tissue. Exp. Cell Res. **131**: 299-318.

Franke, W.W., Schiller, D.L., Moll, R., Winter, S., Schmid, E., Engelbrecht, I., Denk, H., Krepler, R., & Platzer, B. 1981b. Diversity of cytokeratins. Differentiation specific expression of cytokeratin polypeptides in epithelial cells and tissues. J. Mol. Biol. **153**: 933-959.

Franke, W.W., Schmid, E., Grund, C., Geiger, B. 1982a. Intermediate filament proteins in non-filamentous structures; transient disintegration and inclusion of subunit proteins in granular aggregates. Cell **30**: 103-113.

Franke, W.W., Schmid, E., Schiller, D.L., Winter, S., Jarasch, E.D., Moll, R., Denk, H., Jackson, B.W. & Illmensee, K. 1982b. Differentiation-related patterns of expression of proteins of intermediate-size filaments in tissues and cultured cells. Cold Spring Harbor Symp. Quant. Biol. **46**: 431-543.

Frank, W.W., Schmid, E., Wellsteed, J., Grund, C., Gigi, O. & Geiger, B. 1983. Changes of cytokeratin filament organization during the cell cycle: selective masking of an immunologic determinant in interphase PtK2 cells. J. Cell Biol. **97**: 1255-1260.

Franke, W.W., Grund, C., Kuhn, C., Lehto, V-F., & Virtanen, I. 1984. Transient change of organization of vimentin filament during mitosis as demonstrated by a monoclonal antibody. Exp. Cell. Res. **154**: 567-580.

Frayer, W. 1966. Reactivity of the retinal pigment epithelium: an experimental and histopatholgic study. Trans. Am. Ophthalmol. Soc. **64**: 586-643.

Freed, J.J., & Lebowitz, M.M. 1970. The association of a class of saltatory movements with microtubules in cultured cells. J. Cell Biol. **45**: 334-354.

French, S.W., Kondo, I., Irie, T., Ihrig, T.J., Benson, N., & Munn, R. 1982 Morphologic study of intermediate filaments in rat hepatocytes. Hepatology **2**: 29-38.

Fuchs, E. & Green, H. 1978. The expression of keratin genes in epidermis and cultured epidermal cells. Cell **15**: 887-897.

Fuchs, E. & Green, H. 1979. Multiple keratins of cultured human epidermal cells are translated from different mRNA molecules. Cell **17**: 573-582.

Fuchs, E. & Green, H. 1980. Changes in keratin gene expression during terminal differentiation of the keratinocyte. Cell **19**: 1033-1042.

Fuchs, E. & Green, H. 1981. Regulation of terminal differentiation of cultured human keratinocytes by vitamin A. Cell **25**: 617-625.

Fuchs, U., Kivelä, T., & Tarkkanen. A. 1991. Cytoskeleton in normal and reactive human retinal pigment epithelial cells. Invest. Ophthalmol. Vis. Sci. **32**: 3178-3186.

Funahashi, M., Okisaka, S., & Kuwabara, T. 1976. Phagocytosis by the monkey pigment epithelium. Exp. Eye Res. **23**: 217-225.

Gartner, S. 1947. Cyclopia. Arch. Ophthalmol. **37**: 220-231.

Gherardi, E. 1991. Growth factors and cell movement. Eur. J. Cancer. **27**: 403-405.

Geiger, B. 1979. A 130K protein from chicken gizzard: its localisation at the termini of microfilament bundles in cultured chicken cells. Cell **18**: 193-205.

Geiger, B. 1982. Involvement of vinculin in contact-induced cytoskeletal interactions. Cold Spring Harbor Symp. Quant. Biol. **46**: 671-682.

Geiger, B., & Sanger, S.J. 1980. Association of microtubules and intermediate filaments in chicken gizzard cells as detected by double immunofluorescence. Proc. Natl. Acad. Sci. U.S.A. **77**: 4769-4773.

Geiger, B., Avnur, Z., Rinnerthaler, G., Hinssen, H., & Small, V.I. 1984a. Microfilament-organizing centers in areas of cell contact: Cytoskeletal interactions during cell attachment and locomotion. J. Cell Biol. **99**: 83s-91s.

Geiger, B., Kreiss, T.E., Gigi, O., Schmid, E., Mittnacht, S., Jorcano, J.L., von Bassewitz, D.B., & Franke, W.W. 1984b. Dynamic rearrangements of cytokeratins in living cells. Cold Spring Harb. Laboritories, N.Y. Cancer Cells vol. **1**. The Transformed Phenotype: 201-215.

Geiger, B., Tokuyasu, K.T., Dutton, A.H., & Singer, S.J. 1980. Vinculin, and intracellular protein localised at specialised sites where microfilament bundles terminate at cell membranes. Proc. Natl. Acad. Sci. U.S.A. **77**: 4127-4131.

Geiger, B., Tokuyasu, K.T., Dutton, A.H., & Singer, S.J. 1981. Immunoelectron microscope studies of membrane-microfilament interactions: distribution of -actinin, tropomyosin, and vinculin in intestinal epithelial brush border and chicken gizzard smooth muscle cells. J. Cell Biol. **91**: 614-628.

Gilbert, D.S., Newby, B.J., & Anderton, B. 1975. Neurofilament disguise, destruction and discipline. Nature **256**: 586-589.

Gillespie, J.M. 1983. The structural proteins of hair: Isolation, characterization, and regulation of biosynthesis. In Biochemistry and Physiology of the Skin. Ed. L.A. Goldsmith. Oxford University Press, Oxford: 475-510.

Gibbons, I.R. 1968. The biochemistry of motility. Ann. Rev. Biochem. **37**: 521-546.

Goldman, R.D. 1971. The role of three cytoplasmic fibres in BHK-21 cell motility. J. Cell Biol. **51**: 752-762.

Goldman, R.D., & Knipe, D.M. 1972. Functions of cytoplasmic fibres in non-muscle cell motility. Cold Spring Harbour Symp. Quant. Biol. **37**: 523-534.

Goldman, A.I., & O'Brien, P.J. 1978. Phagocytosis in the retinal pigment epithelium of the RCS rat. Science. **210**: 1023-1025.

Goldman, R.D., Goldman, A.E., Green, K.J., Jones, J.C.R., Jones, S.M., & Yang, H-Y. 1986. Intermediate filament networks: Organization and possible functions of a diverse group of cytoskeletal elements. J. Cell Sci. Suppl. **5**: 69-97.

Granger, B.L. & Lazarides, E. 1980. Synemin: A new high molecular weight protein associated with desmin and vimentin flaments in muscle. Cell **22**: 727-738.

Grierson, I., Joseph, J., Millar, M., & Day, J.E. 1988. Wound Repair: The fibroblast and the inhibition of scar formation. Eye. **2**: 135-148.

Grierson I., Millar, L. Yong, J.D., McKechnie, N.M. Hitchins, C. & Boulton, M. 1986. Investigations of the cytoskeletal elements in cultured bovine meshwork cells. Invest. Ophthalmol. Vis. Sci. **27**: 1318-1330.

Guérin, C.J., Anderson, D.H. & Fisher, S.K. 1990. Changes in intermediate filament immunolabeling occur in response to retinal detachment and re-attachment in primates. Invest. Ophthalmol. Vis. Sci. **31**: 1474-1482.

Hall, M.O. & Abrams, T. 1987. Kinetic studies of rod outer segment binding and ingestion by cultured rat RPE cells. Exp. Eye Res. **45**: 907-922.

Hall, M.O. & Quon, D.S. 1980. Plant lectins inhibit phagocytosis of ROS by cultured PE cells. Invest. Ophthalmol. Vis. Sci. (Suppl.) **21**: 162.

Hansson, H.A. 1970. A histochemical study of oxidative enzymes in rat retina damages by visible light. Exp. Eye Res. **9**: 285-296.

Hansson, H.A. 1971. A histochemical study of cellular reactions in rat retina transiently damaged by visible light. Exp. Eye Res. **12**: 270-274.

Hayes, K.C. 1974. Retinal degeneration in monkeys induced by deficiensies of vitamin E or A. Invest. Ophthalmol. **13**: 499-510.

Hayes, K.C., Carey, R.E. & Schmidt, S.Y. 1975. Retinal degeneration associated with taurine deficiency in the cat. Science. **188**: 949-951.

Heath, J.P. & Dunn, G.A. 1978. Cell to substratum contacts of chick fibroblasts and their relation to the microfilament system. A correlated interference-reflexion and high-voltage electron microscope study. J. Cell Sci. **29**: 197-212.

Heaysman, J.E.M., & Pegrum, S.M. 1982. Early cell contacts in culture. *In*: Cell behaviour: a tribute to Michael Abercrombie. Eds. R. Bellairs, A. Curtis, & G. Dunn. Cambridge University Press. pp. 49-76.

Heller, J. 1975. Interactions of plasma retinol-binding protein with its receptor: Specific binding of bovine and human retinol-binding protein to pigment epithelium cells from bovine eyes. J. Biol. Chem. **250**: 3613-3619.

Heller, J. & Bok, D. 1976. A specific receptor for retinol binding protein as detected by the binding of human and bovine retinol binding protein to pigment epithelial cells. Am J. Ophthalmol. **81**: 93-97.

Henderson, D., & Weber, K. 1980. Immunoelectron microscopic studies of intermediate filaments in cultured cells. Exp. Cell Res. **129**: 441-453.

Henderson, D., & Weber, K. 1981. Immunoelectron microscopical identification of the two types of intermediate filaments in established epithelial cells. Exp. Cell Res. 132: 297-311.

Herman, I.M., Crisona N.J., & Pollard, T.D. 1981. Relation between cell activity and the distribution of cytoplasmic actin and myosin. J. of Cell Biol. **90**: 84-91.

Herron, W.L., Reigel B.W., Myers, O.E., & Rubin M.L. 1969. Retinal dystrophy in the rat-A pigment epithelial disease. Invest. Ophthalmol. Vis. Sci. **8**: 595-604.

Herron, W.L. Jr., Reigel, B.W., Brennan E., & Rubin M.L. 1974. Retinal dystrophy in the pigmented rat. Invest. Ophthalmol. Vis. Sci. **13**: 87-94.

Hirokawa, N., Cheney, R.E., & Willard, M. 1983. Location of a protein of the fodrin-spectrin-TW 260/240 family in the mouse intestinal brush border. Cell **32**: 953-965.

Hiscott, P.S., Grierson, I., McCleod, D. 1984. Retinal pigment epithelial cells in epiretinal membranes: an immunohistochemical study. Br. J. Ophthalmol. **68**: 708-715.

Hogan, M.J., Alvarado, J.A., & Weddell, J.E. 1971. Histology of the human eye. An atlas and Textbook. Publ. W.B. Saunders Co. London.

Hollyfield, J.G. 1976. Phagocytic capabilites of the pigment epithelium. Exp. Eye Res. **22**: 457-468.

Hollyfield, J.G., Besharse, J.C., & Rayborn, M.E. 1976. The effect of light on the quantity of phagosomes in the pigment epithelium. Exp. Eye Res. **23**: 623-635.

Hollyfield, J.G. & Ward, A. 1974. Phagocytic activity in the retinal pigment epithelium of the frog, Rana pipiens. I. Uptake of polystyrene spheres. J. Ultrastruc. Res. **46**: 327-338.

Horwitz, A., Duggan, K., Buck, C., Beckerle, M.C., & Burridge, K. 1986. Interactions of plasma membrane fibronectin receptor with talin- a transmembrane linkage. Nature **320**: 531-533.

Horwitz, B., Kupfer, H., Eshar, Z. and Geiger, B. 1981. Reorganization of arrays of prekeratin filaments during mitosis. Immunofluorescence microscopy with multiclonal and monoclonal prekeratin antibodies. Exp. Cell Res. **134**: 281-290.

Hu, D-N, Del Monte M.A., Liu, S., & Maumenee, I.H. 1982. Morphology, phagocytosis and vitamin A metabolism of cultured human retinal pigment epithelium. Birth Defects: Origional Article Series, **18**: 67-79.

Hyams, J.S., & Stebbings, H. 1979. Microtubule associated cytoplasmic transport. *In:* Microtubules. Ed. K. Roberts & J.S. Hyams. Academic Press. N.Y. pp. 487-530.

Hynes, R.O. & Destree, A.T. 1978. 10 nm filaments in normal and transformed cells. Cell **13**: 151-163.

Ingram, V.M. 1969. A side view of moving fibroblasts. Nature **222**: 641-644.

Irons, M.J. & Kalnins, V.I. 1983. Distribution of microtubules in cultured RPE cells from normal and dystrophic RCS rats. Invest Ophthalmol. Vis. Sci. **25**:434-439.

Israel,P., Masterson, E., Goldman, A.I., Wiggert, B. & Chader, G.J. 1980. Retinal pigment epithelial cell differentiation in vitro: Influences of culture-medium. Invest. Ophthalmol. Vis. Sci. **19**: 720-727.

Izzard, C.S., & Lochner, L.R. 1976. Cell-to-substrate contacts in living fibroblasts: an interference reflexion study with an evaluation of the technique. J. Cell Sci. **21**: 129-159.

Johnson, L.V., Walsh, M.L., & Chen, L.B. 1980. Localisation of mitochondria in living cells with rhodamine 123. Proc. Natl. Acad. Sci. USA. **77**: 990-994.

Johnson,L.V., Walsh, M.L., Bockus, B.J. & Chen, L.B. 1981. Monitoring of relative mitochondrial membrane potential in living cells by fluorescence microscopy. J. Cell Biol. **88**: 526-535.

Kampik, A., Kenyon, K.R., Michels, R.G., Green, W.R., de la Cruz, Z.C. 1981. Epiretinal and vitreous membranes comparative study of 56 cases. Arch Ophthalmol. **99**: 1445-1454.

Kasper, M., Moll, R., Stosiek, P., & Karsten, U. 1988. Patterns of cytokeratin and vimentin expression in the human eye. Histochemistry. **89**: 369-377.

Keddie, F.M. & Barajas, L. 1969. Three-dimensional recenstruction of Pityrosporum yeast cells based on serial section electron microscopy. J. Ultrastructure Res. **29**: 260-275.

Keeler, C.E. 1924. The inheritance of a retinal abnormality in white mice. Proc. Natl. Acad. Sci. **10**: 329-333.

Kelly, D.E. 1966. Fine structure of desmosomes, hemi-desmosomes and an adepidermal globular layer in developing newt epidermis. J. Cell Biol. **28**: 51-72.

Kilarski, W. & Koprowski, H. 1976. Observation of whole, cultured human brain cells using 100 kilovolts electron microscopy. J. Microscopie Biol. Cell **25**: 73-80.

Kim, K.H., Rheinwald, J.G. & Fuchs, E. 1983. Tissue specificity of epithelial keratins: Differential expression of mRNAs from two multigene families. Molecular and Cell Biology **3**: 495-502.

Kim, K.H., Stellmach, V., Javors, J., Fuchs, E. 1987. Regulation of human mesothelial cell differentiation: Opposing roles of retinoids and epidermal growth factor in the expression of intermediate filament proteins. J. Cell Biol. **105**: 3039-3051.

Klien, B. 1958. Diseases of the macula. Arch. Ophthalmol. **60**: 175-186.

Koga, N., Koshibu, A., & Uyama, M. 1977. Electron microscope studies on the phagocytotic activity and proliferation of the retianl pigment epithelial cells. Acta Soc. Ophthalmol. Jap. **81**: 707-719.

Kolb, H., & Gouras, P. 1974. Electron microscopic observations of human retinitis pigmentosa, dominantly inherited. Invest. Ophthalmol. **13**: 487-498.

Kreig, T.M., Schafer, M.P., Cheng, C.K., Filpula, D., Flaherty, P., Steinert, P.M. & Roop, D. 1985. Organization of a type I keratin gene. Evidence for evolution of intermediate filaments from a common ancestral gene. J. Biol. Chem **260**: 5867-5870.

Kreis, T.E., & Birchmeier, W. 1980. Stress fibre sarcomeres of fibroblasts are contractile. Cell. **22**: 555-561.

Kurki, P., Ogata, K. & Tan, E.M. 1988. Monoclonal antibodies to proliferating cell nuclear antigen (PCNA)/cyclin as probes for proliferating cell by immunofluorescence microscopy and flow cytometry. J. of Immmunological Methods **109**: 49-59.

Lane, E.B., Goodman, S.L., and Trejdosiewicz, L.K. 1982. Disruption of the keratin filament network during epithelial cell division. EMBO J. **1**: 1365-1372.

Lane, E.B., Hogan, B.L.M., Kurkinen, M., & Garrels, J.I. 1983. Co-expression of vimentin and cytokeratins in parietal endoderm cells of early mouse embryo. Nature **303**: 701-704.

Lane, E.B. & Klymkowsky, M.W. 1981. Epithelial tonofilaments: Investigating their form and function using monoclonal antibodies. Cold Spring Harbor Symp. Quant. Biol. **46**: 387-402.

LaRocca, P.J., & Rheinwald, J.G. 1984. Coexpression of simple epithelial keratins and vimentin by human mesothelium and mesothelioma in vivo and in culture. Cancer Res. **44**: 2991-2999.

LaVail, M.M. 1976a. Rod outer segment disc shedding in relation to cyclic lighting. Exp. Eye Res. **23**: 277-280.

LaVail, M.M. 1976b. Rod outer segment disc shedding in rat retina: Relationship to cyclic lighting. Science **194**: 1071-1074.

LaVail, M.M. 1979. Mice and rats with inherited retinal degenerations. In The Retinal Pigment Epithelium. Ed. K.M. Zinn & M.F. Marmor. Publ. Harvard University Press. London. 357-380.

LaVail, M.M., & Sidman, R.L. 1974. C57BL/6J mice with inherited retinal degeneration. Arch. Ophthalmol. **91**: 394-400.

LaVail, M.M., Sidman, R.L., & Gerhardt C.O. 1975. Congenic strains of RCS rats with inherited retinal dystrophy. J. of Heredity **66**: 242-244.

LaVail, M.M., Sidman, R.L., & O'Neil, D. 1972. Photoreceptor-pigment epithelial cell relationships in rats with inherited retinal degeneration. J. Cell Biol. **53**: 185-209.

Lazarides, E. 1975a. Immunofluorescence studies on the structure of actin filaments in tissue culture cells. J. Histochem. Cytochem. **23**: 507-528.

Lazarides, E. 1975b. Tropomyosin antibody: The specific localization of tropomyosin in non-muscle cells. J. Cell Biol. **65**: 549-561.

Lazarides, E. 1980. Intermediate filaments as mechanical integrators of cellular space. Nature **283**: 249-256.

Lazarides, E. 1982. Intermediate filaments: A chemically heterogenous, developmentally regulated class of proteins. Ann. Rev. Biochem. **51**: 219-250.

Lazarides, E., & Burridge, K. 1975. -actinin: immunofluorescent localization of a muscle structural protein in non-muscle cells. Cell. **6**: 2889-298.

Lazarides, E., & Weber, K. 1974. Actin antibody: The specific visualisation of actin filaments in non-muscle cells. Proc. Nat. Acad. Sci. USA. **71**: 2268-2272.

LeFurgey, A., Ingram, P., Henry, S.C., Murphy, E. & Lieberman, M. 1983. Three-dimensional configuration of the mitochondria in cultured heart cells. Scanning Electron Microscopy **I**: 293-303.

Lehto, V-P, Virtanen, I., & Kurki, P. 1978. Intermediate filaments anchor the nuclei in nuclear monolayers of cultured human fibroblasts. Nature **272**: 175-77.

Liem, K.H., & Shelanski, M.L. 1978. Identity of the major protein in "native" glial fibrillary acidic protein preparation with tubulin. Brain Res. **145**: 196-201.

Lieska, N., Yang, H-Y., & Goldman, R.D. 1985. Prification of the 300 K intermediate filament-associated protein and its in vitro recombination with intermediate filaments. J. Cell Biol. **101**: 802-813.

Leuenberger, P.M., & Novikoff, A.B. 1975. Studies on microperoxisomes. VII. Pigment epithelial cells and other cell types in the retina of rodents. J. Cell Biol. **65**: 324-334.

Lewis, M.R., & Lewis, W.H. 1915. Mitochondria (and other cytoplasmic structures) in tissue culture. Am. J. Anat. **17**: 339-401.

Lin, J. J-L., & Feramisco, J.R. 1981. Disruption of the in vivo distribution of the intermediate filaments in fibroblasts through the microinjection of a specific monoclonal antibody. Cell **24**: 185-193.

Liou, G.I., Bridges, C.D.B., Fong, S.-L., Alvarez, R.A., & Gonzalez-Fernandez, F. 1982. Vitamin A transport between retina and pigment epithelium - an interstitial protein carrying endogenous retinol (interstitial retinol-binding protein). Vision Res. **22**: 1457-1467.

Lucas, D.R. 1954. Retinal dystrophy in Irish setter. J.exp. Zool. **126**: 537-547.

Machemer, R. 1968. Experimental retinal detachment in the owl monkey. II. Histology of the retina and pigment epithelium. Am. J. Ophthalmol. **66**: 396-410.

Machemer, R., & Norton, E.W.D. 1968. Experimental retinal detachment in the owl monkey. I. Methods of production and clinical picture. Am. J. Ophthalmol.**66**: 388-396.

Machemer, R., & Laqua, H. 1975. Pigment epithelium proliferation in retinal detachment (massive periretinal proliferation). Am. J. Ophthalmol. **80**: 1-23.

Machemer, R., Van Horn, D., & Aaberg, T.M. 1978. Pigment epithelial proliferation in human retinal detachment with massive periretinal proliferation. Am. J. Ophthalmol. **85**: 181-191.

Malawista, S.E. 1975. Microtubules and the mobilization of lysosomes in phagocytosing human leukocytes. Anns N.Y. Acad. Sci. **253**:738-749.

Mannagh, J., Arya, D.V., & Irvine,Jr. A.R. 1973. Tissue culture of human retinal pigment epithelium. Invest. Ophthalmol. Vis. Sci. **12**: 52-64.

Maruyama, K., & Ebashi, S. 1965. -actinin, a new structural protein from striated muscle. II. Action on actin. J. Biochem. (Tokyo) **58**: 13-19.

Masterson, E., Goldman, A.I., Chader, G.J. 1981. Phagocytosis of rod outer segments by cultured epithelial cells. Vis. Res. **21**: 143-145.

Mayerson, P.L. & Hall, M.O. 1986. Rat retinal pigment epithelial cells show specificity of phagocytosis in vitro. J. Cell Biol. **103**: 299-308.

McCulloch, C. 1950. The patholigic findings in two cases of choroideremia. Trans. Am. Acad. Ophthalmol. **51**: 565-572.

McKechnie, N.M., Boulton, M., Robey, H.L., Savage, F.J., & Grierson, I. 1988. The cytoskeletal elements of human retinal pigment epithelium: in vitro and in vivo. J. Cell Sci. **91**: 303-312.

McLaughlin, B.J. & Boykins, L.G. 1987. Examination of sialic acid binding on dystrophic and normal retinal pigment epithelium. Exp. Eye Res. **44**: 439-450.

Miller, S.S., & Steinberg, R.H. 1976. Transport of taurine, L-methionine, and 3-O-methyl-D-glucose across frog retinal pigment epithelium. Exp. Eye Res. **23**: 177-189.

Mitchison, T.J., & Kirschner, M. 1984. Dynamic instability of microtubule growth. Nature **312**: 237-242.

Moll, R., Franke, W.W., Schiller, D.L., Geiger, B., & Krepler, R. 1982. The catalog of human cytokeratins: patterns of expression in normal epithalia, tumors and cultured cells. Cell **31**: 11-24.

Moody, M.F., & Robertson, J.D. 1960. The fine structure of some retinal photoreceptors. J. Biophys. Biochem. Cytol. **7**: 87-92.

Mooseker, M.S. & Tilney, L.G. 1975. Organization of an actin filament-membrane complex. Filament polarity and membrane attachment in the microvilli of intestinal epithelial cells. J. Cell Biol. **67**: 725-743.

Mullen, R.J. & LaVail, M.M. 1976. Inherited retinal dystrophy: primary defect in pigment epithelium determined with experimental rat chimeras. Science **192**: 799-801.

Nagle, R.B., Brawer, M.K., Kittelson, J., & Clark, V. 1991. Phenotypic relationships of prostatic intraepithelial neoplasia to invasive prostatic carcinoma. Am. J. of Pathology. **138**: 119-128.

Narfström, K. 1985. Progressive retinal atrophy in the Abyssinian cat. Invest. Ophthalmol. Vis. Sci. **26**: 193-200.

Nguyen-Legros, J. 1978. Fine structure of the pigment epithelium in the vertebrate retina. Int. Rev. Cytol, Suppl. **7**: 287-328.

Novikoff, A.B., Beaufay, H. & DeDuve, C. 1956. Electron microscopy of lysosome-rich fractions from rat liver. J. Biophys. Biochem. Cytol. **2**: 179-184. (suppl.)

Novikoff, A.B., Essner, E., & Quintana, N. 1964. Golgi apparatus and lysosomes. Fed. Proc. **23**: 1010-1022.

Oliver, P.D. & Newsome, D.A. 1992. Mitochondrial superoxide dismutase in mature and developing human retinal pigment epithelium. Invest. Ophthalmol. Vis. Sci. **33**: 1909-1918.

Olmsted, J.B., & Borisy, G.G. 1973. Microtubules. Ann. Rev. Biochem. **42**: 507-540.

Osafune, T. 1973. Three-dimensional structures of giant mitochondria, dictyosomes and "concentric laminar bodies" formed during the cell cycle of Euglena gracilis (Z) in synchronus culture. J. Electron Microcopy **22**: 51-61.

Osborn, M. & Weber, K. 1976a. Tubulin-specific antibody and the expression of microtubules in 3T3 cells after attachment to a substratum. Further evidence for the polar growth of cytoplasmic microtubules in vitro. Exp. Cell Res. **103**: 331-340.

Osborn, M. & Weber, K. 1976b. Cytoplasmic microtubules in tissue culture cells appear to grow from an organising structure towards the plasma membrane. Proc. Natl. Acad. Sci. USA **73**: 867-871.

Osborn, M., & Weber, K. 1979. Microfilament-associated proteins in tissue culture cell viewed by stereo immunofluorescence microscopy. Europ. J. of Cell Biol. **20**: 28-36.

Osborn, M., Franke, W., & Weber, K. 1980. Direct demonstration of the presence of two immunologically distinct intermediate-sized filament systems in the same cell by double immunofluorescence microscopy. Exp. Cell Res. **125**: 37-46.

Owaribe, K. 1988. The cytoskeleton of retinal pigment epithelial cells. In Progress in Retinal Research **8**. Ed. N. Osborne & G. Chader. Permagon Press. 23-49.

Owaribe, K., & Eguchi, G. 1985. Increase in actin content and elongation of apical projections in retinal pigment epithelial cells during development of the chick eye. J. Cell Biol. **101**: 590-596.

Owaribe, K., Araki, M., Hatano, S., & Eguchi, G. 1979. Cell shape and actin filaments. In Cell Motility. Molecules and Organisation. Eds. S. Hatano, H. Ishikawa, & H. Sato. University of Tokyo Press, Tokyo.: 491-500.

Owaribe, K., Kartenbeck, J., Rungger-Brändle, E., & Franke, W.W. 1988. Cytoskeletons of retinal pigment epithelial cells: Interspecies differences of expression patterns indicate independence of cell function from the specific complement of cytoskeletal proteins. Cell Tissue Res. **254**: 301-315.

Owaribe, K., Kodama, R., & Eguchi, G. 1981. Demonstration of contractility of circumferential actin bundles and its morphogenic significance in pigmented epithelium in vitro and in vivo. J. Cell Biol. **90**: 506-514.

Owaribe, K., Sugino, H., & Masuda, H. 1986. Characterization of intermediate filaments and their structural organization during epithelium formation in pigmented epithelial cells of the retina in vitro. Cell Tissue Res. **244**: 87-93.

Paetau, A., Virtanen, I., Stenman, S., Kurki, P., Linder, E., Vaheri, A., Westermark, B., Dahl, D, & Haltia, M. 1979. Glial fibrillary acidic protein and intermediate filaments in human glioma cells. Acta Neuropath **47**: 71-74.

Palade, G.E. 1952. The fine structure of mitochondria. Anat. Rec. **114**: 427-452.

Palade, G.E. 1953. An electron microscope study of the mitochondrial structure. J. Histochem. Cytochem. **1**: 188-211.

Papermaster, D.S. 1982. Preparation of retinal rod outer segments. In Visual Pigments and Purple Membranes. Methods of Enzymology **81** Ed. L. Packer. New York: Academic Press: 48-52.

Pathak, M.A. & Fitzpatrick, T.B. 1974. The role of natural photoprotective agents in human skin. *In*: Sunlight amd man: normal and abnormal photobiologic responses. Ed. T.B. Fitzpatrick, M.A. Pathak, L.C. Harber, M. Seiji, and A. Kukita. Univ. of Tokyo Press. Tokyo. pp. 725-750.

Parry, H.B. 1953. Degenerations of the dog retina. II. Generalizaed progressive atrophy of hereditary origin. Brit J. Ophthal. **37**: 487-502.

Pavalko, F.M., Otley, C.A., & Burridge, K. 1989. Identification of a filamin isoform enriched at the end of stress fibres in chicken embryo fibroblasts. J. Cell Sci. **94**: 109-118.

Pearse, A.G.E. 1961. Localization of oxidative enzymes in rat and chick retina in various physiological conditions. In: The Structure of the Eye. Ed. G.K. Smelser. Acedemic Press, New York. pp. 53-70.

Pfeffer, B., Wiggert, B., Lee, L., Sonnenberg, B., Newsome, D., & Chader, G., 1984. The presence of a soluble interphotoreceptor retinol-binding protein (IRBP) in the retinal interphotoreceptor space. J. Cell Physiol. **117**: 333-341.

Philp, N.J. & Bernstein, M.H. 1980. Receptor specificity in RPE phagocytosis. J. Cell Biol. **87**: 91 (Abstract).

Philp, N.J. & Bernstein, M.H. 1981. Phagocytosis by retinal pigment epithelium explants in culture. Exp. Eye Res. **33**: 47-53.

Philp, N.J., & Nachmias, V.T. 1985. Components of the cytoskeleton in the retinal pigment epithelium of the chick. J. Cell Biol. **101**: 358-362.

Porter, K.R., 1956. The submicroscopic morphology of protoplasm. Harvey Lect. **51**: 175-228.

Porter, K.R., & Yamada, E. 1960. Studies on the endoplasmic reticulum. V. Its form and differentiation in pigment epithelial cells of the frog retina. J. Biophys. Biochem. cytol. **8**: 181-205.

Poselthwaite, A.E., Keski-Oja, J., Balaian, G. & Kang, A.H. 1981. Induction of fibroblast chemotaxis by fibronectin. Localization of the chemotactic region to a 140,000 molecular weight non-geletin-binding fragment. J. Exp. Med. **153**: 494-499.

Pudney, J., & Singer, R.H. 1978. The filamentous framework of chick myoblasts. J. Cell Biol. **79**: 271a.

Ramaekers, F.C.S., Haag, D., Kant, A., Moesker, O. Jap, P.H.K., & Vooijs, G.P. 1983. Coexpression of keratin- and vimentin-type filaments in human metastatic carcinoma cells. Proc. Natl. Acad. Sci. USA **80**: 2618-2622.

Reaven, E.P., & Axline, S.G. 1973. Subplasmalemmal microfilaments and microtubules in resting and phagocytising cultivated macrophages. J.Cell Biol. **59**: 12-27.

Reich-D'Almeida, F.B. & Hockley, D.J. 1975. In situ reactivity of the retinal pigment epithelium. I. Phagocytosis in the normal rat. Exp. Eye Res.**21**: 333-345.

Roop, D.R., Hawley-Nelson, P., Cheng, C.K., & Yuspa, S.H. 1983. keratin gene expression in mouse epidermis and cultured epidermal cells. Proc. Natl. Acad. Sci. **80**: 716-720.

Saari, J.C., Bredberg, L., & Garwin, G.G. 1982. Identification of the endogenous retinoids associated with three cellular retinoid-binding proteins from bovine retina and retinal pigment epithelium. J. Biol. Chem. **257**: 13329-13333.

Sanger, J.W. 1975: Changing patterns of actin localisation during cell division. Proc. Natl. Acad. Sci. U.S.A. **72**: 1913-1916.

Santos-Anderson, R.M., Tso M.O.M. & Wolf E.D. 1980. An inherited retinopathy in collies. A light and electron microscopic study. Invest. Ophthalmol. Vis. Sci. **19**: 1281-1294.

Sarks, S.H. 1976. Ageing and degeneration in the macular region: a clinico-pathological study. Brit. J. Ophthalmol. **60**: 324-341.

Schaafsma, H.E., Ramaekers, F.C.S., van Muijen, G.N.P., Lane, E.B., Leigh, I.M., Robben, H., Huijsmans, A., Ooms, E.C.M., & Ruiter, D.J. 1990. Distribution of cytokeratin polypeptides in human transitional cell carcinomas, with special emphasis on changing expression patterns during tumour progression. Am. J. of Pathology. **136**: 329-343.

Schachner, M. Hedeley-White, E.T., Hsu, D.W. Schoonmaker, G., & Bignami, A. 1977. Ultrastructural localization of glial fibrillary acidic protein in mouse cerbellum by immunoperoxidase labeling. J. Cell Biol. **75**: 67-73.

Schlegel, R. Banks-Schlegel, S., McLeod, J.A. & Pinkus, G.S. 1980. Immunoperoxidase localization of keratin in human neoplasms Am. J. Patholol **110**: 41-49.

Schliwa, M. & van Blerkom, J. 1981. Structural interaction of cytoskeletal components. J. Cell Biol. **90**: 222-235.

Schliwa, M., van Blerkom, J., & Porter, K.R. 1981. Stabilization of the cytoplasmic ground substance in detergent opened cells and a structural and biochemical analysis of its composition. Proc. Natl. Acad. Sci. USA **78**: 4329-4333.

Schliwa, M., Pryzwansky, K.B., & van Blerkom, J. 1982. Implications of cytoskeletal interactions for cellular architecture and behaviour. Phil. Trans. R. Soc. Lond. **B 299**: 199-205.

Schmidt, S.Y., Berson, E.L., Watson, G., & Huang, C. 1977. Retinal degenerations in cat fed casein. III. Taurine deficiency and ERG amplitudes. Invest. Ophthalmol. **16**: 673-678.

Schmid, E., Schiller, D.L., Grund, C., Stadler, J. & Franke, W.W. 1983. Tissue type-specific expression of intermediate filament proteins in a cultured epithelial cell line from bovine mammary gland. J. Cell Biol. **96**:37-50.

Seyfried-William, R., McLaughlin B.J., & Cooper N.G.F. 1984. Phagocytosis of lectin-coated beads by dystrophic and noraml retinal pigment epithelium. Exp. Cell Res. **154**: 500-509.

Sjostrand, F.S. 1953. Electron microscopy of mitochondria and cytoplasmic double membranes. Nature **171**: 30-32.

Small, J.V., & Celis, J.E. 1978. Direct visualization of the 10 nm (100-Å)-filament network in whole and enucleated cultured cells. J. Cell Sci. **31**: 393-409.

Smedtds, F., Ramaekers, F.C.S., Robben, H., Pruszczynski, M., van Muijen, G.N.P., Lane, E.B., Leigh, I.M., & Vooijs, P. 1990. Changing patterns of expression during progression of cervical intraepithelial neoplasia. Am. J. of Pathology. **136**: 657-667.

Spitznas, M., & Hogen, M.J. 1970. Outer segments of photoreceptors and the retinal pigment epithelium. Arch. Ophthalmol. **84**: 810-819.

Spooner, B.S., Yamada, K.M., & Wessells, N.K. 1971. Microfilament and cell locomotion. J. Cell Biol. **49**: 595-613.

Staehelin, L.A. 1974. Structure and function of intercellular junctions. Int. Rev. Cytol. **39**: 191-283.

Steinberg, R.H., Fisher S.K., & Anderson D.H. 1980. Disc morphogenesis in vertebrate photoreceptors. J. Comparative Neurology. **190**: 501-518.

Steinberg, R.H., & Miller, S.S. 1973. Aspects of electrolyte transport in frog pigment epithelium. Exp. Eye Res. **16**: 365-372.

Steinberg, R.H., & Miller, S.S. 1979. Transport and membrane properties of the retinal pigment epithelium. *In*: " The Retinal Pigment Epithelium" Ed. K.M. Zinn & M.F.Marmor. Harvard University Press, London. pp 205-225.

Steinert, P.M., & Parry, D.A.D. 1985. Intermediate filaments: Conformity and diversity of expression and structure. Ann. Rev. Cell Biol. **1**: 41-65.

Steinert, P.M., & Yuspa, S.H. 1978. Biochemical evidence for keratinization by mouse epidermal cell in culture. Science **200**: 1491-1493.

Steinert, P.M., Idler, W.W. & Goldman, R.D. 1980. Intermediate filaments of baby hamster kidney (BHK-21) cells and bovine epidermal keratinocytes have similar ultrastructuras and sub-unit structures. Proc. Natl. Acad. Sci. USA. **77**: 4534-4538.

Steinert, P.M., Idler, W.W., & Zimmerman, S.B. 1976. Self-assembly of bovine epidermal keratin filaments in vitro **108**: 547-567.

Steinert, P.M., Cantieri, J.C., Teller, D.C., Lonsdale-Eccles, J.D. & Dale, B.A. 1981. Characterisation of a class of cationic proteins that specifically interact with intermediate filaments. Proc. Natl. Acad. Sci. USA. **78**: 4097-4101.

Stevens, B.J. 1974. Variation in mitochondrial numbers volume in yeast according to growth conditions. J. Cell Biol. **63**: 336a.

Stossel, T.P. 1974a. Phagocytosis I. New Eng. J. Med. **290**: 717-723.

Stossel, T.P. 1974b. Phagocytosis II. New Eng. J. Med. **290**: 774-780.

Stossel, T.P. 1974.c Phagocytosis II.I New Eng. J. Med. **290**: 833-839.

Stossel, T.P. 1976. The mechanism of phagocytosis. J. of the Reticuloendothelial Soc. **19**: 237-245.

Stossel, T.P. 1982. The structure of cortical cytoplasm. Phil. Trans. R. Soc. Lond. B **299**: 275-289.

Stossel, T.P. & Hartwig, J.H. 1976. Phagocytosis and the contractile proteins of pulmonary macrophages. Cell Motility **3**: 529-544.

Stossel, T.P., Mason, R.J., Hartwig, J. & Vaughan, M. 1972. Quantitative studies of phagocytosis by polymorphonuclear leukocytes: use of emulsions to measure the initial rate of phagocytosis. J. Clin. Invest. **51**: 615-624.

Streeten, B.W. 1961. The sudanophilic granules of the human retinal pigment epithelium. Arch. Ophthalmol. **66**: 391-398.

Strickland, S. & Mohdavi, V. 1978. The induction of differentiation in teratocarcinoma stem cells by retinoic acid. Cell **15**: 393-403.

Strickland, S., Smith, K.K. & Marotti, K.R. 1980. Hormonal induction of differentiation in teratocarcinoma stem cells; generation of pariental endoderm by retinoic acid and dibutyl cAMP. Cell **21**: 347-355.

Sun, T-T. & Green, H. 1978a. Immunofluorescent staining of keratin filaments in cultured cells. Cell **14**: 469-476.

Sun, T-T. & Green, H. 1978b. Keratin filaments of cultured human epidermal cells. Formation of intramolecular disulfide bonds during terminal differentiation. J. Biol. Chem. **253**: 2053-2060.

Sun, T-T., Shih, C., & Green H. 1979. Keratin cytoskeletons in epithelial cells of internal organs. Proc. Natl. Acad. Sci. U.S.A. **76**: 2813-2817.

Szamier, R.B., Berson, E.L., Klien, R., & Meyers S. 1979. Sex-linked retinitis pigmentosa: ultrastructure of photoreceptors and pigment epithelium. Invest. Ophthalmol. Vis. Sci. **18**: 145-160.

Takeuchi, S. 1987. The rearrangement of cytoskeletal systems in epithelial cells accompanying the transition from a stationary to a motile state at the start of epithelial spreading. J. Cell Sci. **88**: 109-119.

Tappel, A.L. 1968. Will antioxidant nutrients slow aging process? Geriatrics. **23**: 97-105.

Tappel, A.L. 1970. Biological antioxidant protection against lipid peroxidation damage. Am. J. Clin. Nutr. 23: 1137-1139.

Tarnowski, B.I., & McLaughlin, B.J. 1988. Phagocytic interactions of sialated glycoproteins, sugar, and lectin-coated beads with rat retinal pigment epithelium. Curr. Eye. Res. **6**: 1079-1089.

Trotter, J.A., Foerder, B.A. & Keller, J.M. 1978. Intracellular fibres in cultured cells: Analysis by scanning microscopy and by SDS-polyacrylamide gel electrophoresis. J. Cell Sci. 31: 369-393.

Troutt & Burnside, M.B. 1989. Role of microtubules in pigment granule migration in teleost retinal pigment epithelial cells. Exp. Eye Res. **48**: 433-443.

Tseng, S.C.G., Jarvinen, M.J., Nelson, W.G., Huang, J-W., Woodcock-Mitchell, J., & Sun, T-T. 1982. Correlation of specific keratins with different types of epithelial differentiation: Monoclonal antibody studies. Cell **30**: 361-372.

Tucker, J.B. 1979. Spatial organization of microtubules. In Microtubules. Ed. K. Roberts & J.S. Hyams. Academic Press. N.Y.: 347-357.

Turksen, K., Opas, M., Aubin, J.E., & Kalnins, V.I. 1983. Microtubules, microfilaments and adhesion patterns in differentiating chick retinal pigment epithelial (RPE) cells in vitro. Exp. Cell Res. **147**: 379-391.

Vikstrom, K.L., Borisy, G.G., & Goldman R.D. 1989. Dynamic aspects of intermediate filament networks in BHK-21 cells. Proc. Natl. Acad. Sci. U.S.A. **86**: 549-553.

Vinores, S.A., Campochiaro, P.A., McGehee, R., Orman, W., Hackett, S.F. & Hjelmeland, L.M. 1990. Ultrastructural and immunocytochemical changes in retinal pigment epithelium, retinal glia, and fibroblasts in vitreous culture. Invest. Ophthalmol. Vis. Sci. **31**: 2529-2545.

Virtanen, I., Kurkinen, M. & Lehto, V.P. 1979. Nucleous-anchoring cytoskeleton in chicken red blood cells. Cell Biol. Int. Rep. **3**: 157-162.

Virtanen, I., Lehto, V.P., Lehtonen, E., Vartio, T., Stenman, S., Kurki, P., Wager, O., Small, J.V., Dahl, D., & Bradley, R.A. 1981. Expression of intermediate filaments in cultured cells. J. Cell Sci. **50**: 45-63.

Wang, Y-L. 1984. Reorganisation of actin filament bundles in living fibroblasts. J. Cell Biol. **99**: 1478-1485.

Wang, Y-L., 1987. Mobility of filamentous actin in living cytoplasm. J. Cell Biol. **105**: 2811-2826.

Wang, E. & Goldman, R.D. 1978. Functions of cytoplasmic fibers in intracellular movements in BHK-21 cells. J. Cell Biol. **79**: 708-726.

Warren, R.H. 1974. Microtubular organization in elongating myogenic cells. J. Cell Biol. **63**: 550-566.

Weber, K., & Groeschel-Stewart, U. 1974. Antibody to myosin: The specific visualisation of myosin-containing filaments in non-muscle cells. Proc. Natl. Acad. Sci. U.S.A. **71**: 4561-4564.

Weber, K., Bibring, T., & Osborn, M. 1975a. Specific visulisation of tubulin containing structures in tissue culture cells by immunofluorescence. Exp. Cell Res. **95**: 111-120.

Weber, K., Pollack, R., & Bibring, T. 1975b. Antibody against tubulin: the specific visualisation of cytoplasmic microtubules in tissue cultre cells. Proc. Natl. Acad. Sci. USA. **72**: 459-463.

Weidman, T.A. & Kuwabara, T. 1968. Postnatel development of the rat retina. An electron microscopic study. Arch. Ophthalmol. **79**: 470-484.

Wiche, G., Depler, R., Arlieb, U., Pytela, R., & Denk, H. 1983. Occurance and immunolocalisation of plectin in tissues. J. Cell Biol. **97**: 887-901.

Willingham, M.C., Yamada, K.M., Yamada, S.S., Pouyssegur, J., & Pastan, I. 1977. Microfilament bundles and cell shape are related to adhesiveness to substratum and are dissociable from growth control in cultured fibroblasts. Cell **10**: 375-380.

Winter, S., Jarasch, E-D., Schmid, E., Franke, W.W. & Denk, H. 1980. Differences in polypeptide composition of cytokeratin filaments, including tonofilaments, from different epithelial tissues and cells. Eur. J. Cell Biol. **22**: 371.

Wolosewick J.J. & Porter, K.R. 1976. Stereo High voltage electron microscopy of whole cells of the human diploid line, WI-38. Am. J. Anat. **147**: 303-324.

Woodcock-Mitchell, J., Eichner, R., Nelson, W.G., & Tung-Tien, S. 1982. Immunolocalization of keratin polypeptides in human epidermis using monoclonal antibodies. J. Cell Biol. **95**: 580-588.

Wu, Y-J. & Rheinwald, J.G. 1981. A new small (40kd) keratin filament protein made by some cultured human squamous cell carcinomas. Cell **25**: 627-635.

Wu, Y-J., Parker, L.M., Binder, N.E., Beckett, M.A., Sinard, J.H., Griffiths, C.T., & Rheinwald, J.G. 1982. The mesothelial keratins: A new family of cytoskeletal proteins identified in cultured mesothelial cells and nonkeratinizing epithelia. Cell **31**: 693-703.

Yen, S-H., & Fields, K.L. 1981. Antibodies to neurofilament, glial filaments and fibroblast intermediate filament protein bind to different cell types of the nervous system. J. Cell Biol. **88**: 115-126.

Young, R.W. 1967. The renewal of photoreceptor cell outer segments. J. Cell Biol. **33**: 61-72.

Young, R.W. 1969. The organisation of vertebrate photoreceptor cells. *In*: The Retina: morphology, function and clinical characterisation. Ed. B.R.Straatsma, M.O.Hall, R.A.allen & F. Crescitelli. University of California Press. pp 177-210.

Young, R.W. 1971a. Shedding of discs from rod outer segments in the rhesus monkey. J. Ultrastruct. Res. **34**: 190-203.

Young, R.W. 1971b. The renewal of rod and cone outer segments in the rhesus monkey. J. Cell Biol. **49**: 303-318.

Young, R.W. 1977. The daily rhythm of shedding and degradation of cone segment membranes in the chick retina. Invest. Ophthalmol. Vis. Sci. **17**: 105-116.

Young, R.W. & Bok, D. 1969. Participation of the retinal pigment epithelium in the rod outer segment renewal process. J. Cell Biol. **42**: 392-403.

Young, R.W. & Bok, D. 1979. Metabolism of the retinal pigment epithelium. *In*: The Retinal Pigment Epithelium. Ed. K.M. Zinn & M.F. Marmor. Publ. Harvard University Press. London. pp 103-123.

Young, R.W. & Droz, B. 1968. The renewal of protein in retinal rods and cones. J. Cell Biol. **39**: 169-184.

Zinn, K.M. & Henkind, B-H. 1979. Anatomy of the human retinal pigment epithelium. In The Retinal Pigment Epithelium. Publ. Harvard University Press, London. pp 3-31.

Zinn, K.M., & Marmor, M.F. 1979. The Retinal Pigment Epithelium. Publ. Harvard University Press, London.

Zimmerman, W.F. 1974. The distribution and proportions of vitamin A compounds during the visual cycle in the rat. Vision Res. **14**: 795-802.